Using systems biology to explore temporal changes in human fibroblast cellular senescence.

Rebekah-Louise Anne Scanlan

Doctor of Philosophy

Biosciences Institute

Newcastle University, UK

March 2025

Acknowledgements.

I would first like to thank my supervisors Daryl Shanley, Carmen Martin-Ruiz, James Wordsworth, and Viktor Korolchuk, for their support and guidance throughout my PhD. Their guidance was instrumental in shaping this project into what it is today.

Additionally, I would like to thank all others who have supported this project and helped me throughout my studies, including Satomi Miwa and Daniel Rico who formed my progress panel, the Shanley lab group, and the postgraduate administrative staff for the Faculty of Medical Sciences. Whether through providing administrative support or feedback on how my work was progressing from year to year, all contributions were crucial in enhancing my experience as a Newcastle University Doctoral Candidate.

Parts of this project would have been impossible without the collaborative effort from the Bohr and Rasmussen lab groups at Copenhagen University. I would like to thank all involved in this research, allowing me to learn from them, and to form these professional connections.

Throughout my PhD I have been fortunate in the vast opportunities I have had access to, including attending conferences nationally and internationally. These opportunities allowed me to keep up with the most up to date research relevant to my studies and apply these fresh perspectives to my own research.

Finally, I would like to thank my family and friends for always encouraging and supporting me. Without them, I would not have found nearly enough time to appreciate the smaller things in life. To my parents, thank you for always believing in me and providing me with everything I could need – I really took being the first in the family to attend university to the extreme! I would especially like to thank my soon-to-be-husband, James Watson, for his unwavering support and generosity throughout my PhD, particularly during these final intense months while I have been in ‘write-up’ mode. Without his care and kindness, I would have been worse off.

Thank you all.

Abstract.

Cellular senescence is a complex phenotype characterised by permanent cell cycle arrest and a senescence-associated secretory phenotype, which includes growth factors and inflammatory cytokines. While primarily thought of as a tumour-suppressive mechanism, senescence also plays roles in wound healing and embryogenesis. Senescent cells are normally transient but accumulate with age due to dysregulated immune clearance, contributing to low-grade chronic inflammation and age-related diseases. Characterising senescent cells is challenging due to phenotype heterogeneity, and the temporal dynamics of senescence remain poorly understood. This thesis employed an integrated approach to investigate human fibroblast senescence at transcriptomic and protein levels. A systematic review identified 119 transcriptomic datasets on human fibroblast senescence, forming the database SenOmic, publicly hosted online and allowing users to filter by variables of interest such as gene and timepoint. Computational modelling of key selected proteins in DNA damage-induced senescence (DDIS) and oncogene-induced senescence (OIS) was also performed, including knockdown interventions. Analysis of SenOmic reinforced the challenges of defining a universal geneset across cell lines and senescence types. However, 28 genes were significantly up- or downregulated across DDIS, OIS, replicative senescence, and bystander senescence compared to proliferating controls, with only one gene present in the KEGG senescence pathway. Distinct phenotypes were also observed, including significantly stronger p53 signalling in DDIS compared to OIS, clustering of samples by time, and significant upregulation of genes involved in protein secretion between days 5-7 in gene set enrichment analysis. Protein level modelling demonstrated the importance of multi-macrolevel analysis, highlighting post-translational modifications and network-wide effects of knockdowns. In conclusion, while unique universal senescence biomarkers remain challenging to identify, conventional senescence markers follow predictable profiles, distinct phenotypic differences exist across timepoints and senescence types, and further interrogation of resources like *SenOmic* with an established framework provides a valuable means to enhance our understanding of senescence.

List of abbreviations.

ACTA2…….	Actin Alpha 2, Smooth Muscle
ALKAL1……...	ALK and LTK Ligand 1
ATM…….	Ataxia-telangiectasia mutated
ATR…….	Ataxia-telangiectasia and Rad3-related
AOA1……..	Ataxia-oculomotor apraxia type 1
APTX……...	Aprataxin
AU……	Arbitrary unit
BYS…….	Bystander senescence
CAFs……	Cancer associated fibroblasts
CCFs……...	Cytoplasmic chromatin fragments
CCN-xx……	Cyclin-xx *e.g. CCNB2*
CDK…….	Cyclin dependent kinase
C/EBPβ……...	CCAAT/enhancer binding protein beta
cGAMP……	Cyclic GMP-AMP
cGAS……...	Cyclic GMP-AMP synthase
CHK…….	Checkpoint kinase
CLDN1……	Claudin-1
COL-x……..	Collagen type-x *e.g. COL1A1, Collagen Type I Alpha 1 Chain*
CR……	Chromatin remodelling
cytoDNA…….	Cytoplasmic DNA
DDIS……	DNA damage-induced senescence
DDR……	DNA damage response
DE……	Differentially expressed
D&Q……	Dasatinib and Quercetin
dNTP……...	Depletion of deoxyribonucleotide triphosphates
dsDNA……	Double stranded DNA
ECM……	Extracellular matrix
EREG……..	Epiregulin
EZH2……...	Enhancer of Zeste 2 Polycomb Repressive Complex 2 Subunit
FGF9……...	Fibroblast Growth Factor 9
GADD45A……...	Growth Arrest and DNA Damage Inducible Alpha

GAS6……..	Growth Arrest Specific 6
GEO……	Gene Expression Omnibus
GSEA……..	Gene set enrichment analysis
KD……	Knockdown
KEGG……..	Kyoto Encyclopedia of Genes and Genomes
KO……	Knockout
IFN……...	Interferon
IL-x……...	Interleukin-x *e.g. IL-6*
IS……..	Immune stimulated
IQR…….	Interquartile range
LogFC…….	Log2 Fold Change
MAPK…….	Mitogen-activated protein kinase
MDM2	Mouse/human double minute 2
MEFs……..	Mouse embryonic fibroblasts
MitoSkip……	Senescence induced through mitotic skipping
mTOR…….	Mammalian target of rapamycin
NBIS……	Nuclear breakdown induced senescence
NF-kB……..	Nuclear factor kappa light chain enhancer of activated B cells
NICD……	Notch intracellular domain
NIPALS……..	Non-linear iterative partial least squares
NIS……..	Notch induced senescence
NS……	Non-immune stimulated
NSD2……..	Nuclear receptor binding SET domain protein 2
OIS……..	Oncogene-induced senescence
ONS……	Office for National Statistics
ORA	Over-representation analysis
OSKM…….	Oct4, Sox2, KLF4, and Myc
PC……	Principal component
PCA…….	Principal component analysis
PD……	Population doubling
PIIPS……...	Proteasome inhibition-induced premature senescence
PTEN……..	Phosphatase and Tensin Homolog
PTM……	Post-translational modification

Rb……	Retinoblastoma
REP…….	Replicative senescence
RNIS……	Ras and Notch induced senescence
ROS……	Reactive oxygen species
SA-β-gal……..	Senescence associated beta galactosidase
SASP……..	Senescence associated secretory phenotype
ssDNA…….	Single stranded DNA
STING…….	Stimulator of interferon genes
TGFβ…….…..	Transforming growth factor beta
TF……	Transcription factor
WT……..	Wildtype

Table of Contents

List of Tables.

List of Figures.

List of Equations and Code.

Chapter 1: Introduction.

1.1 Ageing.

Ageing is a process associated with greying of hair, wrinkled skin, and an increased risk of diseases such as cancer and neurological diseases including Alzheimer's disease and Parkinson's disease (Liu et al., 2024; Niccoli & Partridge, 2012). Ageing is a complex multi-faceted process which affects almost all known organisms (Kirkwood, 2005) with many underlying causes known at the cellular and genetic level. For example, changes to the extracellular matrix (ECM), such as a decreased abundance of type I and type III collagen proteins, leads to the appearance of wrinkled and less elastic skin with age (Reilly & Lozano, 2021; Varani et al., 2006). The progressive loss of function in biological processes with age such as protein homeostasis and DNA repair ultimately leads to increased mortality and a reduction in fertility. In recent years, advances have been made towards extending and improving human lifespan and healthspan: improved medicines, better living conditions and advancement of scientific knowledge have all contributed towards significantly extending human lifespan (**Figure 1.1**).

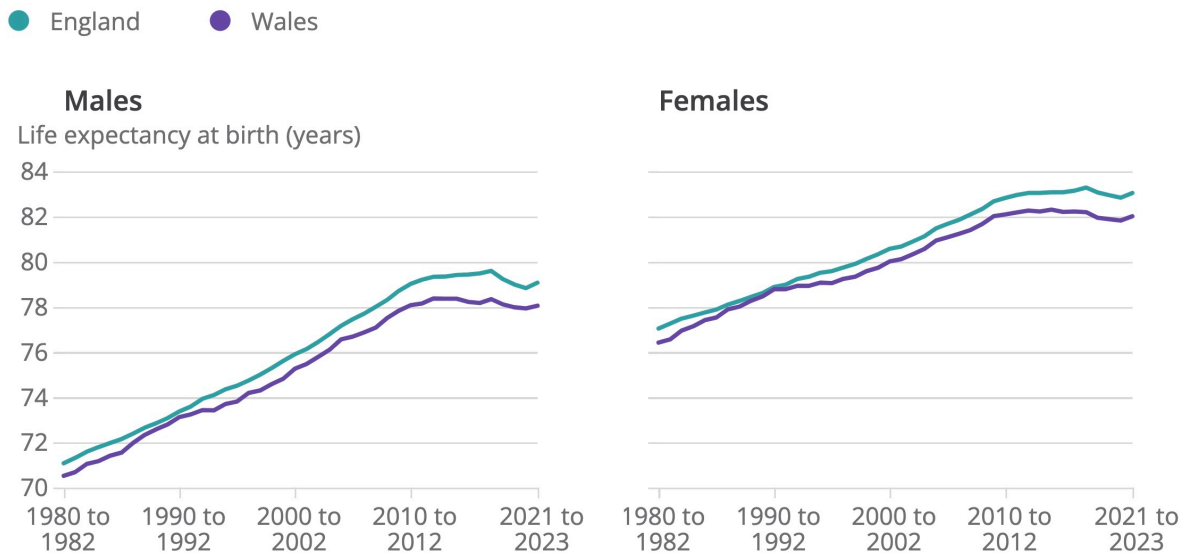

Figure 1.1 – Life expectancy in the United Kingdom.

Life expectancy for males and females in the United Kingdom between 1980 and 2023. Taken from The Office for National Statistics (ONS) ((ONS), 2024).

Ageing has been recognised as one of the greatest risk factors associated with the development of chronic diseases such as type 2 diabetes, cardiovascular diseases, and Alzheimer's disease (Kennedy et al., 2014; López-Otín et al., 2013). Additionally, studies have shown that over 90% of individuals aged 65 and older have at least one chronic disease (Barnett et al., 2012; Marengoni et al., 2011). Most of these diseases have no current cure, with treatments primarily aimed at symptom management and delaying disease progression. Understanding the biology behind ageing and how it influences different disease states will result in the improvement of both healthspan and lifespan in humans.

1.1.1 Hallmarks of ageing.

Ageing is an inherently complex process involving many different interacting processes at the molecular level. There is evidence of ageing being influenced by intrinsically dictated factors such as genetics from studies investigating centenarians (Govindaraju et al., 2015; Sebastiani & Perls, 2012) and premature ageing diseases such as Hutchinson-Gilford progeria syndrome (Paul et al., 2021). While genetics can and does influence ageing, extrinsic environmental factors such as sun exposure, psychological stress, nutrition, access to medicine, and lifestyle choices (such as smoking or physical activity) also play a significant role in the ageing process (Farage et al., 2008). Factors which contribute to ageing, whether intrinsic or extrinsic, interact with one another. For example, smoking can alter DNA through epigenetic modifications (Jenkins et al., 2017; Lee & Pausova, 2013).

Hallmarks of ageing were first introduced in 2013 in a seminal paper by López-Otín et al. (2013). This study proposed nine hallmarks including: (i) stem cell exhaustion, (ii) genomic instability, (iii) telomere attrition, (iv) epigenetic alterations, (v) loss of proteostasis, (vi) deregulated nutrient-sensing, (vii) mitochondrial dysfunction, (viii) altered intracellular communication and (ix) cellular senescence (López-Otín et al., 2013). This list has since been expanded and includes a further three hallmarks: chronic inflammation, dysbiosis, and disabled macroautophagy (López-Otín et al., 2023) (**Figure 1.2**). The hallmarks are split into three different types: primary, antagonistic, and integrative. Primary hallmarks are those reflecting the cellular damage that accumulates with ageing, such as damage to the genome or organelles

(Gladyshev et al., 2021) or telomere erosion (Rossiello et al., 2022). Antagonistic hallmarks have a more complex role in ageing and are those elicited as a response to cellular damage, such as mitochondrial dysfunction and cellular senescence. For example, cellular senescence is beneficial when transient as senescence is primarily considered a tumour suppressive process and has been shown to be beneficial in a wound healing environment (Campisi, 2001; Demaria et al., 2014). However, with age senescent cells tend to accumulate which contributes to chronic low-grade inflammation and increased disease burden (Muñoz-Espín & Serrano, 2014). Integrative hallmarks occur when damage accumulates and a threshold of what the cell can compensate for is passed, resulting in outcomes such as chronic inflammation and stem cell exhaustion.

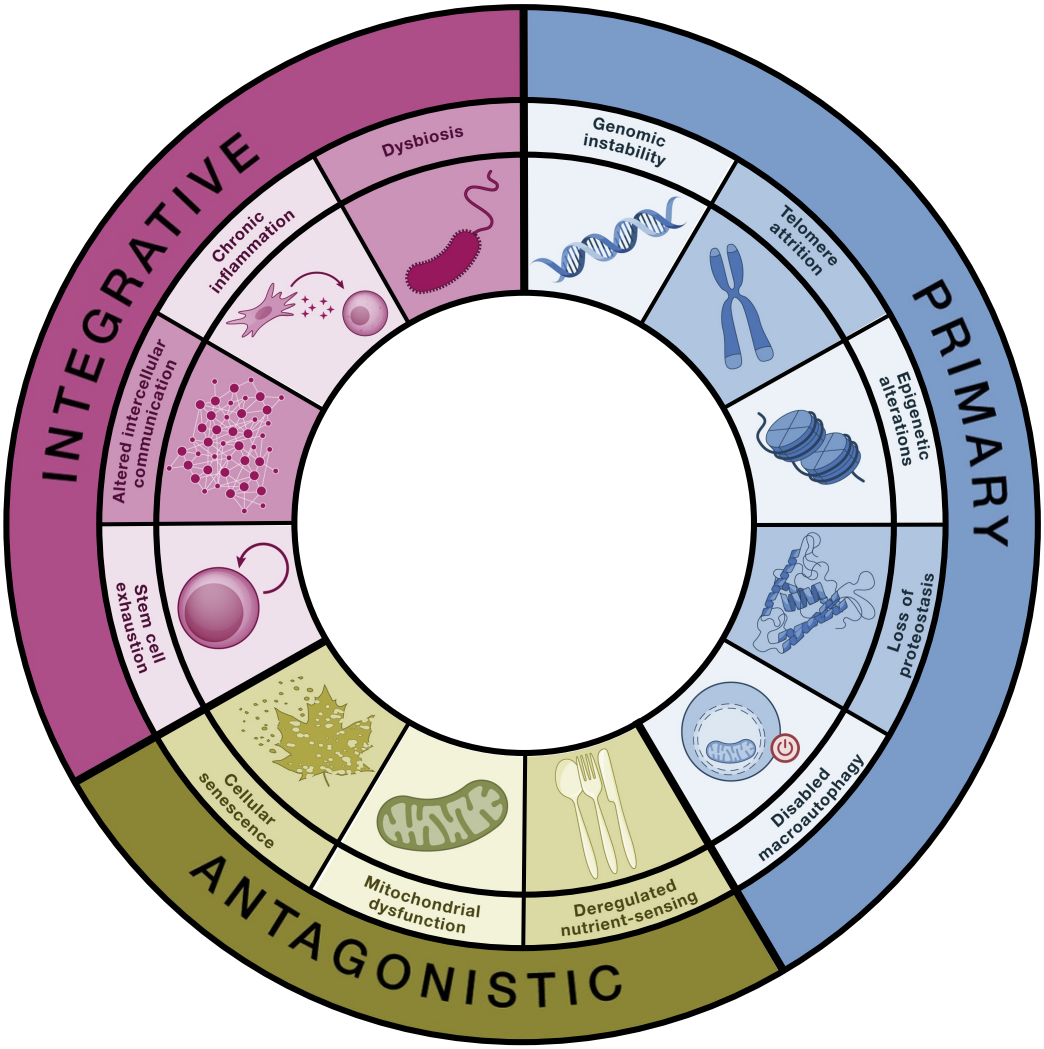

Figure 1.2 – The expanded hallmarks of ageing.

Adapted from López-Otín et al. (2023).

The definition of these hallmarks led to an influx of research into their role in ageing. The majority of research initially investigated singular hallmarks. However, ageing is more complex than individual hallmarks, and as research has progressed and the ageing field advanced, it became more evident that the hallmarks were interacting. For example, telomere attrition is a type of genomic instability and a cause of cellular senescence (Rossiello et al., 2022). Investigating the role of single hallmarks of ageing is experimentally demanding, and researching multiple interacting hallmarks presents a major challenge. One option to investigating complex single or interacting hallmarks is by taking a systems biology approach.

1.2 Systems biology.

Systems biology is the analysis of any complex biological system using a computational or mathematical approach (Kitano, 2002), often addressing multiple levels of complexity in a systematic manner. It presents an integrative approach rather than a reductive one and involves bioinformatics methods to extract knowledge from large datasets and the computational or mathematical simulation of model networks for the detailed study of biological mechanisms. Over the last 20 years, a systems biology approach has been used to explore vast areas of research: to understand disease states such as the dynamics of the spread of foot-and-mouth disease (Keeling, 2005) or the molecular mechanisms behind coronary heart disease (Huan et al., 2013); for the comprehension of molecular interactions such as the synergy between interacting genes (Anastassiou, 2007) or the involvement of cytokines in CD4+ T cell differentiation (Carbo et al., 2013); to explore human response to infection from various influenza strains (Hancioglu et al., 2007; Manchanda et al., 2014); and to investigate breast cancer (Mufudza et al., 2012) or prostate cancer (Ergün et al., 2007). It is possible to explore processes at the molecular and cellular level, through to tissue level, and all the way up to population level, demonstrating the diversity and versatility of systems biology.

Since the introduction of systems biology as a field of scientific research, *in silico* investigation of complex biological systems has advanced significantly due to improvements in computational power, software, technology, and expertise (Colquitt et al., 2011). Taking a systems biology approach over more traditional laboratory

methods has numerous benefits, including gaining a more comprehensive understanding of biological processes by combining knowledge and data from numerous sources. Although it is worth noting that ideally a systems biology approach should be combined with *in vitro* or *in vivo* study as the different types of data can inform one another and lead to hypothesis development. For example, Dalle Pezze et al. (2014) combined *in silico* and *in vitro* approaches to explore the role of signalling in cellular senescence and mitochondrial function. This study, supported by both computational and laboratory work, identified that reactive oxygen species (ROS) or mammalian target of rapamycin (mTOR) inhibition were able to partially rescue senescent cells from the associated dysfunctional mitochondrial phenotype. This was first investigated computationally and then validated experimentally (Dalle Pezze et al., 2014). Taking a combined and integrative approach creates a collaborative effort which will ultimately result in more open research and therefore sharing of knowledge.

A key aim of a systems biology approach is often the development of a computational model of the process being studied. There are various factors to consider when developing a computational model, and the choice of modelling approach depends on what is being investigated. Models can be dynamic or static, discrete or continuous, and stochastic or deterministic. Typically, dynamic models are more useful in systems biology as biological processes inevitably undergo temporal changes, however processes can lend themselves to static modelling rather than dynamic modelling when they achieve prolonged periods of homeostasis. Discrete variables have defined integer values (such as gene expression being either in an ‘on’ or ‘off’ state), while continuous variables (such as membrane potential) have an infinite number of states or values. Regarding stochastic or deterministic models, stochastic modelling accounts for randomness of cellular processes (such as the occurrence of genetic damage). Stochastic models are particularly useful for capturing biological variability and unpredictability. Examples of stochastic modelling include modelling the dynamics of molecular chaperones in ageing (Proctor et al., 2005), and the heterogeneity of cell entry into cellular senescence (Sozou & Kirkwood, 2001). In contrast, deterministic models do not incorporate randomness

and instead use fixed mathematical equations where the same initial conditions always produce the same outcomes.

One advantage of a computational approach is that not every variable needs to be experimentally determined. Instead, modellers can utilise parameter estimations to guide variable behaviour, identifying likely values for the variables which fit within the rest of the system and known data. When parameters are established, the sensitivity to any one or more parameters can be explored by systematic simulation. Knowledge gained can then guide laboratory experiments to confirm whether this is how variables in the biological system work.

As mentioned, ageing is a complex biological system (Kirkwood, 2005). While ageing is often investigated *in vitro* and *in vivo*, it can be difficult to explore multiple mechanisms at once due to the high degree of interactions between cellular processes. Therefore, taking a systems biology approach is an important means to gaining a fuller understanding of the complexity of ageing.

1.2.1 Systems biology of ageing and senescence.

Taking a systems biology approach to understanding ageing can be useful due to the complexity of ageing, but also because if offers the opportunity to combine existing knowledge and data from individual studies to create a more comprehensive understanding (Chandrasegaran et al., 2023). Additionally, a systems biology approach can integrate multiple processes and hallmarks of ageing, for example, into one larger system for investigation.

Many *in silico* mathematical models have investigated ageing and its hallmarks (including cellular senescence), both at the molecular level and at a multiscale level. Examples at the molecular level include: the role of molecular chaperones in ageing (Proctor & Lorimer, 2011; Proctor et al., 2005); mitochondrial function in ageing and senescence (Dalle Pezze et al., 2014; Passos et al., 2010); the dysregulation of various signalling pathway in ageing such as changes in ECM signalling and FOXO signalling (Hui et al., 2016; Smith & Shanley, 2010); age-related diseases such as rheumatoid arthritis (Baker et al., 2013), and amyloid-β aggregation in Alzheimer's

disease (Proctor et al., 2012). An example of multi-scale *in silico* modelling is the whole-body model which explores changes in liver-mediated clearance of low density lipoprotein-cholesterol and how this contributes to an age-related increase in low density lipoprotein-cholesterol (Mc Auley et al., 2012).

Utilising systems biology methods has improved the understanding of ageing and senescence. For example, stochastic *in silico* modelling was able to suggest the reason behind heterogeneity in cell division potential and entry into replicative senescence was due to mitochondrial ROS and nuclear somatic mutations (Sozou & Kirkwood, 2001). This model was later reinforced by laboratory experiments which demonstrated that the production of mitochondrial superoxide increased with replicative cell age, and that mild mitochondrial uncoupling reduced superoxide generation, slowed telomere shortening and delayed entry into replicative senescence (Passos et al., 2007).

1.3 Cellular senescence.

Cellular senescence is one of the antagonistic hallmarks of ageing (**Figure 1.2**) and was first described in 1961 by Hayflick and Moorhead at a time when it was thought that cultured cells could divide indefinitely. In these seminal experiments, young and old cells were co-cultured and it was observed that old cells stopped dividing while young cells continued to divide (Hayflick & Moorhead, 1961). This was termed the Hayflick Limit. Later, this state of arrested cell division in old cells became known as replicative senescence (REP). In 1972, the end replication problem was discovered which explained why old cells stopped dividing and entered REP (Watson, 1972). It is believed that telomere erosion, which occurs with every cell division, is the main cause of entry into REP as cells recognise uncapped telomere ends as a form of double strand DNA (dsDNA) breaks (d'Adda di Fagagna et al., 2003). Telomeres can be replenished by telomerase, however most somatic cells in the human body do not have active telomerase (Collins & Mitchell, 2002). Notably, many cancers have been identified as activating telomerase expression to promote continuous cell proliferation even when there is genetic damage in the cell (Hanahan & Weinberg, 2011).

Many types of senescence have since been discovered including DNA damage-induced senescence (DDIS), oncogene-induced senescence (OIS), bystander secondary senescence (BYS), and senescence in response to chemotherapeutic treatment. Almost all types of senescence are characterised by unresolved DNA damage, however there are exceptions where senescence occurs independent of damage; this is the case when cell proliferation slows down due to decreased levels of Phosphatase and Tensin Homolog (PTEN) leading to PTEN-loss induced cellular senescence (Chen et al., 2005; Song et al., 2012). During senescence, damaged DNA can leak into the cytoplasm as a result of the breakdown of the nuclear lamina (Dou et al., 2017; Freund et al., 2012; Shah et al., 2013), leading to activation of cytosolic DNA-sensing pathways such as cGAS-STING signalling. Likewise, during senescence, leakage of mtDNA into the cytoplasm has been observed, again activating cGAS-STING signalling and thus reinforcing the senescence associated secretory phenotype (SASP) (Dou et al., 2017; Huang et al., 2020; Vizioli et al., 2020).

Senescence is characterised by a stable cell cycle arrest (Huang et al., 2022; Kumari & Jat, 2021; Ogrodnik et al., 2024), with senescence playing a beneficial role in processes such as wound healing, embryonic development and tissue remodelling. Senescent cells are usually transient in tissues and are cleared through a self-regulated process involving the immune system (Lujambio, 2016; Montecino-Rodriguez et al., 2013). Another key characteristic of senescence is the secretion of inflammatory proteins and other molecules, such as extracellular vesicles, which constitute the SASP (Basisty et al., 2020; Coppé et al., 2010; Estévez-Souto et al., 2023; Lopes-Paciencia et al., 2019). The accumulation of senescent cells leads to chronic inflammatory signalling which in turn can promote the development of inflammatory diseases and cancer, all mediated via the SASP.

1.3.1 Cellular senescence and ageing.

Senescent cells have been demonstrated as increasing in abundance with age in multiple human tissues including the skin, liver, lung, and brain (Baker & Petersen, 2018; Dimri et al., 1995; Jurk et al., 2012). This is likely due to impaired immune function and results in chronic low-grade inflammation and increased age-related

disease burden (He & Sharpless, 2017; van Deursen, 2014). Furthermore, mouse models have been developed which have further validated the detrimental effects of senescent cell accumulation, and the age-related benefits of selective removal of senescent cells (Baker et al., 2016; Baker et al., 2011).

Increased presence of senescent cells has been demonstrated to increase the burden of ageing and age-related disorders such as Alzheimer's disease, type 2 diabetes, idiopathic pulmonary fibrosis, and osteoarthritis (Childs et al., 2015; He & Sharpless, 2017; Mylonas & O'Loghlen, 2022). Alzheimer's disease, for example, is a progressive neurodegenerative disease characterised by memory loss and cognitive decline, primarily attributed to the accumulation of amyloid-beta plaques and tau tangles in the brain. There is currently no cure for Alzheimer's disease but rather treatments which focus on symptom management and slowing disease progression. Increasing evidence suggests senescence plays a role in Alzheimer's pathology, with senescent cells detected in the brains of human Alzheimer's disease patients (Baker & Petersen, 2018; Bhat et al., 2012; Saez-Atienzar & Masliah, 2020; Zhang et al., 2019) as well as in Alzheimer's disease mouse models (Bussian et al., 2018; Musi et al., 2018; Wei et al., 2016; Zhang et al., 2019). Importantly, studies using these mouse models have demonstrated that the targeted removal of senescence cells (via senolytic treatment) can reduce amyloid-beta load and tau-pathology, alleviate neuroinflammation, and improve cognitive function (Bussian et al., 2018; Musi et al., 2018; Zhang et al., 2019). These findings highlight the potential of senotherapeutic strategies in mitigating Alzheimer's disease progression and emphasise the need for further research into the role of senescence in age-related diseases.

1.3.2 Functions of cellular senescence.

Cellular senescence is primarily thought to be a tumour protective mechanism due to its role in preventing the replication of genetically damaged cells; however, senescence is also known to play a role in many other processes including development, ageing, embryogenesis, infections, and successful wound healing (Muñoz-Espín et al., 2013; Muñoz-Espín & Serrano, 2014) (**Figure 1.3**). During wound healing, senescent cells have been shown to accumulate at wound sites to induce differentiation of myofibroblasts to accelerate the process of wound healing

(Jun and Lau, 2010). Further supporting the role of senescent cells in wound healing, it has been shown that removal of senescent cells from an acute wound results in an inefficient, delayed healing response (Demaria *et al.*, 2014). A recent computational model demonstrated that the exact timing of accumulation and removal of senescent cells plays an important role in healthy healing, with dysregulation of senescent cell turnover resulting in fibrosis and ulcers (Chandrasegaran, 2023). Senescent cells have also been identified as being present during female reproductive ageing (Secomandi et al., 2022; Velarde & Menon, 2016) although the role of senescence in female reproductive ageing is yet to be fully elucidated.

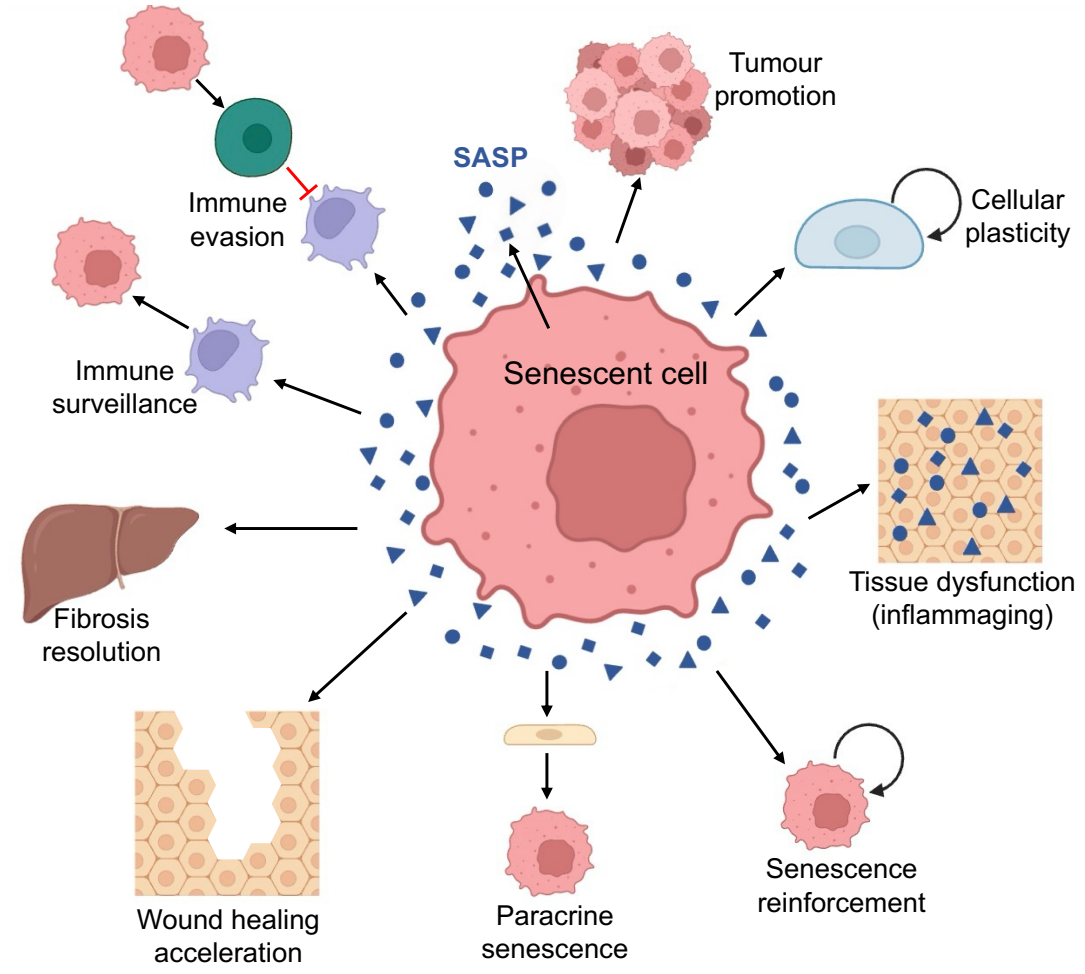

Figure 1.3 – Functions of cellular senescence.

Adapted from Herranz and Gil. (2018).

Unfortunately, despite cellular senescence primarily being recognised as a tumour protective mechanism, accumulation of senescent cells can have detrimental effects

such as inflammaging (Li et al., 2023; Santoro et al., 2021) and the promotion of tumour growth (Schmitt et al., 2022). This paradox highlights the delicate balance between senescent cell persistence and clearance, where disruptions to this balance can drive age-related diseases.

1.3.3 Cellular senescence interventions.

As mentioned above, removal of senescent cells, whether through genetic intervention or therapeutics, has been demonstrated to reduce disease burden and improve mean lifespan in mouse models (Baker et al., 2016; Baker et al., 2011; Jurk et al., 2014). These findings suggest that such an approach in humans could lead to a decreased disease burden, improved healthspan and potentially increased lifespan.

Senotherapeutics is an increasing research area, with a focus on repurposing existing FDA-approved drugs for senescence-targeting rather than developing entirely new molecules. Therapeutic interventions to reduce accumulation of senescent cells is split into two categories: senomorphics and senolytics (Zhang et al., 2023).

Senomorphics suppress markers of senescence, particularly SASP expression. By preventing SASP expression when senescent cells accumulate, senomorphics aim to mitigate the negative impact of senescent cells. Examples of senomorphics include rapamycin, metformin and resveratrol. Rapamycin is a mTOR inhibitor which has been demonstrated to extend mouse lifespan (Chen et al., 2009; Harrison et al., 2009; Miller et al., 2011).

Metformin is a widely used antidiabetic drug with multiple sites of action, primarily prescribed to diabetes patient to help regulate blood glucose levels (Rena et al., 2017). Metformin has been demonstrated to inhibit the expression of inflammatory SASP proteins through interruption of NF-κB function (Moiseeva et al., 2013). There is growing interest in repurposing metformin for the treatment of age-related diseases, including type 2 diabetes. Numerous clinical trials have been designed to investigate whether metformin treatment can delay the onset and progression of age-

related diseases (Barzilai et al., 2016; Justice et al., 2018), reduce the risk of cardiovascular disease (Petrie et al., 2017), or reduce age-related physical decline and frailty (Rennie et al., 2022).

Resveratrol is a natural compound found in foods such as grapes, wine, and blueberries (L. X. Zhang et al., 2021). Resveratrol has shown promise in delaying ageing through the activation of SIRT1, which plays a key role in reducing oxidative stress and suppressing the production of inflammatory protein such as those found in the SASP (Ciccone et al., 2022; Yun et al., 2012). Additionally, resveratrol has been demonstrated to decrease the abundance of senescent-positive cells (Ei et al., 2024), further supporting its potential as an anti-ageing intervention mediated via regulation of senescent cells.

Unlike senomorphics, the aim of senolytics is to selectively induce apoptosis or cell lysis in senescent cells, leading to cell death (Kirkland & Tchkonia, 2020). Notable examples include dasatinib and quercetin (D&Q), fisetin, and navitoclax. Dasatinib, a tyrosine kinase inhibitor initially approved for treatment of chronic myelogenous leukaemia, inhibits BCR-ABL and Src family kinases to induce apoptosis (Schade et al., 2008). Quercetin is a natural flavonoid found in various plants which exhibits antioxidant properties and inhibits the PI3K pathway (Gulati et al., 2006; Zhou et al., 2023). The combination of D&Q has been shown to effectively induce apoptosis in senescent cells *in vitro* (Takaya & Kishi, 2024; Zhao et al., 2025; Zhu et al., 2015). In mouse models, D&Q treatment has improved obesity-induced glucose tolerance and insulin resistance (Palmer et al., 2019; Sierra-Ramirez et al., 2020), ameliorated intervertebral disc degeneration (Novais et al., 2021), and reduced adipose tissue inflammation while improving metabolic function in aged mice (Islam et al., 2023). Currently, D&Q are under investigation in human clinical trials for age-related diseases such as idiopathic pulmonary fibrosis (Justice et al., 2019; Nambiar et al., 2023) and diabetic kidney disease (Hickson et al., 2019). Navitoclax (ABT-263) induces apoptosis in senescent cells *in vitro* by inhibiting anti-apoptotic proteins in the BCL-2 protein family (Zhu et al., 2016) and in *in vivo* mouse models (Gulej et al., 2023; Su et al., 2023). There are associated toxicity issues with navitoclax such as impaired function of bone marrow stromal cells in aged mice (Sharma et al., 2020),

however one study has reported tolerance of navitoclax in aged monkeys alongside reduced neuroinflammation, synaptic dysfunction, senescent cells and SASP expression (Greenberg et al., 2024). Fisetin is a naturally occurring flavonoid present in fruit and vegetables which partially inhibits BCL-2 family proteins leading to apoptosis of senescent cells *in vitro* (Zhu et al., 2017). When fisetin was administered to aged wildtype mice, tissue homeostasis was restored, and median and maximum lifespan was extended (Yousefzadeh et al., 2018). Several clinical trials are scheduled to begin investigating the potential for fisetin use in senescent cell removal and alleviation of age-related diseases (Tavenier et al., 2024). Notably, one clinical trial has observed a reduction in circulating SASP factors and senescent peripheral blood mononuclear cells following fisetin administration (Hambright et al., 2024).

While there are senotherapeutic drugs in human phase clinical trials (Hickson et al., 2019; Justice et al., 2019), there is still a long way to go before any senotherapeutics become routine in clinical practice (Wyld et al., 2020).

1.4 Signalling in cellular senescence.

Senescence is a highly dynamic and metabolically active biological process characterised by permanent cell cycle arrest, a distinct secretory phenotype, and metabolic reprogramming. Senescence is regulated by a complex network of interconnected signalling pathways that collectively contribute to senescence establishment, maintenance, and the impact on the surrounding cellular environment. Key pathways involved include the DNA damage response (DDR), cell cycle regulation, and protein secretion. The intricate crosstalk between these pathways highlights the multifaceted nature of senescence, and understanding the temporal dynamics and regulation of these pathways is crucial for deciphering the role of senescence in human ageing, disease, and for the development of senotherapeutic strategies.

1.4.1 The DNA damage response and cell cycle regulation.

As mentioned, most types of senescence are induced through stimuli which induce genetic damage leading to activation of the DDR. Activation of the DDR results in

one of three outcomes: resolution of the DNA damage and re-entry into the cell cycle, apoptosis, or cellular senescence (**Figure 1.4**).

In brief, when DNA damage occurs, the cell recognises it and activates the protein kinases ataxia-telangiectasia mutated (ATM) and ataxia-telangiectasia and Rad3-related (ATR) (Cimprich & Cortez, 2008; Shiloh, 2003). ATM primarily recognises dsDNA breaks and ATR primarily recognises ssDNA (single strand DNA) (Cimprich & Cortez, 2008; Jazayeri et al., 2006). The activation of ATM and ATR leads to the recruitment of checkpoint kinases (CHK1 and CHK2) (Bartek & Lukas, 2007), which in turn inhibit cyclin dependent kinases (CDKs). CDKs, which include proteins like p53 and p16, are key regulators of the cell cycle. Ultimately, this signalling cascade in response to DNA damage leads to cell cycle arrest providing time for the cell to repair the damaged DNA. However, not all DNA damage is reparable. Because different cell types have varying telomere lengths and erosion rates, cells of different ages and types enter REP at different times, making longitudinal studies of REP particularly challenging.

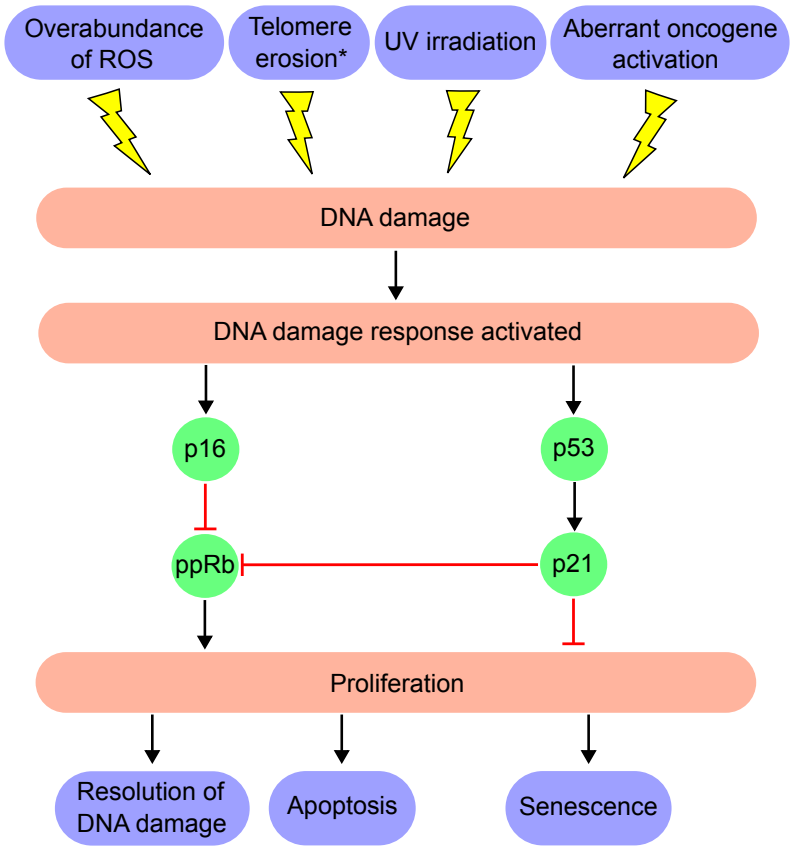

Figure 1.4 – The role of DNA damage in halting cellular proliferation.
*Various stimuli can induce DNA damage. When cells become genetically damaged, the DNA damage response is activated to attempt to repair damaged DNA. If the damage cannot be resolved, then cells will either enter apoptosis or senescence. *When telomere erosion is the cause of genetic damage, the cell cannot resolve the damage unless there is active telomerase.*

In senescent cells, DNA damage is not resolved and persists, leading to the activation of the DDR. When cells experience DNA damage, an early response of the cell is to modify chromatin through the phosphorylation of histone H2AX at ser-139, forming γH2AX foci (Mah et al., 2010). Presence of persistent DNA damage in senescence is supported by experimental data that observe sustained γH2AX foci in senescent cells (Fumagalli et al., 2012; Sedelnikova et al., 2004). There is some evidence that damage within the telomeric region is particularly persistent in senescence (Hewitt et al., 2012). Fumagalli et al. (2012) demonstrated that γH2AX remained in cells for up to 4 months post irradiation at 20 Gy. These γH2AX foci are therefore a marker of senescence as they occur at the beginning of senescence

induction and persist long term. However, γH2AX also occurs in non-senescent cells during cell cycle progression (Turinetto & Giachino, 2015), highlighting the importance of taking a multi-marker approach in identifying senescence.

Activation of the DDR leads to activation of CDK inhibitors and cell cycle arrest. The main pathways inducing cell cycle arrest are the p53/p21 signalling axis, and p16/pRB signalling.

p53 is a tumour suppressor gene and a major transcription factor (TF) often referred to as the “guardian of the genome” due to its critical role in tumour suppression. In normal cellular conditions, p53 protein levels are tightly controlled by negative regulators such as mouse/human double minute 2 (MDM2) (Hunziker et al., 2010; Michael & Oren, 2003). MDM2 promotes p53 degradation through ubiquitination (Michael & Oren, 2003) thereby preventing transcription of p53 target genes. However, upon DNA damage, p53 becomes activated due to inhibition of MDM2, leading to a rapid increase in p53 protein levels. Accumulated p53 is activated and stabilised by post-translational modifications (PTMs) such as phosphorylation (L. Chen et al., 2020; Wang et al., 2023). Stabilised p53 can then form tetramers in the nucleus and bind to target genes leading to activation of the p53 signalling pathway. A key downstream target of p53 is p21. The p53-p21 signalling axis prevents cell cycle progression by inhibiting CDKs and proliferating cell nuclear antigen (PCNA). Upregulation of p53 and p21 is a key phenotype of senescent cells (Herbig et al., 2004; Passos et al., 2010; Waga et al., 1994; Xiong et al., 1993). Additionally, genetic deletion of p21 has been shown to prevent senescence (Brown et al., 1997; Brugarolas et al., 1995), and p21 knockout (KO) *in vivo* resulted in senescence no longer occurring during embryonic development (Muñoz-Espín et al., 2013). Collectively, these studies highlight the importance of the p53-p21 axis in driving cell cycle arrest which is a defining characteristic of cellular senescence.

The p16 and Rb (retinoblastoma) signalling pathway also plays a critical role in inducing cell cycle arrest. When activated by the DDR, p16 binds and inhibits CDK4 and CDK6. This in turn prevents CDK4 and CDK6 phosphorylating Rb. Rb exists in two states: hypophosphorylated (pRB) or hyperphosphorylated (ppRB). In its

hyperphosphorylated state, ppRB is inactive. Inactive ppRB leads to the activation of the TF E2F and resultant transcription of E2F target genes such as DNA polymerase and cyclin E, proteins involved in DNA replication and S-phase entry (Bracken et al., 2004). However, during senescence, p16 is upregulated and activated, leading to the inhibition of CDK4 and CDK6. Without CDK4 and CDK6 activity, Rb is not phosphorylated and exists in its active hypophosphorylated form. pRb binds E2F and prevents transcription of target genes involved in regulating the cell cycle and thus halts cell cycle progression. Moreover, there is growing evidence of p16 interacting with p38 signalling (Kwong et al., 2009; Sun et al., 2007; Wong et al., 2009). p38 is a protein kinase whose activity has been shown to upregulate p16 expression, thus reinforcing the state of cell cycle arrest. Increased p16 expression has been observed with age and multiple age-related diseases such as osteoarthritis and neurodegenerative diseases (Idda et al., 2020). Notably, the role of p16 in senescence has been well studied, particularly in the context of senolytics. Mouse models have been created to investigate senescence, including the INK-ATTAC mouse which selectively removes p16 positive cells upon treatment with drug compound AP20187 (Baker et al., 2016; Baker et al., 2011). Removal of p16-positive senescent cells in INK-ATTAC mice resulted in increased median and maximum lifespan in both male and female mice, and health metrics (such as muscle retention and cataracts) were also improved upon ablation of p16-positive senescent cells.

Thus, p16/Rb signalling and p53 signalling play an important role in the initiation as well as in the maintenance of cellular senescence.

1.4.2 Senescence associated secretory phenotype.

The SASP is involved in numerous non-autonomous processes in senescence including immune clearance of senescent cells (Lujambio, 2016), bystander senescence (Nelson et al., 2018), and autocrine reinforcement of the senescence phenotype *in vitro* (Acosta et al., 2008; Kuilman et al., 2008).

The SASP is traditionally thought to be made up of proteins including cytokines (e.g., IL-6 and IL-8), growth factors (e.g., transforming growth factor beta (TGFβ)), and matrix metalloproteinases (Basisty et al., 2020; Chien et al., 2011; Coppé et al.,

2008). SASP proteins are secreted from the senescent cell and into the surrounding cells and tissues, meaning senescent cells can affect more than just themselves. The SASP can have beneficial or detrimental effects depending on the cellular environment and context. For example, the SASP is involved in signalling to the immune system for clearance of senescent cells (Lujambio, 2016) which is beneficial as senescent cells are then prevented from persisting. Furthermore, the SASP can reinforce the senescent growth arrest *in vitro* (Acosta et al., 2008; Kuilman et al., 2008), and is also essential for embryonic development (Muñoz-Espín et al., 2013; Storer et al., 2013). However, when senescent cells do persist, the SASP can cause chronic inflammatory signalling (Xu et al., 2018) as well as promotion of cancer (Li et al., 2020; Rao & Jackson, 2016; Yoshimoto et al., 2013).

The composition of the SASP can differ depending on the type and stage of cell senescence. For example, in senescence induced via dysfunctional mitochondria, there is the loss of the IL-1α arm of the SASP (Wiley et al., 2016), an otherwise usual element of the SASP in DDIS and OIS. Understanding the differences in SASPs from different types of senescent cells, and how SASP expression changes temporally, would allow for more targeted therapeutics with the aim to modulate the SASP and potentially reduce induction of secondary senescence and inflammatory signalling.

1.4.3 Other signalling pathways in senescence.

While cell cycle arrest and the SASP are key components of cellular senescence, many other pathways and processes have been identified as being involved in senescence. For example, mitochondrial dysfunction and ROS signalling both have been demonstrated as playing a role in senescence induction and maintenance (Davalli et al., 2016; Miwa et al., 2022). Dysfunctional mitochondria have been shown to accumulate during senescence due to impaired mitophagy and mitochondrial biogenesis defects (Correia-Melo et al., 2016; Dalle Pezze et al., 2014; Korolchuk et al., 2017). This leads to an imbalance in mitochondrial dynamics, with increased fission and reduced fusion, resulting in fragmented, damaged mitochondria that contribute to cellular stress. A key consequence of mitochondrial dysfunction is the overproduction of ROS, which can exacerbate DNA damage, activate p53 and p21, and further reinforce the senescence program. Moreover, ROS can amplify SASP

signalling by activating pathways such as NF-κB (Haga & Okada, 2022). ROS signalling has also been implicated in inducing secondary senescence (Nelson et al., 2018).

Beyond mitochondrial dysfunction, many studies have implicated Notch signalling (Hoare et al., 2016; Parry et al., 2018; Teo et al., 2019) and cGAS-STING signalling in senescence (Glück et al., 2017; Gulen et al., 2023; Loo et al., 2020).

Notch signalling is a juxtracrine signalling mechanism involved in various cellular processes including embryogenesis, cell fate specification and proliferation (Balistreri et al., 2016). When a Notch ligand from one cell (such as Jagged-1) binds to a Notch receptor on an adjacent cell, multiple cleavage events of the Notch receptor take place in the receiving cell resulting in the release of the Notch intracellular domain (NICD) into the cell cytoplasm. NICD translocates into the nucleus to enact Notch signalling and transcription of Notch target genes such as *HES1* and *HEY1* (Borggrefe & Oswald, 2009). One study discovered that Notch signalling may act as a temporal regulator of SASP composition through interactions with TGFβ and CCAAT/enhancer binding protein beta (C/EBPβ) (Hoare et al., 2016). More recently, a study demonstrated that Notch signalling mediates juxtracrine secondary senescence in neighbouring cells (Teo et al., 2019). Hoare et al. (2016) described a switch in secretome profile between early and late senescence as being mediated by Notch signalling. During early senescence they observed active Notch signalling and a secretome rich in TGFβ-related proteins, while loss of Notch signalling in late senescence led to a secretome rich in inflammatory-related proteins. This change in Notch signalling activity has been termed the ‘Notch switch’ (Hoare et al., 2016; Hoare & Narita, 2018). Through single cell analysis techniques of hepatocytes from mouse livers, others have found differences in the cell transcriptome between primary and secondary senescent cells, with primary cells having a more C/EBPβ-rich secretome and secondary senescent cells having a more Notch-rich secretome (Teo et al., 2019).

cGAS-STING signalling has recently been highlighted as being involved in senescence (Akbari et al., 2021; Gulen et al., 2017; Yang et al., 2017). This is a

pathway which is evolutionarily conserved across various species and primarily implicated in the innate immune system and the regulation of type I interferons (IFNs) (Hopfner and Hornung, 2020). cGAS-STING signalling has further been linked to other cellular processes such as autophagy regulation, activation of NF-κB (Decout *et al.*, 2021), and senescence (Glück et al., 2017; Gulen et al., 2023). The cGAS (cyclic GMP-AMP synthase) component is a DNA binding protein which binds to free cytoplasmic dsDNA (cytoDNA). CytoDNA can come from foreign sources including viral DNA, or from self-sources such as cytoplasmic chromatin fragments (CCFs). A known correlation exists between age and elevated levels of cytoDNA (Lan *et al.*, 2019), suggesting that cGAS-STING signalling increases with age. When cGAS binds free cytoDNA, cGAS goes through a multistep process to be converted into cyclic GMP-AMP (cGAMP), a cyclic dinucleotide which binds to the STING (stimulator of IFN genes) receptor at the endoplasmic reticulum membrane acting then as the secondary messenger of the cGAS-STING signalling cascade. cGAMP can also fit through gap junctions and enter neighbouring cells to trigger cGAS-STING signalling and prepare neighbouring cells against potential infections (Ablasser et al., 2013). Upon cGAMP binding STING, STING is oligomerised and trafficked to the Golgi, recruiting TBK1. TBK1 becomes active by dimerising and autophosphorylation, leading to STING phosphorylation. In canonical cGAS-STING signalling, IRF3 is recruited and dimerises before translocating into the nucleus to enact target gene transcription of type I IFNs, cytokines such as IL-6 and IL-12 (Decout et al., 2021). NF-κB, which is known to be a major TF driving SASP expression, also plays a role in cGAS-STING signalling. Within the context of cGAS-STING signalling, NF-κB is two-fold as STING can stimulate canonical NF-κB signalling (p50/RelA) and non-canonical NF-κB signalling (p52/RelB) (Abe & Barber, 2014; Hou et al., 2018). Importantly, through NF-κB, cGAS-STING signalling has been found to be involved in the SASP (Loo et al., 2020).

1.4.4 Secondary cellular senescence.

Secondary cellular senescence is not induced from a direct stimulus such as ultraviolet irradiation or oncogene hyperexpression, but rather as a byproduct of primary senescence. There are two subcategories of secondary senescence: juxtacrine bystander senescence and paracrine bystander senescence. Juxtacrine

bystander senescence is induced in a juxtacrine manner between adjacent cells, through signalling pathways such as Notch signalling (Teo et al., 2019). Teo et al. (2019) also observed globally distinct transcriptomes between primary OIS cells and the secondary senescent cells. Paracrine bystander senescence occurs in cells not in the immediate vicinity of the primary senescent cells. Induction of paracrine bystander senescence has been shown to be induced by the SASP (da Silva et al., 2019; Nelson et al., 2012). Some studies have investigated how the depletion of select SASP factors from condition medium (Vassilieva et al., 2020) or inhibition of SASP factor receptors (Acosta et al., 2013; Victorelli et al., 2019) reduces the ability of the SASP to induce secondary senescence. An additional mechanism of paracrine secondary senescence is via ROS and NF-κB signalling, with ROS having been demonstrated as exiting the primary senescent cell and enter neighbouring cells to induce NF-κB activation, leading to SASP induction and consequently senescence induction (Nelson *et al.*, 2018).

Bystander senescence is a biologically significant process with implications in ageing and disease. Unlike primary senescent cells, which directly experience damage, bystander senescence could potentially occur in any cell which is not senescent, even when not in the immediate vicinity of the primary senescent cell. The factors which determine why some cells are more susceptible to secondary senescence, or in fact if all cells are equally susceptible, remains unclear. The spread of secondary senescence contributes to the overall burden of senescent cells. Understanding how bystander senescence is induced, which cells are likely to enter secondary senescence, and the factors which lead to cells being susceptible to induction of secondary senescence will provide deeper insights into human biology. This knowledge could lead to the development of increasingly targeted senotherapeutic strategies (such as treatments which could block non-senescent cells from being susceptible to secondary senescence induction) aimed at reducing the burden of age-related diseases and potentially enhancing both lifespan and healthspan.

1.5 Phenotypes of cellular senescence.

Cellular senescence, as a field of research, has increased rapidly in the past two decades. This was driven in part due to the causal role senescence plays in ageing.

However, while much knowledge has been gained, it has proved difficult to identify a gold standard marker or phenotype which is common to all types of senescence and unique to only senescence. Additionally, the same cell type can present different senescence identities. For example, single cell RNA-seq experiments in WI-38 fibroblasts revealed that the same cell type can enter different senescence programmes following the same induction method (Wechter et al., 2023).

1.5.1 Markers of cellular senescence.

The senescence phenotype is highly heterogenous due to different factors such as mode of senescence induction/entry, cell type, tissue type, and even location of the cell within the tissue. Partly because of the heterogeneity of senescent cells, there is not one specific marker which can identify senescent cells *in vitro* or *in vivo* and multiple markers are required to confirm whether a cell is senescent.

In addition to γH2AX discussed in relation to the DDR above, other common markers used to identify senescent cells include positive senescence associated β-galactosidase (SA-β-gal) staining, increased expression of cell cycle inhibitor proteins such as p16 and p21, and reduced proliferation or replication which can be measured by lower BrdU incorporation into DNA, indicating decreased DNA synthesis. Additional markers of senescence include distinct morphological changes such as enlarged and flattened cell shape, as well as elevated expression of inflammatory proteins. Further markers are detailed in **Figure 1.5**.

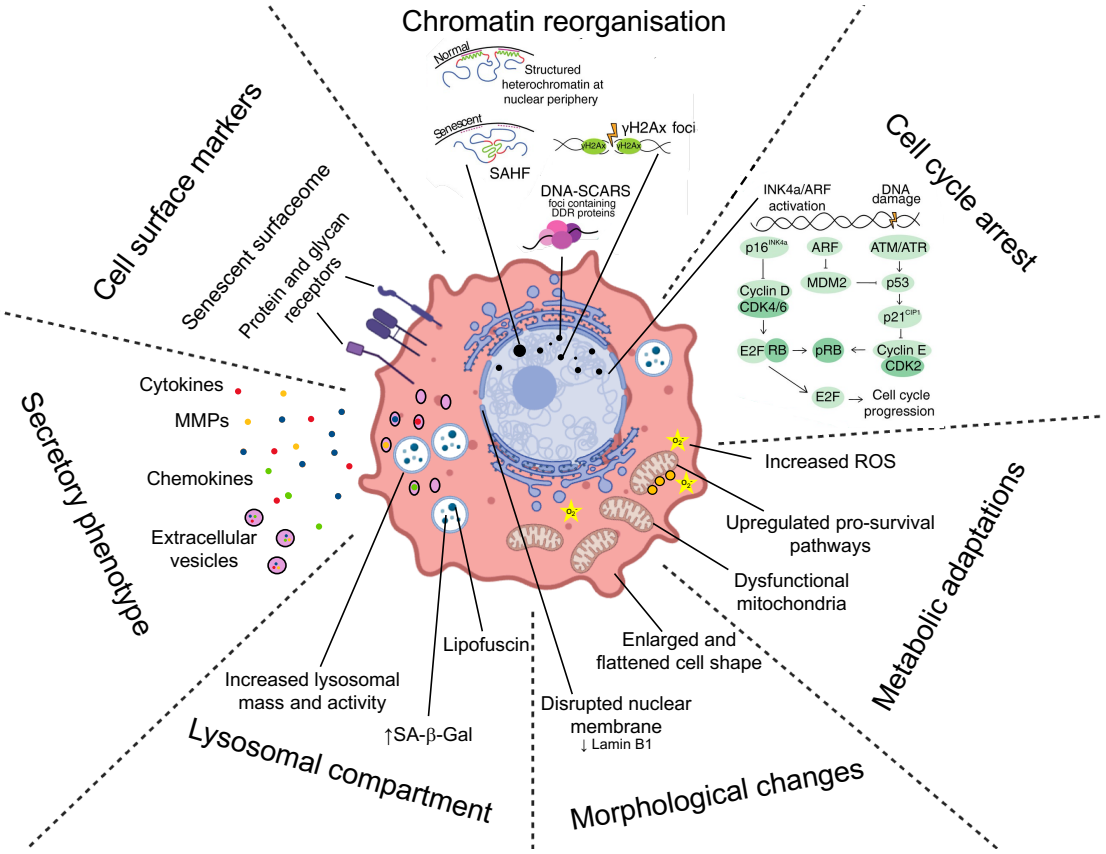

Figure 1.5 – Common markers of cellular senescence.

Adapted from González-Gualda et al. (2021).

Some key markers of senescence are not unique to senescence and can be present in non-senescent cells. For example, β-gal staining is present in some non-senescent cells (Dimri et al., 1995; Going et al., 2002), cell cycle inhibitor proteins are expressed in non-senescent cells (Abbas & Dutta, 2009; Geißler et al., 2013; Witkiewicz et al., 2011), and other cell types experience non-senescent irreversible cell cycle arrest such as post-mitotic neurons. Hence the importance of taking a multi-marker approach to identify senescent cells and the need to identify a specific marker of senescence, such as a gene set (geneset) which is common to many types of senescence, timepoints, and cell types. If a marker, common across all senescent types and unique to only senescence (such as a small set of genes or proteins to test), was identified and introduced as a gold standard for investigating senescence, this would increase the reproducibility and reliability of data, thereby enhancing research into the understanding of senescence.

There is the additional complexity of markers translating from *in vitro* to *in vivo*. For example, it is mentioned above how cell morphology changes are a marker of *in vitro* senescence. However, due to the 3D architecture of tissues and organs, morphology changes are not usually preserved *in vivo*. In addition to senescent cells generally only being present in low numbers in the body (Childs et al., 2015; Idda et al., 2020), a different approach is required when considering *in vivo* senescence as opposed to *in vitro* senescence. While some markers do translate, such as increased expression of p16 and p21, a multi-marker approach is still required. One possibility for assessing *ex vivo* senescence is through flow cytometry, which allows for the simultaneous analysis of multiple markers (González-Gualda et al., 2021). However, this method removes cells from their biological context. Therefore, a possible *in vivo* approach for identifying senescence is the use of a transcriptional signature which can be applied across different types of senescence and cell types.

Multiple studies have attempted to define a core gene signature for the identification of senescent cells (Casella et al., 2019; Hernandez-Segura et al., 2017; Saul et al., 2022). While these studies have provided valuable insights, their findings highlight the complexity and heterogeneity of senescence across different cell types and conditions. Casella et al. (2019) and Hernandez-Segura et al. (2017) conducted transcriptomic analysis in both fibroblast and non-fibroblast cell lines, primarily comparing experimental senescent cells to control proliferating cells. Notably, the gene signature devised by Hernandez-Segura et al. (2017) also compared senescent cells to quiescent cells. More recently, Saul et al. (2022) performed transcriptomic analysis on mouse and human bone marrow samples, comparing senescent cells to proliferating control cells. Individually, these non-systematic studies identified specific genesets they associated with senescence. However, there was minimal overlap between the identified gene signatures, from the genes included to the number of genes identified. These studies highlight the difficulty in determining a core senescence gene signature and illustrate how cell type, senescence type, and even control type can influence the results. Studies like this have demonstrated the intricate nature of senescence and emphasise the need to determine a standardised approach for identification of senescence which can account for differences in senescence type and cell type, as well as have the potential for *in vivo* translation.

1.5.2 Temporal phenotypes of cellular senescence.

Senescent cells are becoming more recognised as distinct from one another. There are many similarities between different types of senescent cells, but the temporal understanding of senescence is far from understood. Many studies investigate only one timepoint, with few studies purposefully investigating the temporal phenotype of senescence. By collating studies investigating different timepoints, the temporal phenotypes of senescence can begin to be investigated.

The strongest temporal evidence regarding senescence is related to SASP composition, first investigated in depth by Coppé et al. (2008) in multiple fibroblast and epithelial cell lines which were either DDIS cells (via irradiation) or OIS cells (via Ras overexpression). This study examined SASP components at multiple time points up to ten days post-senescence induction, revealing that SASP factors, including IL-6 and IL-8, were not expressed until day 7, with a sharp increase by day 10. This finding established that the SASP phenotype was delayed temporally following senescence induction, and has since been corroborated by numerous studies, adding depth to the understanding of SASP dynamics and temporal regulation of it (Freund et al., 2011; Hernandez-Segura et al., 2017; Hoare et al., 2016; Kuilman et al., 2008; Orjalo et al., 2009). Another pivotal study into SASP composition came from Basisty et al. (2020), who performed proteomic analysis of senescent fibroblasts and epithelial cells in various senescence conditions, leading to the creation of the SASP Atlas. This resource contains proteomic data across different senescence conditions, with timepoint of analysis included. For example, there is data for both day 4 and day 7 post-senescence induction in IMR90 fibroblasts induced to senescence via overexpression of Ras (OIS). Beyond generating this publicly accessible proteomic data, the study also identified potential senescence biomarkers which overlap with age markers established in human plasma, including serine protease inhibitors and Growth/differentiation factor 15 (Basisty et al., 2020; Tanaka et al., 2018). However, despite timepoint data being included in the SASP Atlas, there is no emphasis on the temporal evolution of SASP factors, and a comparative analysis was not conducted to see how SASP composition changed between timepoints. This missed opportunity highlights how temporal senescence is still yet to be fully considered or investigated even when the opportunity is available and

reinforces the need for future studies to take a temporal approach to provide a deeper basic understanding of the temporal evolution of senescence.

1.6 Aims.

The aims of this thesis project were:

1. To systematically investigate the literature to create a transcriptomic database relating to cellular senescence in human fibroblasts which contains temporal information. To then explore and utilise this database to elucidate a core signature across types of cellular senescence, cell lines, and sex origin.
2. To explore and utilise the curated database to elucidate a temporal transcriptomic signature in four types of cellular senescence (DDIS, OIS, REP, and BYS), assessing how and whether transcriptomic signatures are unique at different timepoints post-senescence induction.
3. To determine temporal protein phenotypes of cellular senescence in human fibroblasts and computationally model temporal protein changes in DDIS and OIS, including the impact of knockdown interventions. This work will be integrated with the transcriptomic analysis to determine how well different macromolecules translate to one another.
4. Create a future analysis framework to aid in furthering the understanding of biological processes such as cellular senescence, using a KEGG-based analysis approach to visualise whole pathways. This approach will facilitate identification of pathway-wide changes such as in p53 signalling and the inflammatory response.

Chapter 2: Methods.

2.1 Formation of a transcriptomic database of senescent human fibroblasts.

As detailed in **Chapter 1**, understanding the temporal nature of any biological process is important as no biological process is static. Specifically, understanding the basic biology of cellular senescence and how the senescence profile changes temporally is essential given the potential of translational clinical work based on the removal of senescent cells to reduce disease burden (Suda et al., 2025). To begin investigating the temporal profile of human fibroblast senescence, a transcriptomic database was formed of relevant publicly available data for analysis.

All analysis was performed in R version 4.3.0 (R core team, 2023).

2.1.1 Systematic analysis of publicly available data.

Search terms were devised for searching for datasets on **Gene Expression Omnibus** (GEO) and **BioStudies** (formerly ArrayExpress). Each database required a different set of search terms, although there was overlap between studies published on both sites.

The search terms for the smaller BioStudies database were ‘Ageing’ OR ‘Aging’. Once these search terms were applied, the database results were manually filtered.

As GEO is a larger database, specific terms were designed to include relevant MeSH terms and text terms. Initial terms were used in combinations on PubMed PubReMiner (Slater, 2014) to identify additional search terms. Search terms were then inputted in GEO and combined utilising the Advanced Search tool. Search terms and results for GEO are detailed in **Table 2.1**.

Table 2.1 – Systematic search terms and results for GEO.

To select for studies including fibroblasts:		**Number of results per search date:**		
		10 August 2020	06 July 2022	05 October 2023
1	Fibroblasts[MeSH Terms]	100737	149141	167132
2	*fibroblast	100737	149141	167132
3	*fibroblasts	100737	149141	167132
4	“HCA2” OR “HCA” OR “HFF” OR “HFFF” OR “HFFF2” OR “WS1” or “Tig3”	2892	5432	6130
5	“BJ” OR “MRC5” OR “MRC-5” “WI-38” OR “WI38” OR “NHF” OR “NHDF”	1381	1974	2089
6	“IMR90” OR “IMR-90”	8116	9349	9969
7	#1 OR #2 OR #3 OR #4 OR #5 OR #6	106137	157313	175870
To select for studies looking at cellular senescence:				
8	senesce*	5395	10037	11891
9	senescing	80	84	87
10	Cellular Senescence[MeSH Terms]	0	0	0
11	Aging[MeSH Terms]	11870	17857	21258
12	Ageing	11870	17857	21258
13	aging	11870	17857	21258
14	Arrest*	12583	18586	22443
15	“young” AND “old”	9845	15392	17588
16	#8 OR #9 OR #10 OR #11 OR #12 OR #13 OR #14 OR #15	32195	51897	61202
To combine:				
17	#7 AND #16	5063	6175	7281

Taken from Scanlan et al. (2024).

In addition to the search terms for each database, specific inclusion and exclusion criteria were applied to filter the data so only relevant studies were included in the

database. Inclusion criteria applied to both databases, outside of the search terms, were:

- The dataset represented unbiased transcriptomic data for senescent human fibroblasts – where senescence was defined by permanent cell cycle arrest induced by a stimulus in cells that would otherwise be proliferating.
- RNAseq or microarray datasets were stored on GEO (Edgar et al., 2002) or BioStudies (Parkinson et al., 2007) by the deadline date of 05 October 2023.
- There were at least two repeats for all conditions included in a dataset.

Some datasets met the inclusion criteria but could not be analysed by the methods in this thesis. Therefore, exclusion criteria were:

- If datasets were microRNA, long non-coding RNA, or scRNAseq.
- If microarrays were two-colour or custom microarrays.
- Data could not be downloaded from GEO or BioStudies, nor could it be provided when contacting the corresponding author before the deadline date.

The systematic searches were performed independently three times by two individuals. On each occasion the results were compared between individuals to ensure all datasets were identified. The first occasion was on 10 August 2020, the second on 06 July 2022, and the final occasion on 05 October 2023 (**Figure 2.1**). As of the final systematic review, the database created (referred to as SenOmic from here onwards) includes 119 datasets, 14 uniquely induced types of cellular senescence, and 17 human fibroblast cell lines. The main categories can be found detailed in **Appendix Table A2.1**.

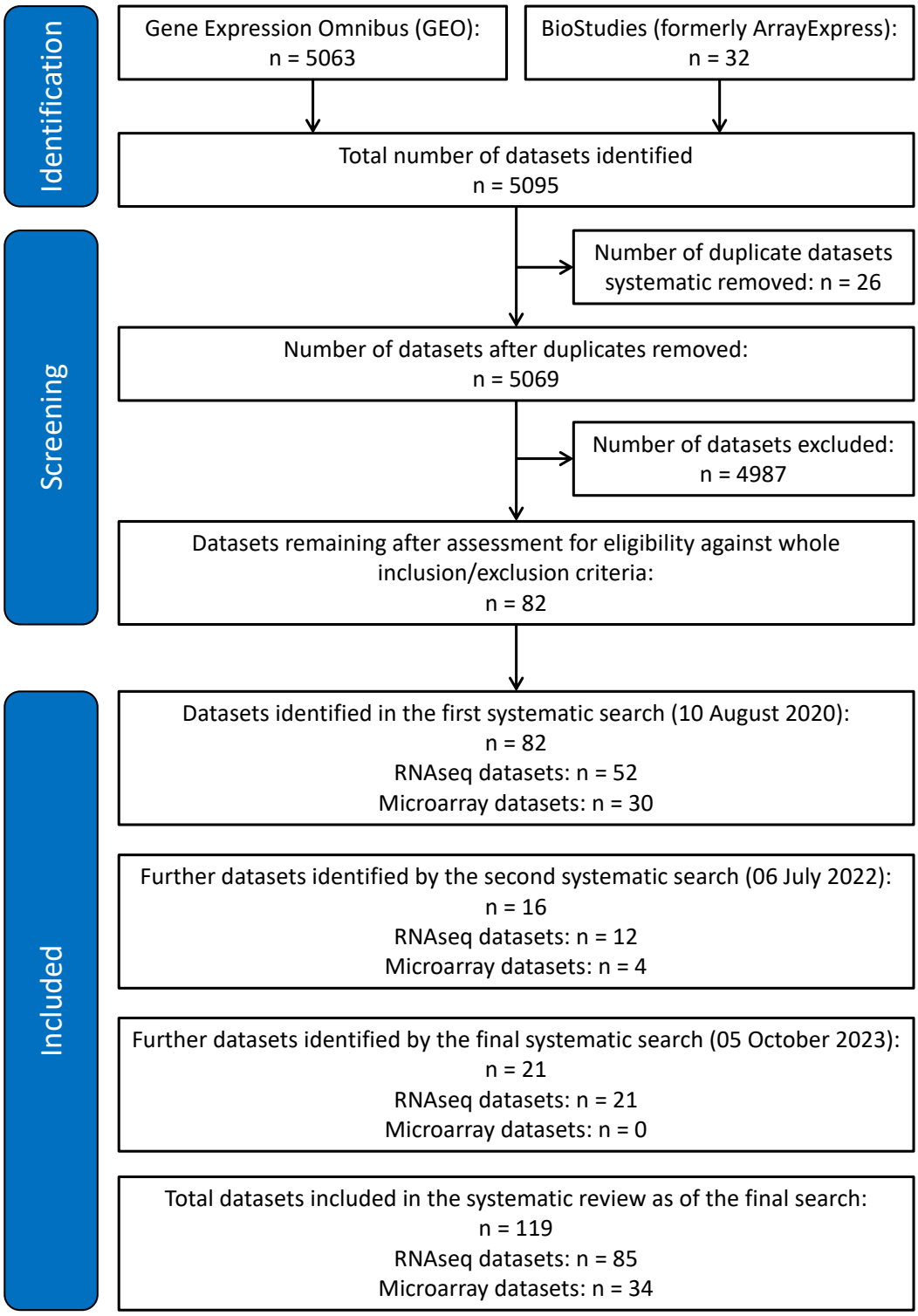

Figure 2.1 – PRISMA flowchart showing identification and exclusion of studies.

Taken from Scanlan et al. (2024).

2.1.2 Processing data and creating the SenOmic database.

For each identified dataset, a comparison matrix which detailed data of interest was constructed in Microsoft Excel and saved as a .csv file. If data of interest was not available on GEO or BioStudies, and the datasets had accompanying publications, papers were checked for missing data. Key data such as senescence type and cell line were available for all datasets; however, in some cases, the timepoint of senescence induction was not stated in the paper or online databases. As this was a key part of constructing a temporal senescence profile, we contacted the corresponding author, but did not do so for any other missing categories. As in **Table 2.2**, a comparison matrix contains all possible relevant information for the dataset and compares samples. The column titled 'X' contains the label for sample comparison. For example, 'D_P' denotes the experimental DDIS sample compared to the control proliferating sample. Completed comparison matrices were combined into a single searchable database in R version 4.3.0 (R core team, 2023).

For downloading and processing both RNAseq and microarray data, the below methods were followed. For specific code details refer to the list of files in the README.md in the following GitHub repository:
https://github.com/rlscanlan/Thesis

For RNAseq datasets, data was downloaded as fastq files from GEO or BioStudies. In R, each file underwent a quality check using the fastqcr R package (de Sena Brandine & Smith, 2019). Moving to the terminal, in a python environment, files were compared using the MultiQC BASH command (Ewels et al., 2016). Continuing in the terminal python environment, adapter trimming and removal of low-quality read ends was carried out using the Cutadapt tool with a Phred score threshold of 25 (Martin, 2011). Once files passed or failed fastqc, the passed files were converted by mapping-based quantification to quant.sf files using Salmon (version 1.1.0) (Patro et al., 2017). To remove additional biases, the –gcBias --seqBias and
-- validateMappings options were used.

For microarray datasets, series matrix files were downloaded from GEO and loaded into R using GEOquery (Davis & Meltzer, 2007), before conversion to esets and

labelling with normalisation and processing information. BioStudies raw data sets were downloaded, and robust multiarray average normalised using affy (Gautier et al., 2004).

Quant.sf files and microarray data underwent differential expression analysis using the R limma package (Ritchie et al., 2015). Data were normalised by cpm or voom commands depending on variance, and plotDensities was used to compare sample curves. Samples with irregular curves not consistent with the rest of the data were removed from further analysis. Log2 fold change (LogFC) and p-values were calculated for each comparison defined in the comparison matrix using the eBayes function before finally being combined into one single database.

Additional new data was identified with the second and third systematic review (**Figure 2.1**). Data was downloaded, processed, and combined with the prior version of the database as described above.

The SenOmic database currently contains 49 variables and 13,248,345 observations. The 49 variables, of which not all have data for, are detailed in **Table 2.2**.

Table 2.2 – Comparison matrix for dataset GSE189789.

X	Cell_line	PD	Study	Treatment	SENvCON	Sen_type
D_P	WI38	NA	An	none	Yes	DDIS
Doridonin_P	WI38	NA	An	Oridonin	Yes	DDIS
Doridonin_D	WI38	NA	An	Oridonin	No	DDIS
Sen_subtype	Subtype_ subtype	Radiation_ dose	Control_ condition	Control_specifics	Control_PD	Control_type
Doxorubicin	Doxorubicin	1μM_12hrs	Prolif	Prolif	NA	Prolif
Doxorubicin	Doxorubicin	1μM_12hrs	Prolif	Prolif	NA	Prolif
Doxorubicin	Doxorubicin	1μM_12hrs	DDIS	Doxorubicin_1μM_12 hrs	NA	DDIS
Control_ subtype	Control_gene_ up	Control_gene_ down	Control_time (days, d)	Time_after_ induction (days, d)	Treatment_ dose	Quiesce_inducer
Prolif	none	none	2.5d	2.5d	NA	NA
Prolif	none	none	2.5d	2.5d	2μM_48hr	NA
Dox	none	none	2.5d	2.5d	2μM_48hr	NA
Disease	Organ	Gene_down	Gene_up	Immortal_line	Immortal_ mechanism	RNAseq_Microarra y
none	Lung	none	none	NA	NA	R
none	Lung	none	none	NA	NA	R

none	Lung	none	none	NA	NA	R
Seq_platform	Single_ Paired	Spot_length	X1or2_colour	Array_type	Pre_SASP_t	ENA_acc
Illumina_HiSeq_2000	Paired	150	NA	NA	Yes	PRJNA784535
Illumina_HiSeq_2000	Paired	150	NA	NA	Yes	PRJNA784535
Illumina_HiSeq_2000	Paired	150	NA	NA	Yes	PRJNA784535
Acc_no	Species	Replicates	Oxygen	CO2	FBS	P_S
GSE189789	Human	3	NA	5%	10%	NA
GSE189789	Human	3	NA	5%	10%	NA
GSE189789	Human	3	NA	5%	10%	NA

The 49 headings detailed here are the 49 variables in SenOmic. Produced as part of the Scanlan et al. (2024) study but not published. DDIS, DNA damage-induced senescence.

2.1.3 Hosting the SenOmic database online.

The size of the database was limiting for online hosting. Therefore, the database was reduced from 49 to 21 variables to allow for easier uploading and accessibility online. Columns which were believed to not impact the outcome of the analysis were removed, such as Oxygen (the oxygen levels cells were grown at) and RNAseq_Microarray (which detailed whether the data was obtain via RNAseq (R) or microarray (M)).

The remaining columns of interest were: Acc_no; Sen_type; Control_type; Gene; LogFC; Pvalues; Sen_subtype; Control_subtype; numeric_time; Cell_line; Treatment; Gene_up; Gene_down; Control_Gene_up; Control_gene_down; PD; Control_PD; Immortal_line; Disease; Organ; SENvCON.

The reduced database was transformed into a Microsoft Power BI report with the aid of Hannah O'Keefe. The Power BI report allows users to access various clusters of the data in easily readable visuals (**Figure 2.2**). Data clusters are accessible by either button or slider selection, with a total of 13 different filters provided to allow users to explore the data. To build the report, Power BI basic functions and DAX programming language were used; specifically, DAX programming language was used to create measures which control the filtering selections such as p-value. The Power BI report is embedded via an iframe in a **Newcastle University research website**.

To update the SenOmic website database with any future systematic reviews or further relevant data identified, it only requires uploading the database file in the correct naming format in our Senescence Microsoft Teams folder which various users have access to and can be invited to.

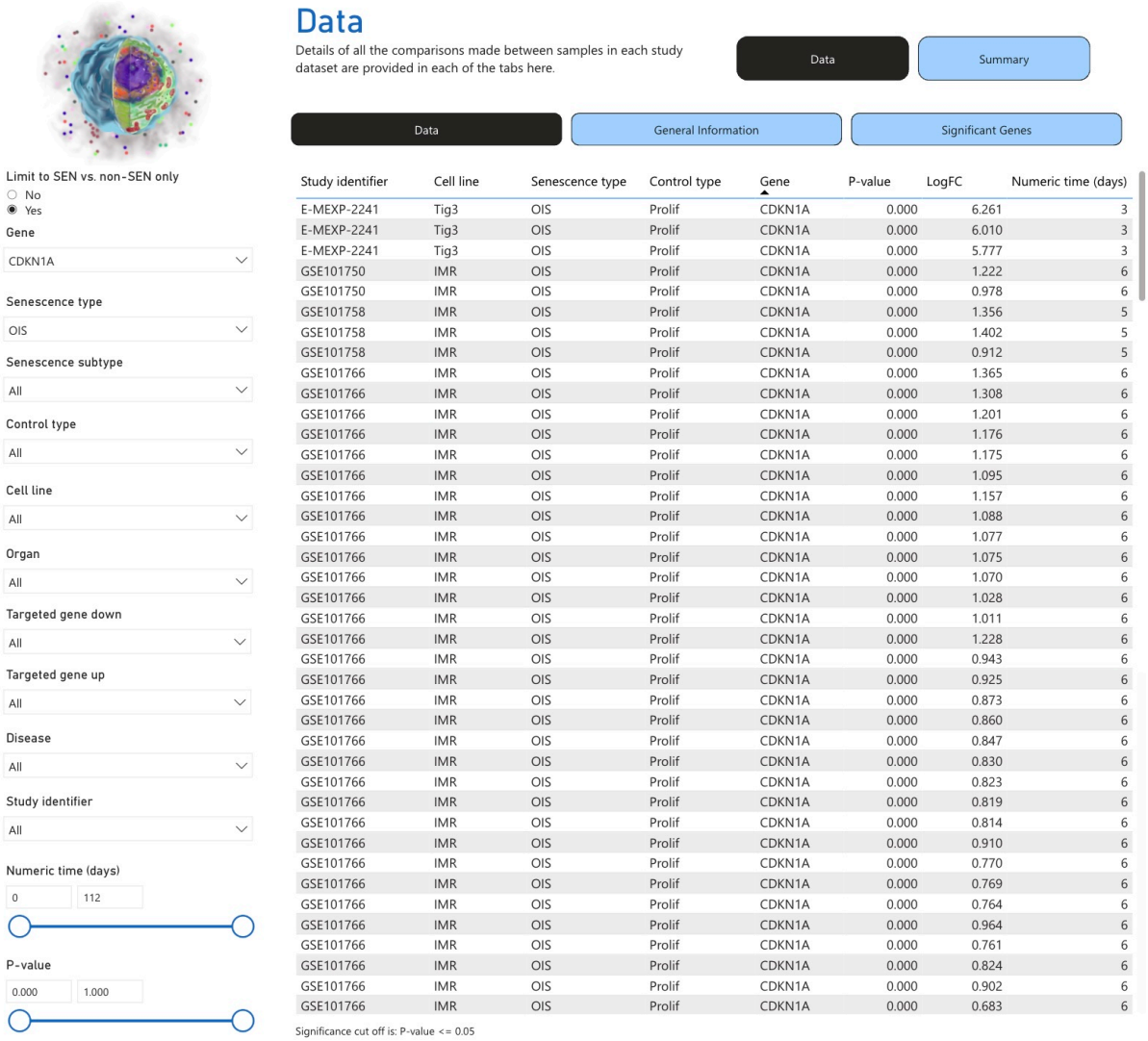

Figure 2.2 – SenOmic database hosted online.

Filters applied here are SEN vs non-SEN is 'Yes', the gene of interest is 'CDKN1A', and oncogene-induced senescence is the senescence type of interest.

2.2 Analysis of SenOmic.

Various types of analysis were performed on the data contained in SenOmic, detailed below. For the majority of the SenOmic analysis in this thesis, unless specifically stated, an interquartile range (IQR) was applied to data.

2.2.1 Removal of outliers using an interquartile range.

Outliers were initially identified due to the maximum LogFC in SenOmic being 151148.7 and the minimum LogFC being -151593. Both values originated from the same study (dataset GSE178115 (Yang et al., 2022)) and represent highly irregular

LogFC values. Additionally, following principal component analysis (PCA) on SenOmic without outlier removal, it became evident that outliers were skewing results and would likely bias any further analysis (discussed in **Section 2.2.2** in more detail). To prevent skewing of analysis, outliers were removed using an IQR filtering method. The IQR is the range between the first quartile (Q1 or 25th percentile) and the third quartile (Q3, or 75th percentile), representing the middle 50% of data. Outliers were defined as anything less than $Q1 - 1.5 \times IQR$ or greater than $Q3 + 1.5 \times IQR$. Applying this method removes extreme values outside of the typical spread of data, minimising the effect of outliers on analysis and producing more robust results. Other than select data presented in **Section 2.2.2**, all data analysed in this thesis underwent this IQR filtering method.

For the analysis performed in **Chapter 3**, the IQR was calculated for each gene per senescence type; for temporal analysis in **Chapter 4** the IQR was calculated for each gene in each senescence type per time_group. This is the method utilised in Scanlan et al. (2024).

2.2.2 Optimising and performing principal component analysis.

When transforming the SenOmic data.frame (referred to as 'total_data' from here onwards) into a data.matrix for PCA, it became apparent that although each dataset is bulk RNAseq data, not every type of analysis was made equal; meaning not all genes were tested in every dataset. Of the 27086 unique genes tested in total, 1031 genes appeared only once in all SenOmic; for example, *TAGLN2P1* was present in only 1 of the 1069 comparisons (GSE175686 (Barnes et al., 2022)), with even a gene as common as *TP53* missing from 5 of the comparisons. Therefore, when using the pivot_wider function from the tidyr library (Wickham *et al*., 2024) to transform the data into the correct format for PCA, the data became overwhelmingly full of missing (NA) values. Due to the introduction of a large proportion of NA data when transforming total_data into a data.matrix, PCA needed to be optimised. Four methods were explored (referred to as PCA Methods 1-4).

PCA Method 1 involved using the prcomp function which is included in base R as part of the stats library (R core team, 2023). prcomp is one of the common PCA

methods in R and uses the singular value decomposition method which cannot handle missing data well. When converting the total_data data.frame into a data.matrix, 54.245% of data had NA values. One option to overcome this is to use na.omit (a function which is part of the base R stats library). However, when performing na.omit with prcomp on the total_data data.matrix with **Code 2.1**, R was unable handle the amount of missing values and data, giving the error code '*Error in svd(x, nu = 0, nv = k) : a dimension is zero)*'.

Code 2.1.

```
Sen.pca = prcomp(na.omit(c[c(3:27088)], center = TRUE, scale.
= TRUE)
```

This code uses prcomp in conjunction with na.omit to perform PCA. Extracted from GitHub file Thesis.R, line 159.

Another option would be to impute values for all NA values. This approach would involve estimating values for over 50% of the data which would be a complex undertaking due to the nature of the data. The data.matrix is made up of LogFC values and therefore there is the argument that 0 could be imputed for all NA values as a LogFC value of 0 would represent no change in expression between the experimental and control sample. However, this method increases the risk of artificial patterns and biases which can skew and distort data.

To optimise and curate the best PCA method for the SenOmic database, various options were considered. PCA Method 1 involved imputing all NA values to equal 0 followed by employing the prcomp method (**Figure 2.3**). While a PCA plot was visualised, the first two principal components (PCs) account for just less than 40% of the total variance in the data. Although it is evident there are some data outliers within the 1069 datasets represented on the PCA plot, the majority of data cannot be distinctly visualised due to the overlap and disproportionate axes scaling. Therefore, moving forward prcomp was not considered for PCA of SenOmic.

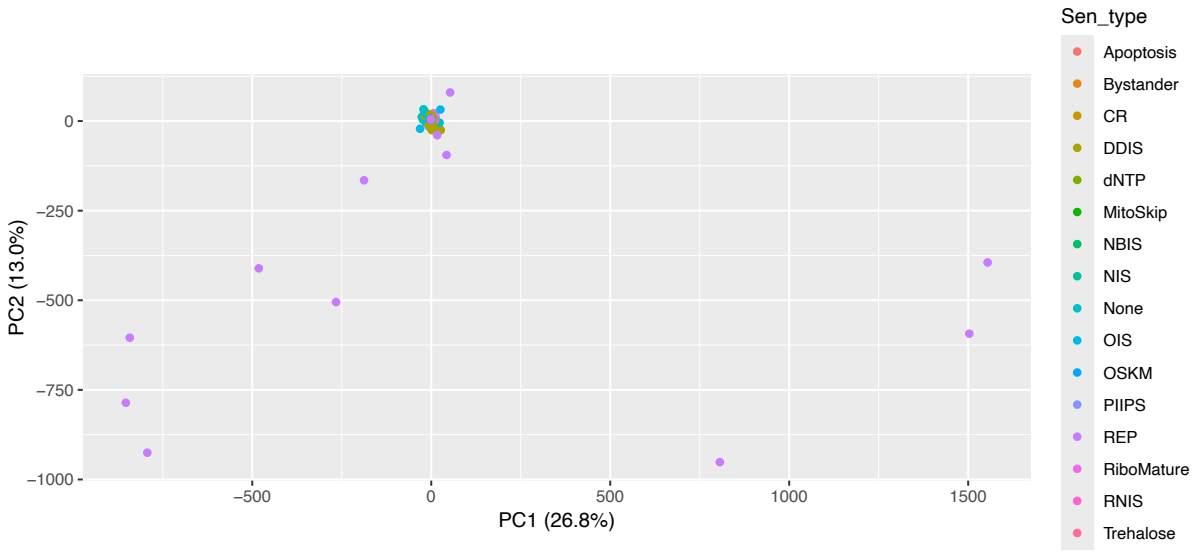

Figure 2.3 – PCA of total_data using PCA Method 1.

PCA produced using prcomp on total_data without IQR filtering when missing data was imputed to equal 0.

Instead of the base R prcomp function to conduct PCA, the pcaMethods library (Stacklies et al., 2007) was consulted. pcaMethods contains many approaches to performing PCA. Of interest was the non-linear iterative partial least squares (NIPALS) method which can deal with missing data by excluding missing values from the appropriate inner products. For PCA Methods 2-4, the NIPALS method from pcaMethods was employed. The number of PCs to be investigated can be selected for in the NIPALS method. To optimise PCA in this thesis, NIPALS was performed with nPCs = 2, nPCs = 5, and nPCs = 15 for all data during optimisation.

PCA Method 2 used the same data as in PCA Method 1, and PCA was performed using the NIPALS method from pcaMethods (**Figure 2.4**). The total amount of data variance explained by the PCs (indicated by the cumulative R2 x 100) increases with the number of PCs investigated: 77.8% with 2 PCs (**Figure 2.4A**); 90.72% with 5 PCs (**Figure 2.4B**); 97.62% with 15 PCs (**Figure 2.4C**). These values represent a substantial improvement over the less than 40% of variance explained when using the previously discussed PCA Method 1. Furthermore, the variance of data covered by the first two PCs increases to 78.23% when nPCs = 5 or nPCs = 15, demonstrating that investigating a higher number of PCs produces more reliable data

but that 5 PCs appears sufficient for analysis. The variance explained using NIPALS, even with 54.245% of data missing, illustrates the importance of optimising a PCA method to effectively deal with specific types of data.

Figure 2.4 – PCA of total_data using PCA Method 2.

PCA using the NIPALS method from the pcaMethods library on total_data without IQR filtering. This method was performed with 2 PCs (A), 5 PCs (B), and 15 PCs (C).

While there were differences in variance of data covered by the PCs, there were limited visual differences when plotting the PCA. There were 1069 datapoints represented on each PCA plot, and the majority of them overlapped in the top left of the plot – an issue which also arose when using PCA Method 1 (**Figure 2.3**). Due to most data overlapping and disproportionate axes scaling, it was difficult to identify any visual differences. There was a slight difference in position of two points when nPCs = 2 compared to nPCs = 5 or nPCs = 15 (**Figure 2.4**), encircled in red. While there was likely more than just this difference, it was difficult to identify any. Additionally, clustering based on senescence type cannot be observed with this lack of clarity. As discussed, there was a large amount of overlap on the PCA plot and disproportionate axes scaling which was due to outlier data and a lack of optimisation of the PCA method.

While the NIPALS method can tolerate some missing data in a data.matrix it can typically only tolerate up to 5%, and 54.245% data was missing in this analysis. Therefore, two further options were explored to optimise PCA: (i) PCA Method 3 – missing data was imputed to equal 0 as in PCA Method 1, and then NIPALS performed with nPCs = 2, nPCs = 5, and nPCs = 15 on total_data with no IQR filtering (**Figure 2.5**) and with IQR filtering (**Figure 2.6**); (ii) PCA Method 4 – columns of data where more than 50% of values were missing, meaning that specific gene did not have LogFC expression for over 50% of the comparisons, were removed in total_data without IQR filtering (**Figure 2.7**), and total_data with IQR filtering (**Figure 2.8**).

For PCA Method 3, missing LogFC data was imputed to equal 0 to investigate if showing no expression change between experimental and control samples would result in appropriate results. Imputing NA to equal 0 reduced the percentage of missing data to 0% as expected. The NIPALS method was performed for nPCs = 2, nPCs = 5, and nPCs = 15, and demonstrated that when there was no IQR filtering (**Figure 2.5**) or there was IQR filtering (**Figure 2.6**) that the axes were still disproportionate, even when there were less data points after IQR filtering.


```
nipals calculated PCA
Importance of component(s):
                  PC1    PC2
R2            0.6427 0.1393
Cumulative R2 0.6427 0.7819
27086   Variables
1069    Samples
0       NAs ( 0 %)
2       Calculated component(s)
```

```
nipals calculated PCA
Importance of component(s):
                  PC1    PC2     PC3     PC4     PC5
R2            0.6425 0.1394 0.06191 0.03976 0.02346
Cumulative R2 0.6425 0.7819 0.84377 0.88353 0.90700
27086   Variables
1069    Samples
0       NAs ( 0 %)
5       Calculated component(s)
```

```
nipals calculated PCA
Importance of component(s):
                  PC1    PC2     PC3     PC4     PC5
R2            0.6425 0.1394 0.06191 0.03976 0.02346
Cumulative R2 0.6425 0.7819 0.84377 0.88353 0.90700
                  PC6     PC7     PC8     PC9     PC10
R2            0.01233 0.01093 0.009405 0.008261 0.006211
Cumulative R2 0.91933 0.93026 0.939665 0.947926 0.954137
                 PC11    PC12    PC13    PC14    PC15
R2            0.006051 0.00504 0.004253 0.003659 0.003171
Cumulative R2 0.960188 0.96523 0.969481 0.973140 0.976311
27086   Variables
1069    Samples
0       NAs ( 0 %)
15      Calculated component(s)
```

Figure 2.5 – PCA of total_data using PCA Method 3.

PCA using the NIPALS method from the pcaMethods library on total_data without IQR filtering when missing data was imputed to equal 0. This method was performed with 2 PCs (A), 5 PCs (B), and 15 PCs (C).

The first two PCs accounted for 78.195% of the variance when there had been no IQR filtering (**Figure 2.5**), but interestingly less variance was accounted for after IQR

filtering albeit not by much (76.53-76.6% – **Figure 2.6**). There were some clear differences in plotting depending on whether the data have been IQR filtered or not, namely the axes limits were smaller after filtering and there were less datapoints plotted, but the trends of the remaining Sen_type remain similar. For example, trehalose (coloured in **pink**) is explained more by PC2 than PC1 in both plots.

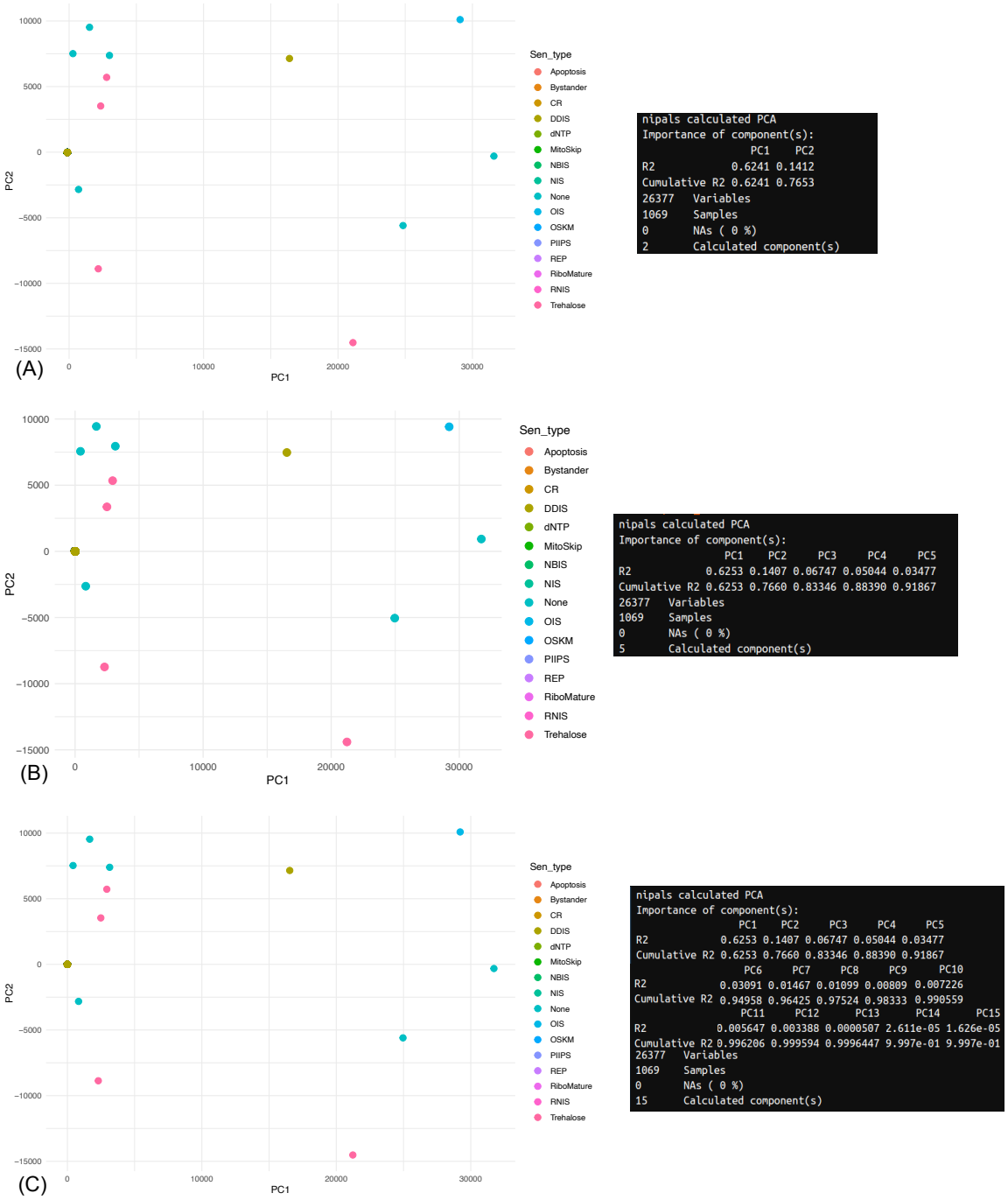

Figure 2.6 – PCA of IQR filtered total_data using PCA Method 3.

PCA using the NIPALS method from the pcaMethods library on total_data with IQR filtering when missing data was imputed to equal 0. This method was performed with 2 PCs (A), 5 PCs (B), and 15 PCs (C).

PCA Method 3 still produced results which were unable to be effectively visualised, and the method potentially introduced biases to the data. Therefore, PCA Method 4 was devised. Using **Code 2.2** the threshold for missing data per column was set to

50%. If more than 50% of the data for each column (gene) was missing, then that column was removed from the data.frame, in this case total_data without IQR filtering (**Figure 2.7**) and with IQR filtering (**Figure 2.8**).

Code 2.2.

```
Threshold = 0.5
new_df = c[, colMeans(is.na(c)) <= threshold]
cols_to_keep = colMeans(is.na(c)) <= threshold
df_kept = c[, cols_to_keep]
```

Removal of columns when gene LogFC expression data was missing for over 50% of comparisons. Extracted from GitHub file Thesis.R, lines 330-334.

Performing PCA Method 4 without IQR filtering visually produced plots similar to previous methods, however importantly the percentage of missing data was dropped to 2.838% (**Figure 2.7**) which the NIPALS method can effectively handle. Additionally, 78.6% of data variance was explained by PC1 and PC2. Despite these positive outputs, the visual output remained equally unreadable due to overlap and disproportionate axes scaling.

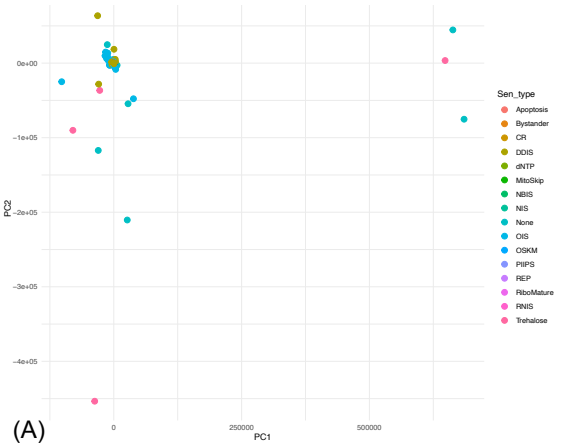

(A)

```
nipals calculated PCA
Importance of component(s):
                  PC1    PC2
R2            0.6462 0.1398
Cumulative R2 0.6462 0.7860
12378   Variables
1069    Samples
375533  NAs ( 2.838 %)
2       Calculated component(s)
```

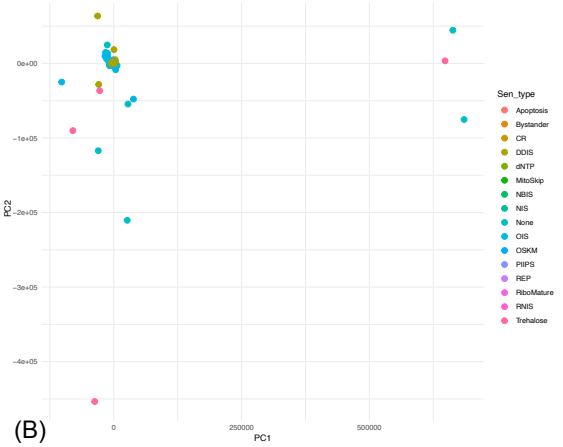

(B)

```
nipals calculated PCA
Importance of component(s):
                  PC1    PC2     PC3     PC4     PC5
R2            0.646 0.1399 0.05292 0.04231 0.02348
Cumulative R2 0.646 0.7859 0.83881 0.88112 0.90460
12378   Variables
1069    Samples
375533  NAs ( 2.838 %)
5       Calculated component(s)
```

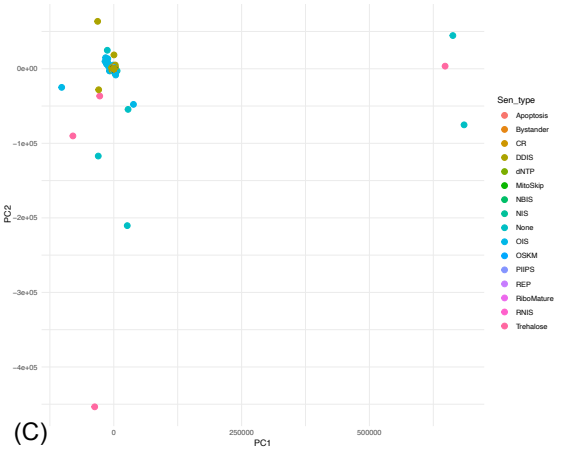

(C)

```
nipals calculated PCA
Importance of component(s):
                  PC1    PC2     PC3     PC4     PC5
R2            0.646 0.1399 0.05292 0.04231 0.02348
Cumulative R2 0.646 0.7859 0.83881 0.88112 0.90460
                  PC6    PC7     PC8     PC9    PC10
R2            0.01317 0.0112 0.009775 0.008131 0.006629
Cumulative R2 0.91777 0.9290 0.938750 0.946881 0.953510
                 PC11     PC12     PC13     PC14     PC15
R2            0.006421 0.005352 0.003872 0.003389 0.003178
Cumulative R2 0.959931 0.965283 0.969155 0.972544 0.975722
12378   Variables
1069    Samples
375533  NAs ( 2.838 %)
15      Calculated component(s)
```

Figure 2.7 – PCA of total_data using PCA Method 4.

PCA using the NIPALS method from the pcaMethods library on total_data without IQR filtering when genes which had data missing for more than 50% of comparisons were removed. This method was performed with 2 PCs (A), 5 PCs (B), and 15 PCs (C).

IQR filtering was performed on total_data and PCA Method 4 carried out. This resulted in a total of 17.255% missing data and the first two PCs accounting for a maximum of only 23.402% of data variance (**Figure 2.8**). While the amount of missing data was much lower than PCA Method 2 which investigated data which had also undergone IQR filtering, it accounted for much less of the data variance (**Figure 2.4**). When comparing PCA Method 4 between non-IQR filtered and IQR filtered data, the statistics clearly indicate that removal of outliers increased variation within the dataset. This suggests that outliers were heavily influencing the data variation. This observation is further supported in the PCA visualisation as after IQR filtering the axes were no longer disproportionate. While distinct clustering was still difficult to discern, individual datapoints became more distinguishable (**Figure 2.8**).

Figure 2.8 – PCA of IQR filtered total_data using PCA Method 4.

PCA using the NIPALS method from the pcaMethods library on total_data with IQR filtering when genes which had data missing for more than 50% of comparisons were removed. This method was performed with 2 PCs (A), 5 PCs (B), and 15 PCs (C).

Regardless of the PCA Method utilised, finding any trends in Sen_type was difficult due to the sheer volume of data that was plotted. Additionally, many of the colours were very similar for different Sen_types; in the future, specifying more distinct colours would allow for better visualisation. Additionally, while nPCs = 15 produced data which more accurately explained the variance in data, it also required a higher computing power. When typically compared to nPCs = 5, the amount of variance explained by the first 2 PCs is similar if not exactly the same, therefore it was practical to continue with nPCs = 5 as this takes less computational power while producing likewise data.

While numerous methods were explored here, it is favourable to first not remove data. However, when there is such a large amount of missing data (as there was in data.matrix of total_data), there were only two suitable options: impute the missing data, or remove columns which had a large percentage of missing data. While imputation of missing data can be reliable if estimations are used, with such a large amount of data missing it was deemed unsuitable. Likewise, while imputing missing data to equal 0 meant there was no missing data in the data.matrix, assuming over 50% of the data was equal to the same value is an unsuitable approach.

Therefore, the two preferred PCA methods are PCA Method 2 followed by PCA Method 4. This is because PCA Method 2 does not impute or remove any data. However, when there is a large percentage of missing values an alternative approach (PCA Method 4) needs to be taken. In summary, the data should determine which method is applied.

PCA was not performed as part of the Scanlan et al. (2024) study and is only reported in this thesis.

2.2.3 Venn diagrams, heatmaps and gene set enrichment analysis.

Using the formula in **Equation 1**, the p-value was inverted for some analyses to create the p_i value. The p_i value variable was named ‘MegaP’ and is referred to as MegaP throughout this thesis. Combining the p-value and LogFC into a singular value as done here is not a new method in bioinformatics (Xiao et al., 2014). Using a

MegaP value created a scale which put p-values for significant upregulation at the opposite end of the scale to p-values for significant downregulation, with non-significant values in the middle.

$$p_i = \frac{1}{p} \times \frac{LogFC}{|LogFC|} \qquad \textbf{Equation 1}$$

Inclusion of only significantly expressed data based on the MegaP value was achieved through **Code 2.3**. A MegaP value of 20 represents a positive LogFC value with a p-value of 0.05, and a MegaP value of -20 represents a negative LogFC with a p-value of 0.05.

Code 2.3.

```
SigDDISGenes = DDIS_T4 %>%
  mutate(Significant_MegaP = case_when(
    MedianMegaP <= -20 ~ 'Yes',
    MedianMegaP >= 20 ~ 'Yes',
    TRUE ~ 'No'
  ))
```

Example code used to select only significantly expressed genes based on MegaP value. Extracted from GitHub file Thesis.R, lines 1562-1567.

The R library VennDiagram was used to plot both pairwise (using the draw.pairwise.venn function) and four-set (using the draw.quad.venn function) Venn diagrams (Chen & Boutros, 2011).

Heatmap analysis was performed using the heatmap.2 function from the gplots library (Warnes et al., 2022).

Over-representation analysis (ORA) was carried out using the Gene Set Enrichment Analysis (GSEA) command from the ClusterProfiler library (Wu et al., 2021), using the GSEA index h.all.v7.0.symbols.gmt to explore defined genesets.

2.2.4 Analysis of sex differences.

To explore sex differences a new variable needed adding to the database which denoted the sex origin of the cell line. First, the types of Cell_line in the data needed defining. The unique cell lines in the FourSen_df with IQR applied were BJ, HFF, MRC/MRC5, Tig3, HDF, HFL1, HCA2, IMR, LF1, WI38, CAF, and FL2 (determined by **Code 2.4**).

Code 2.4.

```
unique(FourSen_df_IQR$Cell_line))
```

This code can be altered to find the unique values of any variable in any data.frame. Extracted from GitHub file Thesis.R, line 494.

Next, the sex origin of each Cell_line needed determining. The sexes of cell lines CAF and FL2 were undetermined; HCA2, BJ, HFF, MRC/MRC5, Tig3, HDF, and HFL1 all originate from male samples (Cellosaurus, n.d.-a, n.d.-b; Friedman & Koropchak, 1978; Jacobs et al., 1970; Marthandan, Baumgart, et al., 2016); IMR, LF1, and WI38 cells all originate from female samples (Cellosaurus, n.d.-c; Friedman & Koropchak, 1978; Marthandan, Baumgart, et al., 2016; Nichols et al., 1977). The mutate function from the library dplyr (Wickham et al., 2023) was utilised to create the variable ‘Sex’ (**Code 2.5**)

Code 2.5.

```
DF = FourSen_df_IQR %>%
  mutate(Sex = case_when(
    Cell_line %in% c("BJ", "HFF", "MRC", "MRC5", "Tig3",
"HDF", "HFL1") ~ "Male",
    Cell_line %in% c("HCA2", "IMR", "LF1", "WI38") ~ "Female",
    Cell_line %in% c("CAF", "FL2") ~ "N/A"
  ))
```

Code to create the Sex variable based on cell type. Extracted from GitHub file Thesis.R, lines 496-501.

For any sex-based analysis, CAF and FL2 data were excluded due to them not having a determined sex. Additionally, as CAFs are derived from cancer patients they were excluded on this basis.

Following the protocols detailed in **Sections 2.2.2** and **2.2.3**, PCA, Venn, heatmap and ORA were conducted to explore if there were any sex differences in the *in vitro* senescence transcriptome.

2.2.5 Knockdown analysis.

A different subset of SenOmic was required to investigate the impact of gene knockdowns (KDs) on senescence. The exact code used is detailed in GitHub file Thesis.R.

First, total_data was filtered for SENvCON == “Yes”, Control_type == “Prolif”, and Sen_type == “OIS” or “DDIS”, creating the base KD data.frame. IQR filtering was then employed following the protocol in **Section 2.2.1**. Once the KD_IQR data.frame was formed, it was filtered to exclude numeric_time == 28, and to only include experimental samples with gene KDs which were “p53”, “RELA”, or “none”, and control samples with gene KDs of “none”.

Analysis of KDs were then performed through the creation of a function which would plot either p53 KD data or RELA KD data in both DDIS and OIS as well as when no KD had been introduced for direct comparison using the ggplot2 library (Wickham, 2016).

For statistical analysis of KD data, the Wilcoxon signed-rank test in the stats R library was employed for paired sample statistical analysis (Bauer, 1972), comparing expression of a gene when there was no gene inhibition to gene expression when there was gene inhibition.

2.2.6 Temporal analysis.

Time_groups (variable 'numeric_time2') were introduced for temporal analysis. To the IQR filtered FourSen_df data.frame, **Code 2.6** was applied to add the numeric_time2 variable which would facilitate temporal analysis.

Code 2.6.

```
sen3 = sen3 %>%
  mutate(numeric_time2 = case_when(
    Sen_type %in% c("DDIS", "OIS") ~ case_when(
      numeric_time <= 4 ~ "0-4",
      numeric_time > 4 & numeric_time <= 7 ~ "5-7",
      numeric_time > 7 & numeric_time <= 11 ~ "8-11",
      numeric_time > 11 & numeric_time <= 14 ~ "12-14",
      numeric_time > 14 ~ "15+",
      is.na(numeric_time) ~ "NA",
     TRUE ~ NA_character_
    ),
    Sen_type == "REP" ~ case_when(
      numeric_time < 41 ~ "0-40",
      numeric_time >= 41 ~ "41+",
      TRUE ~ NA_character_
    ),
    TRUE ~ NA_character_
  ))
```

Code used to introduce the variable 'numeric_time2' which was the defined time_groups. Extracted from file NewSenAnalysis_RS_20234.R, line 635-652.

As with KD analysis, statistical analysis of temporal data employed the Wilcoxon signed-rank test in the stats R library for paired sample statistical analysis (Bauer, 1972), comparing gene expression between DDIS and OIS in the same time_group.

2.3 Qualitative protein analysis of human senescent fibroblasts.

2.3.1 Non-systematic literature search to build a protein network.

The literature was non-systematically reviewed to determine a temporal protein profile in senescent human fibroblasts. For a study to be considered in this review, it had to be of senescent human fibroblasts in either DDIS or OIS, and it had to have experimental analysis performed at the protein level. Timepoint of analysis was also a requirement. From this non-systematic search and the transcriptomic analysis of **Chapter 4**, key pathways and proteins of senescence were chosen to be incorporated into the model. These included: cell cycle arrest, Ras expression, the inflammatory SASP, p38 signalling dynamics, and Notch signalling. The proteins and pathways chosen are in no way exhaustive of the entire process of senescence, however they are well-documented and understood aspects of senescence.

For each of these proteins, the involvement of them with other proteins in senescence and any information relating to their temporal profile in DDIS and OIS was recorded in a Microsoft Excel file (**Appendix Table A2.2**). Collating the identified studies made it possible to determine temporal behaviour of proteins which could then be qualitatively modelled. When there was no available published temporal protein data, transcriptomic data from the analysis of SenOmic was used as the best available proxy although it is recognised that the transcript and protein levels do not always align.

After reviewing the literature and collating data, criteria were established that described the temporal molecular protein phenotype of senescence in human fibroblasts. A total of eight protein-level phenotypes were identified to describe the normal senescence phenotype, including:

- p21 and p16 are continued to be expressed once senescence has been induced from more than 4 days.
- There is higher p53 activation and p21 expression in DDIS than in OIS.
- There is higher p16 expression in OIS than in DDIS.
- Expression of p16 increases later in DDIS than in OIS.
- Changes in Notch signalling activity is temporally associated with a switch in the SASP profile.

- There is a stronger inflammatory phenotype in OIS than in DDIS.
- The inflammatory phenotype begins to be established on days 5 to 8 after senescence induction.
- There is more p38 phosphorylation in OIS than in DDIS.

In addition to the normal senescence phenotype, four KD phenotypes were established. As with the normal senescence phenotype criteria, KD phenotype criteria were established based on the non-systematic review of the literature and the transcriptomic analysis in **Chapter 4**. These included:

- Knockdown of p53 results in upregulation of p16 expression.
- Knockdown of p53 results in decreased p21 expression.
- Knockdown of p53 results in upregulation of p38 in DDIS.
- Knockdown of RelA results in decreased p53 signalling.

The model's robustness and success as a qualitative representation of senescence were evaluated based on its ability to meet both the normal and KD senescence criteria.

2.3.2 Building the computational model of senescence.

Once the pathways to be modelled were selected, protein networks including reactions and interactions in senescence were designed in CellDesigner (Funahashi, 2008). CellDesigner uses the Systems Biology Graphical Notation (Le Novère et al., 2009). In this graphical notation, different molecular components can have different visual representations (such as shape or colour), and interactions can be represented as arrows (for formation reactions) or bars (for inhibition reactions). These reactions and interactions were informed from the non-systematic literature search (**Appendix Table A2.2**).

Most reactions in the model code were straight forward reactions involving protein formation (F), degradation (D), activation (A) or a backwards reaction (B). However, some reactions were more complex and required Michaelis-Menten kinetics to be applied. The equations used in the model code were **Equations 2–4**.

```
function NonCompetitiveInhibition(km, ki, Vmax, I, S)
          Vmax * S / ((km + S) * (1 + I / ki))
end
```

***Equation* 2**

```
function NonCompetitiveInhibitionNoSub(Vmax, km, ki, I)
      Vmax / (km * (1 + I / ki))
end
```

***Equation* 3**

```
function NonCompetitiveInhibitionWithKcatNoSub(km, ki, kcat, E, I)
      kcat * E / (km * (1 + (I / ki)))
end
```

***Equation* 4**

2.3.3 Development of the cellular senescence model code.

Protein networks created in CellDesigner were converted to text-based code using Antimony. A base model consisting of reactions, reaction rates, and initial parameters was developed using Tellurium (Choi et al., 2018) and Antimony. Antimony provides an extensive vocabulary for defining components and reactions within a network, and Tellurium is an open-source Python-based platform which enables simulation and visualisation of biochemical networks. The Antimony model was loaded into Tellurium for simulation, which was performed in a Python 3.6 environment (Foundation, 2016) using the Spyder graphical interface (Contributors, 2024).

Specific inputs were introduced into the model code to induce either DDIS or OIS (**Table 2.3**). The inputs were developed based on knowledge from published literature. All expression and time units in the simulations were arbitrary (AU). Inputs chosen to induce cellular senescence were ‘DDR’, ‘RAS’, ‘kDDRF’, ‘kRASF’ and ‘kDDRFRAS’. Values of ‘DDR’ and ‘RAS’ denoted the initial concentration in each cellular state, whereas ‘kDDRF’, ‘kRASF’ and ‘kDDRFRAS’ were parameter values which determined the rate of formation of the DDR, RAS, and the DDR dependent on RAS respectively. To simulate DDIS, a strong DDR and kDDRF was required as

previously discussed. In contrast, OIS simulation required overexpression of RAS (achieved through high RAS and kRASF values) as well as high kDDRFRAS.

Table 2.3 – Inputs for inducing the different senescence types.

Inputs	Cellular states simulated	
	DDIS	**OIS**
RAS	0.5	5*
DDR	5*	0
kDDRF	14*	0.01
kRASF	0.3*	1*
kDDRFRAS	0.5	5.75*

**Induced once the model was determined to have reached equilibrium.*

KDs of p53 and RelA were introduced into model simulations through an inducible event which downregulated the respective proteins and the formation of them (**Code 2.7 and 2.8**). KDs were induced at the same as senescence induction, a decision based on the methods described in p53 and RelA KD studies in SenOmic.

Code 2.7.

```
at 35 after (time>0): p53 = 0.01;
at 35 after (time>0): kp53F = 0.1;
at 35 after (time>0): kp53F2 = 0.1;
```

Code to induce a p53 knockdown. Extracted from GitHub file CellularSenPaper.py, lines 287-289.

Code 2.8.

```
at 35 after (time>0): NFkB = 0.01;
at 35 after (time>0): kp65A = 0.1;
at 35 after (time>0): kpNFkBB = 3;
```

Code to induce a RelA knockdown. Extracted from GitHub file CellularSenPaper.py, lines 291-293.

Additionally, an inducible event termed the Notch switch was introduced into the model network. The Notch switch creates a dynamic change in Notch signalling activity. Activation of the Notch switch results in diminished Notch signalling through the downregulation of NICD levels. As Notch signalling is mediated via cell-cell interaction and this is a single cell level model, an event was needed to induce the Notch switch. The Notch switch was implemented through the introduction of an event in the model code at Time 65 (**Code 2.9**). This arbitrary time coincided with around day 5 post-senescence induction.

Code 2.9.

```
at 65 after(time>0): NICD = 0.01;
at 65 after(time>0): kNICDD = 5;
```

Code to induce the Notch switch. Extracted from GitHub file CellularSenPaper.py, lines 284-285.

The senescence model is qualitative, not quantitative, thus values used are not from experimental analysis but rather from the behaviour profile of proteins understood from the non-systematic review.

Scripts containing model networks, reactions and parameter values are titled ModelA.py, ModelB.py, and CellularSenPaper.py, and are available in the following GitHub repository: ***https://github.com/rlscanlan/Thesis***

2.3.4 Visualisation of simulated temporal protein expression.

Models were simulated over a time period of 0-100 AU for a total of 1000 data points. This was done for every model iteration, in both DDIS and OIS, and again when either the p53 or RelA KD were induced. Datafiles containing the simulated protein value for all proteins and timepoints were saved as .csv files for each simulation. The datafiles were loaded into R using the read.csv function which is part of base R. Using the ggplot2 library (Wickham, 2016), temporal simulation graphs of proteins were visualised. Details can be found in file datafiles_graphs.R available on the following GitHub repository: ***https://github.com/rlscanlan/Thesis***

2.3.5 Dynamic sensitivity analysis of the computational model.

Dynamic sensitivity analysis, conducted by Alvaro Martinez-Guimera, was performed in both DDIS and OIS conditions at four distinct timepoints (pre-senescence, Time = 20; post-senescence induction, Time = 40; pre-Notch switch, Time = 60; post-Notch switch, Time = 80) in The Cellular Senescence Model network. The X-method was followed for calculating scaled sensitives to parameter perturbations as 'events' at specific simulation time points using SIMBIOLOGY, MATLAB (Yue et al., 2006).

2.4 Creation of KEGG-based analysis framework.

Studying entire pathways is a common bioinformatic method. Typically, results are visualised using approaches such as heatmap analysis and ORA or GSEA. Another less utilised approach is investigating specific defined KEGG (Kyoto Encyclopaedia of Genes and Genomes) pathways and visualising the results on the KEGG pathway map. With the KEGG website (found at the following link: **https://www.genome.jp/kegg/**) combined with the KEGGrest (Tenenbaum & Maintainer, 2024) and pathview libraries (Luo & Brouwer, 2013), it is possible to visualise results on a KEGG pathway map.

In collaboration with the Bohr and Rasmussen laboratories at Copenhagen University, the role of cytosolic DNA-sensing pathways in the neurodegenerative disorder ataxia-oculomotor apraxia type 1 (AOA1) which is caused by Aprataxin (APTX) inactivation mutations was investigated. APTX KO microglial cells were produced using CRISPR technology. Control and experimental cells underwent immune stimulation through the introduction of dsDNA. RNAseq analysis was performed on the four sample conditions as detailed in Madsen et al. (2023). Laboratory analysis was performed by Helena Madsen and Mansour Akbari, and bioinformatic analysis was performed by Louise Pease and I.

Sample conditions in this study included: APTX WT (wildtype) microglial cells without immune stimulation (NS – APTX1_NS), APTX WT microglial cells with immune stimulation (IS – APTX1_IS), APTX KO microglial cells without immune stimulation (APTX0_NS), and APTX KO microglial cells with immune stimulation (APTX0_IS). Condition comparisons were drawn between samples as below:

- APTX1_NS versus APTX1_IS
- APTX1_NS versus APTX0_NS
- APTX0_NS versus APTX0_IS

Paired end sequencing files for each sample and sequencing run were aligned to the HG38 genome using HISAT2. Salmon (Patro et al., 2017) and DESeq2 (Love et al., 2014) were used to identify differentially expressed (DE) genes. Significantly ($q < 0.05$) DE genes and transcripts for each of the comparisons were then identified.

KEGG pathway analysis was performed on significantly ($q < 0.05$) DE genes within KEGG pathway hsa04623 (cytosolic DNA-sensing pathway – *Homo sapiens* (human)) using R packages KEGGrest (Tenenbaum & Maintainer, 2024) and pathview (Luo & Brouwer, 2013).

2.5 Summary of methods and code used.

Methods in **Sections 2.1**, **2.2.1**, **2.2.3**, **2.2.5**, **2.2.6**, and **2.3** all detail methods created for and utilised in the Scanlan et al. (2024) study. Methods detailed in **Section 2.4** were created and utilised in the Madsen et al. (2023) study. Methods detailed in **Sections 2.2.2** and **2.2.4** were created for this thesis.

All code used throughout this thesis can be found in the following GitHub repository: ***https://github.com/rlscanlan/Thesis***

Chapter 3: The transcriptomic phenotype of human senescent fibroblasts.

3.1 Background.

There are well characterised and recognised transcriptomic phenotypes of senescence, such as stable cell cycle arrest and expression of the SASP (Coppé et al., 2010; Muñoz-Espín & Serrano, 2014). Typically, the SASP is composed of inflammatory proteins, growth factors, and matrix metalloproteinases, however unique SASPs have been identified in response to different senescence inducers. For example, the loss of the IL-1α arm of the SASP when senescence is induced from dysfunctional mitochondria (Wiley et al., 2016). These unique SASP compositions are often not followed up with further research, but it is interesting to observe different senescence inducers resulting in different SASP compositions. Understanding the transcriptomic phenotype of the SASP is important as it is often a target of senotherapeutics research to aid in alleviating symptoms such as chronic low-grade inflammation, the reduction of disease burden and advanced ageing.

While some phenotypes such as the SASP are well characterised, there is yet to be a unique and reliable biomarker of senescence identified which can be used as a standard when it comes to experimental analysis (Matjusaitis et al., 2016). Identification of a gold standard biomarker, such as a small set of genes unique to senescence, will allow for more robust and reproducible senescence experiments ultimately leading to advancement of basic biology and more advanced senotherapeutics. Most experimental studies take a multi-marker approach to confirm senescence; however, there is no consensus over the best markers to use and most, if not all, markers are not unique to senescence. For example, β-gal staining is present in non-senescent cells (Dimri et al., 1995; Going et al., 2002), and cell cycle inhibitor proteins such as p53 are expressed in non-senescent contexts such as the normal progress of the cell cycle (Abbas & Dutta, 2009; Geißler et al., 2013; Witkiewicz et al., 2011). Additionally, further work is required regarding translation of biomarkers from an *in vitro* to an *in vivo* environment as not all current biomarkers do translate. For example, changes in cellular morphology are observed *in vitro*

including the cell becoming enlarged and flattened (González-Gualda et al., 2021), however this phenotype does not translate to *in vivo* contexts due to the complexity of tissue architecture. Expression levels of genes or proteins may also differ between an *in vitro* and an *in vivo* environment which has biological context.

The aim of this chapter was to systematically investigate the literature to create a transcriptomic database. This database was then bioinformatically investigated with the aim of gaining a comprehensive understanding of the *in vitro* senescent transcriptome; to find commonalities between senescence types, cell lines, and the sex origin of senescent cells. In addition, the impact of the KD of key TFs p53 and RelA on the senescent transcriptome was also investigated.

3.2 Results and Discussion.

The results of this chapter were obtained using methods detailed in **Section 2.2**. **Figures 3.5**, **3.7**, **3.14**, **3.15**, and **Table 3.1** were published in Scanlan et al. (2024), and **Figures 3.9, 3.10, 3.11** and **3.12** were newly produced for this thesis using the methods detailed in Scanlan et al. (2024).

The senescent transcriptomic phenotype was investigated using SenOmic, allowing for exploration of senescence heterogeneity. Unless otherwise stated, the SenOmic data analysed in this chapter was of experimental senescence cells compared to proliferating control cells and has undergone IQR filtering.

3.2.1 Utilising SenOmic to explore senescence heterogeneity.

As described in **Chapter 2**, SenOmic is a database containing temporal transcriptomic data for senescent human fibroblasts, with 49 variables across 119 datasets identified from the systematic analysis. **Table 3.1** details the identifying factors (study ID and associated publications) and selected main variables (senescence types, control types, timepoint analysed, and genes targeted for up- or downregulation) of all 119 datasets. In SenOmic there are 1069 unique comparisons. In the simplest dataset there were only two samples analysed – an experimental and a control sample. In that case, only one comparison can be drawn. For several datasets there were multiple sample types and therefore more comparisons were

possible. Most datasets investigated one type of senescence and timepoint, such as GSE40349 (Aksoy et al., 2012) and GSE94395 (Baar et al., 2017); nonetheless, certain datasets investigated multiple senescence types such as GSE41318 (Acosta et al., 2013) or timepoints such as E-MTAB-5403 (Hernandez-Segura et al., 2017).

Table 3.1 – Dataset information for the 119 studies in SenOmic.

Study ID	Publication	Senescence type	Control type	Cell lines	Timepoints (days, d)	Gene(s) up	Gene(s) down	Number of replicates per sample
GSE103938	(Aarts et al., 2017)	OIS, OSKM	Prolif	IMR	10d	none	mTOR	3
GSE94928	(Aarts et al., 2017)	OSKM	Prolif	IMR	14d, 20d	none	p21, mTOR	3
GSE41318	(Acosta et al., 2013)	OIS, BYS	Prolif	IMR	7d	none	none	3
GSE40349	(Aksoy et al., 2012)	OIS	Prolif	IMR	7d	none	pRb, E2F7, pRb_E2F7	2
GSE56293	(Alspach et al., 2014)	REP	Prolif	BJ	97PD	none	p38	2
GSE94395	(Baar et al., 2017)	DDIS	Prolif	IMR	10d	none	none	3
GSE33710	(Benhamed et al., 2012)	OIS	Prolif	WI38	7d	none	none	3
GSE112084	(Martínez-Zamudio et al., 2020)	OIS	Prolif, Quiesce	WI38	1d, 2d, 3d, 4d, 6d	none	none	2
GSE122918	(Martínez-Zamudio et al., 2020)	OIS	Prolif	WI38	3d, 6d	none	ETS1, JUN, RELA	4
GSE143248	(Martínez-Zamudio et al., 2020)	REP, OIS	Prolif	WI38	0.5d, 1d, 2d, 3d, 4d, 6d, 11d, 18d, 26d,	none	none	2

					33d, 42d, 57d, 88d			
GSE133660	(Buj et al., 2019)	dNTP	Prolif	IMR	7d	none	p16	3
GSE134747	(Carvalho et al., 2019)	OIS	Prolif	BJ	1d, 2d, 3d, 5d	GR	RELA	4
GSE130727	(Casella et al., 2019)	DDIS, REP, OIS	Prolif	IMR, WI38	5d, 8d, 10d	none	none	2
GSE130100	(Chan et al., 2020)	OIS	Prolif	BJ	14d	none	none	3
GSE130099	(Chan et al., 2020)	OIS	Prolif	BJ	6d	none	none	3
GSE19864	(Chicas et al., 2010)	OIS	Prolif, Quiesce	IMR	7d	none	pRb, p107, p130	2
GSE2487	(Collado et al., 2005)	OIS	Prolif, Immortal	IMR	3d	SmallT, E6_E7, SmallT_E6_E7	none	2
E-MTAB-4920	(Contrepois et al., 2017)	DDIS	None	WI38	20d	none	H2AJ	3
GSE76125	(Correia-Melo et al., 2016)	DDIS	Prolif	MRC	10d	Parkin	Mitochondrial	3
E-MTAB-2086	(Criscione et al., 2016; Lackner et al., 2014)	REP	Prolif	IMR	30PD, 50PD, 70PD	none	none	2

GSE109700	(De Cecco et al., 2019)	REP	Prolif	LF1	56d, 112d	none	none	3
GSE70668	(Dikovskaya et al., 2015)	OIS	Prolif	IMR	4d	none	none	3
GSE99028	(Dou et al., 2017)	DDIS	Prolif	IMR	7d	none	cGAS	2
GSE151745	(Omer et al., 2020)	DDIS	None	WI38	8d	none	G3BP1	2
GSE101766	(Georgilis et al., 2018)	OIS	Prolif	IMR	6d	none	See table legend†	3
GSE101750	(Georgilis et al., 2018)	OIS	Prolif	IMR	6d	none	PTBP1	3
GSE101758	(Georgilis et al., 2018)	OIS	Prolif	IMR	5d	none	EXOC7, PTBP1	3
GSE98216	(Saint-Germain et al., 2017)	OIS	None	IMR	8d	none	none	3
GSE127116	(Hari et al., 2019)	OIS	Prolif	IMR	5d, 8d	none	LTR2, LTR10	3
E-MTAB-5403	(Hernandez-Segura et al., 2017)	DDIS	Prolif, Quiesce	HCA2	4d, 10d, 20d	none	none	6
GSE61130	(Herranz et al., 2015)	OIS	Prolif	IMR	7d	ZFP36L1	none	3
GSE122079	(Guerrero et al., 2019)	OIS	Prolif	IMR	6d, 7d	none	caspase, ION pump	3

GSE72407	(Gonçalves et al., 2021)	OIS, DDIS	Prolif	IMR	6d, 7d	none	none	8
GSE42368	NA	DDIS	Prolif	FL2	1d	none	DINO	2
E-MEXP-2241	(Jacobsen et al., 2010)	OIS	Prolif	Tig3	3d	none	miR34a	3
GSE117444	(Mitra et al., 2018)	NA	Prolif, Quiesce	10-5_12-1 *	7d	none	none	3
GSE45276	(Kennedy et al., 2011)	OIS	Prolif	IMR	7d	none	none	4
GSE53379	(Kirschner et al., 2015)	OIS, DDIS	Prolif, Quiesce, Immortal	IMR	7d	E1A	p53	3
GSE93535	(Lämmermann et al., 2018)	DDIS	Quiesce	HDF161 *	15d	unknown	unknown	3
GSE108278	(Lau et al., 2019)	OIS	Prolif	IMR	4d, 10d	none	IL1R	2
GSE75643	(Lenain et al., 2017)	OIS	Prolif, Quiesce	Tig3	4d, 10d	SV40smallT	none	3
GSE134088	NA	DDIS	Prolif	IMR	2d	none	none	3
GSE94280	(Lizardo et al., 2017)	REP	Prolif	BJ	44PD	none	none	3
GSE42509	(Loayza-Puch et al., 2013)	OIS	Prolif, Quiesce	BJ	5d	none	none	2

GSE131503	(Borghesan et al., 2019)	BYS	Prolif	HFF	3d	none	none	2
GSE63577	(Marthandan, Baumgart, et al., 2016)	REP	Prolif	BJ, WI38, IMR, HFF, MRC	26PD, 46PD, 52PD, 57PD, 62PD, 64PD, 72PD, 74PD	none	none	3
GSE64553	(Marthandan et al., 2015)	REP	Prolif	HFF, MRC	22PD, 26PD, 30PD, 34PD, 38PD, 42PD, 48PD, 52PD, 58PD, 74PD	none	Complex I	3
GSE60883	(Marthandan et al., 2014)	NA	Prolif	MRC	36PD	none	none	3
GSE77682	(Marthandan, Menzel, et al., 2016)	DDIS	None	MRC	5d	none	none	3
E-MTAB-3101	(Mellone et al., 2016)	DDIS	Prolif	HFF	7d	TGFb	none	3
GSE85082	(Muniz et al., 2017)	OIS	Prolif	WI38	3d	none	none	3
GSE28464	(Narita et al., 2011)	OIS	Prolif	IMR	4d	none	none	3
GSE54402	(Nelson et al., 2014)	OIS	Prolif	IMR	NA	none	none	4

GSE42212	(Neyret-Kahn et al., 2013)	OIS	Prolif	WI38	5d	none	none	3
GSE62701	(Contrepois et al., 2017)	DDIS	Prolif	WI38	21d	none	H2AJ	4
GSE120040	(Paluvai et al., 2018)	OIS, CR	Prolif	BJ	14d	none	none	2
GSE128055	(Pantazi et al., 2019)	OIS, RiboMature	Prolif	MRC	NA	none	none	3
GSE24810	(Kumari et al., 2021; Rovillain et al., 2011)	OIS	Immortal, Quiesce	HMF3A *	7d, 14d	E1A, E7	laminA, p53, E2F, p21	3
GSE113060	(Parry et al., 2018)	OIS	Prolif	IMR	6d	none	HMGA1	6
GSE37318	(Martinez-Zubiaurre et al., 2013)	DDIS	Prolif	CAF	1d	none	none	4
GSE13330	(Pazolli et al., 2009)	REP, DDIS	Quiesce	BJ	4d, 85PD	none	none	6
GSE60340	(Purcell et al., 2014)	REP, DDIS	Prolif, Quiesce, Immortal	LFS_MDAH041 *	5d, 8d, 18PD, 29PD, 200PD	none	p53	3
GSE52848	(Nelson et al., 2016; Rai et al., 2014)	OIS	Prolif	IMR	8d	none	none	2

GSE53356	(Nelson et al., 2016; Rai et al., 2014)	REP	Prolif	IMR	88PD	none	none	2
GSE128711	(Schade et al., 2019)	DDIS	Prolif	HFF	1d	none	p130, pRb, p130_pRb	2
GSE105951	(Sen et al., 2019)	REP	Prolif	IMR	77PD, 79PD	none	p300, CBP	2
GSE36640	(Shah et al., 2013)	REP	Prolif	IMR	90PD	none	none	5
GSE19018	NA	REP	Prolif	IMR	30PD, 48PD, 53PD	none	none	3
GSE23399	(Chan et al., 2016)	DDIS	Prolif	CAF	1d, 3d, 7d	none	none	2
GSE60652	(Takebayashi et al., 2015)	OIS	Prolif	IMR	6d	none	pRb	2
GSE74324	(Tasdemir et al., 2016)	OIS	Prolif, Quiesce	IMR	4d, 12d	none	p53, BRD4, RELA, p16_p21, p53_pRb	3
GSE75207	(Tordella et al., 2016)	OIS	Prolif	IMR	7d	none	ARID1B	3
GSE75291	(Tordella et al., 2016)	CR	Prolif	IMR	6d	none	none	3
GSE132370	(Vizioli et al., 2020)	DDIS	Prolif	IMR	10d	none	HDAC	3
GSE132369	(Vizioli et al., 2020)	DDIS	Prolif	IMR	10d	Parkin	mitochondrial	3

GSE140961	(Wakita et al., 2020)	DDIS	None	Tig3	12d	none	BRD4	3
GSE81368	(Wang et al., 2017)	DDIS, REP	Prolif	CAF	NA	none	none	3
GSE133292	(X. Zhang et al., 2021)	DDIS	Prolif, Quiesce	BJ	12d, 28d	none	p53	2
GSE98240	(Yosef et al., 2017)	DDIS	Prolif	BJ	3d	none	p21	3
GSE59522	(Young et al., 2009)	OIS	Prolif	IMR	0.08d, 0.33d, 2d, 4d,6d, 8d	none	none	3
GSE98440	(Zirkel et al., 2018)	REP	Prolif	IMR	NA	none	none	3
GSE189789	(An et al., 2022)	DDIS	Prolif	WI38	2.5d	none	none	3
GSE175686	(Barnes et al., 2022)	DDIS	Prolif	BJ	1d	none	none	3
GSE153921	(Innes et al., 2021)	OIS	Prolif	IMR	5d	none	XPO7	3
GSE168994	(Lee et al., 2021)	DDIS	Prolif	IMR	10d	none	none	2
GSE156648	(Leon et al., 2021)	OIS	Prolif	IMR	4d	DOT1L	DOT1L	3
GSE139563	(López-Antona et al., 2022)	BYS	Prolif	IMR	4d, 7d, 10d	none	none	2
E-MTAB-9714	(Mangelinck et al., 2020)	DDIS	Prolif	WI38	9d	none	H2AJ	6
GSE144752	(Montes et al., 2021)	OIS	Prolif	BJ	3d	none	MIR31HG, YBX1	3

GSE112530	(Park et al., 2021)	REP, DDIS, OIS, NBIS	Prolif	HDF	8d, 10d, 12d	none	none	3
GSE77074	NA	DDIS	Prolif	HDF	5d	none	none	4
GSE124609	(Sabath et al., 2020)	REP	Prolif	WI38	4d	none	none	2
GSE141991	(Liu et al., 2021)	OIS	Prolif	IMR	7d	none	METTL14	3
GSE200479	(Zhu et al., 2022)	OIS	Prolif	BJ	14d	none	CBS, p53, NF1	3
GSE169037	(Anerillas, Herman, Rossi, et al., 2022)	DDIS, apoptosis	Prolif, apoptosis	IMR	2d	none	none	3
GSE145650	(Gonçalves et al., 2021)	OIS	Prolif	IMR	6d	none	COX2	8
GSE178115	(Yang et al., 2022)	REP	Prolif	HDF	3d, 8d, 15d	none	none	3
GSE72404	(Hoare et al., 2016)	OIS, NIS, RNIS	Prolif	IMR	6d	none	none	6
GSE102537	(Debès et al., 2023)	REP	Prolif	IMR	NA	none	none	2
GSE155903	(Guerrero et al., 2022)	OIS	Prolif	IMR	6d	none	none	4
GSE179465	NA	MitoSkip	Prolif	HCA2	21d	none	none	3
GSE180406	(Rey-Millet et al., 2023)	REP	Prolif	MRC	PD71, PD75	TRF2	none	3

GSE184892	(Muto et al., 2023)	Trehalose	Prolif	Primary skin fibroblast *	1d, 3d, 14d	none	none	3
GSE190998	(Anerillas, Herman, Munk, et al., 2022)	DDIS	Prolif	WI38	8d	none	NTRK2, BDNF	3
GSE191055	(Hasegawa et al., 2023)	REP	Prolif	HDF	NA	none	none	3
GSE198396	(T. W. Wang et al., 2022)	DDIS	Prolif	HCA2	12d	none	none	3
GSE210020	(Cho et al., 2022)	REP	Prolif	HDF	NA	none	none	3
GSE212085	(Marin et al., 2023)	DDIS	Prolif	IMR	10d	none	none	3
GSE213993	(Rossi et al., 2023)	DDIS	Prolif	WI38	10d	none	BAFF	2
GSE214409	(Y. Wang et al., 2022)	OIS	Prolif	IMR	7d	WSTF	none	3
GSE221104	(Anerillas et al., 2023)	DDIS	Prolif	WI38	8d	none	none	3
GSE222676	NA	DDIS	Prolif	IMR	7d	none	ABCA1	2
GSE235768	(Skea et al., 2023)	DDIS, PIIPS	Prolif	BJ, HFL1	3d, 9d, 10d	none	none	3
GSE175533	(Chan et al., 2022)	DDIS, REP	Prolif	WI38	1d, 2d, 3d, 4d, 7d, PD50, PD52, PD53	none	none	3
GSE224070	(McHugh et al., 2023)	DDIS, OIS	Prolif	IMR	10d	none	COPB2	3

GSE224071	(McHugh et al., 2023)	OIS	Prolif	IMR	10d	none	none	3
GSE225095	(Papaspyropoulos et al., 2023)	DDIS	Prolif	IMR	7d	none	none	2
GSE234417	(Gulen et al., 2023)	DDIS	Prolif	WI38	20d	none	none	4
GSE196610	(Victorelli et al., 2023)	DDIS	Prolif	IMR, MRC5	10d	mtDNA	BAK, BAX	3

*Prolif, proliferating cells; Quiesce, quiescent cells; Immortal, immortalised cells; PD, population doublings; CAF, cancer associated fibroblast; BYS, bystander induced senescence; DDIS, DNA damage-induced senescence; OIS, oncogene-induced senescence; REP, replicative senescence; CR, chromatin remodelling induced senescence; NBIS, nuclear breakdown induced senescence; NIS, Notch induced senescence; RNIS, Ras and Notch induced senescence; OSKM, senescence induced as a by-product of pluripotency induction via transcription factors Oct4, Sox2, Klf4 and c-Myc; dNTP, depletion of deoxyribonucleotide triphosphates; RiboMature, senescence induced through ribosomal disruption; MitoSkip, senescence induced via mitotic skipping; PIIPS, proteasome inhibition-induced premature senescence; Trehalose, senescence induced though high concentrations of trehalose. * Identifies primary fibroblast cell lines. †CEBPb, ABCD4, AKR1C1, ALOX5, ASB15, BPIL1, BRD8, C20, CCL23, CTDSPL, DCAMKL3, DUSP11, EMR4, ERCC3, GPRC5D, HSPC182, IFNA17, IL15, IL17RE, ITCH, KCNA5, KCNQ4, LOC399818, LOC51136, MAP3K6, MCFP, NRG1, PEO1, PLCB1, PPP1CB, PROK2, PTBP1, PTPN14, RNF6, SHFM3, SKP1A, TMEM219, UBE2V2, p16, p38, p53, RELA. Taken from Scanlan et al. (2024).*

SenOmic is composed of data from 17 different cell lines, originating either from the lungs or the skin; temporal data spanning from point of induction (day 0) up to 112 days post-senescence induction; and importantly, data from 14 different types of senescence. The different types of senescence include: replicative senescence (REP) from telomere erosion (Bodnar et al., 1998); DNA damage-induced senescence (DDIS) which can be induced in a number of ways including ultraviolet and ionising irradiation or the use of compounds such as etoposide, leading to constitutive activation of the DNA damage response (DDR) and the expression of cell cycle inhibitors; oncogene-induced senescence (OIS) occurring through the aberrant activation of oncogenes such as RAS or BRAF; secondary paracrine bystander senescence (BYS) in which neighbouring cells become senescent in response to secreted factors from primary senescent cells; senescence induced through chromatin remodelling (CR) (Paluvai et al., 2018; Tordella et al., 2016); the breakdown of the nuclear barrier leading to nuclear barrier induced senescence (NBIS); Notch induced senescence (NIS) through ectopic NICD activation as well as Ras and Notch (combined) induced senescence (RNIS) (Hoare et al., 2016); OSKM induced senescence as a by-product of trying to induce pluripotency; induction of senescence through the disruption of ribosomal function (RiboMature) (Pantazi et al., 2019); depletion of deoxyribonucleotide triphosphates (dNTP) induced senescence (Buj et al., 2019); senescence induction through mitotic skipping through inhibition of CDK1 and MDM2 (MitoSkip) (Johmura et al., 2014); inhibition of the proteasome with drugs such as bortezomib, leading to proteasome inhibition-induced premature senescence (PIIPS) (Skea et al., 2023); and highly concentrated treatment with trehalose (Trehalose) (Muto et al., 2023). Control cells could be proliferating or quiescent, and some lines were immortalised or treated with agents that immortalised them as part of the study. Twenty studies compared senescent cells to cells immortalised primarily through hTERT activation, although one study used immortalised cells with p53 KO (Purcell et al., 2014).

While all datasets induced senescence, 53 studies also explored the effect of introducing treatments such as sh/siRNAs against specific genes, and other datasets used diseased patient cells such as those from breast cancer (Chan et al., 2016), non-small-cell lung cancer (Martinez-Zubiaurre et al., 2013), and Li-Fraumeni

syndrome, an inherited syndrome causing vulnerability to rare cancers (Malkin, 1993) due to mutation of p53 (Purcell et al., 2014). Further datasets investigated the overexpression of genes such as the mitochondrial related gene *Parkin* (Correia-Melo et al., 2016; Victorelli et al., 2023; Vizioli et al., 2020), while another dataset treated senescent cells with compound "1201," an alcoholic extract from the plant *Solidago alpestris,* which had unknown effects on gene expression (Lämmermann et al., 2018).

Given the extent and richness of the data collated through this work, it was considered essential that such a resource is publicly available to improve collaboration and sharing of knowledge, and, importantly, to allow others to investigate future hypotheses of interest outside of those explored in this work. Therefore, as detailed in **Section 2.1.3**, SenOmic was hosted online on a website which allows users to filter for multiple variables to find studies and genes of interest. For example, using the **SenOmic online database**, data can be filtered to present only comparisons that meet multiple criteria such as 'OIS in skin fibroblasts with p53 inhibition versus proliferating controls'. The median LogFC and p-values are also calculated, and the data is available to be downloaded for further analysis.

Like any repository, SenOmic offers diverse applications. To address the aims of this thesis, a specific subset of the database was analysed. Consequently, certain aspects of SenOmic, such as distinctions between senescence and quiescence, were not explored. Similarly, the analysis of KDs focused only on p53 and RelA KDs in DDIS and OIS despite the perturbation of other genes such as p21 and Rb being documented in multiple studies.

3.2.2 Exploring differences and similarities in senescent human fibroblasts.

SenOmic first needed to be filtered to explore specific aims. The analysis in this section focused on senescence heterogeneity as found in SenOmic with the following filters applied:

- SENvCON == "Yes", meaning all comparisons were drawn between senescent cells and non-senescent cells.

- Treatment == “none”, meaning cells had only been treated for senescence induction (e.g. Ras overexpression to induce oncogene-induced senescence) and nothing further (e.g. a gene KD).
- Disease == “none”, ensuring only non-diseased cells were included as diseased cells may introduce variation which alters the transcriptome.
- Control_type == “Prolif”, ensuring the only control types included were of proliferating cells.

This first filtering step created the data.frame referred to as ‘SENvCON_df’ in this thesis and in coding scripts. In SENvCON_df, there were 220 unique comparisons in 104 datasets. Within these 220 comparisons were 14 types of senescence summarised in **Table 3.2**. Despite there being 14 types of senescence in these 220 comparisons, 89% of the data was comprised of DDIS, OIS, REP and BYS datasets.

Table 3.2 – Summary of SENvCON_df.

Sen_type	Number of comparisons	Number of unique datasets	Sen_type	Number of comparisons	Number of unique datasets
BYS	6	3	OIS	79	52
CR	2	2	OSKM	3	2
DDIS	54	35	PIIPS	2	1
dNTP	1	1	REP	57	22
MitoSkip	1	1	RiboMature	1	1
NBIS	3	1	RNIS	1	1
NIS	1	1	Trehalose	9	1

A summary of the number of sample comparisons in the SENvCON_df, prior to interquartile range filtering, and the number of unique datasets these comparisons are found in. BYS, bystander induced senescence; DDIS, DNA damage-induced senescence; OIS, oncogene-induced senescence; REP, replicative senescence; CR, chromatin remodelling induced senescence; NBIS, nuclear breakdown induced senescence; NIS, Notch induced senescence; RNIS, Ras and Notch induced senescence; OSKM, senescence induced as a by-product of pluripotency induction

via transcription factors Oct4, Sox2, Klf4 and c-Myc; dNTP, depletion of deoxyribonucleotide triphosphates; RiboMature, senescence induced through ribosomal disruption; MitoSkip, senescence induced via mitotic skipping; PIIPS, proteasome inhibition-induced premature senescence; Trehalose, senescence induced though high concentrations of trehalose.

Trehalose-induced senescence had more unique comparisons compared to BYS and therefore had a higher percentage of data pertaining to it in SENvCON_df. Despite this, BYS was chosen for future analysis for two reasons: (i) BYS is a more widely researched area and is more biologically relevant, and (ii) while there are fewer comparisons in BYS, they were from three unique datasets rather than a single dataset, meaning any patterns identified are more likely to represent true findings rather than artifacts which could have been introduced by potential biases or errors stemming from experimental design.

As 89% of the data in SENvCON_df was comprised of BYS, DDIS, OIS, and REP, analysis of SenOmic in Chapter 3 (with the exception of the KD analysis) includes only this data. Outliers from SENvCON_df were removed prior to analysis following the protocol detailed in **Section 2.2.1**, producing the data.frame 'SENvCON_IQR_df'. Following this, SENvCON_IQR_df was further filtered to the senescence types of interest using **Code 3.1**, forming the data.frame 'FourSen_df' which was analysed below. FourSen_df contained 196 unique sample comparisons, representing 18.5% of the total SenOmic database. Filtering of SenOmic to produce FourSen_df is visualised in **Appendix Figure A3.1**.

Code 3.1.

```
FourSen_df = filter(SENvCON_IQR_df, Sen_type == "DDIS" |
Sen_type == "OIS" | Sen_type == "BYS" | Sen_type == "REP")
```

Code to filter for only DDIS, OIS, BYS, and REP to create the data.frame FourSen_df. Extracted from GitHub file Thesis.R, line 57.

PCA was first performed on all columns of the transformed FourSen_df data.matrix following PCA Method 2, with nPCs = 15 as detailed in **Section 2.2.2**. This was taken

as the first step to avoid deleting data. While more than 99% of the data variance was accounted for in the first three PCs, 56.865% of the data was comprised of NA values (**Figure 3.1**).

```
nipals calculated PCA
Importance of component(s):
                    PC1    PC2     PC3      PC4       PC5       PC6
R2            0.8692 0.1071 0.02006 0.003322 0.0001264 5.053e-05
Cumulative R2 0.8692 0.9763 0.99637 0.999691 0.9998175 9.999e-01
                     PC7       PC8       PC9      PC10      PC11
R2            1.761e-05 1.253e-05 8.371e-06 6.114e-06 4.842e-06
Cumulative R2 9.999e-01 9.999e-01 9.999e-01 9.999e-01 9.999e-01
                    PC12      PC13      PC14      PC15
R2            3.660e-06 3.476e-06 2.786e-06 2.620e-06
Cumulative R2 9.999e-01 9.999e-01 9.999e-01 9.999e-01
25842   Variables
196     Samples
2880246         NAs ( 56.865 %)
15      Calculated component(s)
```

Figure 3.1 – PC information for FourSen_df using PCA Method 2 when nPCs = 15.

Despite the high volume of NAs, visualisation was still attempted (**Figure 3.2**). As observed during the optimising of PCA, when there is a high percentage of NA data, it is difficult to discern any observation of the PCA plot. When plotting the FourSen_df data.matrix, only REP studies were initially visible (**Figure 3.2A**). To be certain all data was plotted and the code was functioning correctly, labels for each Comparison were added (**Figure 3.2B**), demonstrating all four senescence types were present in the PCA; however, because of outlier data the axes were disproportionate resulting in overlap between datasets. To better visualise the data, Cartesian axis limits were utilised. Using Cartesian axis limits rather than xlim and ylim ensured data outside of the set limits remained included in the plotted data and therefore the data visualised within the set limits was not altered. Limits were set to x(-0.01, 0.01) and y(-0.01, 0.01) allowing for a closer visualisation of the spread when using PCA method 2 (**Figure 3.2C**). Even with extremely small axes limits such as these, data was still largely overlapped, and it was difficult to make many relevant observations suggesting this method of PCA was inappropriate for this data. In addition to this, there are more appropriate methods to visualising and understanding PCA outlined during PCA optimisation (**Section 2.2.2**).

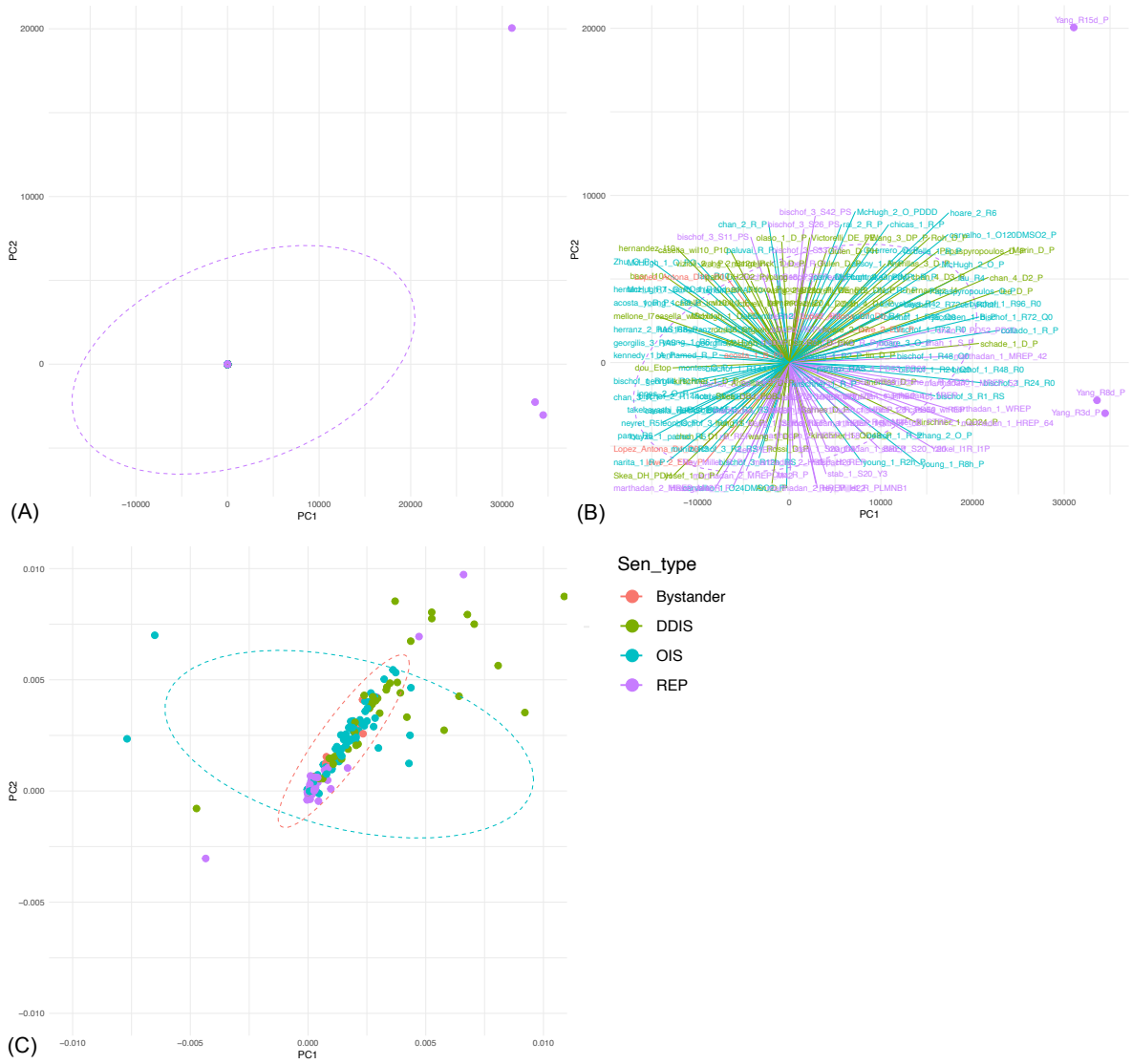

Figure 3.2 – PCA of FourSen_df using PCA Method 2.

(A) PCA of FourSen_df when nPCs = 15, with confidence ellipses plotted per Sen_type. (B) Labels for Comparisons were added, and (C) Cartesian axes limits applied for better visualisation.

As discussed in **Section 2.2.2**, NIPALS cannot tolerate a high volume of missing data. Therefore, the secondary preferred PCA Method 4 was employed: removing any column for which the LogFC gene expression data was comprised of 50% or more NA values. Removing columns with an over 50% NA content led to a reduction in missing data from 56.865% to 14.356% (**Figure 3.3**). This was still a high percentage of missing data, however it was a vast improvement. While missing data

is reduced, so was the total variance accounted for by the PCs: 26.66% with 2 PCs (**Figure 3.3A**); 53.91% with 5 PCs (**Figure 3.3B**); 67.80% with 15 PCs (**Figure 3.3C**).

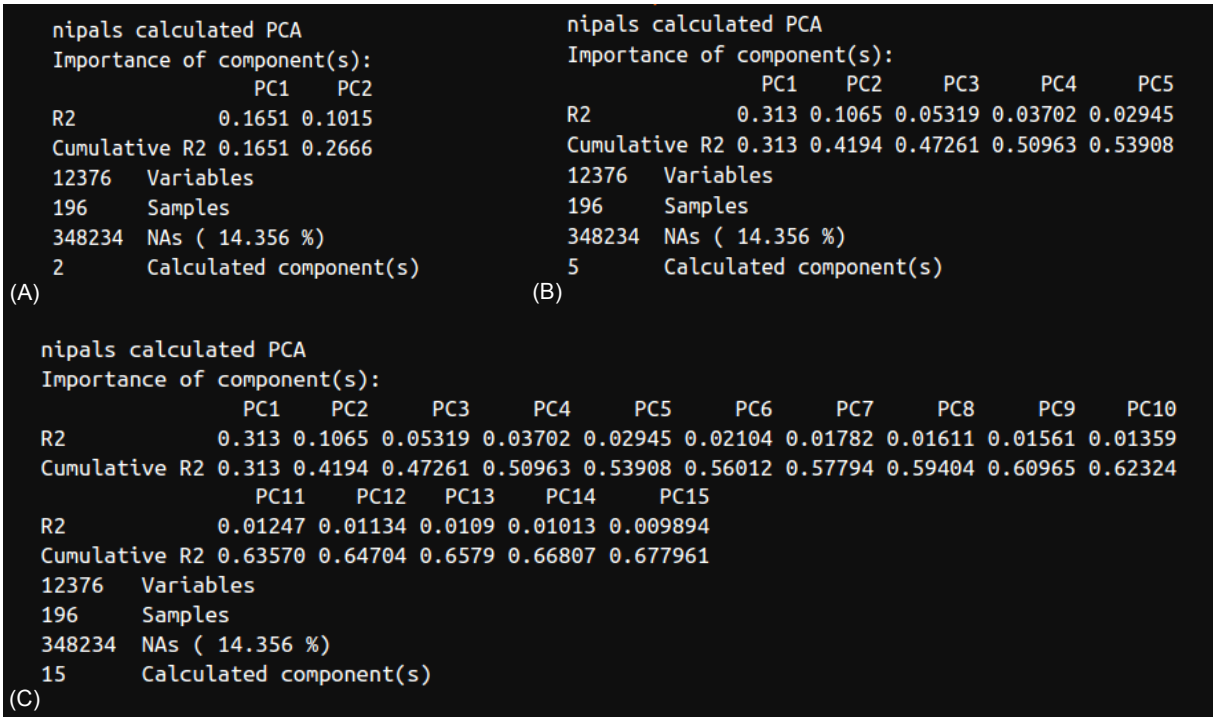

Figure 3.3 – PC data of FourSen_df using PCA Method 4.

Information of the PCs when (A) nPCs = 2, (B) nPCs = 5, and (C) nPCs =15.

The total variance in the data explained by the first two principal components (PCs) was 41.94%, regardless of whether the number of PCs (nPCs) was set to 5 or 15. Therefore, nPCs = 5 was chosen for all subsequent PCA visualisations, as it required less computational power while providing results that were equally accurate and consistent with higher levels of detail. Based on PC1 and PC2, data was visualised on a biplot and labelled by Sen_type (**Figure 3.5**). Confidence ellipses were plotted in colours matched to the labelled variable (in this case Sen_type) on the PCA plots to aid in observing any clustering by Sen_type. Overlap between all senescence types was observed, suggesting and supporting the assumption that senotherapeutics will be beneficial for all types of senescence and not just specific senescence types. However, there was also clear distinctions between all four senescence types, suggesting different senescence types have different transcriptomic profiles. Therefore, when developing senotherapeutics, it may be valuable to consider the senescence stimulus to better understand how the cell

responds and how this knowledge can be utilised to improve efficiency of senotherapeutics. Interestingly, BYS has the most distinct cluster compared to any other type of senescence. One possibility to explain this is that BYS is a secondary type of senescence while the rest are primary types. BYS exhibited an upward trend along PC2 and was more distributed along PC2, whereas the other senescence types were primarily distributed along PC1. OIS also exhibited an upward trend along PC2 while REP and DDIS exhibited a downward trend along PC2. Interestingly, the experimental design of the three BYS studies in this analysis induced BYS through OIS as the senescence stimulus (Acosta et al., 2013; Borghesan et al., 2019; López-Antona et al., 2022). This could be a possible explanation for why both BYS and OIS exhibited an upward trend along PC2 and REP and DDIS did not. It would be interesting to explore if BYS induced from different types of primary senescence would match that of the BYS studies plotted in **Figure 3.4**, or if they would be more similar to the senescence which acted as a stimulus for BYS induction. Data to explore this theory and fit within the SenOmic parameters does not currently exist and would need performing in a laboratory setting for incorporation into this analysis. SenOmic only contains paracrine induced bystander senescence types, however future work should consider and compare differences between paracrine induced and juxtacrine induced bystander senescence to see if there are any observable differences.

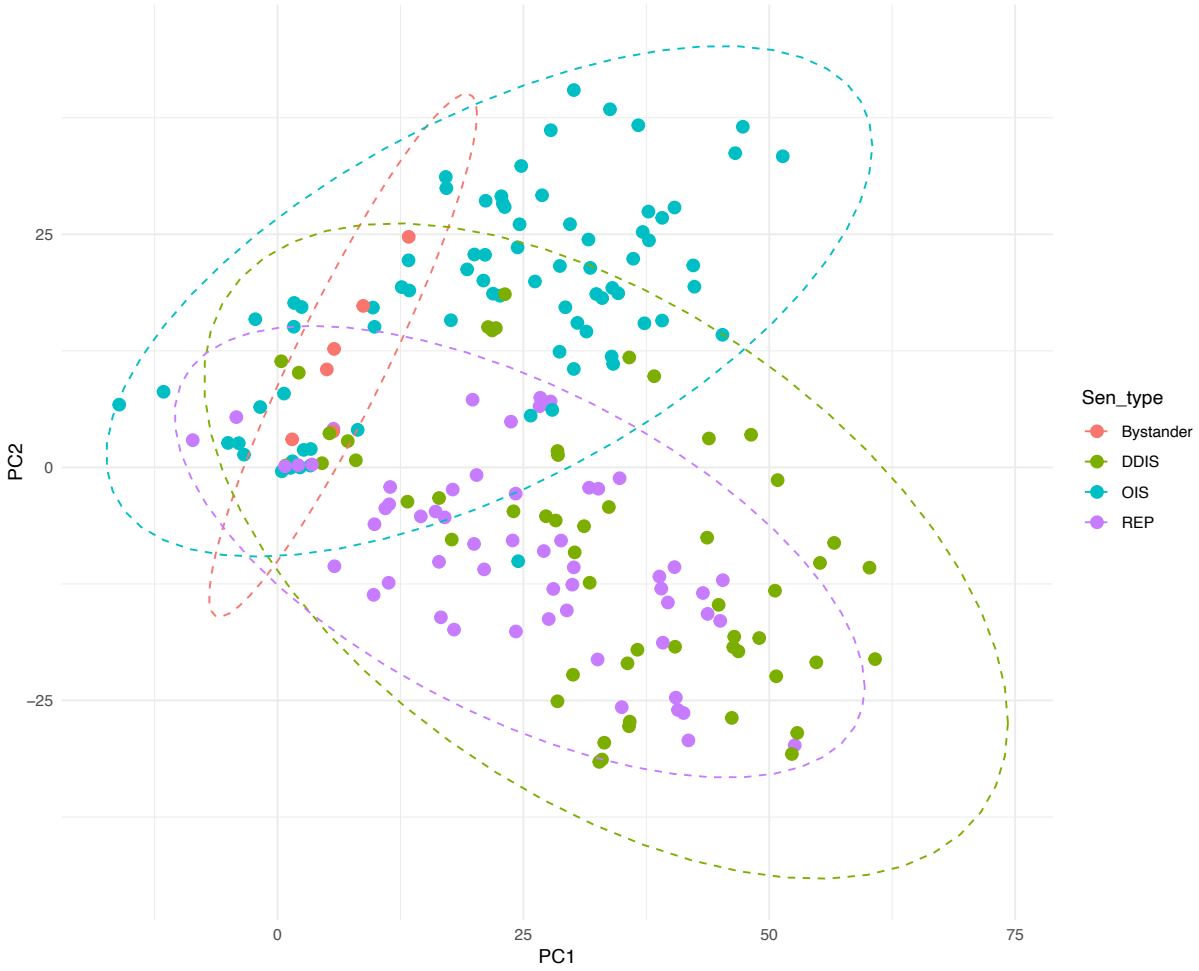

Figure 3.4 – PCA of FourSen_df labelled by Sen_type.

PCA produced using PCA Method 4 and labelled by Sen_type with confidence ellipses added to illustrate clustering. DDIS, DNA damage-induced senescence; OIS, oncogene-induced senescence; REP, replicative senescence; PC, principal component.

Moving forward, investigations were performed to examine the unique and shared features of the different senescence types. To do this, median p-values, LogFC, and MegaP were determined for each Gene in each of the senescence types. Median MegaP values were used to plot the Venn diagram so that genes which showed repeated significant change including both increases and decreases compared to proliferating cells were excluded from the set of genes that showed significant change in a consistent direction.

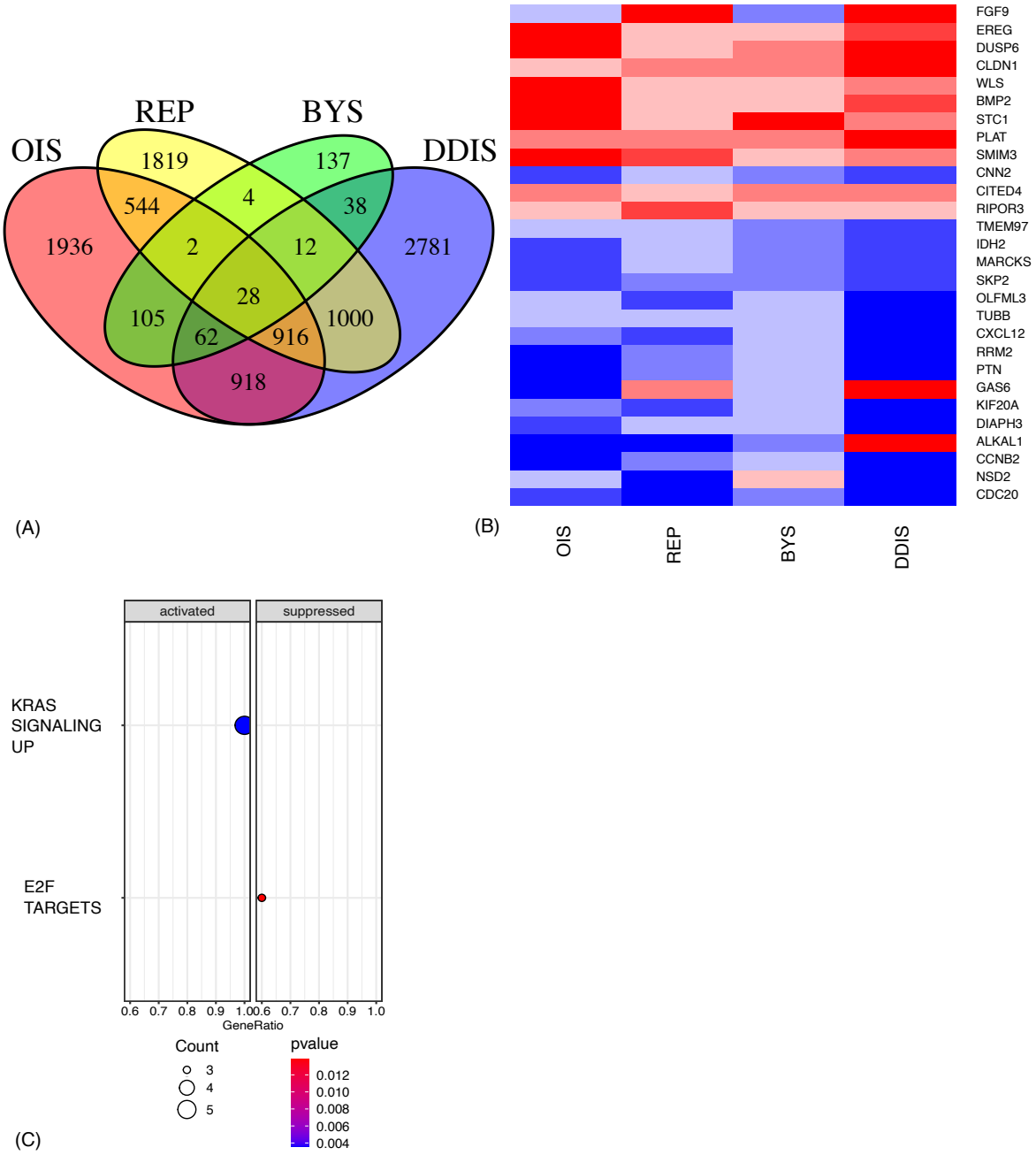

Figure 3.5 – Significant genes and pathways across the four types of senescent transcriptomes.

(A) Venn diagram of genes with median MegaP value that is significant across OIS, REP, BYS and DDIS. (B) Heatmap of the 28 genes that were significant for all four senescence inducers. Upregulated, red; downregulated, blue. (C) Dot plot of pathways from ORA of significantly activated and suppressed pathways for the 28 genes common in OIS, REP, BYS and DDIS. p-*value refers to the significance of the overrepresentation of the pathway and count reflects the number of genes associated with the pathway. OIS, oncogene-induced senescence; REP, replicative*

senescence; BYS, bystander induced senescence; DDIS, DNA damage-induced senescence; ORA, over-representation analysis. Taken from Scanlan et al. (2024).

A total of 28 genes were identified as significantly expressed in DDIS, OIS, BYS, and REP (**Figure 3.5A**), and were plotted on a heatmap following the method described in **Section 2.2.3** (**Figure 3.5B**). From here onwards, these 28 genes will be referred to as the Core Geneset. Within the Core Geneset, 14 genes were consistently downregulated across all senescence types, 10 genes were consistently upregulated across all senescence types, and expression of 4 genes were dependent on senescence type. The majority of the Core Geneset were expressed in the same direction across all senescence types, for example *EREG* (Epiregulin) is upregulated across all senescence types to varying degrees compared to proliferating cells. *EREG* is a protein coding gene for the protein epiregulin which is an epidermal growth factor involved in many biological processes; of note, wound healing is one of these processes and the role of senescence in wound healing is well documented (Chandrasegaran et al., 2024; Demaria et al., 2014; Jun & Lau, 2010).

While most genes in the Core Geneset have the same expression profile across all senescence types, interestingly some genes have a different expression profile dependent upon the senescence type: *FGF9* (Fibroblast Growth Factor 9) and *GAS6* (Growth Arrest Specific 6) are both upregulated in REP and DDIS, and downregulated in OIS and BYS; *ALKAL1* (ALK and LTK Ligand 1) is downregulated in OIS, REP and BYS, but upregulated in DDIS; *NSD2* (nuclear receptor binding SET domain protein 2) is upregulated in BYS and downregulated in DDIS, OIS, and REP. The fact that *NSD2* is specifically upregulated in the secondary type of senescence but not in primary types of senescence is worth noting as *NSD2* is a protein coding gene. The NSD2 protein has histone methyltransferase activity and can alter the epigenetic makeup of the cell, specifically the mono- and di-methylation of H3K36 (R. Chen et al., 2020; Weirich et al., 2024). This suggests that changes to the epigenome may play an important role in the induction of secondary senescence as these cells are not subjected to any direct DNA damage-inducing stimulus to arrest the cell cycle. It would be interesting for future work to take a multi-omic approach

and investigate the epigenome of primary versus secondary senescence in complex with the transcriptome and proteome.

Interestingly, of the Core Geneset, only one gene is present in the cellular senescence KEGG pathway (**Figure 3.6**): *CCNB2* (cyclin B2 – labelled CycB on the KEGG pathway). Cyclin B2 is involved in regulation of cell cycle progression, specifically the G2M checkpoint (Gong & Ferrell, 2010). In all four types of senescence *CCBN2* is significantly downregulated compared to proliferating cells, suggesting that cell cycle progression has been halted. While CCNB2 is found in the senescence KEGG pathway, it is not considered one of the typical senescence biomarkers as its function is not exclusive to senescence as it has an important role in regulating the cell cycle across all cells. The remaining 27 genes in the Core Geneset are likewise not considered typical senescence genes, and were consequently excluded from further discussion or analysis in this thesis. These results highlight the importance of re-evaluating the biomarker criteria for senescence studies, as genes not previously linked to senescence could provide new insights and improve the accuracy of senescence detection in various biological contexts.

When performing over-representation analysis (ORA) on the Core Geneset, only KRAS signalling upregulation is significantly activated and E2F targets significantly suppressed (**Figure 3.5C**). The lack of significantly enriched pathways is likely due to the limited number of genes available in the Core Geneset. The identification of only 28 genes and two pathways significantly enriched across the four types of senescence mainly reflected that BYS cells had fewer significant changes across all BYS studies (a total of 388 significant genes compared to DDIS, OIS and REP which all identify over 4000 significant genes). However, another possibility is that there are inherent differences between primary and secondary senescence types.

When deriving biological insight from ORA, it is necessary to consider whether up- and down-regulated genes were analysed as separate groups or combined. When analysed as separate groups, interpretation is straightforward: pathways identified as activated from up-regulated genes indicates pathway activation, while pathways identified as suppressed from up-regulated genes is indicative of pathway

suppression. However, when taking a combined gene approach as in this analysis, the direction of pathway regulation is not immediately clear as up- and down-regulated genes may be contributing to identification of an activated or suppressed pathway. Therefore, it is important to consider the direction of regulation of individual genes to understand the impact on pathway activity.

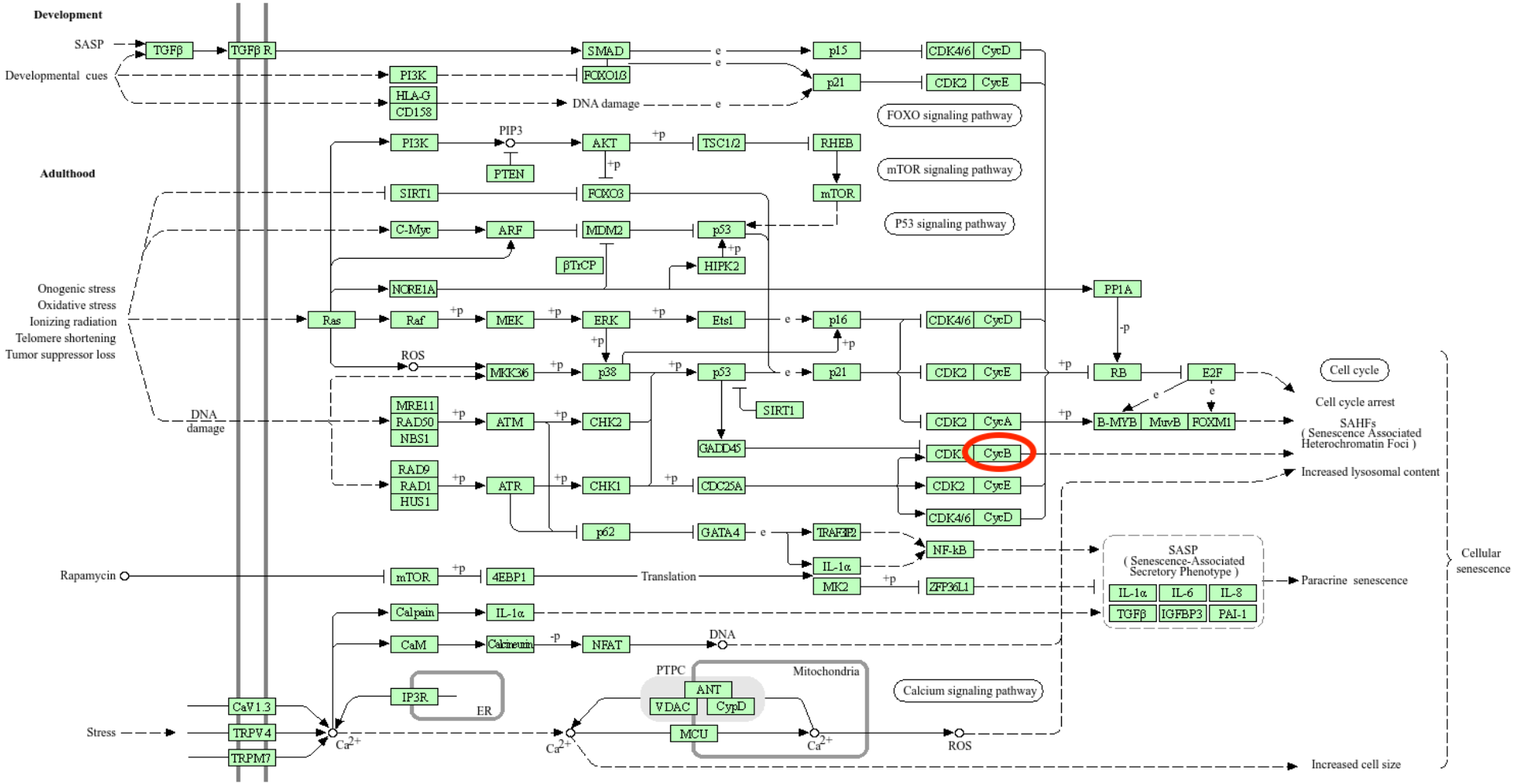

Figure 3.6 – Cellular senescence KEGG pathway.

CCBN2, identified by the Core Geneset, is encircled in red. The human pathway code is hsa04218 and is available at the following link: ***https://www.genome.jp/entry/pathway+hsa04218****.*

Two other studies have reported on identifying a core senescent gene signature in human fibroblast cells (Casella et al., 2019; Hernandez-Segura et al., 2017). Hernandez-Segura et al. (2017) identified a 55 gene signature in their non-systematic review of data which included six different fibroblast lines (BJ, IMR90, HFF, MRC5, WI38, and HCA2) for three different senescence types (REP, OIS, and DDIS). There was no overlap between our Core Geneset and the 55 gene signature identified by Hernandez-et al. (2017); however, *CNTLN*, *MEIS1, PLK3*, and *TSPAN13* were consistent with our 916 significantly expressed genes which excluded BYS. The study performed by Casella et al. (2019) which included two fibroblast cells lines (WI38 and IMR90) for three types of senescence (REP, OIS, and DDIS) identified a 68 gene signature for cellular senescence, and only *CLDN1* (Claudin-1) was consistent with our Core Geneset. In both the Casella et al. (2019) study and our study, *CLDN1* was upregulated. Claudin-1 is an integral membrane protein involved in tight junctions (Furuse et al., 1998). Therefore, the upregulation of *CLDN1* could indicate increased membrane activity such as that observed with SASP expression. Interestingly, KD of claudin-1 has been reported to significantly impair wound healing (Volksdorf et al., 2017), further highlighting its potential role in senescence. *ANP32B, CDCA7L, DHRS7, ELMOD1, HIST1H1A, HIST1H1D, HIST2H2AB*, *ITPRIPL1, JCAD, KIAA1671, LBR, LRP10, PAM, PARP1, PTMA,* and *SLC9A7* from our 916 significantly expressed genes which excluded BYS were consistent with the 68 gene signature observed by Casella et al. (2019). Between Casella et al. (2019) and Hernandez-Segura et al. (2017), only *POFUT2* was consistent across the core signatures identified. Notably both studies included non-fibroblast cells, and Hernandez-Segura et al. (2017) only included genes that were also significantly different to quiescent cells. These differences could account for the minimal overlap between the two core gene signatures and our Core Geneset.

A further study has reported on a core senescence gene signature comprising 125 genes and referred to as SenMayo; however, this analysis was conducted in human and mouse bone marrow samples (Saul et al., 2022). Ultimately, it would be advantageous to identify a core senescence gene signature across multiple cell types and tissues. When comparing the SenMayo gene signature to Hernandez-Segura et al. (2017), only one gene was common to both gene signatures (*TNFRSF10C),* and there were no common genes between the SenMayo and

Casella et al. (2019) gene signatures. Notably four genes (*BMP2*, *EREG*, *PLAT*, and *CXCL12*) were shared between SenMayo and the Core Geneset identified in this work (**Figures 3.5A-B**).

The analysis presented thus far in this thesis, the Hernandez-Segura et al. (2017) study, the Casella et al. (2019) study, and the Saul et al. (2022) study together reinforce the difficulties and complexity of identifying a clear and consistent transcriptional biomarker profile of senescence. One possible explanation for the lack of any clear core senescence signature is that the senescence profile may change temporally and our above data spans from day 0 to 28 days post senescence induction, while Hernandez-Segura et al. (2017) and Casella et al. (2019) only investigate up to 10 days post senescence induction.

Further laboratory validation would be required to confirm if the genes comprising the Core Geneset are an appropriate geneset to consult when investigating senescence; validation would especially have to take place *in vivo* to see if there is total or partial translation between *in vitro* and *in vivo* environments. Although, 28 genes seem like a large number to test for every time senescence is investigated, it is a smaller geneset than the gene signatures put forward by Hernandez-Segura et al. (2017), Casella et al. (2019), and Saul et al. (2022), making the Core Geneset identified here a more feasible option for translational potential.

Due to the lack of observable data regarding the Core Geneset, ORA was performed on the 916 significantly expressed genes common to DDIS, OIS, and REP, as well as the 388 significantly expressed genes specific to BYS (**Figure 3.7**).

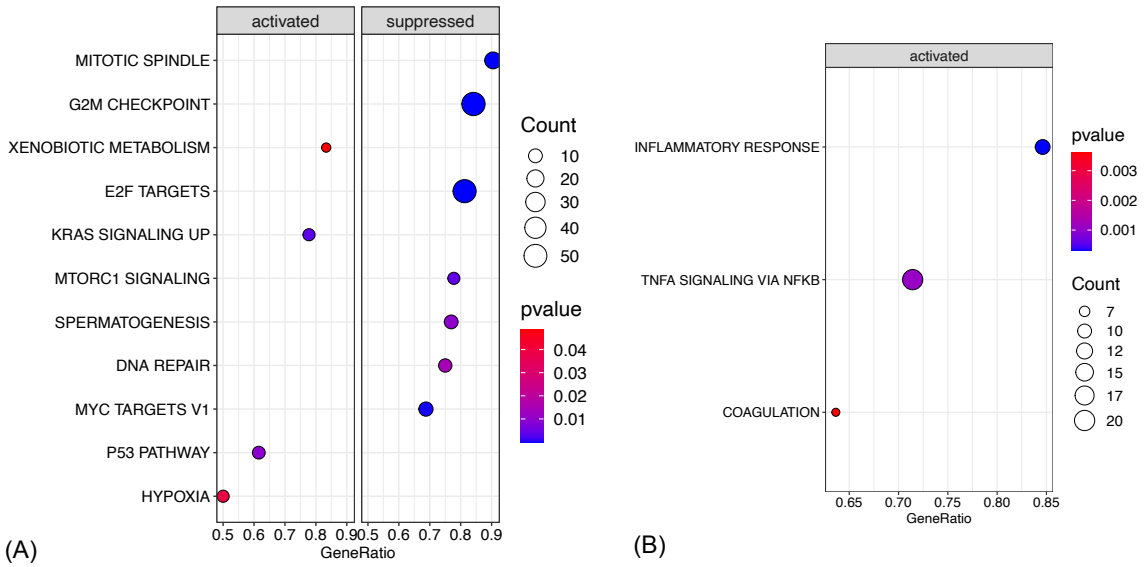

Figure 3.7 – Significant pathways for different senescence groups.

Dot plot of pathways from ORA showing pathways that are activated and suppressed between (A) the 916 genes common in OIS, REP and DDIS (p-value < 0.05), and (B) the 388 genes common to BYS (p-value < 0.05). p-value refers to the significance of the overrepresentation of the pathway and count reflects the number of genes associated with the pathway. DDIS, DNA damage-induced senescence; OIS, oncogene-induced senescence; BYS, bystander senescence. Taken from Scanlan et al. (2024).

ORA of the 916 genes common to primary senescence types of OIS, DDIS, and REP identified significant suppression of the mitotic spindle, G2M checkpoint, E2F targets, and DNA repair (**Figure 3.7A**), suggesting inhibition of the cell cycle and the DDR. This is supported by the fact senescence is considered a permanent state of cell cycle arrest (Kumari & Jat, 2021) and *CCNB2* was identified as significantly downregulated (**Figure 3.5B**). The suppression of DNA repair in senescent cells indicates that they are not attempting to resolve their genetic damage but are instead actively preventing DNA repair. Senescence is characterised by a state of permanent cell cycle arrest ending with immune-mediated senescent cell removal. This observation suggests that there could be an underlying mechanism which recognises senescent cells have entered a pathway of delayed cell death. As a result, cellular resources may be redirected from DNA repair and towards processes such as SASP and immune system signalling which would reinforce the senescent state and promote immune-mediated clearance.

Significant activation of xenobiotic metabolism, KRAS signalling, the p53 pathway and hypoxia pathway were also identified, alongside the significant inhibition of MTORC1 signalling, spermatogenesis, and MYC targets V1. Activation of the p53 pathway is somewhat expected as p53 signalling is a well-known aspect of cellular senescence, with p53 and p21 both acting as biomarkers for senescence identification (González-Gualda et al., 2021). Suppression of MTORC1 signalling is controversial as some studies have found that mTOR signalling is required for senescence (for example, PTEN-loss induced cellular senescence (Jung et al., 2019)), and that inhibition of mTOR with rapamycin can delay senescence progression (Demidenko & Blagosklonny, 2008; Xu et al., 2014). Moreover, there is a focus in ageing research on rapalogue therapies and how inhibition of mTOR can extend lifespan (Weichhart, 2018).

BYS is a type of secondary senescence and it distinctly clustered in PCA from the primary senescence types (**Figure 3.4**). A total of 388 genes were identified as significantly expressed in BYS compared to proliferating control cells (**Figure 3.5A**). ORA was performed on the 388 genes significantly expressed in BYS, identifying only the significant activation of three pathways (**Figure 3.7B**). The limited number of pathways enriched in the 388 geneset is likely due to the fewer genes available in the geneset. Intriguingly, these pathways included the activation of the inflammatory response and TNFA signalling via NFKB. The inflammatory SASP is well recognised in senescence (Coppé et al., 2010), yet these pathways were not significantly enriched in the primary senescence types. One possibility for why this could be is that it has been demonstrated by numerous studies that the SASP and NF-κB are causal in inducing BYS (Acosta et al., 2013; Nelson et al., 2018). Notably, there was no overlap between the significantly enriched pathways between the primary senescence types and secondary bystander senescence.

The ORA (**Figure 3.5C** and **Figure 3.7**) strongly suggest that the common changes in expression for senescent cells, with the exception of BYS cells, is the suppression of the cell cycle and DDR, with different inducers suppressing different genes within these pathways. The fact that BYS cells were not suppressing these pathways is interesting. Of the four senescence inducers, BYS had the fewest studies and

comparisons, which increases the impact of outlier studies when calculating the median MegaP value. Thus, this difference may simply reflect that BYS cells have less data available. However, it may also reflect the difference between primary and secondary senescence which is not yet well understood (Admasu et al., 2021; Teo et al., 2019).

3.2.3 Observed differences in cell lines and organ origin.

SenOmic contains many variables which can be used to explore the heterogeneity of senescent cells. Understanding how different cells and cell types respond to inducers of senescence is important as this can dictate which senotherapeutics would be most effective or how they are applied, i.e. would a lotion/gel be better for skin fibroblasts compared to an oral drug? This work cannot answer this question, but it can begin to help explore what specific targets could be of interest.

To investigate how cell line and organ of origin influence the senescent transcriptome, PCA was conducted and labelled by cell line or organ (**Figure 3.8**). Due to the large number of cell lines in the database, it was difficult to determine clear clustering based on cell line. Additionally, confidence ellipses were not plotted for all cell lines as some cell lines were represented by minimal datapoints (**Figure 3.8A**). Most cell lines exhibited similar distributions on the PCA plot; however, BJ cells (coloured **peach**), HCA2 cells (coloured **olive-green**) and HFF cells (coloured **light-green**) displayed distinct clustering patterns. These findings suggest that while some cells exhibit unique transcriptomic profiles, the majority share similar characteristics. Regarding the organ origin of cells (which was either the skin or lung), distinct differences were observed such as skin fibroblasts being primarily distributed along PC1 and lung fibroblasts being primarily distributed along PC2 (**Figure 3.8B**). A considerable amount of overlap was also evident, suggesting that senotherapeutics may be broadly relevant for treating senescent cells across different tissue environments. However, this approach of broadly treating senescent cells throughout the body should be used with caution to minimise off-target effects.

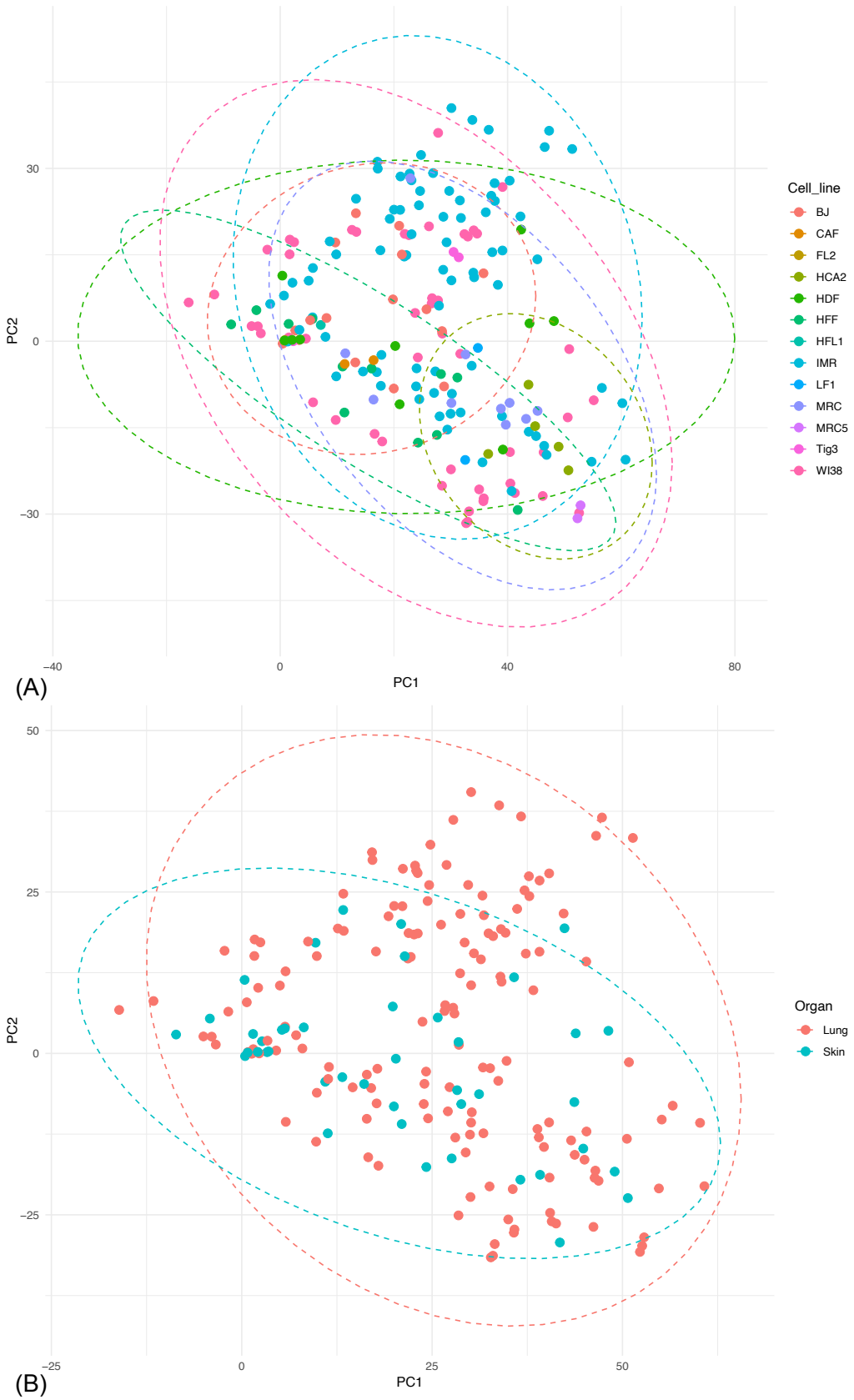

Figure 3.8 – PCA of FourSen_df labelled by organ and cell line.

PCA of comparisons of (A) cell lines and (B) organ in FourSen_df with IQR filtering when nPCs = 5.

Encouragingly, but increasing complexity, there were aspects of both uniqueness and similarity when labelling by organ, just as there was when labelling by Sen_type. Therefore, the next step was to plot a Venn diagram of significantly expressed genes following the pairwise protocol detailed in **Section 2.2.3** to determine if there was a specific core signature and how this compared to the Core Geneset of 28 genes identified by Sen_type-based analysis.

As with the previous Venn diagram, the significant median MegaP values were plotted (**Figure 3.9**). Although there were more genes unique to each organ than common to them both (2718 genes significantly and uniquely expressed in only skin fibroblasts, and 2096 genes significantly and uniquely expressed in lung fibroblasts), there were 1294 genes significantly expressed in both senescent skin and lung fibroblasts. Performing heatmap analysis on a set of 1294 genes is challenging as annotating the expression direction of each gene can become unfeasible.

When comparing these 1294 genes to the Core Geneset identified as significantly expressed in DDIS, OIS, REP, and BYS (**Figure 3.2A**), 27 of the genes were significantly expressed in lung fibroblasts and 24 genes were significantly expressed in skin fibroblasts. In senescent lung fibroblasts *GAS6* was not significantly expressed, while *BMP2*, *CITED4*, *RIPOR3,* and *ALKAL4* were not significantly expressed in senescent skin fibroblasts.

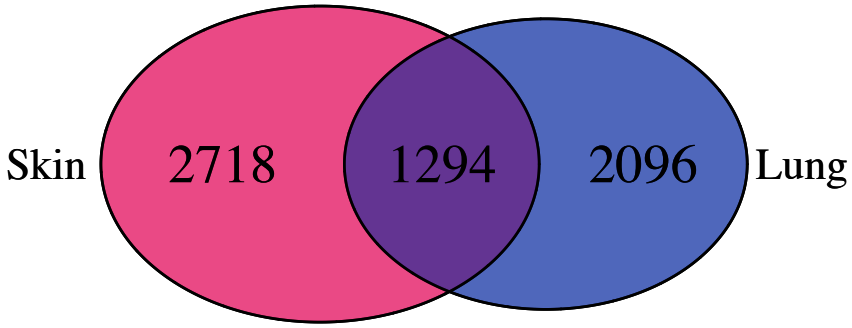

Figure 3.9 – Significant genes grouped by organ type.
Venn diagram of genes with a significant median MegaP value in skin and lung fibroblasts.

Of the 1294 significantly expressed genes common to both skin and lung, when performing ORA, no genesets were significantly enriched (p-value < 0.05 or p-value < 0.1). Therefore, ORA was performed without a significance threshold to determine if any pathways were enriched in the 1294 genes (**Figure 3.10**). There were many expected enriched pathways including suppression of the mitotic spindle, G2M checkpoints and E2F targets, and activation of the inflammatory response and p53 pathway. Noted earlier was the significant enrichment of genes involved in suppression of DNA repair in DDIS, OIS and REP cells (**Figure 3.7A**) which suggested senescent cells are not trying to resolve the genetic damage caused by the senescence inducing stimuli. These pathways were also identified as a commonly enriched pathway in both skin and lung fibroblasts, although they were not significantly enriched. While this observation is noteworthy, significantly expressed genes being involved in the activation of apoptosis was also observed. Together these findings support the earlier suggested theory that senescent cells have entered a delayed cell death pathway, with cellular resources being redirected to promote cell death rather than repair. These cellular changes, however, could also represent cells being redirected into a state of cell maintenance rather than repair.

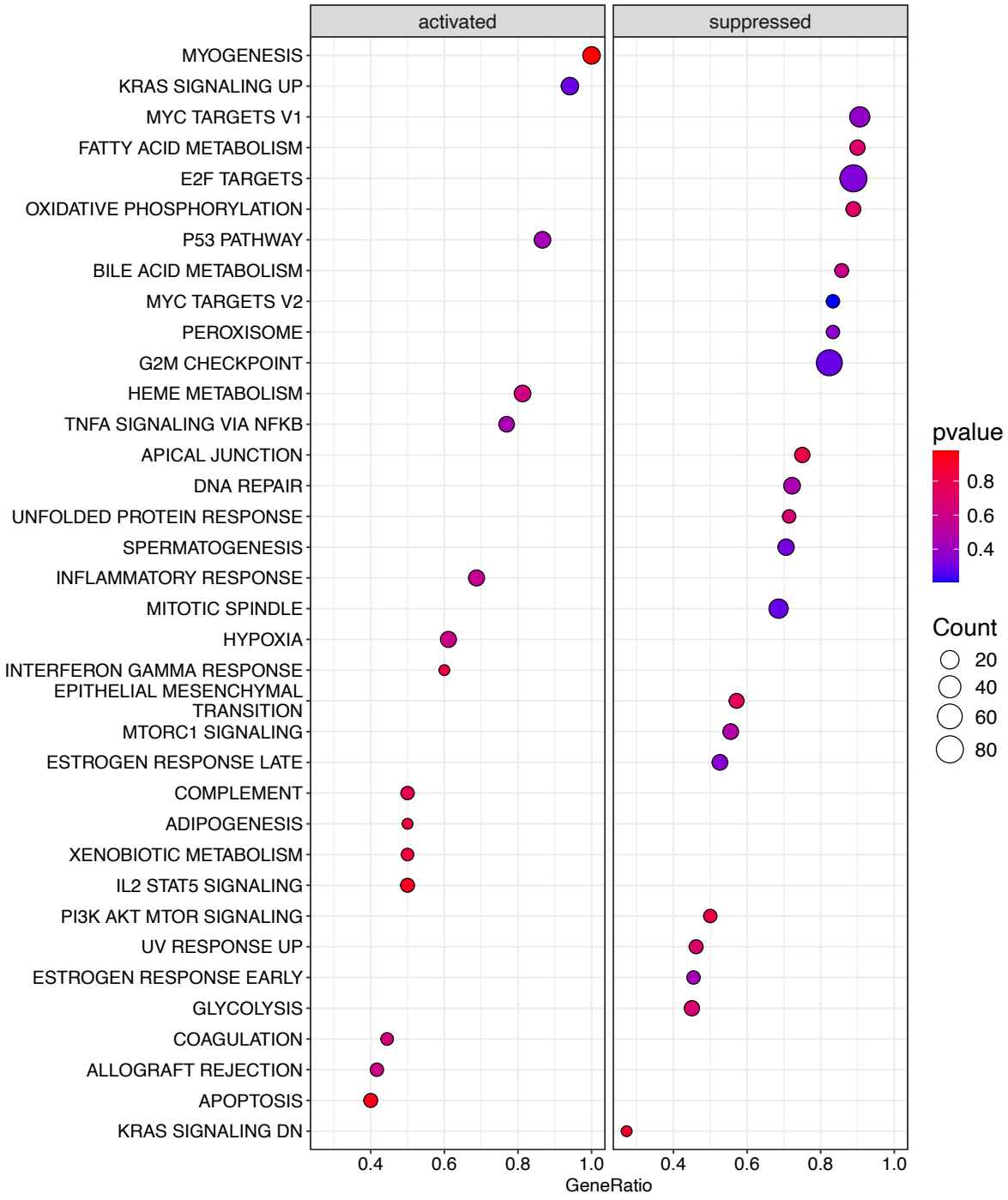

Figure 3.10 – ORA of significant pathways in senescent lung and skin fibroblasts.

Dot plot of pathways from ORA of activated and suppressed pathways identified in the 1294 genes common in both skin and lung fibroblasts. p-*value refers to the significance of the overrepresentation of the pathway and count reflects the number of genes associated with the pathway.*

Likewise, when performing ORA separately on all significantly expressed genes in skin or lung fibroblasts, there were no significantly enriched genesets (p-value < 0.05). With a more lenient threshold of p-value < 0.1, only the suppression of MYC targets V2 was identified in the lung specific genes (**Appendix Figure A3.2**), while no enriched genesets for skin specific genes were identified. Although no genesets were identified as significantly enriched, numerous pathways were enriched when analysing the 3390 expressed genes in lung cells (**Figure 3.11**), and the 4012 expressed genes in skin cells (**Figure 3.12**) with no significance threshold.

The majority of enriched genesets were shared between lung and skin fibroblasts, with some of these expected for senescent cells and observed in previous ORA such as the suppression of E2F targets and the mitotic spindle. However, notable differences were observed between the two organ types. For example, genes significantly expressed in senescent lung fibroblasts were enriched in the activation of inflammatory related pathways including IFNα, IFNγ, IL2-STAT5, and IL6-JAK-STAT3 signalling, but were suppressed in senescent skin fibroblasts. This suggests that lung fibroblasts may exhibit a greater predisposition to inflammatory responses, and potentially a stronger SASP compared to skin fibroblasts. Unique genesets identified included activation of protein secretion and hedgehog signalling as well as suppression of notch signalling and WNTβ catenin signalling in senescent lung fibroblasts (**Figure 3.11**), and the suppression of TGFβ signalling and the ROS pathway in senescent skin fibroblasts (**Figure 3.12**).

Figure 3.11 – ORA of significant pathways in senescent lung fibroblasts.

Dot plot of pathways from ORA of activated and suppressed pathways identified in the 3390 genes expressed in lung fibroblasts. p-value refers to the significance of the overrepresentation of the pathway and count reflects the number of genes associated with the pathway.

Figure 3.12 – ORA of significant pathways in senescent skin fibroblasts.

Dot plot of pathways from ORA of activated and suppressed pathways identified in the 4012 genes expressed in skin fibroblasts. p-value refers to the significance of the overrepresentation of the pathway and count reflects the number of genes associated with the pathway.

An organ-based investigation into the senescence transcriptome revealed a great amount of overlap in gene expression and pathway enrichment, suggesting that broad-use senotherapeutics could be effective across multiple tissue types. However, the analysis also identified genes and pathways unique to the specific organ type.

For example, the TGFβ signalling pathway was identified as suppressed in senescent skin fibroblasts, although not significantly (**Figure 3.12**), but was not identified in senescent lung fibroblasts (**Figure 3.11**). This observation is interesting as TGFβ signalling is a well-established driver of fibrosis (Biernacka et al., 2011). The apparent suppression of TGFβ signalling in senescent skin fibroblasts may indicate an effect to potentially reduce fibrosis. In contrast, the lack of detectable changes in TGFβ signalling in senescent lung fibroblasts suggests genes associated with TGFβ signalling remain largely unchanged compared to proliferating control cells, implying that senescence in lung fibroblasts may not alter TGFβ signalling activity. Together this suggests that the specific cell environment should be considered in future senescence research and in the design of senotherapeutics. This has significant implications for future senescence research, particularly translation into senotherapy in a clinical setting.

3.2.4 Sex differences in cellular senescence.

In all biology, there are observed differences between the sexes from as obvious as reproductive organs, to females being more predisposed to autoimmune diseases while males are more susceptible to bacterial infections (Dias et al., 2022; Klein & Flanagan, 2016). There are many age-related diseases which show sex-bias in humans, including diabetes and heart disease which males are more predisposed to suffer from, and females having a higher death rate due to Alzheimer's disease (Fritz García et al., 2024). Moreover, studies have identified sex differences in senescence, with higher p21 mRNA levels in female leukocytes compared to males (Guan et al., 2022), longer telomere lengths in females (Gardner et al., 2014), a greater degree of telomere uncapping in females (Walker et al., 2016), and significant sex-dependent differences observed in SASP proteins (Martín-Escolano et al., 2023). Understanding how biological sex influences ageing and senescence is increasingly important in the context of an ageing global population and evolving gender dynamics, including a rise in individuals seeking gender-affirming hormone therapy (Das & Dusetzina, 2023).

SenOmic exclusively contains *in vitro* data; therefore, any investigation of sex differences using this database is conducted within the context of *in vitro* studies. Investigating sex differences *in vitro* may not reveal much as typically there are no

sex hormones included during cell culture and key biological context is missing. However, SenOmic offers the opportunity to investigate sex differences across multiple studies and datasets, making any observations more likely to be robust compared to *in vitro* studies which rely on a single dataset. It is imperative to note that most cells in SenOmic are not from primary patient cells, which means sex differences may not be fully observable due to the loss of cell-specific characteristics over time.

Sex needed adding as a variable to SenOmic as it did not previously exist. As previously mentioned, the cell types included in the FourSen data.frame were CAF, FL2, BJ, HFF, MRC/MRC5, Tig3, HDF, HFL1, HCA2, IMR, LF1, and WI38. As detailed in **Section 2.2.4**, the biological sex of each cell line was identified, and the variable ‘Sex’ was added to the data.frame using the mutate function from the dplyr library (Wickham et al., 2023) – detailed in **Code 2.5**.

(A)

```
nipals calculated PCA
Importance of component(s):
                  PC1    PC2     PC3     PC4     PC5
R2            0.3138 0.1069 0.05341 0.03719 0.02958
Cumulative R2 0.3138 0.4207 0.47412 0.51131 0.54090
12375   Variables
193     Samples
336623  NAs ( 14.094 %)
5       Calculated component(s)
```

(B)

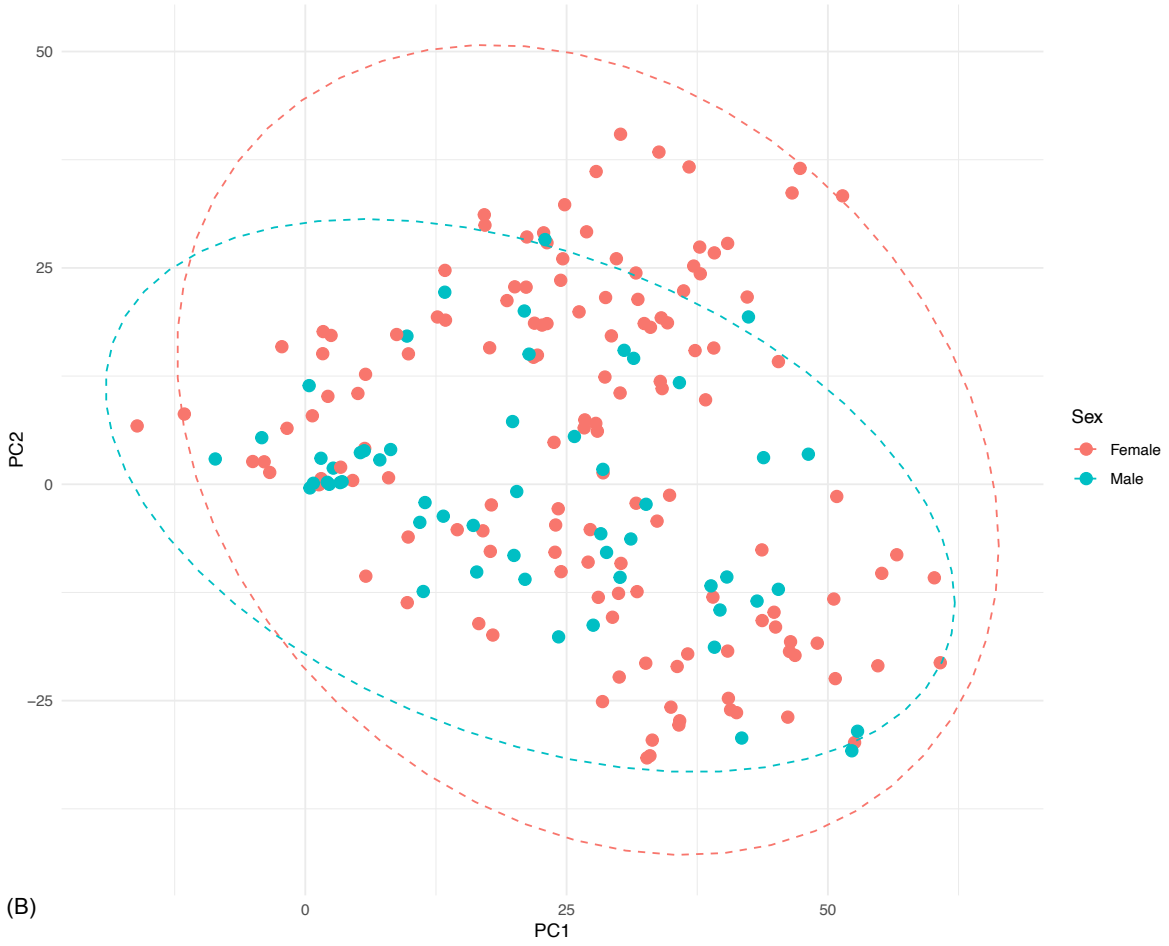

Figure 3.13 – PCA of FourSen_IQR labelled by variable Sex.

Using PCA Method 4, PC statistics when nPCs = 5 (A) and biplot with confidence ellipses labelled by Sex (B).

Removal of the two cell lines which had an indeterminate sex origin reduced the percentage of missing data from 14.356% (**Figure 3.3B**) to 14.094% (**Figure 3.13A**), and the total variance accounted for in the dataset by the first two PCs increased from 41.94% to 42.07%. These changes were minimal. PCA and visualisation of the data including the cell lines whose Sex was 'NA' showed no obvious difference other than the addition of 2 datapoints (**Appendix Figure A3.3**), suggesting that these studies did not strongly influence the overall transcriptomic phenotype.

Both male and female cells showed similar distributions along PC1, indicating shared variance in the primary PC of the data. Additionally, both sexes exhibited an upward trend along PC2. However, a notable difference in clustering patterns was observed, with male cells forming a more compact cluster compared to the broader distribution of female cells (**Figure 3.13B**). Overall, PCA labelled by 'Sex' revealed minimal differences between male and female cells. This lack of distinction could be attributed to several factors: the *in vitro* nature of these experiments lacking the complex biological context of *in vivo* systems; the possibility that cells have undergone extensive passaging and/or adaptation and have thus lost some of their original characteristic; the influence of other factors (such as the age of the cell donor and organ of origin); or the potential that there were simply no significant transcriptomic differences between the sexes in senescent human fibroblasts. Investigation of sex differences should be considered further with *in vivo* models and/or with primary cells *in vitro* to fully elucidate the truth of whether there are any sex-based differences when it comes to senescence in human fibroblasts, as these results could have potential impacts on senotherapy regimes.

During this sex differences analysis, the wrong sex was assigned to cell line 'HCA2' which represents five datapoints in **Figure 3.13**. As this was identified post-submission analysis was not re-conducted, therefore it is worth noting that these five datapoints may have contributed towards the minimal differences identified in clustering between the sexes.

3.2.5 Knockdown of p53 and RELA in DDIS and OIS.

While it is important to look at how genes are expressed in normal cellular senescence conditions, it is also important to understand how senescent cells respond to KDs as this will improve the basic understanding about the biology of senescence, which will aid in senotherapeutic design. In this section, different data was used compared to previous sections in this chapter. Previously KD data was excluded, but to understand the impact KDs have on the senescent transcriptome it had to be included. Therefore, the data.frame detailed in **Section 2.2.5** was created for analysis.

In the SenOmic database there were 85 different unique genes knocked down. Nine datasets introduced *TP53* (p53) or *RELA* (RelA) KDs, all conducted in either DDIS or OIS conditions. The genes selected for KD analysis were chosen based on two key characteristics of senescence: cell cycle arrest mediated by p53 signalling and p16 signalling (Freund et al., 2011; Kumari & Jat, 2021), and the expression of the inflammatory SASP (Acosta et al., 2013; Coppé et al., 2010). These are two well established characteristics of senescence, making the expression of related genes particularly relevant in KD analysis.

When investigating the impact of knocking down p53, there were seven unique datasets, two in DDIS and five in OIS. Genes directly related to p53 signalling were first investigated: *TP53* (p53), *CDKN1A* (p21), and *MDM2* (MDM2). As expected, KD of p53 resulted in downregulation of p53 (**Figure 3.14A**), p21 (**Figure 3.14B**), and MDM2 (**Figure 3.14C**); significant downregulation in DDIS for all three genes, and significant downregulation of p21 in OIS. Observation of significant downregulation across all three genes in DDIS but not in OIS suggests that DDIS may be more dependent on p53 signalling as a means to induce cell cycle arrest compared to OIS. The next genes investigated were *CDKN2A* (p16 – **Figure 3.14D**) and *MAPK14* (p38 – **Figure 3.14E**). In OIS, the expression of both genes remained largely unchanged when a p53 KD was introduced. However, in DDIS, the median expression of p16 increased (although not significantly) and the expression of p38 was significantly increased (p-value < 0.05) after introduction of the p53 KD. These findings support the hypothesis by Freund et al. (2011) that p53 is restraining expression of p38. The analysis then turned to inflammatory SASP-related genes. *IL1B* (IL-1β – **Figure 3.14F**), *IL6* (IL-6 – **Figure 3.14G**), and *CXCL8* (IL-8 – **Figure 3.14H**) after p53 KD were chosen to be investigated. In DDIS, p53 KD resulted in significant upregulation of IL-1β, while median expression levels of IL-6 and IL-8 also increased but not significantly. In OIS when a p53 KD was introduced, expression of all three genes remained consistent with expression when there was no genetic manipulation. These findings suggest that p53 may suppress the inflammatory SASP, potentially through p38 regulation. Identification of increased expression of SASP-related genes in response to a p53 KD could explain the lack of initial inflammatory SASP activity in senescent cells.

Overall, significant changes in gene expression were observed primarily in DDIS, suggesting that DDIS is more reliant on p53 signalling than OIS. Genes associated with cell cycle arrest tended to be downregulated following p53 KD (**Figure 3.14 A–D**) while inflammatory SASP genes tended to be upregulated (**Figure 3.14 E–H**). These observations highlight the complex role of p53 in senescence and the pathways p53 activity can influence.

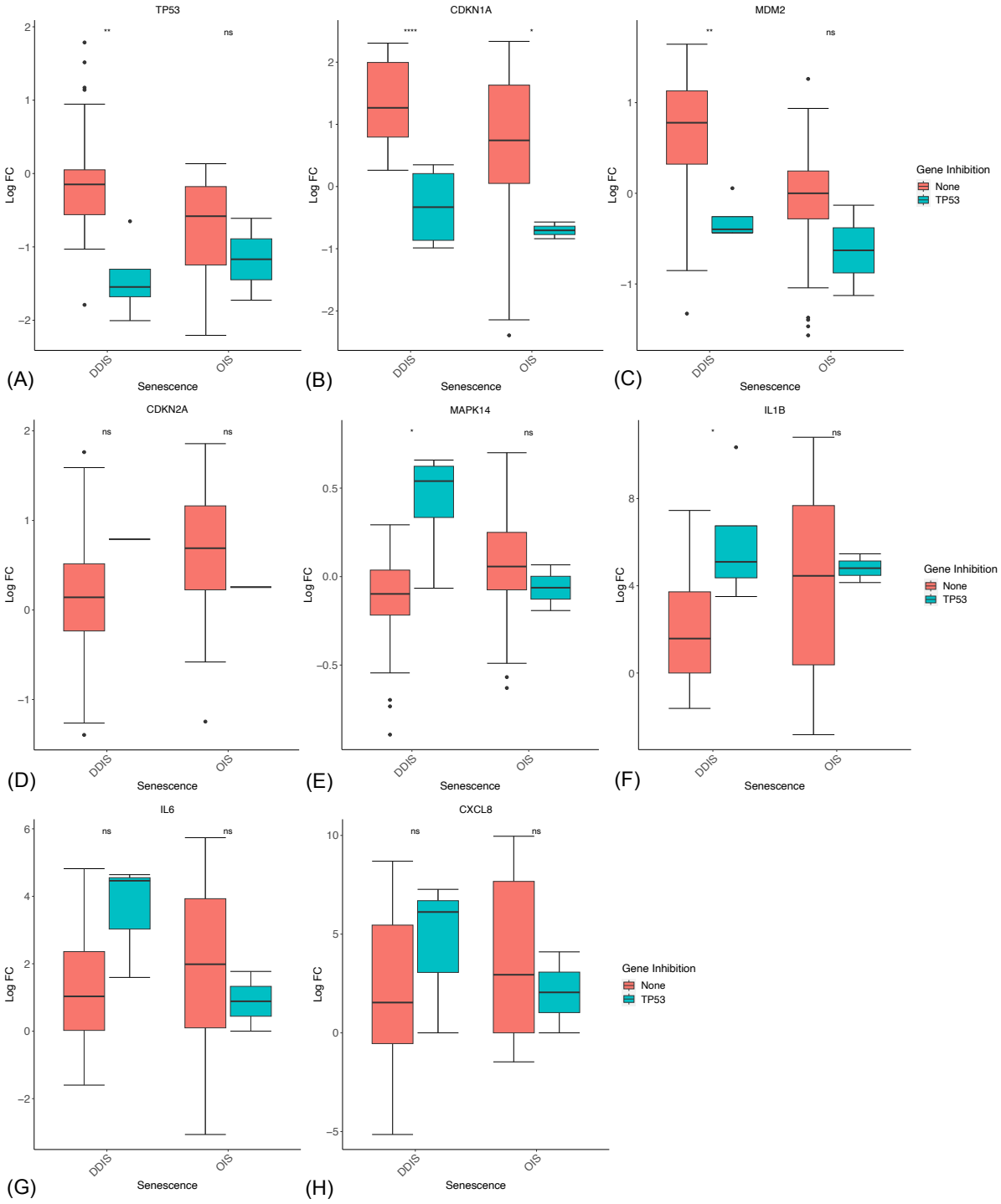

Figure 3.14 – Expression of senescence related genes when p53 is knocked down.

*Gene expression in DDIS and OIS with and without p53 inhibition. Control samples are proliferating samples. DDIS, DNA damage-induced senescence; OIS, oncogene-induced senescence; LogFC, log2 fold change; p-value refers to significance in expression of the gene with and without p53 inhibition; *p-value <0.05; **p-value <0.01; ***p-value <0.001. Taken from Scanlan et al. (2024).*

Four studies examined the impact of a *RELA* (RelA) knockdown on senescence, focusing exclusively on OIS. Therefore, only OIS results will be discussed below. To maintain consistency with the p53 KD analysis, the same set of genes were investigated.

Interestingly, KD of RelA resulted in the downregulation of p53-signalling related genes p53 (**Figure 3.15A**), p21 (**Figure 3.15B**), and MDM2 (**Figure 3.15C**), although none of these changes were statistically significant. This trend suggests a connection between RelA and p53. The expression of p16 remained relatively similar as observed by the similar median expression (**Figure 3.15D**), while p38 showed a non-significant trend towards increased expression in response to the RelA KD (**Figure 3.15E**).

NF-κB, a major TF involved in the transcription of inflammatory genes (Liu et al., 2017), is made up of two main subunits. The most common subunit conformation of NF-κB includes RelA, as a p50-RelA heterodimer (Hoffmann & Baltimore, 2006). As expected due to the role RelA is known to play in the expression of inflammatory genes, there was an observable downregulation of IL-1β (**Figure 3.15F**), IL-6 (**Figure 3.15G**), and IL-8 (**Figure 3.15H**) in response to the RelA KD. While this was only significant (p-value < 0.05) for IL-6 expression, expression of IL-1β and IL-8 both decreased and median expression was lower. The median expression of all three inflammatory genes became lower than 0 LogFC after the introduction of the RelA KD, highlighting the importance of NF-κB in regulating the inflammatory SASP.

These findings further highlight the role of NF-κB in regulating the SASP – a well-documented process (Chien et al., 2011; Ouvrier et al., 2024; Salminen et al., 2012). Of note, it has also been observed that RelA potentially promotes p53 signalling; when RelA was knocked down, p53 signalling (demonstrated with p53, p21 and MDM2) had a lower median expression compared to standard OIS samples (**Figures 3.15A-C**). This suggests there could be a regulatory feedback loop between p53 and NF-κB in senescence which acts to promote cell cycle arrest and secretion of SASP proteins to promote immune clearance.

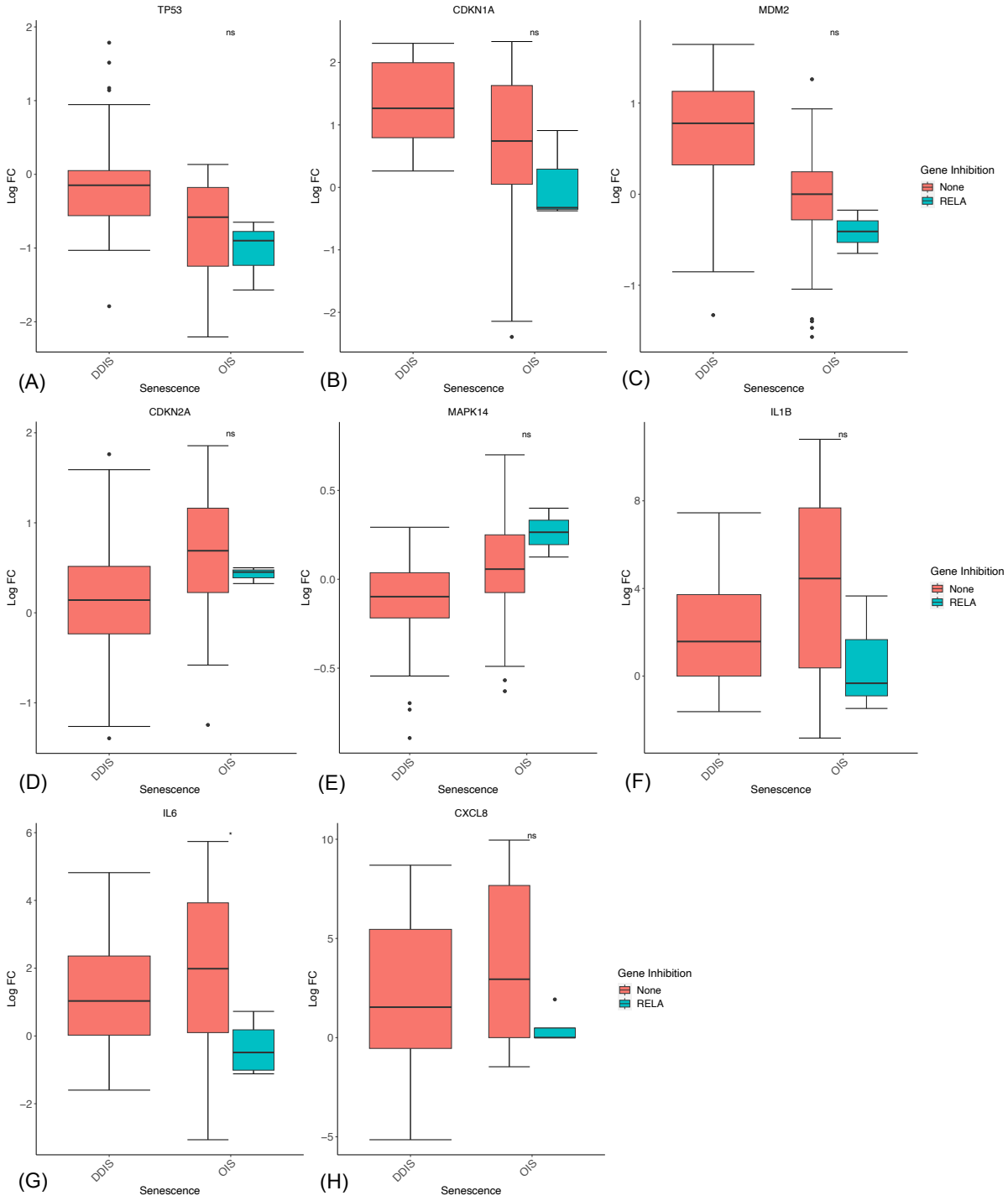

Figure 3.15 – Expression of senescence related genes when RelA is knocked down.

Gene expression in OIS with and without RelA inhibition. Control samples are proliferating samples. DDIS, DNA damage-induced senescence; OIS, oncogene-induced senescence; LogFC, log2 fold change; p-*value refers to significance in expression of the gene with and without RelA inhibition;* *p-value *<0.05. Taken from Scanlan et al. (2024).*

KD data observed at the transcriptomic level (**Figures 3.14** and **3.15**) was used to aid in informing the protein computational model in **Chapter 5**.

3.3 Conclusion.

This study highlights the heterogeneity and variety of factors that influence the senescent transcriptome, supported by other non-systematic studies (Casella et al., 2019; Hernandez-Segura et al., 2017; Saul et al., 2022). By creating SenOmic and systematically examining the senescence transcriptome of human fibroblasts, this study contributes to a comprehensive understanding of the complexity of the transcriptomic phenotype of senescence; additionally, it highlights gaps in current knowledge that could be the basis for future work, particularly in relation to secondary senescence and how the transcriptome (and other omics such as epigenomics) may differ from primary senescent cells.

PCA was performed on the IQR filtered FourSen_df and labelled for different groups: Sen_type (**Figure 3.4**), cell line (**Figure 3.8A**), organ (**Figure 3.8B**), and sex (**Figure 3.13**). Visualisation of the PCA demonstrated that senescence type is the biggest determining factor on the senescence transcriptome – particularly with the identification of BYS, a secondary type of senescence, as having a distinctive transcription pattern. This study highlights the differences between primary senescence (DDIS, OIS, and REP) and secondary senescence (BYS); particularly how there was no identification of cell cycle arrest or the DDR in BYS cell transcriptomes (**Figure 3.7B**), which was otherwise present in primary senescence cells (**Figures 3.5C** and **3.7A**). Despite all the data referring to *in vitro* studies, the analysis points to factors such as cell line, organ and sex likely having a larger influence in *in vivo* systems as they provide biological context such as sex hormones.

Interestingly, investigating KDs in the senescent transcriptome led to several clear conclusions. The effects of p53 and RELA KDs revealed a stronger dependence on p53 signalling in DDIS compared to OIS (**Figures 3.14 A-C**), the role of NF-κB signalling in SASP induction was reinforced (**Figures 3.15 F-H**), and a connection between RelA and p53 was revealed, as a RelA KD resulted in the downregulation of p53-related genes (**Figures 3.15 A-C**). These distinct differences between senescent

types are valuable for senotherapeutic strategies, as it suggests compounds which target p53 signalling pathways, for example, may be more effective in DDIS.

While this work established a robust foundation for investigating the transcriptome of human senescent fibroblasts, incorporating a multiomic and temporal approach would enhance the depth of understanding in senescence research. Therefore, to support this systematic analysis, the temporal dynamics of senescence was explored in the upcoming chapters; temporal changes in the expression of core senescence-associated proteins were analysed at the transcript level (**Chapter 4**), and a qualitative computational model was developed to simulate temporal protein expression in DDIS and OIS (**Chapter 5**). Together these approaches provide a more comprehensive understanding of the dynamic nature of senescence and how the senescence phenotype changes temporally.

Chapter 4: The temporal transcriptome of human senescent fibroblasts.

4.1 Background.

4.1.1 Temporal investigation of senescence at the transcript level.

With the advancement of high-throughput technologies over the past few decades, more laboratories now have the capacity and accessibility to perform omic analysis. As technologies have advanced, the cost of performing such experiments has reduced. This has allowed for more thorough research to be conducted and has led to an increase in temporal omic analysis. Despite temporal analysis becoming more popular, it is still an underutilised area of research; partly because it is still resource-intensive to assess multiple timepoints in a laboratory setting. However, cells are not static. Cells are inherently dynamic and ever changing, therefore it is impossible to truly understand how a cell, or a specific protein or pathway, is behaving by assessing only one or limited timepoints.

The gap in temporal knowledge is particularly evident in the study of cellular senescence. Although there are some well characterised temporal phenotypes of senescence, the overall temporal understanding of senescence is limited. It is well established that senescent cells first enter cell cycle arrest, typically following DNA damage of such a degree it is unresolvable. However, how long cell cycle inhibitors are expressed and whether this expression is maintained through to late senescence is not well evidenced. Although, some studies do suggest p21 and p16 expression is transient (He & Sharpless, 2017; Kumari & Jat, 2021; Robles & Adami, 1998). Furthermore, some studies suggest TGFβ signalling is active following senescence induction and that TGFβ signalling reduces as senescence progresses (Hoare et al., 2016; Tominaga & Suzuki, 2019). The best evidenced and understood temporal dynamics of senescence relate to the SASP, a secretory phenotype composed of molecules including inflammatory cytokines, growth factors, and matrix metalloproteinases (Basisty et al., 2020; Chien et al., 2011; Coppé et al., 2008). The development of the SASP is known to be delayed by 4–7 days following senescence induction (Coppé et al., 2008; Hernandez-Segura et al., 2017; Orjalo et al., 2009). Many proteins and/or genes typically increase in expression beyond the initial

expression point, however most studies do not explore beyond day 10 post-senescence induction and therefore SASP composition in late senescence is unknown.

In **Chapter 3**, senescence was investigated as a whole biological process to further the understanding of senescence heterogeneity and how different factors influence the transcriptome. Building upon this, the following two chapters examine the temporal transcriptomic and protein profiles of senescence in human fibroblasts to advance our understanding of how senescence evolves over time. By integrating core and temporal phenotypes, this work seeks to uncover key molecular transitions that define progression of senescence. Such insights can inform the improvement and targeted development of senotherapeutics to alleviate senescence-associated disease burden, ultimately improving healthspan. Specifically, this chapter aims to explore and utilise SenOmic to elucidate core temporal transcriptomic signatures in senescence, including the temporal analysis of specific identified genes and recognised senescence-related genes.

4.2 Results and Discussion.

The results in this chapter were obtained using the methods detailed in **Section 2.2**. **Figure 4.1** was created using the methods detailed in **Section 2.2.2**. **Figures 4.8**, **4.9**, **4.10**, and **4.11** are published in Scanlan et al. (2024). **Figure 4.7** was produced at the same time of analysis as Scanlan et al. (2024) but not published. **Figures 4.2**, **4.3**, **4.4**, **4.5**, and **4.6** were created using the methods published in Scanlan et al. (2024) but were produced at a later timepoint.

In **Chapter 4**, time_groups were created in FourSen_df for BYS, DDIS, OIS, and REP; the four types of senescence investigated in detail in the previous chapter. Different time_groups were applied to REP compared to DDIS, OIS, and BYS as the methods of senescence induction vary greatly; with REP being a natural long-term replicative induced senescence compared to a faster induced form of senescence. Interestingly, PCA identified DDIS as being more similar to REP than to OIS (**Figure 3.4**). Despite this, the time_groups were still split for REP, and DDIS, OIS, and BYS as the time it takes for senescence induction to occur is what is important when investigating the temporal profile.

For REP analysis the time_groups created were (i) 0–40, and (ii) 41+. Most REP studies in SenOmic did not state the time point after induction, often the population doubling (PD) is reported but not always. Creation of two groups, 0–40 days after senescence induction and 41+ days after senescence induction, was chosen under the assumption that waiting 41+ days reflected a deliberate attempt to look at long term senescence and therefore the study would have noted the time point.

As the time taken to induce DDIS, OIS, and BYS differs from that of REP, the following time_groups of time after induction (in days) were created for temporal analysis on DDIS, OIS, and BYS: (i) 0–4, (ii) 5–7, (iii) 8–11, (iv) 12–14, (v) 15+. These time_groups were chosen based on knowledge in published senescence work and guided by the data available in the SenOmic database. Although 15+ days was created as a time_group, only DDIS was represented across 4 studies and five comparisons. In DDIS and OIS, there were 7 additional comparisons which did not have a defined timepoint and therefore they were excluded from temporal analysis.

The first time_group, spanning 0–4 days post-senescence induction, was selected based on multiple studies observing an early fibrogenic, TGFβ-rich SASP prior to the onset of inflammatory SASP induction (Hoare et al., 2016; Ito et al., 2017). By defining 0–4 days as its own time_group, this allowed the opportunity to investigate the early transcriptomic composition of cells becoming senescent prior to establishment of the inflammatory SASP.

The second time_group, 5–7 days post-senescence induction, was selected as this time frame likely captures the upregulation and expression of inflammatory SASP genes. Previous studies have identified the onset of the inflammatory SASP as occurring between 5 to 8 days post-senescence induction (Coppé et al., 2010). Having distinct time_groups which should encompass the establishment of senescence and the induction of the inflammatory SASP created the opportunity to explore what causes this distinctive switch in gene expression, allowing for a more detailed understanding of the temporal nature of the senescent transcriptome.

The third time_group, 8–11 days post-senescence induction, was defined because most studies investigating late senescence timepoints typically only focus up to 10 days post-senescence induction. Therefore, this time_group will contain the majority of the later senescence timepoint data. And indeed, in the FourSen_df data.frame, time_group 8–11 days represents 72% of the data for DDIS, OIS, and BYS datasets after day 8.

Finally, time_groups 12–14 days and 15+ days post-senescence induction were defined as distinct time_groups rather than a singular 12+ time_group due to significant variability in the timepoints observed beyond day 15; one DDIS study was performed at day 28 post-senescence induction (X. Zhang et al., 2021) and it is possible day 28 post-senescence induction has a different transcriptomic phenotype to day 14 for example. Additionally, there was more data availability for days 12–14 post-senescence induction compared to 15+. Therefore, having them as distinct time_groups reduces the risk of skewed results or the appearance of artifacts in the analysis.

First, PCA was performed following the PCA Method 4 protocol detailed in **Section 2.2.2** (**Figure 4.1**).

Regarding REP, the PCA revealed distinct clustering patterns between the 0–40 days (coloured **gold**) and 41+ days (coloured **blue**) time_groups. Time_group 0–40 days showed a distribution primarily along PC1, while time_group 41+ days displayed an upward distribution predominantly along PC2.

Furthermore, there was clear clustering and separation of transcriptomic profiles within the defined DDIS, OIS, and BYS time_groups, reflecting distinct shifts in gene expression patterns over time. During senescence establishment (time_group 0–4 – coloured **peach**) and SASP expression (time_group 5–7 – coloured **purple**), the majority of data variance was explained by PC1. Notably, time_group 5–7 exhibited a unique downward distribution on PC2, suggesting that the activation of the inflammatory SASP might be driven by a distinct set of transcriptomic changes compared to earlier and later stages of senescence. This downward trend could also

reflect a temporary switch in gene networks as cells transition from senescence establishment to SASP expression, and SASP expression to late senescence.

Comparison of time_groups 0–4, 5–7, and 8–11 (coloured **pink**) revealed particularly interesting clustering dynamics. While the variance in time_groups 0–4 and 5–7 was primarily explained by PC1, there was a notable transition in time_group 8–11, where the variance became primarily explained by PC2. Additionally, there was a change in the direction of distribution along PC2: from a downward trend in time_group 5–7 to and upward trend in time_group 8–11. This transition could represent a switch in cellular states, such as those moving from the induction of inflammatory proteins to later stage senescence.

Time_groups 12–14 (coloured **green**) and 15+ (coloured **teal**) displayed an upward trend along PC2 as observed in time_group 8–11; although with a less pronounced slope. While time_group 12–14 showed a relatively even distribution across PC1 and PC2, time_group 15+ demonstrated slightly less variation explained by PC1 and a more prominent upward trend along PC2. Both time_groups exhibited looser clustering compared to earlier time_groups which could be attributed to the limited number of studies in these time_groups. Alternatively, it may reflect late senescence as lacking a consistent transcriptomic phenotype.

Interestingly, the upward distribution along PC2 observed in time_groups 8–11, 12–14, and 15+ aligned with the clustering of time_group 41+ for REP, suggesting that 41+ represents a late-stage REP phenotype. In contrast, time_group 0–40 likely encompasses a mixture of cells transitioning into senescence and early senescence as the clustering is most similar to time_group 0–4.

These observations emphasise the importance of considering temporal dynamics when investigating senescence and highlight the inherently dynamic nature of senescence. The distinct clustering patterns and transitions observed across time_groups highlight how gene expression profiles evolve temporally. Moreover, this analysis may provide insight into the mechanisms driving variability within each time_group, offering valuable insights into factors contributing towards the senescence phenotype and its heterogeneity.

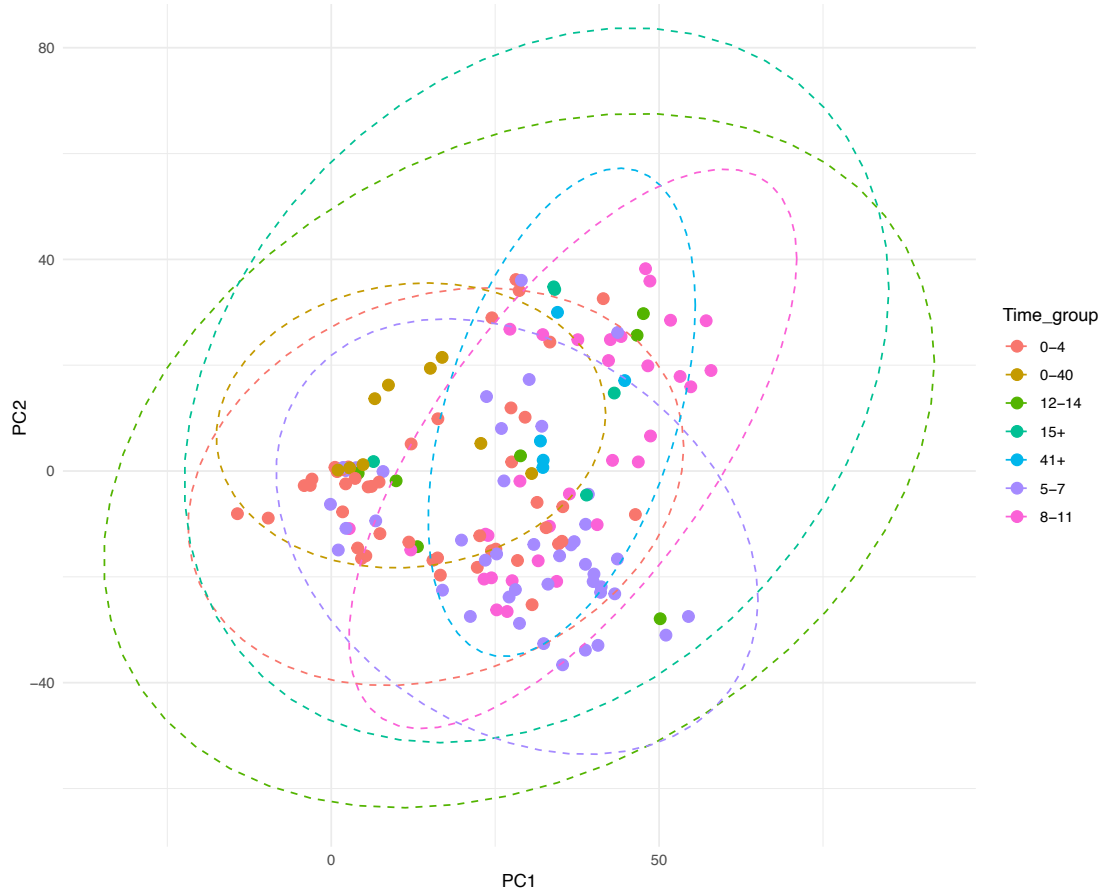

Figure 4.1 – PCA of FourSen_df labelled via time_group.

Time_groups 0-40 and 41+ are for REP datasets; Time_groups 0-4, 5-7, 8-11, 12-14 and 15+ are for BYS, DDIS, and OIS datasets. PCA Method 4 was employed on the FourSen_df data.frame with the addition of confidence ellipses during visualisation. REP, replicative senescence; BYS, bystander induced senescence; DDIS, DNA damage-induced senescence; OIS, oncogene-induced senescence.

4.2.1 Temporal similarities between the transcriptomes of DDIS and OIS.

To investigate the temporal profile of senescence in more detail, Venn diagrams and ORA comparing the described time_groups for DDIS and OIS were performed. Time_group 15+, Sen_type == “REP,” and Sen_type == “BYS” were excluded from any further analysis in this section. Time_group 15+ was excluded due to limited data for these timepoints; BYS was excluded due to it being a form of secondary senescence which has distinct clustering compared to DDIS and OIS (**Figure 3.4**);

REP was excluded due to the difference in time_groups. A median value for LogFC, p-value, and MegaP for each gene was calculated for each senescence type and time_group.
There were 42 comparisons available in days 0–4 post-senescence induction – composed of 14 DDIS datasets, and 28 OIS datasets. This was the largest set of data for any of the DDIS/OIS time_groups devised, illustrating that the majority of experimental senescence analysis takes place during early timepoints – potentially under the assumption that the profile would be the same at these time points as at a later timepoint. However, as illustrated in the PCA (**Figure 4.1**) this is not the case. Later timepoints in senescent cells should therefore be investigated in laboratory settings to enhance the understanding of basic senescence biology.

To begin analysing time_group 0–4, the significantly expressed genes in DDIS and OIS were investigated. To do this, the data.frame which contained the data for time_group 0–4 days was filtered by its median MegaP value. If the median MegaP value was <= -20, or >= 20, then the gene was significantly expressed, and anything in that range was plotted as a Venn diagram (**Figure 4.2A**). Interestingly, there was a much larger number of significantly expressed genes in DDIS than in OIS. Despite this, 684 genes were commonly significantly expressed in both DDIS and OIS in comparison to proliferating control cells. ORA was performed on these 684 genes and numerous significant pathways were identified; including suppression of E2F targets, G2M checkpoint, DNA repair, mitotic spindle (**Figure 4.2B**), all which support that senescent cells are entering a state of cell cycle arrest.

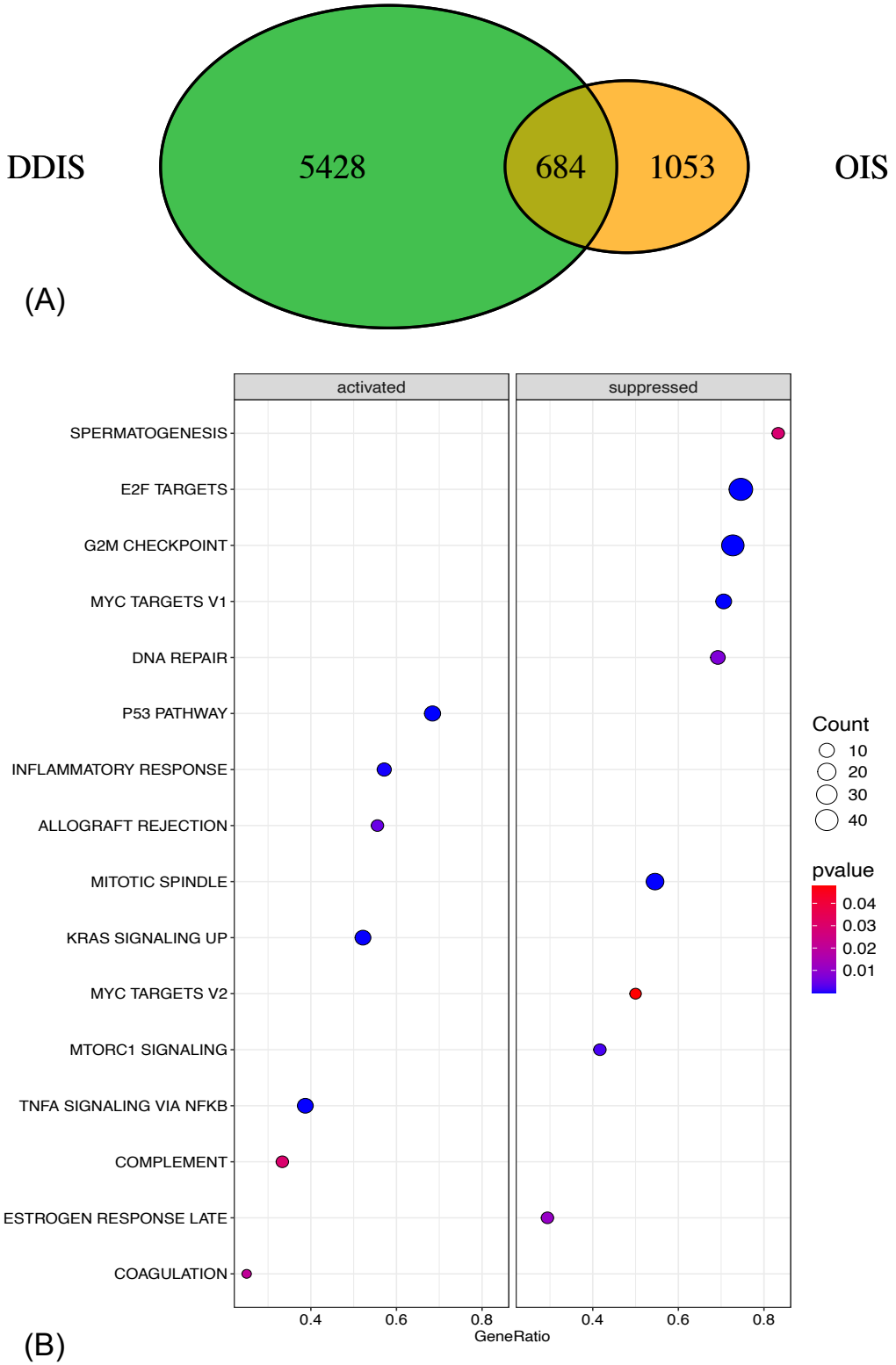

Figure 4.2 – Significant genes and pathways 0–4 days after senescence induction.

(A) Venn diagram of genes with a median MegaP value that is significant across DDIS and OIS 0-4 days post-senescence induction. (B) Dot plot of pathways from ORA of significantly activated and suppressed pathways identified in the 684 genes

common in DDIS and OIS. p-value refers to the significance of the overrepresentation of the pathway and count reflects the number of genes associated with the pathway. DDIS, DNA damage-induced senescence; OIS, oncogene-induced senescence; ORA, over-representation analysis.

There were 41 comparisons available in time_group 5–7 – composed of 9 DDIS datasets, and 32 OIS datasets. 1461 genes were identified as significantly expressed in DDIS and OIS compared to proliferating control cells (**Figure 4.3A**). ORA of the 1461 genes identified many significant pathways, with many similar to time_group 0-4, including suppression of the G2M checkpoint, E2F targets, and activation of the p53 pathway and inflammatory response (**Figure 4.3B**). However, some pathways were not significantly enriched including suppression of DNA repair (although this was identified when there was no p-value applied to the ORA – **Appendix Figure A4.1**). Interestingly, several additional pathways were significantly enriched for time_group 5–7 compared to time_group 0–4, including the activation of inflammatory related pathways such as IL6 JAK STAT3 signalling, IL2 STAT5 signalling, and the interferon gamma response. The enrichment of these inflammatory-related pathways aligns with the known timing of SASP expression. One of the most notable and interesting pathways identified as significantly enriched in the 1461 geneset was the activation of protein secretion. This finding supports and enhances the established understanding of SASP as being delayed following senescence induction (Coppé et al., 2008; Hernandez-Segura et al., 2017; Hoare et al., 2016). The upregulation of protein secretion at this timepoint likely reflects the senescent cells preparing for and actively secreting SASP-related proteins.

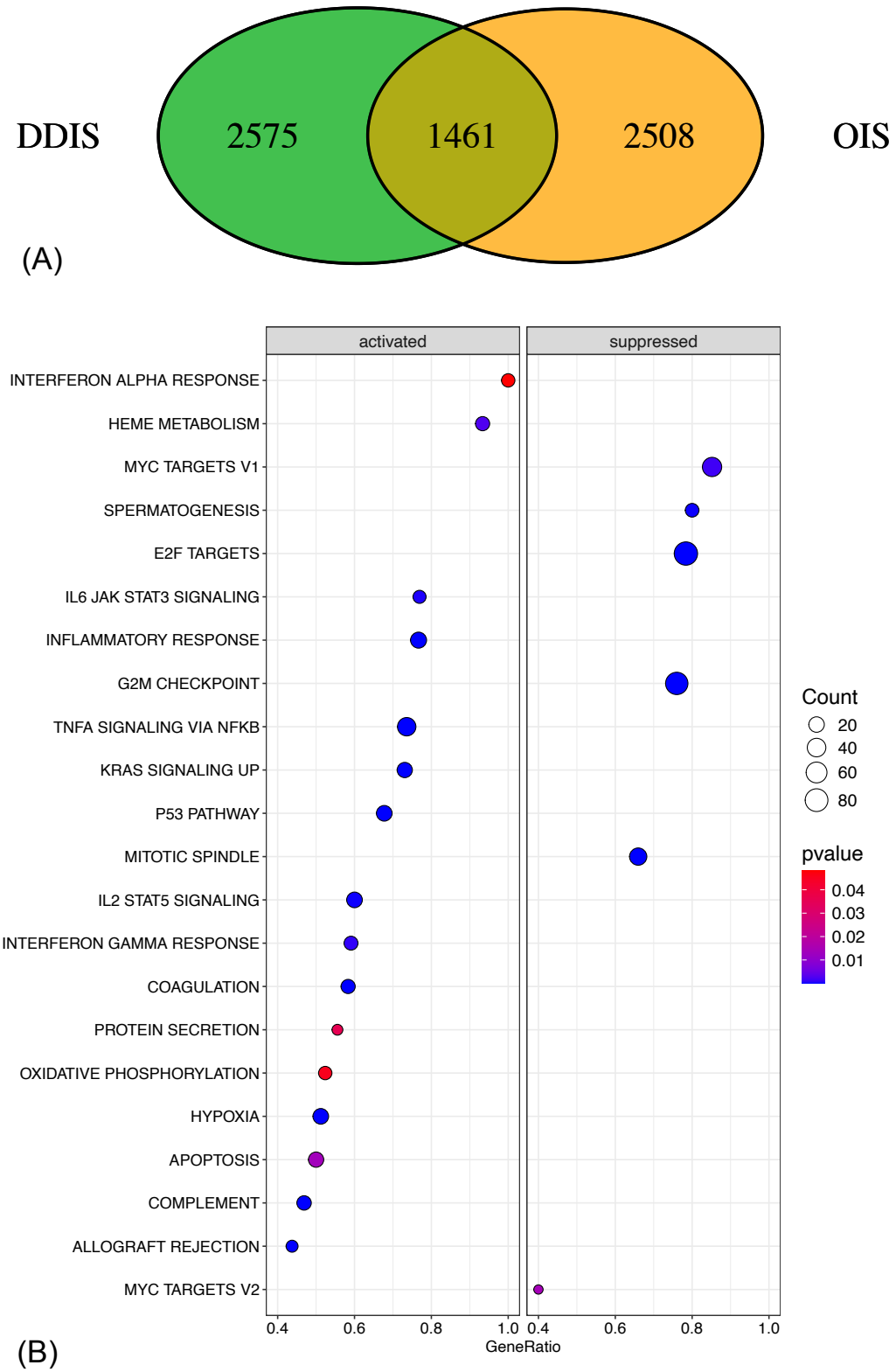

Figure 4.3 – Significant genes and pathways 5–7 days after senescence induction.

(A) Venn diagram of genes with a median MegaP value that is significant across DDIS and OIS 5-7 days post-senescence induction. (B) Dot plot of pathways from ORA of significantly activated and suppressed pathways identified in the 1461 genes

common in DDIS and OIS. p-value refers to the significance of the overrepresentation of the pathway and count reflects the number of genes associated with the pathway. DDIS, DNA damage-induced senescence; OIS, oncogene-induced senescence; ORA, over-representation analysis.

There were 31 comparisons available in time_group 8–11 – consisting of 20 DDIS datasets and 11 OIS datasets. 1922 genes were identified as significantly expressed compared to proliferating control cells in DDIS and OIS (**Figure 4.4A**). ORA of these 1922 genes revealed many significantly enriched pathways (**Figure 4.4B**), allowing an insight into temporal-associated senescence changes at late time points.

Several pathways enriched in earlier time_groups were also identified in time_group 8–11, such as the suppression of E2F targets, the G2M checkpoint and mitotic spindle all of which suggest active maintenance of cell cycle arrest rather than senescent cells relying only on the initial induction of cell cycle arrest. Additionally, activation of inflammatory-related pathways such as IL6 JAK STAT3 signalling and IL2 STAT5 signalling were observed, supporting the idea that even at later stages of senescence, cells are maintaining a pro-inflammatory state. However, time_group 8–11 revealed new pathways not seen at earlier timepoints, including activation of the epithelial mesenchymal transition, angiogenesis, and adipogenesis. These findings suggest that at mid-late timepoints of senescence, cells undergo morphological and phenotypical changes that could influence the microenvironment, neighbouring cells, and tissue remodelling processes. These changes are based on *in vitro* analysis and may not directly translate to *in vivo* systems; however, it would be interesting to see if these changes are reflected *in vivo* as this may represent a factor which influences disease burden.

Interestingly, the protein secretion pathway was not identified at this time_group even when there was no p-value threshold applied during ORA. This could indicate that once the protein secretion machinery has been synthesised, it may not need to be produced continuously. This suggests a potential shift in focus during mid-late senescence to remodelling of the microenvironment, which could result in inducing bystander senescence or signalling to the immune system for clearance. Further investigations into the mechanics of protein secretion at the protein level would

provide valuable insight into the dynamic nature of senescence, which could lead to the identification of new therapeutic targets to prevent the secretion of SASP-related proteins and thus mitigating the low-level chronic inflammation associated with senescence and ageing.

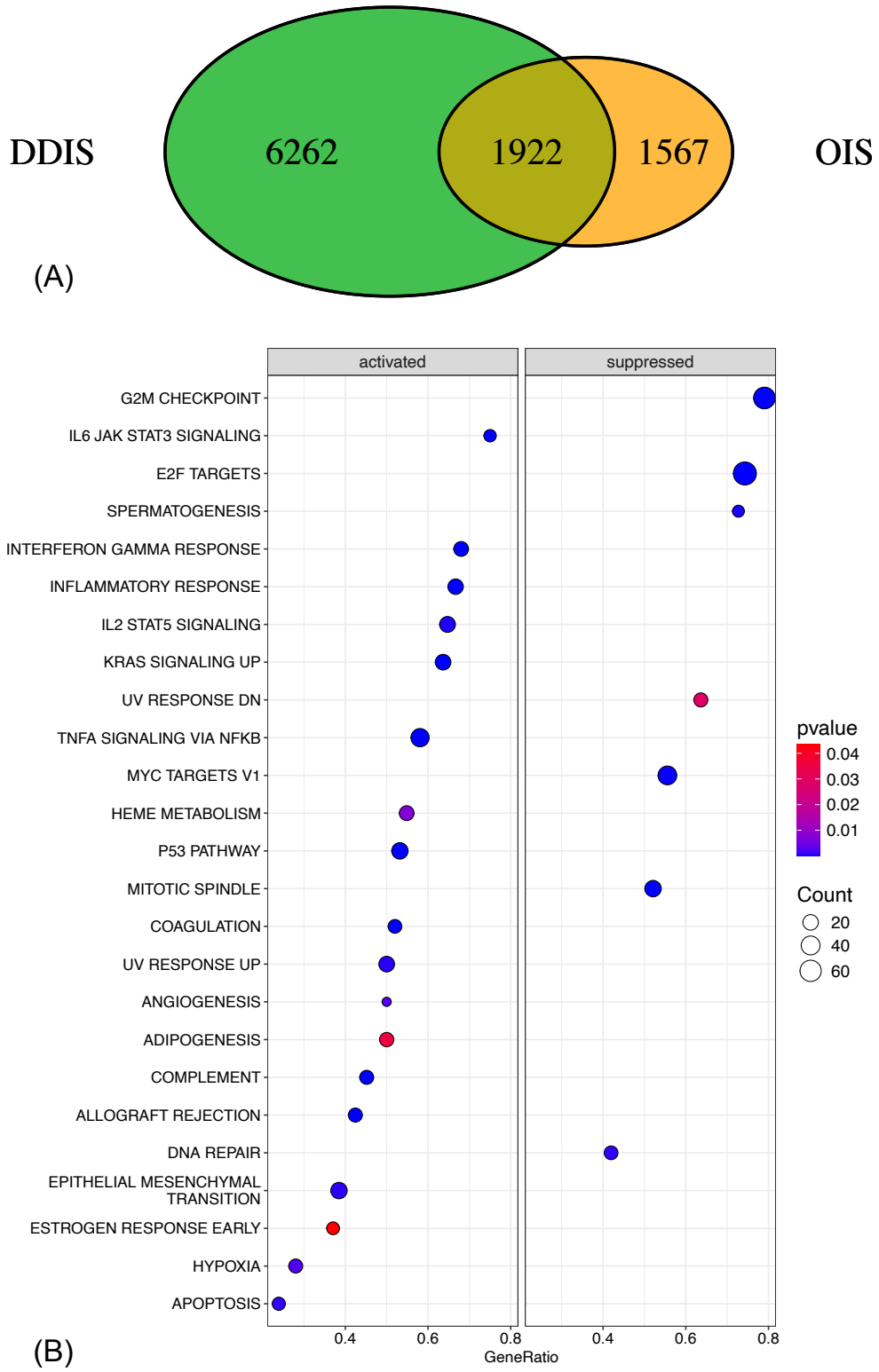

Figure 4.4 – Significant genes and pathways 8–11 days after senescence induction.

(A) Venn diagram of genes with a median MegaP value that is significant across DDIS and OIS 8-11 days post-senescence induction. (B) Dot plot of pathways from ORA of significantly activated and suppressed pathways identified in the 1922 genes

common in DDIS and OIS. p-value refers to the significance of the overrepresentation of the pathway and count reflects the number of genes associated with the pathway. DDIS, DNA damage-induced senescence; OIS, oncogene-induced senescence; ORA, over-representation analysis.

There were 7 comparisons available in time_group 12–14 – consisting of 3 DDIS datasets, and 4 OIS datasets. This was the smallest amount of data for any of the time_groups analysed, however 880 genes were still identified as significantly expressed in DDIS and OIS compared to proliferating control cells (**Figure 4.5A**).

ORA of these 880 genes revealed enriched pathways that were similar to those identified by the previous time_groups, including the suppression of E2F targets, the G2M checkpoint and mitotic spindle, alongside activation of the p53 pathway and inflammatory response. These findings are consistent with ongoing maintenance of cell cycle arrest and the pro-inflammatory environment as being key characteristics of senescent cells (**Figure 4.5B**).

The only unique pathway that was significantly enriched in the time_group 12–14 was the activation of glycolysis (**Figure 4.5B**). This could represent a shift in the metabolic demands of senescent cells at late timepoints as the cell dynamically adapts to the changing cell environment. However, it is important to consider the limitations of studies performed *in vitro*, as the cell culture environment could have influenced the transcriptomes of cells. *In vitro* conditions, which often involve high glucose concentrations and lack the nutrient regulation found in tissues, may artificially stimulate glycolysis. Therefore, while the activation of glycolysis in this time_group may reflect a metabolic shift in senescent cells, further research in *in vivo* systems is necessary to determine whether this shift is consistent across different biological contexts or is just a product of the experimental circumstances.

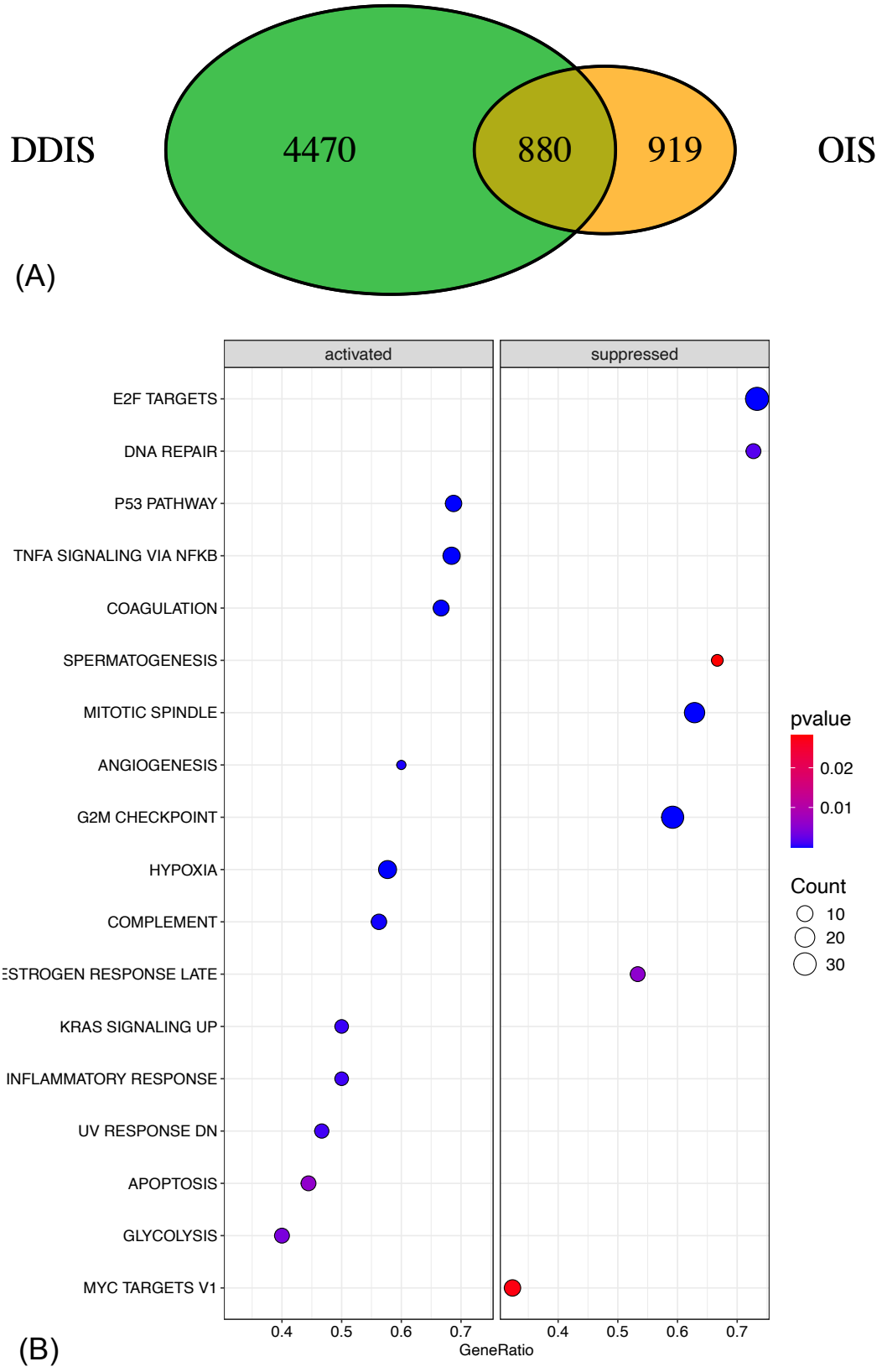

Figure 4.5 – Significant genes and pathways 12–14 days after senescence induction.

(A) Venn diagram of genes with a median MegaP value that is significant across DDIS and OIS 12-14 days post-senescence induction. (B) Dot plot of pathways from

ORA of significantly activated and suppressed pathways identified in the 880 genes common in DDIS and OIS. p-value refers to the significance of the overrepresentation of the pathway and count reflects the number of genes associated with the pathway. DDIS, DNA damage-induced senescence; OIS, oncogene-induced senescence; ORA, over-representation analysis.

There were several common pathways identified as enriched across all timepoints, such as the suppression of E2F targets and the G2M checkpoint, and the activation of the p53 pathway and the inflammatory response. This suggests that no matter the timepoint, maintenance of cell cycle arrest and the expression of inflammatory proteins are core characteristics of senescence. Interestingly, no timepoint identified the cellular senescence pathway as significantly enriched in the ORA.

Moreover, activation of the apoptosis pathway was identified as significantly enriched in time_groups 5–7, 8–11 and 12–14 (**Figures 4.3B**, **4.4B**, and **4.5B**). Although the apoptosis pathway was not identified as significantly enriched in time_group 0–4, it was observed when no p-value threshold was applied (**Appendix Figure A4.2**). This could suggest, that while the DNA damage incurred as part of senescence induction was not enough to directly induce apoptosis, it sufficed to activate the transcription of apoptosis-related genes. As senescence progressed, the expression of these genes became more pronounced, resulting in identification of significant activation of the apoptosis pathway in the ORA, potentially indicating a progression towards cell death. This aligns with the theory discussed in **Chapter 3** which suggested that senescence may act as a delayed-death pathway, where cells survive for a time but are ultimately driven towards apoptosis or other forms of cellular removal. Another noteworthy finding was the identification of activation of protein secretion only in the 5–7 time_group, which corresponds with the onset of the SASP. This supports the idea that protein secretion and the associated inflammatory phenotype begin to emerge at this stage of senescence, contributing to the senescent cell's role in modulating the tissue microenvironment. Together, temporal ORA revealed the identification of common pathways and core characteristics of senescence as well as pathways unique to specific timepoints.

There were 72 genes common genes to DDIS and OIS across all four time_groups – hereafter referred to as the Temporal Geneset. The LogFC expression of these 72 genes was explored in heatmap analysis (**Figure 4.6**).

For the majority of the Temporal Geneset, the direction of gene expression was the same across all timepoints. In some cases, such as with *EZH2* (Enhancer Of Zeste 2 Polycomb Repressive Complex 2 Subunit – marked with a single black asterisk in **Figure 4.6** for ease), the expression profile did change temporally; in DDIS during days 0–4 post-senescence induction, *EZH2* LogFC was lower than in proliferating control cells, however this became even lower at days 5–7, and lowered again at days 8–14. Interestingly, in OIS while *EZH2* is still expressed less in senescent cells than in control cells, its profile differs from DDIS in that it began to increase compared to proliferating control cells at days 12–14 post-senescence induction. *EZH2* is the protein coding gene for the protein EZH2 which has histone methyltransferase activity and is involved in transcriptional regulation of genes, including repression of tumour suppressor genes (Tan et al., 2014). While there were many similarities between the expression of the Temporal Geneset in DDIS and OIS, there were also some differences. *SERPINE2, IGFBP7*, *NIPAL3, PAM, AVPI1, PRDX6, MTAP,* and *FABP5* have different profiles depending on senescent type – indicated on the heatmap with a double black asterisk (**Figure 4.6**). The profile between senescence types is completely different for *NIPAL3, PAM, AVPI1, MTAP,* and *FABP5*, while only partially different for *SERPINE2, IGFBP7,* and *PRDX6.*

There were a limited number of common genes between the Core Geneset and the Temporal Geneset: *MARCKS*, *SKP2*, *PTN,* and *DIAPH3* all showed the same directional change of expression in both analysis pipelines. When compared to the human cellular senescence KEGG pathway (**Figure 3.6**), only *CCNA2* was identified in the Temporal Geneset. While *LMNB1* is not considered a typical senescence gene, it is identified as downregulated in the Temporal Geneset across all timepoints and both senescence types (**Figure 4.6** – indicated by a triple black asterisk). LMNB1 is one of the core proteins which form the nuclear lamina, and the breakdown of the nuclear lamina is well a recognised biomarker of senescence (Freund et al., 2012).

Figure 4.6 – Temporal LogFC expression of the Temporal Geneset.

Heatmap of the 72 genes significantly expressed across all timepoints. Upregulated, red; downregulated, blue; DDIS, DNA damage-induced senescence; OIS, oncogene-induced senescence.

4.2.2 Temporal expression of senescence-related transcripts.

As part of the analysis in this thesis, a temporal graph of gene expression of every gene in the human transcriptome was conducted and is accessible at the following link: **Transcriptomic_Temporal_Graphs**. It would be impossible to analyse every gene in this manner, hence selected genes and pathways were chosen for further interrogation.

When trying to determine a core geneset for the senescent transcriptome across multiple types of senescence and timepoints (**Figure 3.5A-B**), 28 genes were identified. As previously stated in **Section 3.2.2**, only *CCNB2* was present in the human senescence KEGG pathways. Likewise, 72 significantly expressed genes were identified in both DDIS and OIS across the four time_groups (0–4 days, 5–7 days, 8–11 days, and 12–14 days post-senescence induction), and only one of these is present in the cellular senescence KEGG pathway – *CCNA2*. Interestingly, both of these genes code for cyclin proteins which are involved in regulating the cell cycle. When downregulated, as they both are, this suggests cells are undergoing cell cycle arrest (**Figures 3.5B** and **4.6**).

In REP, *CCNB2* expression is lower than in proliferating control cells from days 0–40, however this becomes comparable to proliferating control cells at 41+ days (**Figure 4.7A**). In contrast, *CCNA2* expression is lower than proliferating control cells at both REP time points (**Figure 4.7B**). In DDIS and OIS, expression of both *CCNB2* and *CCNA2* are lower than proliferating control cells at all timepoints, with expression levels steadily declining from days 0–4 to days 5–7 and days 8–11. Interestingly, although expression levels remained below that of proliferating controls cells at days 12–14 post-senescence induction for both genes, they do begin to trend upwards compared to days 8–11 (**Figure 4.7**). This could possibly reflect that the control cells are themselves entering a pre-senescent state; with some studies using time-matched proliferating control cells while others used freshly cultured proliferating control cells. This observed trend may indicate cell cycle progression is slowing down. Alternatively, this observation may represent senescent cells heading towards cell cycle re-entry. Studying later timepoints would aid in clarifying this observation. As CCNB2 is involved in controlling progression of the cell cycle from G2 to mitosis (Gong & Ferrell, 2010), and CCNA2 is required during phases S and G2 of the cell

cycle (Pagano et al., 1992), observing immediate downregulation of these genes strongly supports senescent cells as entering immediate cell cycle arrest following senescence-inducing stimulus. Additionally, the immediate downregulation of both genes indicates that the process for cell cycle arrest must be tightly and rapidly controlled.

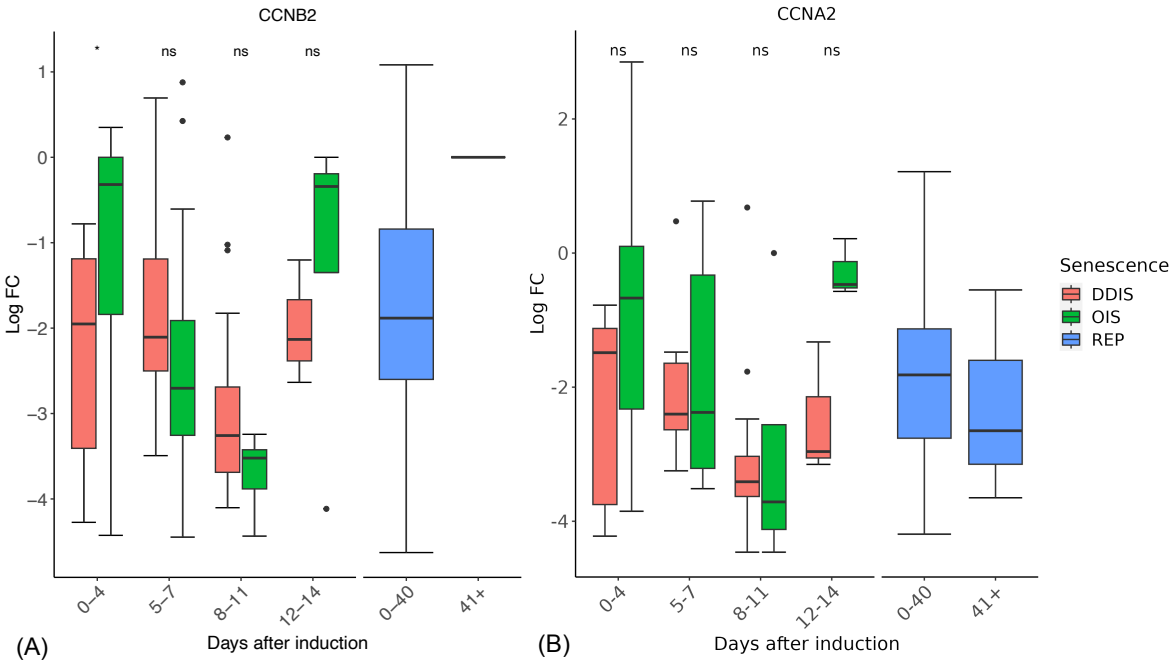

Figure 4.7 – Temporal expression of CCNB2 and CCNA2 in senescence.
*Temporal expression of the CCNB2 and CCNA2 in senescence measured in days after the initial senescence-inducing stimulus in DDIS, OIS, and REP. DDIS, DNA damage-induced senescence; OIS, oncogene-induced senescence; REP, replicative senescence; LogFC, log2 fold change; p-value refers to significance in expression between DDIS and OIS, *p-value <0.05. Figures produced using the methods and data from Scanlan et al. (2024).*

The temporal profile of the remaining 27 genes from the Core Geneset can be found in **Appendix Figures A4.3–4.5** (**A4.3** presenting the genes which did not follow a uniform expression pattern across all senescence types, **A4.4** presenting upregulated genes, and **A4.5** presenting downregulated genes). In summary, all genes with sufficient data showed the same profile of expression in the heatmap; however, there were a small number of genes which had a notable lack of data. For instance, the gene *ALKAL1* was present in only 13 of the 1069 comparisons within

the entire SenOmic database, making it impossible to discern a clear temporal expression profile for this gene across the different senescent types (**Appendix Figure A4.3A**).

In this section, select genes known to be involved or associated with senescence were investigated in more depth to understand the temporal evolution of the senescent transcriptome.

Common to all types of senescence is cell cycle arrest, resulting from changes to the cell cycle in response to stimuli that often induce DNA damage (Kumari & Jat, 2021). Therefore, to begin, the temporal profile of genes related to the DDR and the cell cycle were investigated. DDR genes were of particular interest as ORA of significantly expressed genes in DDIS, OIS and REP identified suppression of DNA repair as significantly enriched (**Figure 3.2D**).

ATM, *CHEK1* and *CHEK2* (**Figures 4.8 A-C**) are key components of the DDR (Maréchal & Zou, 2013; Stracker et al., 2009; van Jaarsveld et al., 2020). ATM primarily recognises dsDNA breaks and directly activates CHEK2 (Jazayeri et al., 2006), whereas CHEK1 is downstream of ATR which primarily recognises ssDNA breaks (Cimprich & Cortez, 2008). *ATM* expression exhibited no clear temporal trend, with median expression levels remaining similar to proliferating control cells across all timepoints in REP, DDIS, and OIS, with the exception of DDIS at days 0–4 when expression was lower, and days 12–14 when expression was higher than control cells (**Figure 4.8A**). Likewise, *CHEK2* expression was comparable with the proliferating control cells across all timepoints (**Figure 4.8C**). In contrast, *CHEK1* expression was consistently reduced across all senescence types and timepoints (**Figure 4.8B**). The absence of upregulation in these DDR genes may be due to the time intervals being too broad. If data were collected at hourly intervals within the first 24 hours following senescence induction, a clearer expression profile might emerge. Alternatively, cells may already maintain baseline levels of these proteins, allowing for rapid activation upon DNA damage through PTMs such as phosphorylation. Since CHEK1 and CHEK2 activity is primarily regulated through phosphorylation by ATM and ATR (Ahn et al., 2000; Cimprich & Cortez, 2008), this could explain the lack of significant changes in gene expression.

One of the primary functions of CHEK1/2 is the stabilisation of the p53 protein (Chehab et al., 2000). p53 signalling is known to be active in senescence (Mijit et al., 2020; Rufini et al., 2013), therefore temporal expression of *GADD45A* (Growth Arrest And DNA Damage Inducible Alpha) (**Figure 4.8D**), *TP53* (**Figure 4.8E**), *MDM2* (**Figure 4.8F**), and *CDKN1A* (**Figure 4.8G**) was investigated in DDIS, OIS, and REP in comparison to control proliferating cells. Despite the expectation that p53 (*TP53*) would be expressed in senescence, transcript levels of p53 did not increase in senescence across all timepoints, with some timepoints demonstrating lower p53 expression in senescent cells compared to control cells (**Figure 4.8E**). This likely reflects the pulsatile signalling of p53 (Hunziker et al., 2010; Sun et al., 2011). While p53 activity is largely regulated through PTMs and coactivators (Fielder et al., 2017), it is also a short-lived protein that must be transcriptionally regulated to some extent. However, the rapid pulsatile nature of p53 signalling may prevent detection of meaningful changes in average mRNA levels when measured at broad time intervals. This could also explain the absence of increased *ATM*, *CHEK1* and *CHEK2* expression following senescence induction. *GADD45A*, a downstream p53 target (Kastan et al., 1992), exhibited a rapid increase in days 0–4 post-senescence induction compared to control cells and continued to rise across all timepoints. Additionally, *GADD45A* expression was significantly higher in DDIS compared to OIS between days 0–11, and although not significantly higher at days 12–14, expression remained substantially elevated (**Figure 4.8D**). MDM2, which binds and inactivates p53 in a feedback loop (Michael & Oren, 2003), followed a similar temporal profile, being significantly higher in DDIS compared to OIS between days 0–11 post-senescence induction, and consistently elevated across all timepoints in DDIS compared to control cells (**Figure 4.8G**). Additionally, p21 (*CDKN1A*) expression was elevated across all timepoints and senescence types compared to control cells (**Figure 4.8G**). However, p21 expression was significantly higher in DDIS than in OIS during days 0–7 post-senescence induction, whereas p21 expression was significantly higher in OIS than in DDIS during days 8–11. Notably, systematic analysis provided little indication that p53 activity declines before day 11, with p21, GADD45A, and MDM2 expression trending upwards between days 8–11 compared to days 5–7 in both DDIS and OIS, remaining elevated above proliferating controls even at days 12–14 days post-senescence induction. It has been widely suggested that p21 is transient in senescence and required only for induction (He & Sharpless,

2017; Kumari & Jat, 2021). For instance, in DDIS, p21 levels have been reported to decrease by day 8 (Robles & Adami, 1998), and suggested that p53 activity peaked around day 4 post-senescence induction. However, these findings do not support this as p53 signalling remained elevated up to days 8–11 (**Figures 4.8D and 4.8F-G**). Even at days 12–14, p21 expression in DDIS remained higher than in proliferating control cells. Two frequently cited studies on REP describe p21 levels as transient and declining over extended passaging (Alcorta et al., 1996; Stein et al., 1999). However, in this analysis, median expression of p21 in REP is above proliferating control cell levels for days 0–40 and 41+ (**Figure 4.8G**). The transcriptomic findings suggest p21 is not transiently expressed in senescence and is instead sustained throughout senescence establishment and maintenance.

Interestingly, while p21 was significantly higher in DDIS compared to OIS up to day 11 post-senescence induction (**Figure 4.8G**), p16 (*CDKN2A*) was significantly higher in OIS compared to DDIS up to day 11 post-senescence induction, and non-significantly higher at days 12–14 (**Figure 4.8H**). The increase in p16 expression was less pronounced in DDIS, however it exhibited an upward trend up to days 8–11 post-senescence induction. This contrasts with studies which suggest p16 mRNA increases at later timepoints such as at day 12 in DDIS (Robles & Adami, 1998), or after 30 weeks of passaging in REP (compared to 10 weeks for p21) (Stein et al., 1999). However, more recent protein studies have shown that p16 expression increases as early as 2 days post-senescence induction in DDIS and OIS, with a stronger Western blot signal in OIS at day 8 compared to DDIS (Hoare et al., 2016), aligning with the findings of this analysis. While p16 dynamics in senescence remain controversial, this analysis suggests that p16 expression is maintained into late senescence, appears earlier in OIS than in DDIS, and is significantly higher in OIS than in DDIS (**Figure 4.8H**).

Unlike other cell cycle associated genes assessed, *RB1* expression was consistently downregulated across all timepoints in DDIS and OIS, remaining comparable to or slightly lower than control levels in REP (**Figure 4.8I**). Rb is primarily regulated through PTMs, alternating between hypo- and hyperphosphorylated states, with the hypophosphorylated state inducing cell cycle arrest (Bracken et al., 2004). Thus,

PTM-mediated regulation of Rb may explain the observed reduction in RB1 expression in senescent cells compared to proliferating controls.

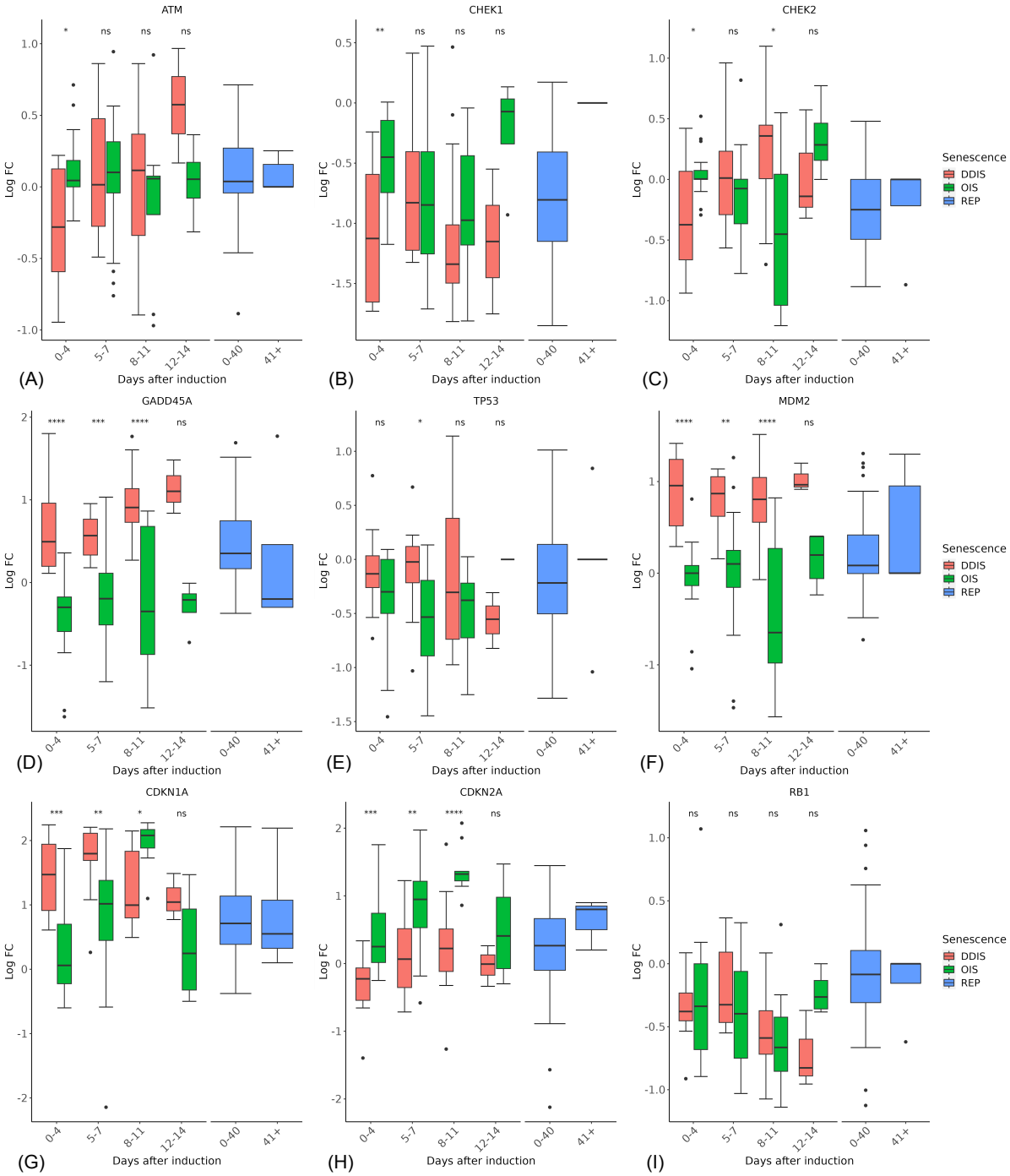

Figure 4.8 – Temporal expression of DDR and cell cycle related genes in senescence.

*Temporal expression of the DDR, p53 signalling and cell cycle signalling in senescence measured in days after the initial senescence-inducing stimulus in DDIS, OIS, and REP. DDIS, DNA damage-induced senescence; OIS, oncogene-induced senescence; REP, replicative senescence; LogFC, log2 fold change; p-value refers to significance in expression between DDIS and OIS, *p-value <0.05; **p-*

*value <0.01; ***p-value <0.001; ****p-value <0.0001. Taken from Scanlan et al (2024).*

Once cells stop proliferating and arrest, there are numerous studies which suggest senescent cells secrete fibrogenic proteins such as TGFβ and experience collagen remodelling (Jun & Lau, 2010; Muñoz-Espín & Serrano, 2014).

COL1A1 (Collage type I Alpha 1 Chain) and COL1A2 were selected for analysis as they encode type I collagens, the most abundant structural protein in the ECM with a crucial role in maintaining tissue architecture, providing mechanical strength and supporting cell adhesion, migration, and signalling (Kadler et al., 2007; Ricard-Blum, 2011). Temporal downregulation of *COL1A1* and *COL1A2* was observed, with a more pronounced – and at certain timepoints, significantly greater – reduction in OIS than in DDIS (**Figure 4.9A-B**). Notably, *COL1A2* expression remained significantly lower in OIS compared to DDIS up to day 11 post-senescence induction. Interestingly, by days 12–14 post-senescence induction, the median expression of both *COL1A1* and *COL1A2* (as indicated by the line in the box plot) returned to levels similar to that of the proliferating control cells. This suggests that collagen matrix remodelling may occur again at late timepoints in senescence. Further investigation into collagen synthesis and degradation during late-stage senescence could provide insight into this intriguing observation.

At the protein level, elevated TGFβ expression and an associated fibrogenic SASP has been reported immediately following senescence induction (Tominaga & Suzuki, 2019). However, this was not reflected at the transcriptomic level as there were no initial increases in *TGFβ* (**Figure 4.9C**), in its receptor (*TGFBR1* – **Figure 4.9D**), or in *ACTA2* (Actin Alpha 2, Smooth Muscle) (**Figure 4.9E**) which is upregulated in response to TGFβ activity (Fakatava et al., 2023; Fujii et al., 2010). One possible explanation for the lack of increased expression at the transcript level of TGFβ-related genes, despite reports of TGFβ protein activity in early senescence, is that cells may already have abundant levels of TGFβ–related proteins prior to senescence induction. Following entry into senescence, these proteins may be downregulated. Alternatively, the detection of TGFβ in protein studies could

represent TGFβ which was released as a byproduct of apoptosis, as some cells may enter apoptosis rather than senescence. Since ACTA2 is regulated by TGFβ, the observed decline in *ACTA2* expression from days 0–4 to days 5–7 post-senescence induction (**Figure 4.9E**) may support the hypothesis that TGFβ signalling is downregulated following senescence induction, rather than being activated as an immediate response to senescence.

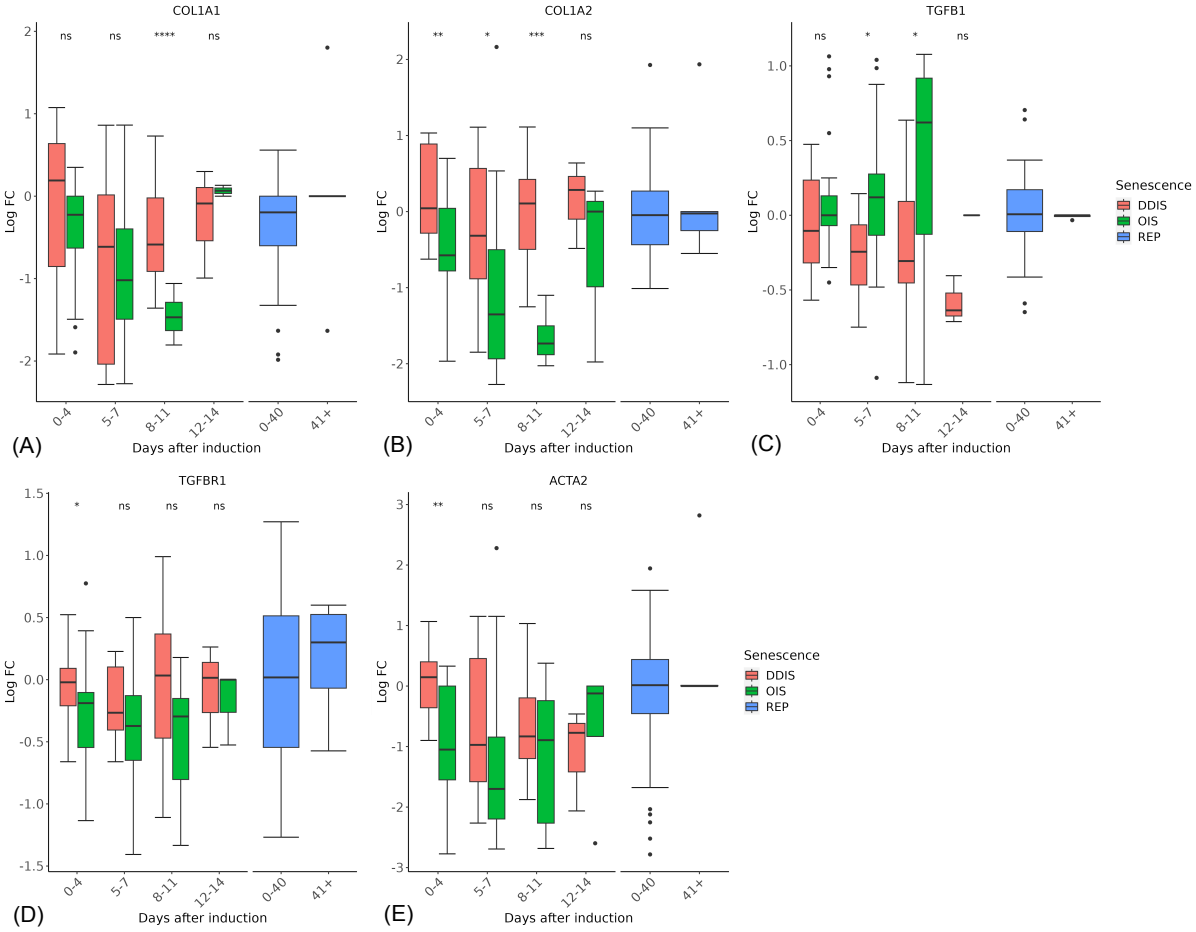

Figure 4.9 – Temporal expression of collagens and TGFβ response genes in senescence.

*Temporal expression of collagens and TGFβ response genes in senescence measured in days after the initial senescence-inducing stimulus in DDIS, OIS, and REP. DDIS, DNA damage-induced senescence; OIS, oncogene-induced senescence; REP, replicative senescence; LogFC, log2 fold change; p-value refers to significance in expression between DDIS and OIS, *p-value <0.05; **p-value <0.01; ***p-value <0.001; ****p-value <0.0001. Taken from Scanlan et al. (2024).*

Finding disparity between the protein and transcript level demonstrate the importance of investigating more than just one type of macromolecule when it comes to understanding a biological processes.

Senescent cells exhibit an inflammatory SASP which is not immediately upregulated upon senescence induction but rather emerges between days 5 and 8 post-senescence induction (Coppé et al., 2008; Freund et al., 2011; Hoare et al., 2016). The posttranslational regulator p38 (*MAPK14)* is involved in inflammation. At the protein level, p38 is phosphorylated in senescent cells in a time dependent manner (Freund et al., 2011), however at the transcriptomic level p38 expression remained similar to proliferating control cells across all timepoints for DDIS, OIS and REP, with the exception of a downregulation in expression at days 12–14 in DDIS (**Figure 4.10A**). Notably, Freund et al. (2011), also reported that expression of total p38 protein did not change, only its phosphorylation status. Interestingly, p38 expression was significantly higher in OIS between days 5–11 than in DDIS, and higher at the remaining timepoints although not significantly.

The SASP is a key phenotype of senescent cells, largely driven by NF-κB, a major transcriptional regulator of inflammation (Oeckinghaus & Ghosh, 2009). NF-κB is primarily composed of two subunits, with the most common conformation the heterodimer p50-RelA (Hoffmann & Baltimore, 2006). In senescence, the NF-κB subunit RelA has been shown to have a high level of binding in complexes at transcriptional promoters (Chien et al., 2011), suggesting the active homo/heterodimer in senescence involves RelA. NF-κB is essential for the production of the inflammatory SASP (Chien et al., 2011; Freund et al., 2011), and co-suppression of NF-κB with p53 leads to bypass of cell cycle arrest (Beauséjour et al., 2003). Among the most well-characterised inflammatory SASP components are IL-8 (*CXCL8* – **Figure 4.10B**), IL-6 (**Figure 4.10C**), and IL-1β **Figure 4.10D**). At days 0-4 post-senescence induction, IL-8 and IL-6 expression levels were comparable to proliferating control cells (**Figures 4.10B-C**), however IL-1β expression was already strongly upregulated. This is likely due to the dual role of IL-1β as part of the SASP but also functioning upstream of SASP induction, reinforcing the inflammatory

phenotype by amplifying NF-κB transcriptional activity (Yang et al., 2019). At days 5–7 post-senescence induction, IL-8 and IL-6 expression were rapidly upregulated compared to proliferating control cells in alignment with published studies (Acosta et al., 2013; Coppé et al., 2008), alongside further increased expression of IL-1β. This upregulation continued through days 8–11. However, at days 12–14, all three genes were rapidly downregulated to near-control levels, potentially indicating a regulatory mechanism which limits inflammatory signalling in late senescence. Interestingly, while not statistically significant, IL-8, IL-6, and IL-1β expression was higher in OIS compared to DDIS across days 0–11 post-senescence induction, suggesting that OIS may exhibit a stronger SASP. Nevertheless, the SASP remains a critical feature across different senescence types, reinforcing its role as a key phenotype of senescence.

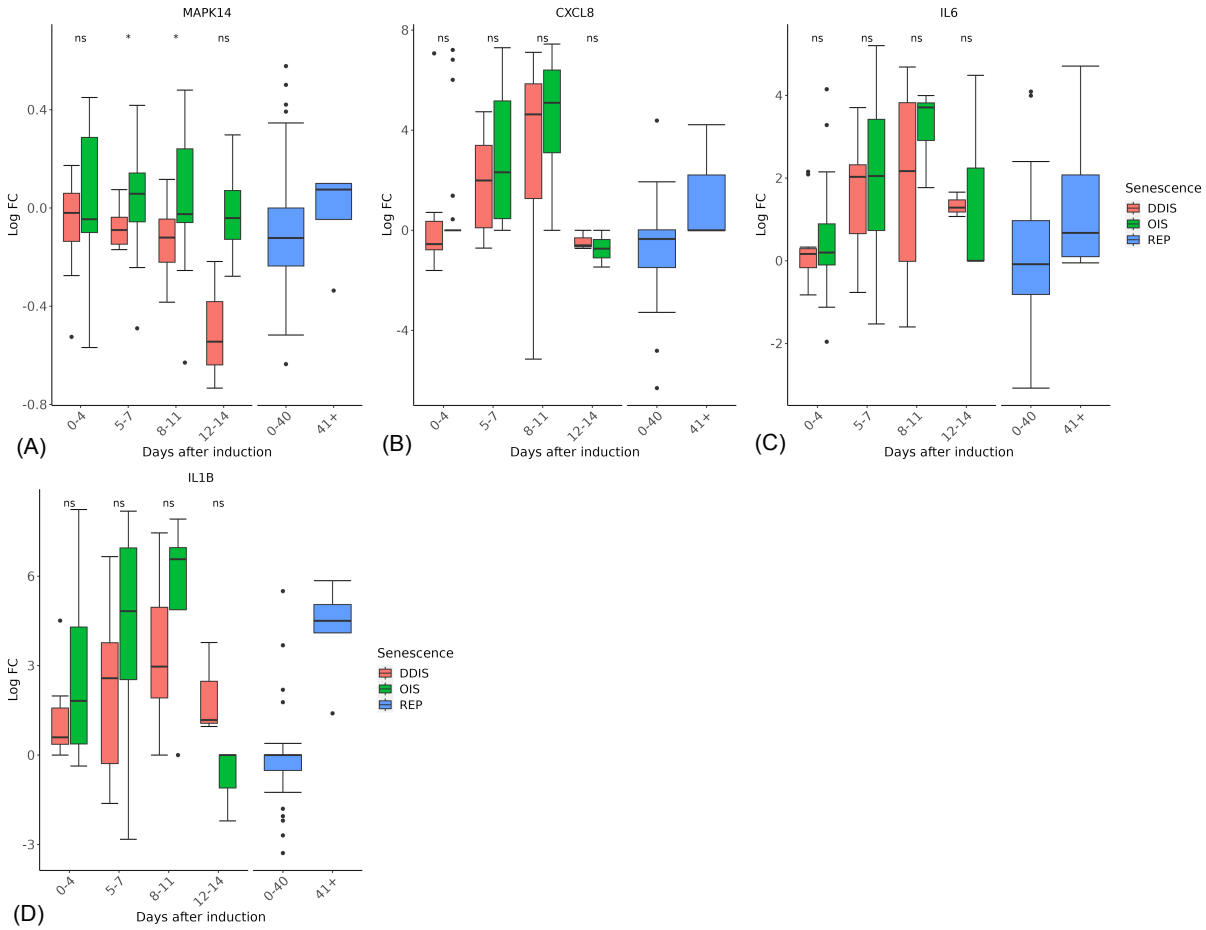

Figure 4.10 – Temporal expression of inflammatory genes in senescence.

Temporal expression of inflammatory-related genes in senescence measured in days after the initial senescence-inducing stimulus in DDIS, OIS, and REP. DDIS, DNA damage-induced senescence; OIS, oncogene-induced senescence; REP, replicative

*senescence; LogFC, log2 fold change; p-value refers to significance in expression between DDIS and OIS, *p-value <0.05. Taken from Scanlan et al. (2024).*

While it is well established that certain TFs are involved in the transcription of inflammatory genes, the process which leads to the induction of the SASP is still unclear. If the early fibrogenic SASP observed at the protein level is accurate, what triggers this sudden switch from a fibrogenic to an inflammatory phenotype? There are several theories such as the theory that p38 activates NF-κB (Freund et al., 2011). The study by Freund et al. (2011) demonstrated p38 becoming phosphorylated around day 4 post senescence induction, and although we see no changes in gene expression of p38 (**Figure 4.10A**) this does not exclude PTMs from occurring. Another theory, derived from one of the most comprehensive temporal protein analyses of *in vitro* human senescence, implicated Notch signalling in regulating the switch in SASP composition (Hoare et al., 2016). The study by Hoare et al. (2016) suggested that the early SASP is rich in TGFβ-related proteins and active Notch signalling. At 4–5 days post-senescence induction (in both DDIS and OIS), Notch signalling began to break down as TGFβ-related proteins also decreased and expression of inflammatory SASP proteins increased. This suggests that Notch downregulation may serve as a molecular switch, promoting the transition from a fibrogenic to an inflammatory SASP.

Due to the detailed protein profile demonstrated by Hoare et al. (2016), the role of Notch signalling at the transcript level was explored. Notch signalling is a juxtacrine signalling mechanism where a ligand from one cell binds the Notch receptor of an adjacent cells, resulting in multiple cleavage events and the release of the NICD. The NICD then translocates from the cytosol to the nucleus to enact Notch target gene transcription (Bray, 2006). Notch signalling is therefore mediated at the protein level and, if it were to be active in early senescence, we may not see an upregulation of the receptor as it would have to already exist to elicit immediate Notch signalling – however downregulation compared to control proliferating cells could show a change from normal state. Expression of the *NOTCH1* receptor gene, as well as two well-known Notch target genes, *HEY1* and *HES1*, were investigated. It is worth noting that Notch transcriptional activity needs further investigation to fully understand it's action

as *HES1* is not always responsive to active Notch signalling (Kopan & Ilagan, 2009; Lee et al., 2007).

Analysis of *NOTCH1* revealed that expression is higher in OIS than in DDIS, being significantly higher at day 0–4 (p-values < 0.01) and 8–11 days (p-values < 0.001) (**Figure 4.11A**). Both *HES1* and *HEY1* showed an increase in median expression compared to control proliferating cells at 0–4 days in DDIS and OIS. Expression remained similar at days 5–7 for *HEY1* (**Figure 4.11B**) before decreasing at days 8–11, while median *HES1* expression decreased from days 0–4 to days 5–7 (**Figure 4.11C**). These results correspond with the study by Hoare et al. (2016), who observed an initial increase in Notch signalling activity (demonstrated via the presence of the NICD and HES1) followed by a decrease between days 4–6.

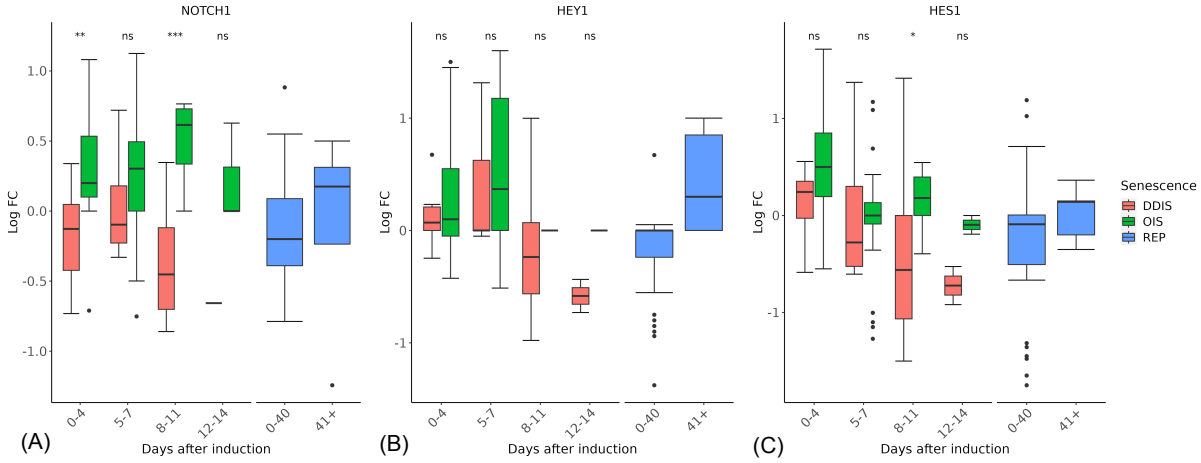

Figure 4.11 – Temporal expression of Notch related genes in senescence.

*Temporal expression of inflammatory-related genes in senescence measured in days after the initial senescence-inducing stimulus in DDIS, OIS, and REP. DDIS, DNA damage-induced senescence; OIS, oncogene-induced senescence; REP, replicative senescence; LogFC, log2 fold change; p-value refers to significance in expression between DDIS and OIS, *p-value <0.05; **p-value <0.01; ***p-value <0.001. Taken from Scanlan et al. (2024).*

4.3 Conclusion.

SenOmic provides a valuable resource for examining the senescence transcriptome in human fibroblast cells, offering the flexibility to explore a variety of variables based on different study designs and aims. It is worth noting, however, that there are limited

studies at later timepoints. Further exploration into late timepoints of senescence is still required to fully elucidate the complexities of dynamic temporal changes in senescence.

Notably, time_groups displayed distinct clustering patterns (**Figure 4.1**) demonstrating the senescence profile dynamically evolves with time. Although, despite these distinct clustering profiles, similarities were still observable. This was supported with ORA of each time_group in DDIS and OIS which identified shared significantly enriched pathways such as suppression of E2F targets and the G2M checkpoint (**Figure 4.2B**, **4.3B**, **4.4B** and **4.5B**), but also significantly enriched pathways which were unique to the time_group. For example, protein secretion was only identified as enriched at days 5–7 (p-value < 0.05 – **Figure 4.3B**) and was not found when no threshold value was applied at any other time_group. Identification of activation of protein secretion only enriched during days 5–7 post-senescence induction aligns with published protein profiles which detail SASP expression is delayed (Acosta et al., 2013; Coppé et al., 2008; Freund et al., 2011). Additionally, expression of SASP factors IL-8 and IL-6 being upregulated at days 5–7 post-senescence induction compared to proliferating control cells (**Figures 4.10B-C**) further highlighted the delayed SASP.

While some temporal protein phenotypes aligned with this transcriptomic analysis, some did not. For example, p21 and p16 were not transient as some studies have suggested (He & Sharpless, 2017; Kumari & Jat, 2021; Robles & Adami, 1998), as expression of both genes persisted into late senescence (**Figure 4.8G-H**). Additionally, TGFβ signalling has been identified as active and upregulated in early senescence (Tominaga & Suzuki, 2019), however this transcriptomic analysis did not identify any increased expression in TGFβ or TGFβ–related genes (**Figure 4.9**).

Other notable observations include, significantly stronger p53 signalling in DDIS compared to OIS (**Figure 4.8**), stronger expression of inflammatory genes in OIS compared to DDIS (**Figure 4.10**), and significantly stronger p16 and p38 expression in OIS compared to DDIS (**Figures 4.8H** and **4.10A**). Together, these findings emphasise the importance of considering the stage of senescence a cell may be at,

as well as identifying phenotypes both common and unique to multiple senescence types and across multiple timepoints.

Chapter 5 – The temporal protein profile of human senescent fibroblasts.

5.1 Background.

Understanding how a biological process evolves temporally is important to truly understanding the biology of it. Temporal research is becoming increasingly popular and more achievable in a laboratory setting as techniques improve and become cheaper; however, time-series data and investigations into temporal changes is still often limited. Understandably investigating multiple timepoints, particularly late time points, can demand significant resources. A cheaper and more environmentally friendly alternative to laboratory experimentation is computational modelling. Equally, many experimental approaches focus on a single pathway, while computational modelling allows for the simultaneous analysis of multiple pathways; anecdotally, experimental studies rely on reagents, such as antibodies, that occasionally do not work, a hindrance that is avoided with modelling studies. Nevertheless, any exemplary systems biology study should combine laboratory and computational work in which one experiment complements and provides the other with data and hypotheses to test, and vice versa. There have been various *in silico* investigations into cellular senescence, including the role of mitochondrial dysfunction in senescence (Dalle Pezze et al., 2014; Passos et al., 2010) and understanding the heterogeneity behind cell division potential and entry into replicative senescence (Sozou & Kirkwood, 2001).

Many senescent studies explore the protein level, however this is often for a single timepoint and a single senescence type. The study performed by Basisty et al. (2020) notably produced ‘The SASP Atlas’, a resource containing proteomic data from different cell types, timepoints, and as a result of multiple senescence inducing stimuli. While this resource provides much understanding of senescence at the protein level, no comparison was made between the different timepoints to aid in understanding the temporal evolution of senescence. Combining the results of this study and other single timepoint investigations, it is possible to devise phenotypic profiles which describe temporal senescence at the protein level. For example, initially after induction, senescent cells experience an increase in expression of cell cycle inhibitors such as p53 and p21 (Freund et al., 2011; Kim et al., 2017; Young et

al., 2009). Additionally, Notch signalling has been identified as influencing the SASP and temporal profile of senescent cells though a dynamic switch in signalling activity (Hoare et al., 2016; Ito et al., 2017; Teo et al., 2019). Combining profiles from multiple studies can successfully lead to the building of a protein network and simulation of senescence, with outputs of the model providing new insights which can be tested in laboratory experiments.

Chapter 4 investigated the temporal transcriptomic profile of senescent human fibroblasts, and while many observations were supported by protein profiles in the literature, some genes did not follow the same profile. For example, p53 is known to be active in senescence but gene expression of p53 was similar to proliferating controls in DDIS and lower than proliferating controls in OIS (**Figure 4.8E**). Additionally, gene expression does not directly indicate if any PTMs such as phosphorylation or ubiquitination have taken place. To truly understand any biological process, it must be investigated across the different macromolecule types of the cell. Understanding how a process, whether that be cellular senescence or a disease such as Alzheimer's disease, progresses for different macromolecule types will allow for improved and better targeted therapeutics, as well as improved basic understanding of human biology.

The aim of this chapter was to collate temporal protein phenotypes of cellular senescence to qualitatively model temporal protein expression during DDIS and OIS in human fibroblasts. KD perturbations were also introduced into the model network to see how KDs of major TFs impacted the whole network and to demonstrate the robustness of the model. Data to inform this model was collected from a non-systematic review as described in **Section 2.3**. Combined with **Chapter 4**, **Chapter 5** has taken an integrated approach (although not a multi-omic approach) to understanding the temporal nature of senescence in human fibroblasts.

5.2 Results and Discussion.

The results of this chapter were obtained using methods detailed in **Section 2.3**. **Figures 5.1C**, **5.4**, and **5.5** were published in Scanlan, et al. (2024), and **Figures 5.1A-B**, **5.2**, **5.3**, and **5.6** were produced using the same methods detailed in Scanlan et al. (2024).

5.2.1 Determining a temporal protein network of senescence.

One option to model the protein phenotype of cellular senescence would be to take the proteins outlined in the KEGG cellular senescence pathway (**Figure 3.6**). The KEGG cellular senescence pathway includes pathways such as p53 signalling, FOXO signalling, and the cell cycle. However, the cellular senescence KEGG pathway is composed of 157 proteins. Modelling all 157 proteins would be a huge computational undertaking even before considering whether published expression data exist for each protein.

To build the model network, pathways (and thus proteins) were selected based on the non-systematic review performed as detailed in **Section 2.3.1**. Temporal data availability was much more limited for protein profiles than for transcriptomic data. Only DDIS and OIS were considered when developing the computational model of senescence due to these types of senescence being the most commonly investigated in the literature, with 66% of data in SenOmic comprising only DDIS and OIS studies. The identified pathways for inclusion in the model networks were cell cycling, Ras signalling, inflammatory SASP signalling, p38 signalling dynamics, and Notch signalling. The inclusion of these pathways is justified later in this section.

A total of twelve molecular protein phenotypes were established defining cellular senescence as an outcome of the non-systematic review, four of which were related to how senescent cells responded when key network components were knocked down. During model development, the simulation outputs were compared to the criteria and assessed on whether they met them or not. To successfully be considered an accurate representation of the temporal protein profile of human senescent fibroblasts, all twelve criteria had to be fulfilled in model simulations (**Table 5.1**).

It was essential to include senescence inducers in each iteration of the model, forming a core foundation for constructing a network representative of senescence. Both DDIS and OIS are known to require overwhelming activation of the DDR leading to cell cycle arrest (Kumari & Jat, 2021), with hyperactivation of an oncogene such as RAS additionally required for OIS (Liu et al., 2018). In all stages of model

development, both the DDR and RAS were incorporated as a source of senescence stimulus. In simulations, DDIS was induced by introducing an input which would simulate DNA damage and activation of the DDR to induce cell cycle inhibitor expression and the resultant arrest. OIS was induced through RAS expression which leads to the activation of p38/p16 with subsequent DDR activation and cell cycle arrest.

Table 5.1 – Molecular protein phenotype criteria of cellular senescence.

Senescent cell phenotype	How established is this phenotype at the protein level*	Is this phenotype reflected in the transcriptomic analysis?	Do model simulations match the senescent cell phenotype criteria?		
			Model A	Model B	Model C
p21 and p16 are continued to be expressed once senescence has been induced from more than 4 days †	3	Y	Y	Y	Y
There is higher p53 activation and p21 expression in DDIS than in OIS	0	Y	N	N	Y
There is higher p16 expression in OIS than in DDIS	1	Y	Y	Y	Y
Expression of p16 increases later in DDIS than OIS	0	Y	N	N	Y
Changes in Notch signalling activity is temporally associated with a switch in the SASP profile	1	Y	N	N	Y
There is a stronger inflammatory phenotype in OIS than in DDIS	2	Y	N	Y	Y

The inflammatory phenotype begins to be established on days 5 to 8 post-senescence induction ††	3	Y	N	N	Y
There is more p38 phosphorylation in OIS than in DDIS	1	N	N	N	Y
KNOCKDOWN CRITERIA					
Knockdown of p53 results in upregulation of p16 expression	0	Y	N	N	Y
Knockdown of p53 results in decreased p21 expression	3	Y	Y	Y	Y
Knockdown of p53 results in upregulation of p38 in DDIS	3	Y	N	N	Y
Knockdown of RelA results in decreased p53 signalling	0	Y	N	Y	Y

**0 denotes no studies can be found related to this phenotype at the protein level; 1 denotes limited published studies support this described phenotype at the protein level; 2 denotes multiple studies support this described phenotype at the protein level; 3 denotes this is a well-established protein phenotype in senescent cells. † 4 days post-senescence induction correlated with arbitrary time 60 in model simulations. †† 5-8 days post-senescence induction correlates with arbitrary time 65-85 in model simulations. Y, yes; N, no; DDIS, DNA damage-induced senescence; OIS, oncogene-induced senescence; SASP, senescence associated secretory phenotype. Taken from Scanlan et al. (2024) with 'Model A' and 'Model B' columns added for this thesis.*

To ultimately meet all phenotypic criteria, a qualitative model was developed in stages (**Figure 5.1**). DDIS and OIS were induced in each iteration of the model until all twelve criteria were met. Taking this stepwise approach allowed for easier identification of proteins and interactions which were incorrect and resulting in phenotype errors.

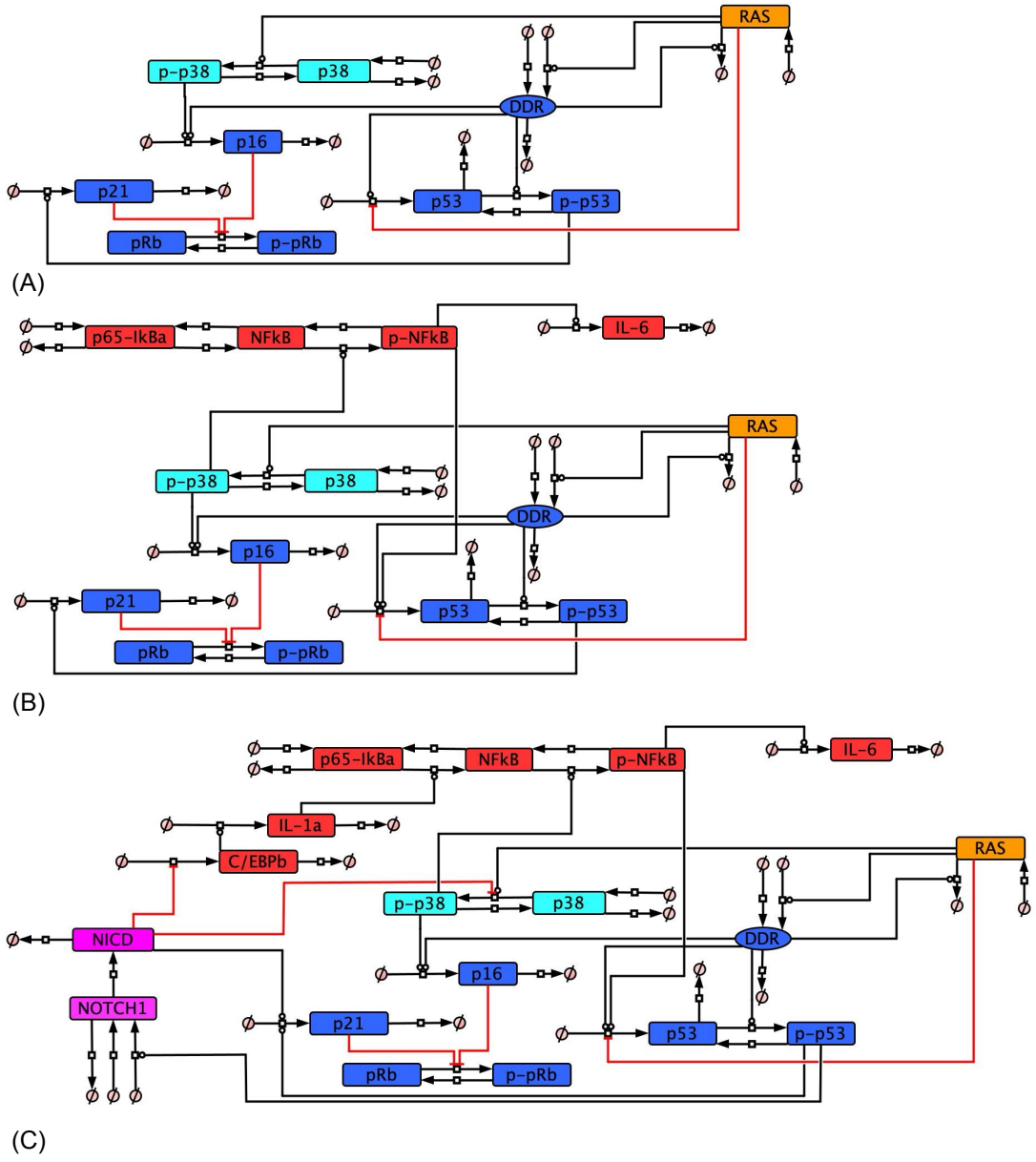

Figure 5.1 – Development of The Cellular Senescence Model.

*Model A was the first iteration of the cellular senescence model (A); Model B was the second iteration (B); Model C was the final iteration and named The Cellular Senescence Model (C). All interactions in the network have been non-systematically searched in the literature, providing evidence to justify the network (**Appendix Table A2.2**).*

Each iteration of the model network built upon the previous model by incorporating additional proteins and network interactions. The first model developed, Model A (**Figure 5.1A**), consisted of proteins involved in regulation of the cell cycle and the DDR, alongside RAS and p38. As previously mentioned, cell cycle arrest is a key phenotype of senescence. The p53/p21 axis and p16/pRb interaction were chosen to represent cell cycle regulatory proteins. These proteins are well-established in cell cycle control and senescence, with multiple studies providing protein level data on their roles in senescence (Freund et al., 2011; Kim et al., 2017; Young et al., 2009). Moreover, p38 phosphorylation dynamics were included as species in the model as p38 has been shown to play a role in regulating p16 expression through RAS in a p53-independent manner (Kwong et al., 2009; Sun et al., 2007; Wong et al., 2009), making it an essential component of cell cycle arrest in OIS. Transcriptomic analysis presented in this thesis further revealed that p16 expression was significantly higher in OIS compared to DDIS from day 0–11 post-senescence induction (**Figure 4.8H**), further supporting its critical role in the OIS pathway and justifying its inclusion in the model network.

To build upon Model A, Model B (**Figure 5.1B**) introduced inflammatory SASP proteins. The SASP is a key characteristic of senescent cells which contributes to secondary senescence (Acosta et al., 2013; Coppé et al., 2010; Kuilman & Peeper, 2009) and signalling to the immune system for senescent cell removal (Krizhanovsky et al., 2008; Muñoz-Espín & Serrano, 2014). Therefore, the ability of a model to capture SASP dynamics is essential. As observed in the literature the SASP begins to be established 5–8 days after senescence induction (Coppé et al., 2010) and is controlled by proteins including p38 (Freund et al., 2011) and NF-κB (Chien et al., 2011). NF-κB was chosen for inclusion as it is a key TF of inflammatory proteins and inflammatory signalling in senescence (Chien et al., 2011; Liu et al., 2017). The most common subunit conformation of NF-κB is p50-RelA (Hoffmann & Baltimore, 2006), and therefore a p50-RelA heterodimer was chosen to represent NF-κB. In the model network NF-κB is introduced as three species: p65-IκBA (inhibited), NFκB (uninhibited and likely to be active), and p-NFκB (phosphorylated with increased activity). p65 is another name for RelA. IL-6 was introduced as a variable to represent the inflammatory aspect of the SASP.

In Model C (the Cellular Senescence Model, **Figure 5.1C**), Notch signalling (through variables NOTCH and NICD) and additional inflammatory proteins (IL-1α and C/EBPβ) were incorporated as protein species. Notch signalling was introduced as a mechanism to modulate temporal SASP expression as dynamic changes in Notch signalling activity have been shown to influence temporal SASP composition (Hoare et al., 2016; Ito et al., 2017). An event termed 'the Notch switch' (as described in **Section 2.3.3**) was introduced to the model network. This allowed for inducing a dynamic change in Notch signalling at a specific timepoint, allowing for modulation of the SASP.

The Cellular Senescence Model integrates five interconnected signalling pathways (**Figure 5.1C**): cell cycle and DDR-related proteins, Ras signalling, p38 signalling, inflammatory SASP signalling, and Notch signalling. This model can be adapted to investigate various dynamic aspects of senescence, such as the impact of changes in Notch signalling (Hoare et al., 2016; Teo et al., 2019) or the consequences of p53 KD or inhibition (Kumari et al., 2021; X. Zhang et al., 2021; Zhu et al., 2022).

A key advantage of computationally modelling biological processes is the ability to introduce perturbations, such as KDs, to explore how the entire network is affected – an approach which would be difficult to achieve in a laboratory setting where experimental measurements are often limited to a specific small number of proteins. To demonstrate the utility of the model, p53 and RelA KDs were separately introduced at the time of senescence induction. Both p53 and RelA were chosen as they are important TFs in any cellular process and are specifically relevant in senescence (Chien et al., 2011; Mijit et al., 2020). Furthermore, these genes were investigated in the transcriptomic analysis of **Chapter 4**.

5.2.2 Developing and simulating the Cellular Senescence Model.

DDR and RAS variables were included as sources of senescence stimulus as described in **Table 2.3**. In all models, senescence and KDs (when introduced) were induced at Time = 35 (AU).

In the first model (Model A – **Figure 5.1A**), p53 signalling became activated upon senescence induction as evidenced by the expression of p53 (**Figure 5.2A**),

phosphorylation and consequent activation of p53 (pp53 – **Figure 5.2B**), and sustained expression of p21 (**Figure 5.2C**). p53 KD also resulted in downregulation of p21 expression in both DDIS and OIS. Additionally, p16 expression was sustained following senescence induction and was higher in OIS compared to DDIS (**Figure 5.2D**). The upregulation and sustained expression of these cell cycle inhibitors upon senescence induction indicated cell cycle arrest. Total p38 remained similar upon senescence induction as observed in Freund et al. (2011) (**Figure 5.2E**), however phosphorylated p38 (pp38) was the same in DDIS and OIS (**Figure 5.2F**) in contradiction to the established criteria.

These results met three of the established criteria: sustained p21 and p16 expression, higher p16 expression in OIS compared to DDIS, and a p53 KD resulting in downregulated p21 expression (**Table 5.1**). However, some simulation outputs contradicted other criteria. For example, higher p53 signalling was not observed in DDIS compared to OIS, and p53 KD did not lead to upregulated p16 expression; instead, p16 expression remained unchanged regardless of the perturbation. Notably, both of these phenotypes were identified in the transcriptomic systematic analysis in **Chapter 4**, and had minimal supporting evidence at the protein level. However, the lack of protein-level evidence does not necessarily indicate these phenotypes do not occur at the protein level; rather it highlights a lack of experimental studies specifically investigating these phenotypes. Further protein-level analyses, whether *in silico*, *in vitro* or *in vivo*, would be required to validate these specific criteria. The development of this model in this thesis will enable deeper *in silico* investigation of these phenotypes.

The ability of Model A to meet the defined criteria was partially constrained by the limited signalling pathways and proteins included in the network. Nonetheless, the ability of the model to meet one quarter of the established criteria demonstrated a solid foundation on which to build a more robust and refined model.

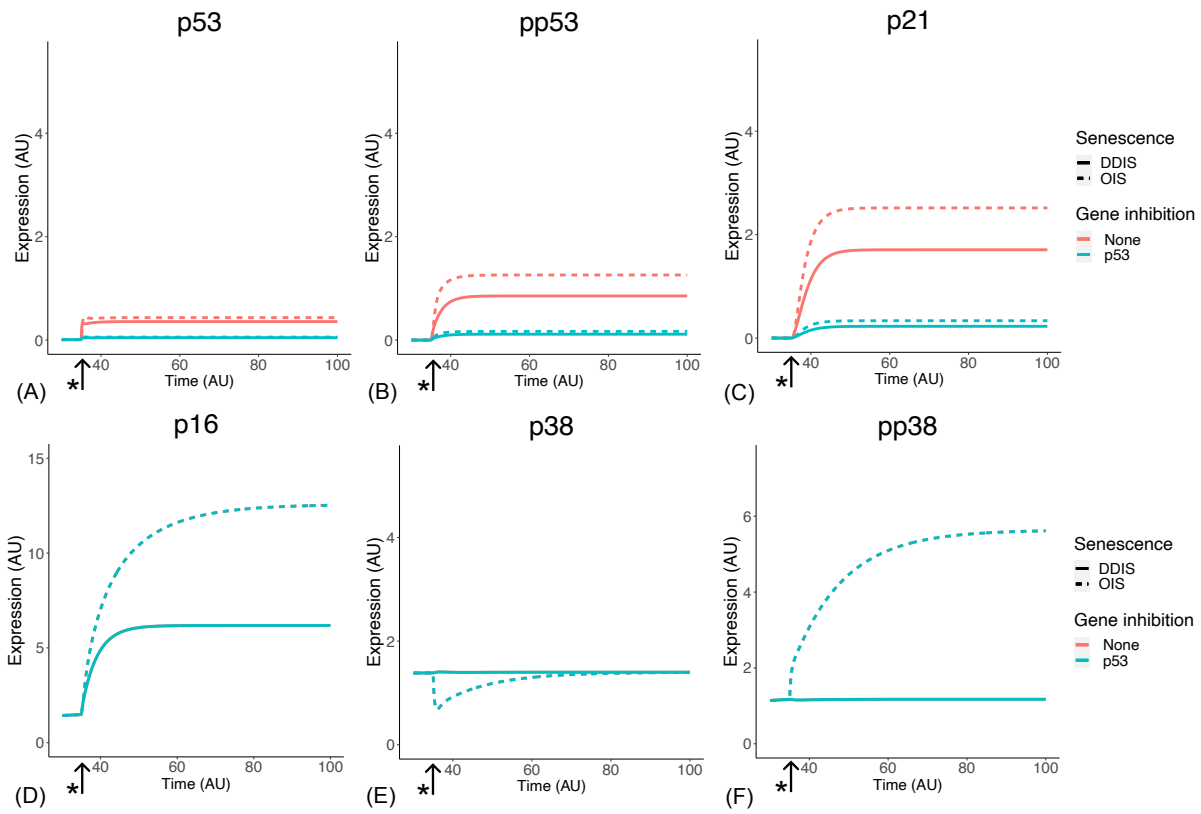

Figure 5.2 – Simulation of proteins in Model A.

*Simulations show temporal expression of p53 (A), phosphorylated p53 (B), p21 (C), p16 (D), p38 (E), and phosphorylated p38 (F). A p53 KD was introduced in all proteins (A-F). Units are arbitrary (AU). *Senescence and/or KD induced. DDIS, DNA damage-induced senescence; OIS, oncogene-induced senescence. Produced using the same method as described in Scanlan et al. (2024).*

As mentioned, a critical component of senescence is the inflammatory SASP. The SASP is involved in numerous processes in senescence including immune clearance (Krizhanovsky et al., 2008; Muñoz-Espín & Serrano, 2014) and inducing bystander senescence (Acosta et al., 2013; Nelson et al., 2018). Therefore, to model cellular senescence, the SASP must be included. Consequently, NF-κB (in three different cellular states – inhibited, uninhibited, and phosphorylated) and IL-6 were introduced into the model network of Model B (**Figure 5.1B**).

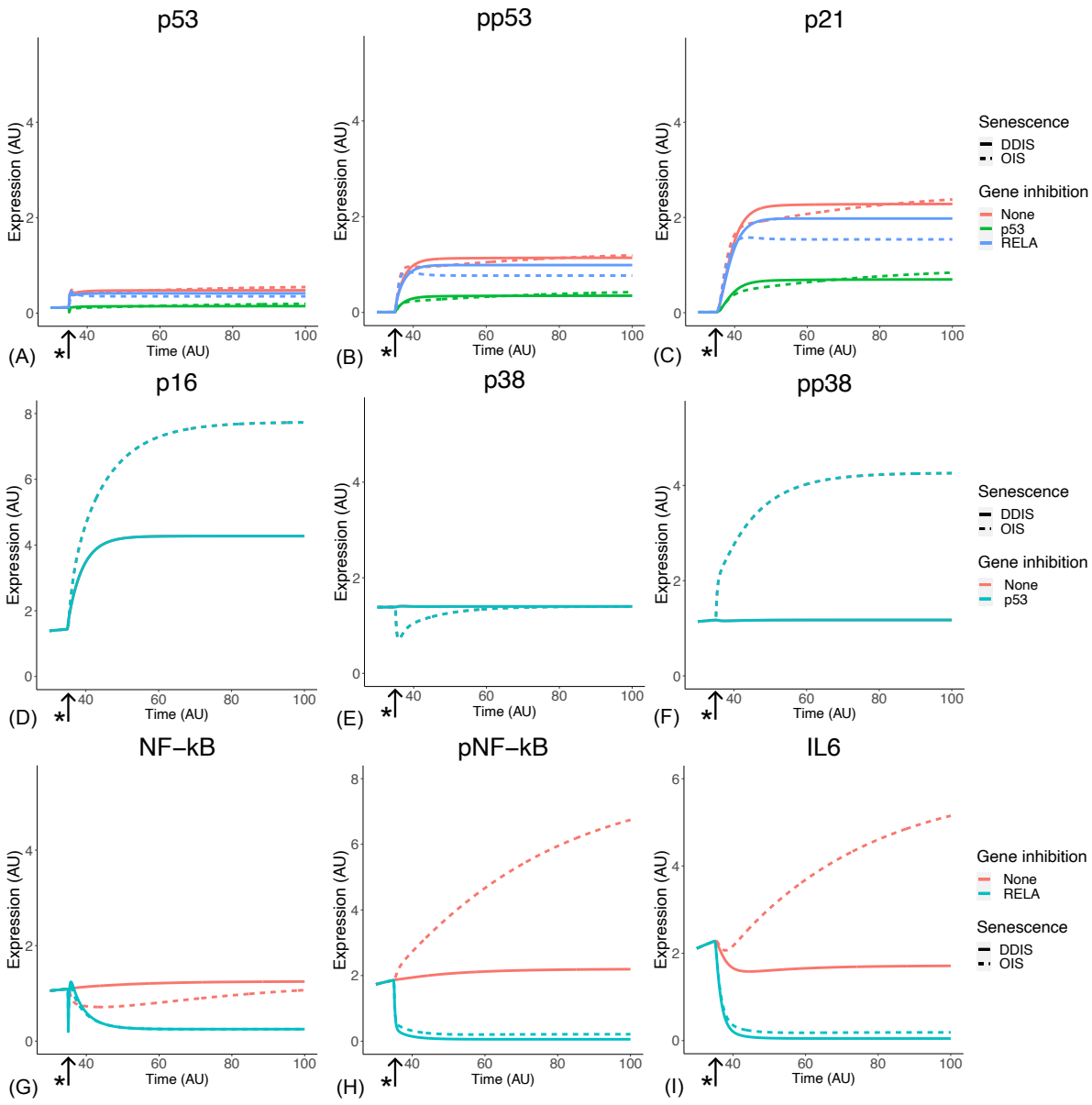

Figure 5.3 – Simulation of proteins in Model B.

*Simulations showing temporal expression of p53 (A), phosphorylated p53 (B), p21 (C), p16 (D), p38 (E), phosphorylated p38 (F), NF-KB (G), phosphorylated NF-KB (H), and IL6 (I). Different KDs were introduced to different proteins, p53 and RELA KD to (A-C), p53 KD to (D-F), and RELA KD to (G-I). Units are arbitrary (AU). *Senescence and/or KD induced. DDIS, DNA damage-induced senescence; OIS, oncogene-induced senescence. Produced using the same method as described in Scanlan et al. (2024).*

Model B was able to meet the same criteria as Model A as well as additional criteria, whereby p53 signalling became activated upon senescence induction (**Figure 5.3A-C**), KD of p53 resulted in decreased p21 expression (**Figure 5.3C**), and p16

expression was sustained and higher in OIS than in DDIS (**Figure 5.3C-D**). However, p38 expression and phosphorylation remained the same in Model B as it did in Model A and therefore did not satisfy the established p38-related criteria (**Figure 5.3E-F, Table 5.1**).

While expression of p53 signalling and p38 signalling were the same in Model B as in Model A, the addition of inflammatory protein species provided the opportunity for simulations to meet additional criteria. There was a stronger inflammatory phenotype in OIS compared to DDIS demonstrated by increased expression of IL-6 and the active form of NF-κB (**Figure 5.3G-I**). Interestingly, we observed less total NF-κB expression (**Figure 5.3G**) and more NF-κB phosphorylation (**Figure 5.3H**). This observation illustrates the complexity of cellular processes and the importance of investigating processes in multiple macromolecule types as direct NF-κB phosphorylation, a PTM, cannot be observed at the transcript level. Additionally, the introduction of a RelA KD decreased p53 signalling illustrated by decreased pp53 and p21 expression (**Figures 5.3B-C**), further demonstrating the additional ability for Model B to meet more criteria than Model A and therefore be a better representation of senescence.

Results of Model B were able to meet five of the established criteria: sustained p21 and p16 expression, higher p16 expression in OIS compared to DDIS, there is a stronger inflammatory phenotype in OIS and DDIS, KD of p53 resulted in downregulated p21 expression, and KD of RelA results in decreased p53 signalling. However, despite the introduction of NF-κB and IL-6, Model B still did not meet all twelve criteria to be considered a successful representation of cellular senescence. Importantly, inflammatory SASP-associated proteins were induced immediately upon senescence induction, a behavioural profile not observed in published protein literature (Coppé et al., 2010; Kuilman & Peeper, 2009) nor in the transcriptomic analysis of **Chapter 4**. A mechanism which modulated temporal SASP induction was therefore required. One possible mechanism for modulating the SASP is dynamic changes in Notch signalling (Hoare et al., 2016).

Thus, additional inflammatory proteins and Notch signalling were added to the protein network of Model C (henceforth referred to as the Cellular Senescence Model

– **Figure 5.1C**). To model a change in Notch signalling dynamics, the NOTCH1 receptor and NICD were introduced as protein species in the model network. As Notch signalling is a juxtacrine mechanism and this model is at the single cell level, to induce a change in Notch receptor activity an inducible event termed the 'Notch switch' was introduced as described in **Section 2.3.3**. When activated, NICD expression (the active cleaved component of the Notch receptor) is downregulated. Downregulation of NICD represents less ligand-receptor activity as less NICD is released from NOTCH1; indicating less Notch signalling as there is less NICD to translocate into the nucleus and enact Notch-mediated transcription.

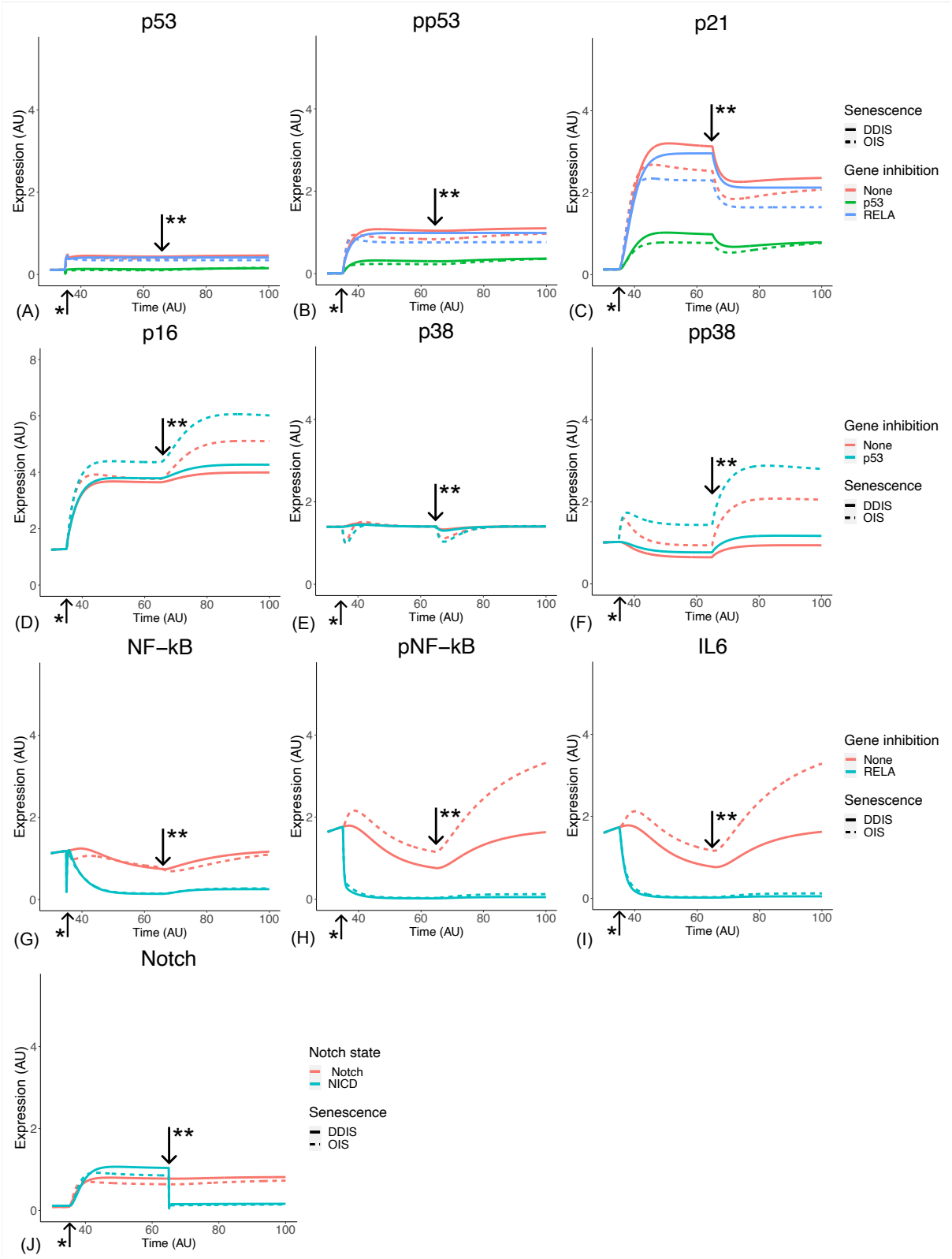

Figure 5.4 – Simulation of proteins in The Cellular Senescence Model.

Simulations show temporal expression of p53 (A), phosphorylated p53 (B), p21 (C), p16 (D), p38 (E), phosphorylated p38 (F), NF-KB (G), phosphorylated NF-KB (H), IL6 (I), and Notch (J) in DDIS and OIS. Different KDs were introduced to different proteins, p53 and RELA KD to (A-C), p53 KD to (D-F), and RELA KD to (G-I). Units

*are arbitrary (AU). *Senescence and/or KD induced. **Notch Switch induced. DDIS, DNA damage-induced senescence; OIS, oncogene-induced senescence; NICD, Notch intracellular domain. Taken from Scanlan et al. (2024).*

Simulation outputs of the Cellular Senescence Model (**Figure 5.1C**) successfully met all twelve predefined criteria pertaining to normal and KD senescence temporal protein phenotypes (**Table 5.1**). Upon senescence induction, p53 signalling was activated, with higher levels observed in DDIS compared to OIS (**Figures 5.4A-C**). Model perturbations further confirmed expected molecular phenotypes and interactions: p53 KD led to a reduction in p21 expression, as indicated by the lower **green** line relative to the **pink** line (**Figure 5.4C**), while RelA KD resulted in decreased p53 signalling, evidenced by the lower **blue** line compared to the **pink** line in simulation graphs (**Figures 5.4A-C**). As expected, due to p53 being a direct mediator of p53 signalling, a p53 KD had a bigger effect on p53 signalling than the RelA KD. Although the observed impact of a RelA KD on p53 signalling has not been explicitly reported at the protein level, it was identified in this transcriptomic KD analysis (**Figure 3.15B-D**). The ability of simulations to reproduce this phenotype at the protein level indicates a potentially intriguing feedback loop between RelA and p53 which warrants further investigation in future *in vitro* or *in vivo* work.

Further related to cell cycle regulator proteins and their criteria, p21 and p16 were sustained into late senescence and persisted beyond activation of the Notch Switch (**Figures 5.4C-D**). Notably, p16 expression was stronger in OIS and was upregulated later in DDIS compared to OIS. Stronger p16 expression in OIS supports the greater involvement of p16 in inducing cell cycle arrest in OIS, aligning with analysis in this thesis (**Figure 4.8H**) and with published studies showing the involvement of p38 signalling (via Ras) as inducing p16 activity (Kwong et al., 2009; Sun et al., 2007; Wong et al., 2009). Unlike p53 signalling, which has been shown in this transcriptomic analysis and modelling to play a more dominant role in DDIS compared to OIS (**Figures 3.14B-D** and **4.8D-G**). This distinction further highlights the differences in regulatory mechanisms of senescence, reinforcing the complexity of cell cycle control in different senescence contexts even though the result of cell cycle arrest is the same. Moreover, p53 KD led to an upregulation of p16 expression (**Figure 5.4D**). The upregulation of p16 following p53 KD suggested that p53 may

restrain p16 activity. However, one study reported decreased p16 transcript expression upon p53 KD in OIS (Georgilis et al., 2018). Interestingly, while activation of the Notch Switch resulted in a slight downregulation of p21, p16 expression increased – particularly in OIS, further highlighting the greater role of p16 in OIS compared to DDIS. Sustained expression of cell cycle inhibitor proteins into late senescence suggests they are continually expressed to aid in maintenance of cell cycle arrest, an observation further supported by transcriptomic analysis (**Figures 4.8G-H**).

Overall, p38 expression remained stable throughout DDIS and OIS simulations, consistent with the transcriptomic analyses in this thesis (**Figure 4.10A**) and published protein data (Freund et al., 2011). However, phosphorylated p38 (pp38) increased, with higher phosphorylation observed in OIS compared to DDIS. Additionally, p53 KD increased p38 activity, as indicated by the **blue** line compared to the **pink** line (**Figure 5.4F**). This finding supports previously published protein profiles (Freund et al., 2011) and transcriptomic analysis in this thesis (**Figure 3.14F**).

In the previous model iteration (Model B), there was a stronger inflammatory phenotype in OIS compared to DDIS, but these proteins were immediately upregulated upon senescence induction (**Figures 5.3G-I**). In simulation of the Cellular Senescence Model, simulations captured both a stronger inflammatory response in OIS and a delayed induction of inflammatory proteins (**Figure 4.5G-I**), consistent with published protein profiles (Coppé et al., 2008; Hernandez-Segura et al., 2017; Kuilman et al., 2008). Although NF-κB expression remained similar between DDIS and OIS, there was more pNF-κB in OIS, which likely contributed to the increased inflammatory response observed in OIS compared to DDIS, which we also observed in our systematic transcriptomic analysis (**Figure 4.10**). Both the systematic analysis and computational modelling suggest that SASP factors in DDIS are not delayed but rather expression is reduced in comparison to OIS. For example, median expression of the *IL6* transcript initially increased between days 5 and 7 in both DDIS and OIS, but the range of expression was larger in OIS (**Figure 4.10C**). This was also observed at the protein level in model simulations (**Figure 5.4I**). While both transcriptomic analyses and computational analyses support stronger SASP

expression in OIS, the primary role of SASP – whether in senescence maintenance, bystander induced senescence, or other – is unknown.

The Notch switch was introduced to the network of the Cellular Senescence Model as a mechanism to modulate temporal SASP expression. At Time = 65 (AU) in model simulations, Notch signalling activity dynamically transitioned from active to inactive. Following senescence induction and establishment, Notch signalling was active indicated by expression of the NICD. Upon induction of the Notch switch, NICD was downregulated indicating reduced Notch signalling activity (**Figure 5.4J**). These simulation results recapitulated published protein profiles in senescence (Hoare et al., 2016) and are further supported by the systematic analysis of *HES1* transcript expression (**Figure 4.11C**). These findings highlight the role of Notch signalling in controlling temporal SASP expression and suggest that therapeutic targeting of Notch signalling could reduce inflammatory SASP expression in senescent cells, reducing bystander senescence and chronic low-grade inflammation when the timely removal of senescent cells by the immune system becomes dysregulated.

In conclusion, the Cellular Senescence Model successfully met all twelve molecule phenotype criteria established (**Table 5.1**). This model represents an important contribution to the senescence field by integrating data from multiple studies of single timepoints or limited timepoints to simulate temporal protein changes during senescence. Notably, this is the first model to explore temporal protein changes in senescence, providing a more comprehensive and realistic understanding of senescence. However, this model is at the single cell level. The impact of non-autonomous senescence mechanisms could not be explored to further the understanding of senescence in multicellular environments such as those in tissue composition; although as with the Notch switch, events can be introduced to mimic non-autonomous mechanisms. Furthermore, this computational model demonstrates that events (such as the Notch switch) and perturbations (such as a p53 KD) can be introduced with relative ease into the model network. In this context, the model presented here is a valuable tool for future studies aiming to further dissect the molecular mechanisms of senescence and how different interventions may alter a senescent cell.

5.2.3 Dynamic sensitivity analysis of the Cellular Senescence Model.

The Cellular Senescence Model was able to satisfy all twelve defined criteria, but it is important to explore how sensitive simulations are to variations in parameter values. Dynamic sensitivity analysis was used here as it assesses the sensitivity of each protein species to model parameters as time in the simulation progresses. It does this by individually changing each parameter value (by 10% in this case) and running the simulation to see how protein expression is affected.

Four time points were assessed throughout the simulation period, one before senescence was induced (Time = 20) and three during senescence (Time = 40, = 60, and = 80). Time 40 and 60 were both before the Notch switch was induced, whereas time 80 was post-Notch switch induction. These times were chosen to provide a varied and in-depth understanding of the sensitivity of proteins at senescence induction, during senescence establishment, and into the late inflammatory state of senescence.

At all four time points assessed, in both DDIS and OIS, protein species were mostly sensitive to parameters which were involved in inducing senescence or the Notch switch – which was expected as these parameters influence the overall outcome of protein expression. Sensitivities were similar between senescence types, however there were some key differences due to different inputs being used to stimulate senescence induction.

Prior to senescence induction (Time 20 – **Figure 5.5A**) there was minimal sensitivity of protein species to parameters. The two parameters which caused the most sensitivity of proteins were kDDRD (in DDIS simulations) and kRASD (in OIS simulations). Both of these parameters form part of the reaction to downregulate DDR signalling and RAS expression respectively. In the computational model, DDIS was induced through high activation of the DDR which leads to induction of cell cycle inhibitors, whereas OIS was induced through the strong activation of RAS and the DDR dependent upon RAS (rather than a genotoxic stress such as ultraviolet irradiation). Therefore, it was expected that most protein species would be sensitive to kDDRD and kRASD parameters specifically in DDIS and OIS. After senescence induction, sensitivity of most protein species to kDDRD remained similar to Time 20,

however protein sensitivity to kDDRF massively increased in DDIS (Time 40 – **Figure 5.5B**). Furthermore, pNF-κB, IL-6, pp38 and RAS all became highly sensitive to kRASF following induction of DDIS. In OIS however, after senescence induction, most proteins became highly sensitive to kDDRFRAS and kRASF, both of which were used as inputs to induce OIS in the model. As senescence progresses, but prior to activation of the Notch switch, sensitives remain similar in DDIS and OIS however there were some notable differences. These included an increased sensitivity of pRb, NF-κB and the inhibited form of NF-κB to kDDRF in DDIS, and an increased sensitivity of p53, NF-κB and inhibited NF-κB to kDDRFRAS in OIS (Time 60 – **Figure 5.5C**). The final timepoint analysed occurred after the Notch switch was induced. As expected, the majority of proteins became sensitive to kNICDD (one of the parameters altered during the Notch switch event) in both DDIS and OIS (Time 80 – **Figure 5.5D**).

Most protein species were sensitive to direct inputs which induce either senescence or induction of the Notch switch, suggesting that, if there were dose differences in senescence induction but with the same drug, you may see different outcomes in the transcriptome and therefore at the protein level. In SenOmic, for example, there are eight studies which induce DDIS using etoposide. However, there were three differing doses of etoposide treatment with different treatment regimens depending upon the study design, all which could lead to changes in the senescence phenotype.

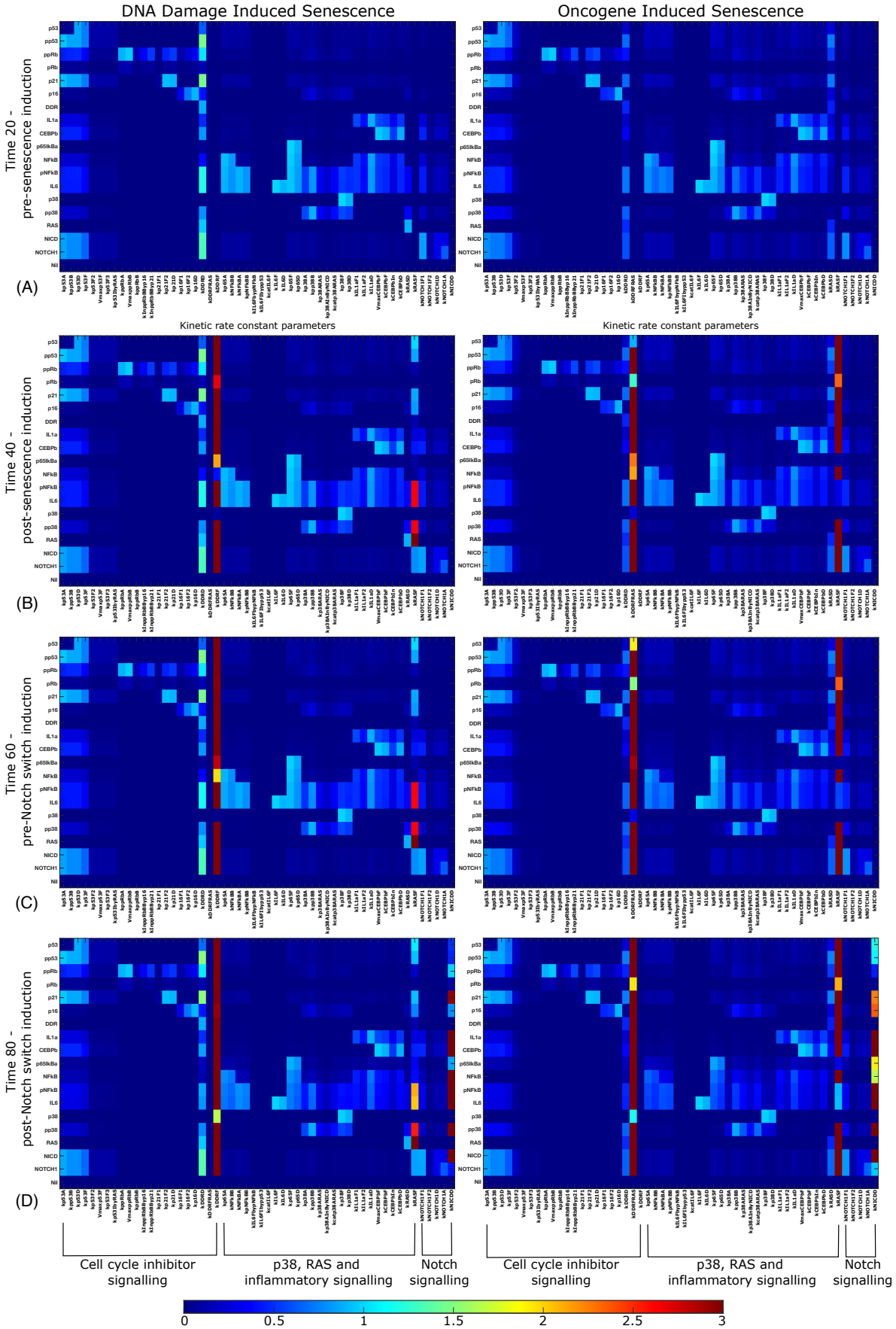

Figure 5.5 - Dynamic sensitivity analysis of the Cellular Senescence Model.

Dynamic sensitivity analysis of senescence simulations. Four timepoints – Time 20

(A), Time 40 (B), Time 60 (C), and Time 80 (D) – were selected in the simulation period of DDIS and OIS, and dynamic sensitivity analysis was performed on all parameters. DDIS, DNA damage-induced senescence; OIS, oncogene-induced senescence.

5.2.4 Future perspectives and adaptations of the Cellular Senescence Model.

It has been demonstrated during model development that additional pathways of interest can be introduced into the model network and that perturbations such as KDs can also be introduced. There are many possibilities when it comes to further developments of this model as the current protein network is not exhaustive of cellular senescence. For example, one possibility is the introduction of an early fibrogenic TGFβ-rich SASP.

Numerous studies have reported TGFβ expression in senescent human fibroblasts, with many of these studies observing an increase in TGFβ or TGFBR1 mRNA expression at an undisclosed timepoint (Acosta et al., 2013; Hubackova et al., 2012). At the protein level, Hoare et al. (2016) observed weak staining of TGFβ in both OIS and DDIS, with this peaking at different times dependent on the senescence type; in OIS, TGFβ expression peaked at day 4 before declining, while TGFβ expression peaked at days 1–2 in DDIS. While some studies do support an early fibrogenic SASP in senescence, this is not supported at the transcriptomic level in this interrogation of SenOmic (**Figures 4.9C-E**). This thesis has suggested that perhaps the TGFβ present in protein studies may be what was already present in the cell or from cells which have entered apoptosis in response to the damaging stimulus, and goes further to suggest that TGFβ signalling may be downregulated and not activated in response to senescence induction due to downregulation of the *ACTA2* transcript from as early as the first time_group (days 0–4 – **Figure 4.9E**). Despite this uncertainty, it is possible to introduce TGFβ-related signalling into the Cellular Senescence Model after performing a non-systematic review (**Figure 5.6**) as described in **Section 2.3.1**.

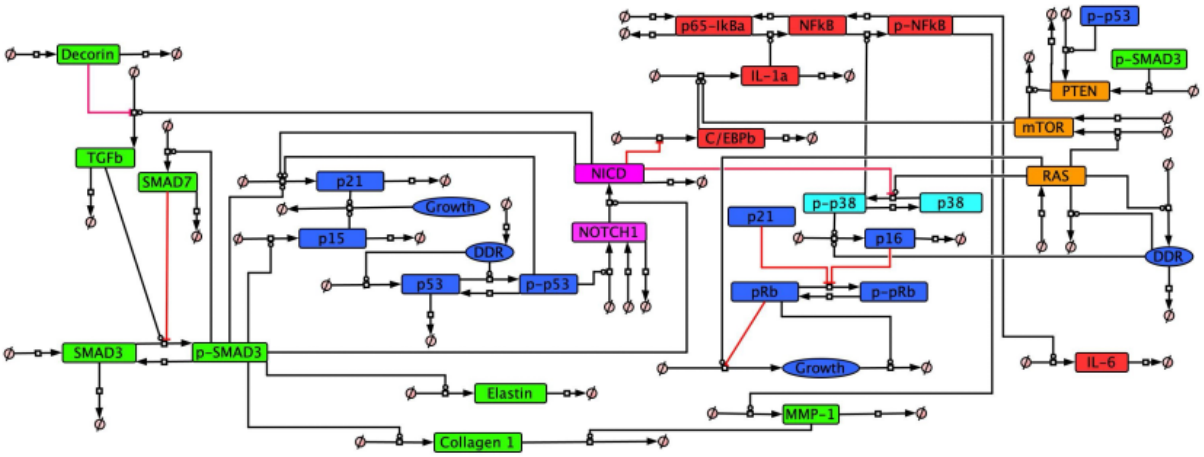

Figure 5.6 – Protein network of Model D.

A non-systematic review of the literature was performed with TGFβ signalling in mind as described in **Section 2.3.1**. From this non-systematic review, the network of Model D was produced. Proteins such as p15 and PTEN were added to the network to expand upon the cell cycle signalling and metabolic-related proteins. Additionally, TGFβ signalling was added to the network, represented by TGFβ, Decorin, SMAD3, SMAD7, Elastin, and Collagen1. Not all of these proteins had temporal expression information available in the context of cellular senescence, however they have been demonstrated as interlinked within TGFβ signalling (**Appendix Table A5.1**). Model D was not simulated but demonstrates the versatility of computational modelling, as well as providing a potential future direction which could be performed in conjunction with laboratory experiments investigating TGFβ signalling in early senescence; experiments which could investigate the theory that the expression of TGFβ after senescence induction is not representative of initial increased TGFβ signalling, but rather a byproduct of TGFβ which was already present in cells and in those which may have entered apoptosis. With additional experimental evidence, TGFβ signalling could be accurately simulated. Results from computational simulations could then guide laboratory experiments for validation, and vice versa.

5.3 Conclusion.

In conclusion, this Chapter highlights the advantages of taking a systems biology approach to studying senescence, emphasising the importance of taking an integrated multi-macromolecule approach. **Chapter 5** collated data from various studies in a non-systematic review aimed at building a temporal profile of protein

phenotypes in senescent human fibroblasts. From this non-systematic review, supported by systematic analysis of SenOmic, twelve criteria were able to be devised pertaining to normal and KD senescence phenotypes. A model of senescence was built in stages, adding additional complexity with each stage of the model, to satisfy the twelve criteria. The Cellular Senescence Model successfully demonstrated the capability to meet all twelve criteria, supporting both published literature and the transcriptomic analysis in this thesis.

Several interesting observations emerged in this work, offering insights which have not been extensively explored previously. Notably, SASP expression appeared weaker in DDIS compared to OIS (**Figures 4.10** and **5.4G-I**). The base code for the model was the same for DDIS and OIS simulations, the only difference was the parameter value for the senescence inducing parameters. The parameters for inducing senescence were chosen based on the literature understanding of DDIS and OIS, and it is intriguing to observe how slight changes in parameter values can lead to significantly different outcomes when using the same base code. This observation was further enhanced by the dynamic sensitivity analysis which identified the model as being sensitive to parameters which either induced senescence or the Notch switch (**Figure 5.5**). The Cellular Senescence Model was further able to demonstrate its adaptability at introducing inducible events and perturbations such as the Notch switch and p53 KD, showcasing its potential for future modifications. Furthermore, with additional temporal protein data from *in vitro* and *in vivo* analyses, the cellular senescence model can be further developed. For example, incorporation of TGFβ signalling and related fibrogenic proteins as outlined in Model D (**Figure 5.6**).

This work underscores the importance of taking an integrated approach to investigate both the transcriptomic and protein levels of senescent human fibroblasts. While direct phosphorylation cannot be observed at the transcript level, it can be observed at the protein level. Likewise, transcription of genes following phosphorylation and activation of a protein can be observed at the transcript level. Taking an integrative approach, such as described here, provides a robust framework for investigating complex biological processes across multiple macromolecule types.

Chapter 6 – KEGG-based analysis framework: cGAS-STING signalling and the adaptability of the framework.

6.1 Background.

The KEGG pathway database provides a comprehensive bioinformatics resource which integrates genomic, chemical, and systemic functional information into databases including genes, diseases, and pathways (Kanehisa et al., 2025). In this chapter, the KEGG resource is used to investigate cytosolic DNA sensing (specifically cGAS-STING signalling) in different cellular states. Utilising KEGG and related libraires allows for a broad overview of how whole pathways change in response to different cellular contexts, such as disease states or in response to therapeutic interventions.

cGAS-STING signalling is an evolutionarily conserved pathway primarily implicated in the innate immune response (Hopfner & Hornung, 2020) and implicated in different disease states such as rheumatoid arthritis (Liu & Pu, 2023) and acute kidney injury (Sun et al., 2023). Furthermore, cGAS-STING signalling has been linked to ageing and senescence (Glück et al., 2017; Gulen et al., 2023; Lan et al., 2019), specifically to the SASP in senescence (Gulen et al., 2023; Schmitz et al., 2023; Yang et al., 2017). Upon detection of cytosolic dsDNA (either foreign or self-originating), cGAS binds the dsDNA and in a multistep process is converted to cGAMP. cGAMP is a secondary messenger which primarily binds to and activates the protein STING. Once STING is activated, in canonical cGAS-STING signalling, IRF3 is recruited and translocates to the nucleus to enact targeted gene expression of genes including type I IFNs, IL-6, and IL-12 (Decout et al., 2021).

There has been increasing interest in cGAS-STING signalling in senescence due to its innate ability to increase transcription of inflammatory genes. Multiple studies have observed cGAS as recognising self cytoDNA in senescent cells – for example, cGAS has been experimentally shown to co-localise with CCFs in senescent cells (Dou et al., 2017), and to also recognise CCFs in senescent cells (Glück et al., 2017). In cell culture experiments, KO of cGAS or STING in mouse embryonic fibroblasts (MEFs) compromised the senescence phenotype compared to WT MEFs when trying to induce senescence – evidenced through reduced p16 activation and SA-β-gal

staining in the KO MEFs. This was found in multiple modes of senescence induction including oxidative stress, aberrant RAS activation, and the use of DNA damaging agents (Glück et al., 2017). This study was further able to demonstrate that when cGAS was knocked out, the senescent bystander effect was not present, highlighting the role of cGAS-STING in promoting bystander senescence.

cGAS-STING signalling is also of interest in other cellular contexts such as the immune system and autoimmune diseases (Hopfner & Hornung, 2020; Liu & Pu, 2023). Towards understanding the basics of cGAS-STING signalling, one study has modelled the dynamics of cGAS-STING signalling and was able to form hypotheses such as how the inhibition of TREX1 (a DNA exonuclease) effected the inflammatory IFN response, as well as exploring small molecule inhibitors of cGAS and how they were able to achieve reduced expression of inflammatory proteins (Gregg et al., 2019).

In collaboration with the Bohr and Rasmussen laboratories at Copenhagen University, the role of cytosolic DNA-sensing, specifically cGAS-STING signalling, was investigated in microglial cells with or without an APTX KO to mimic the disease AOA1. RNAseq was performed and data analysed on samples as detailed in **Section 2.4** and Madsen et al. (2023). Part of the bioinformatic analysis of this paper involved investigating the human cytosolic DNA-sensing pathway as defined by the KEGG Pathway database, for which the pathway code is hsa04623 (**Figure 6.1**). The KEGG-based framework used in this analysis can be adapted to investigate any cellular state (for example, senescence or aged cells). The aim of this chapter is to present the applications of this KEGG-based analysis framework though the work conducted in Madsen et al. (2023) and to discuss how it can be applied to future analysis of SenOmic, such as with the cellular senescence pathway itself (hsa04218) or p53 signalling pathway (hsa04115).

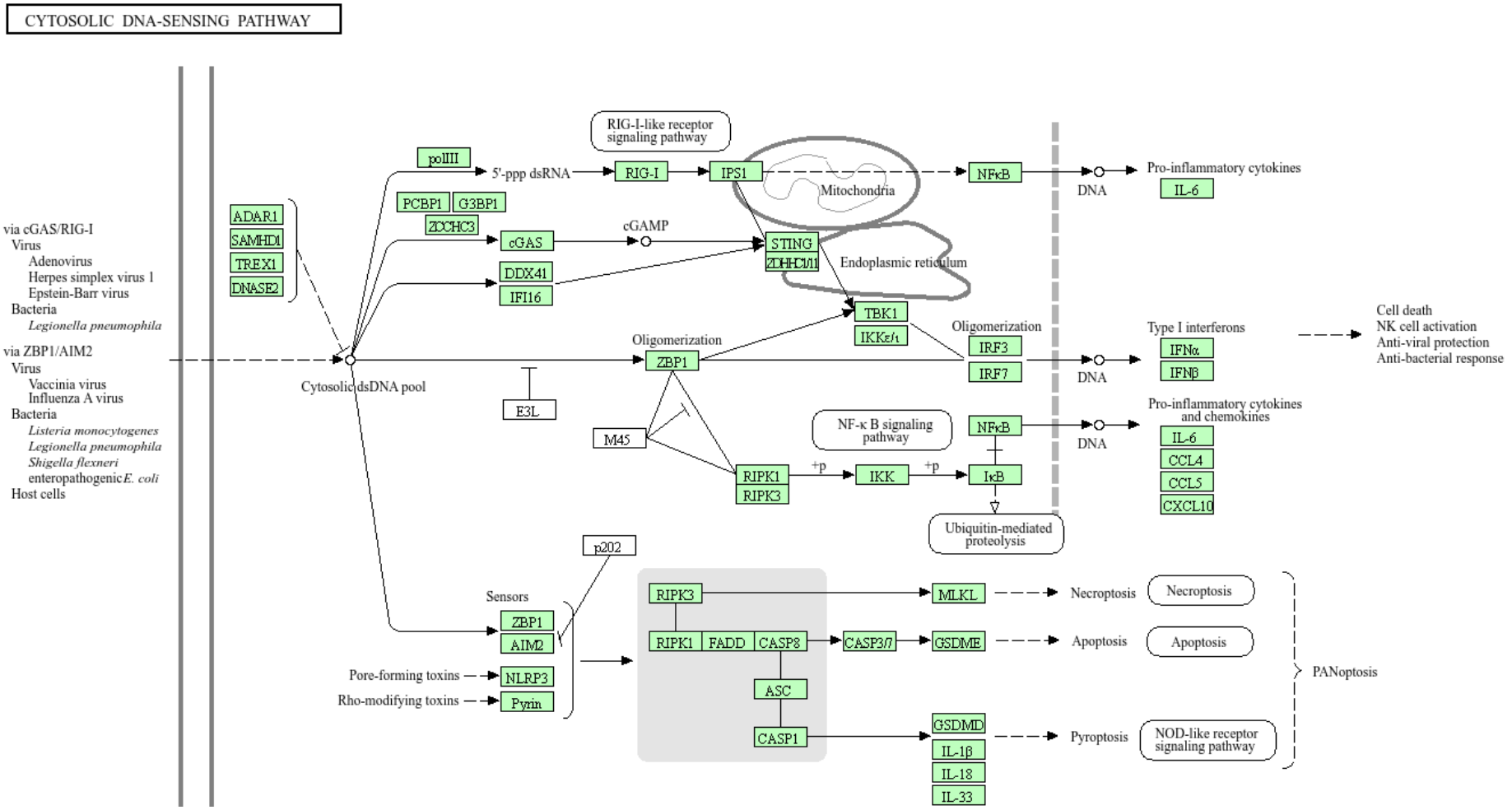

Figure 6.1 – Cytosolic DNA-sensing KEGG pathway.

The human pathway code hsa04623 details the cytosolic DNA-sensing KEGG human pathway and is available at the following link: ***https://www.genome.jp/pathway/hsa04623***.

6.2 Results and discussion.

In the Madsen et al. (2023) study, cGAS-STING signalling was investigated in microglial cells with APTX KO to mimic AOA1. In this chapter, the KEGG pathway analysis framework developed and how it can be applied to future work senescence-associated data is the primary focus of discussion.

6.2.1 – KEGG pathway analysis.

Enrichment analysis of the APTX KO microglial cells compared to APTX WT microglial cells identified a dysregulated response to viral infections and a dysregulated innate immune response suggesting altered cytosolic DNA-sensing dynamics in the absence of functional APTX (Madsen et al., 2023). Thus, for this study, the KEGG cytosolic DNA-sensing pathway (**Figure 6.1**) was further interrogated and the KEGG-based analysis framework developed.

Genes, which were significantly ($q < 0.05$) DE under the different APTX and immune stimulation statuses were overlaid with the KEGG cytosolic DNA-sensing pathway (**Figures 6.2-6.4**). This analysis demonstrated how cytosolic DNA-sensing was altered between the different sample comparisons: APTX1_NS versus APTX0_NS (**Figure 6.2**); APTX1_NS versus APTX1_IS (**Figure 6.3**); APTX0_NS versus APTX0_IS (**Figure 6.4**). Understanding the results is relatively straightforward due to the KEGG-based technique of presenting the whole pathway. There were clear significant differences between each of the comparisons made. For example, when there was no immune stimulation (NS), there was a significant decrease in expression of TREX1, CASP1, IL-18, and RIG-I when APTX was knocked out (**Figure 6.2**), which suggested APTX KO dysregulated DNA- and RNA-sensing pathways. Already, this was an interesting observation as it suggested that the KO of APTX effected the base expression of mediators of cytosolic DNA-sensing pathways. If KEGG analysis had not been performed in addition to the other bioinformatic analysis conducted in the paper (such as ORA and heatmap analysis), this observation could have been easily missed. Moreover, when there was IS, there were similarities between the pathway in APTX WT cells (**Figure 6.3**) and APTX KO cells (**Figure 6.4**), but there were also distinct differences. Importantly, when APTX KO cells were stimulated with dsDNA, there was no significant effect detected on

STING (**Figure 6.4**), suggesting APTX KO cells were unable to correctly activate the cGAS-STING pathway as observed in the WT cells (**Figure 6.3**).

Performing KEGG pathway analysis in this manner allowed for easy visualisation of the pathway as a whole and how the pathway can change in response to different experimental conditions.

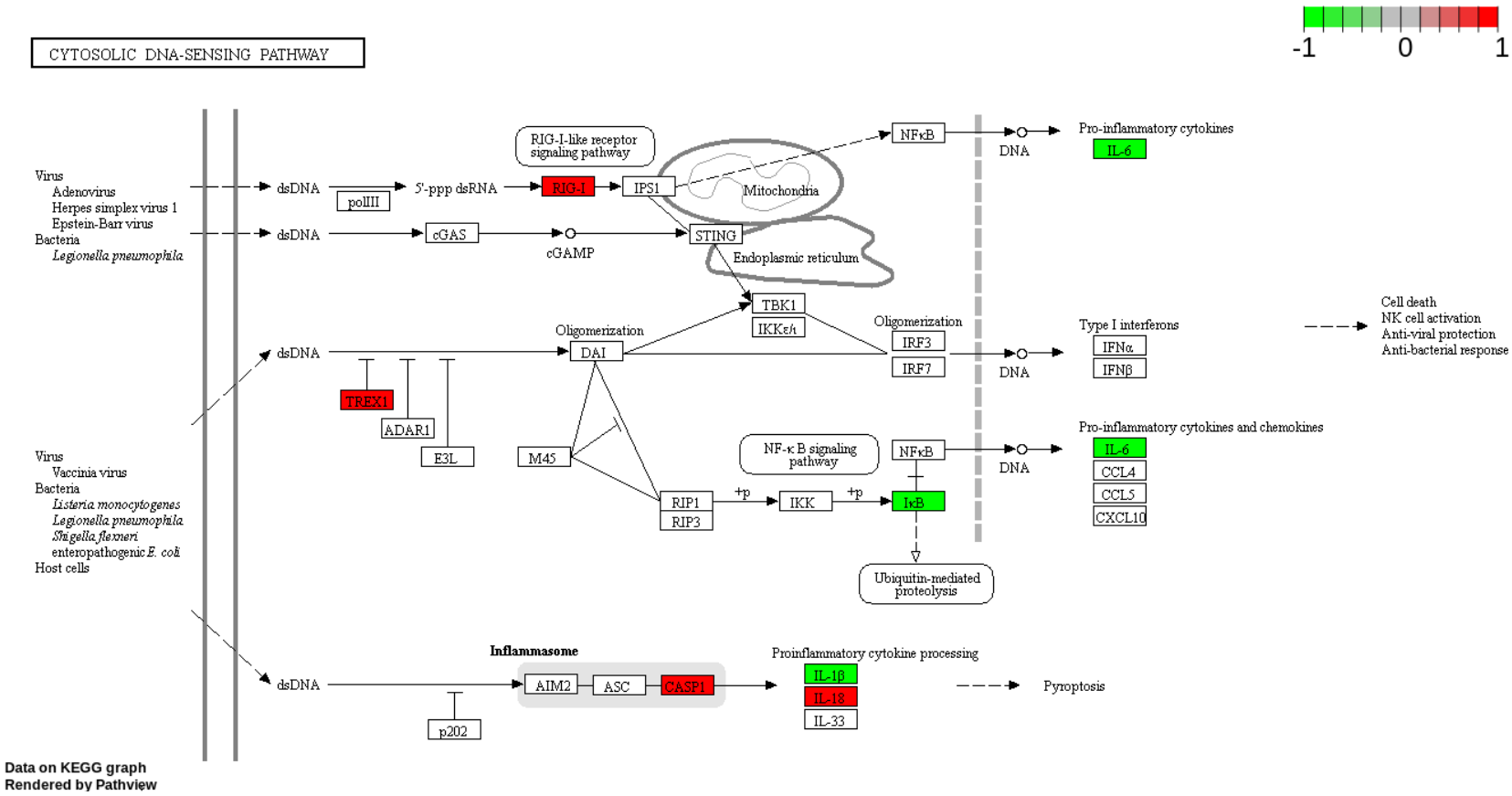

Figure 6.2 – Comparison of the cytosolic DNA-sensing pathway in non-stimulated APTX WT versus APTX KO cells.

Analysis of the cytosolic DNA-sensing human KEGG pathway in non-stimulated APTX WT versus non-stimulated APTX KO microglial cells. Green, downregulation; red, upregulation. Taken from Madsen et al. (2023).

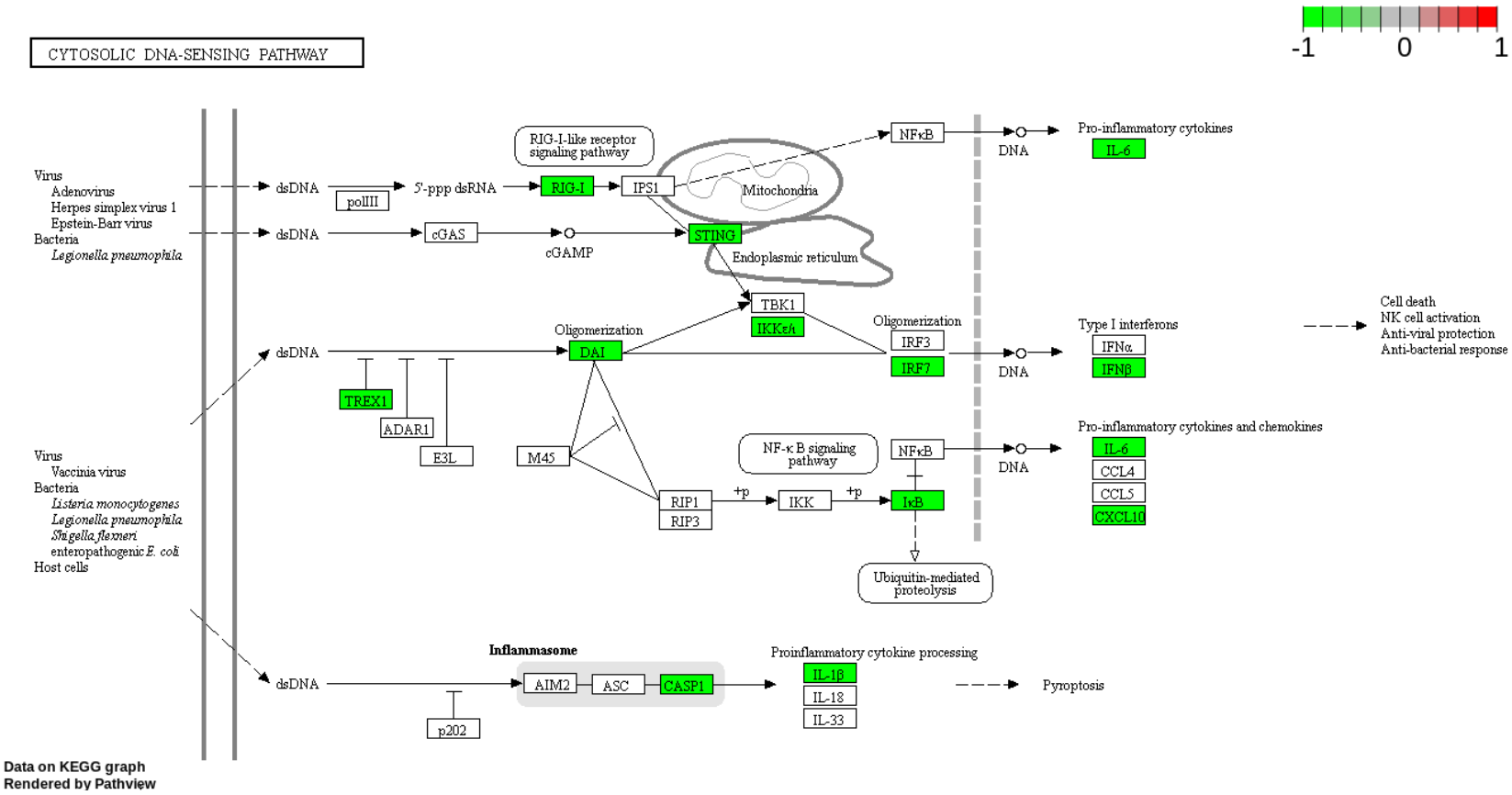

Figure 6.3 – Comparison of the cytosolic DNA-sensing pathway in non-stimulated versus immune-stimulated APTX WT cells.

Analysis of the cytosolic DNA-sensing human KEGG pathway in non-stimulated APTX WT versus immune-stimulated APTX WT microglial cells. Green, downregulation; red, upregulation. Taken from Madsen et al. (2023).

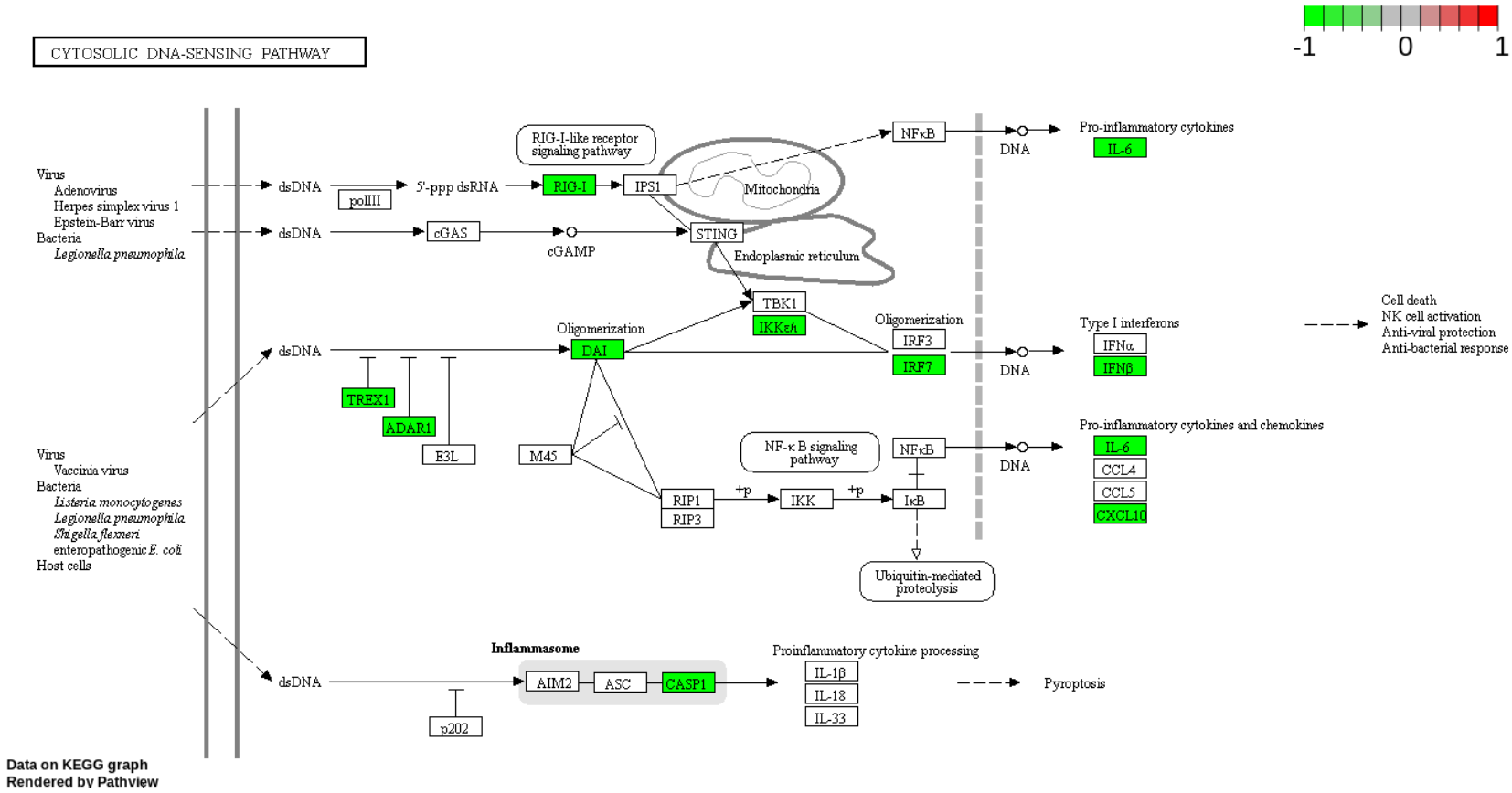

Figure 6.4 – Comparison of the cytosolic DNA-sensing pathway in non-stimulated versus immune-stimulated APTX KO cells.

Analysis of the cytosolic DNA-sensing human KEGG pathway in non-stimulated APTX KO versus immune-stimulated APTX KO microglial cells. Green, downregulation; red, upregulation. Taken from Madsen et al. (2023).

6.2.2. – Adaptation of KEGG analysis framework.

The KEGG-based analysis framework described in this study can be applied to any transcriptomic dataset which compares two different samples. SenOmic, for example, contains 1069 unique sample comparisons across 119 RNAseq datasets.

RNAseq data can be processed, aligned and analysed following any traditional RNAseq analysis pipeline, including the one used in this thesis. Once significantly DE genes were identified, the results can be visualised using libraries KEGGrest and pathview as described in **Section 2.4** and explored in the previous section. Additionally, although KEGG primarily focuses on genes, genomes, and metabolites, proteomic data can be integrated by mapping protein information to corresponding gene IDs. This would then enable pathway visualisation at the protein level, facilitating multi-omic analysis when data is available.

If specific pathways have been identified in prior analysis, such as in ORA or GSEA, KEGG can be searched for associated pathways. For example, in the temporal transcriptomic analysis of senescent cells versus non-senescent proliferating cells, **Figures 4.2, 4.3, 4.4,** and **4.5** all identified activation of p53 signalling as being significantly enriched at all timepoints. The KEGG pathway code for p53 signalling in humans is hsa04115. Therefore, to investigate the p53 signalling pathway within the context of SenOmic datasets, ‘hsa04115’ could be substituted in the file ‘RS_Enrichment_analysis_APTXwork.R’ where ‘hsa04263’ is specified, and the whole p53 signalling pathway can be investigated and visualised at the different timepoints.

6.3 Conclusion.

Investigating cGAS-STING signalling in different disease and cellular settings, such as AOA1 and senescence, is important for developing future therapies. Therefore, by taking the integrated biochemical and computational approaches described in Madsen et al. (2023) and outlined in **Section 2.4**, the impact on the whole cytosolic DNA-sensing pathway can be explored.

As mentioned, the study by Gregg et al. (2019) developed a computational model of cGAS-STING signalling under normal signalling conditions. By applying this KEGG-

based analysis framework to multiple datasets investigating cGAS-STING signalling across different cellular states, data can be gathered to enhance this model and create a more comprehensive computational model of cGAS-STING signalling with the inclusion of various perturbations such as age, senescence, and disease states like AOA1. This approach exemplifies the integration of *in silico* modelling with *in vitro* experimentation, where computational predictions can inform experimental design, and experimental results can refine and validate the model. Collaborative research efforts like this highlight a successful systems biology approach which enables a deeper mechanistic understanding of complex signalling pathways and facilitates the development of targeted therapeutic strategies.

An advantage of this KEGG-based analysis framework is that it can be applied to any KEGG pathway. KEGG is a long-established database consistently funded since 1995. As this resource is constantly updated to reflect the understanding of biological processes, KEGG pathways can change when updated (as seen between **Figure 6.1** and **Figures 6.2–6.4**). In this case, **Figure 6.1** is the most up to date version of cytosolic DNA-sensing pathways in humans and the analysis performed in Madsen et al. (2023) was performed prior to the updating of the KEGG pathway.

Using this KEGG-based framework provides an interesting and valuable approach to investigating and interrogating specific pathways. It is particularly striking to see how different parts of the pathway can be up- or downregulated depending on the cellular state, whether this is normal proliferating cells, senescent cells, or diseased cells. It is especially interesting as the whole pathway is visualised, not just the effectors which are often the focus of investigations. For example, with cGAS-STING signalling, it is often only the target genes and proteins cGAS and STING themselves which are investigated in laboratory settings. However, with this KEGG-based analysis framework, the entire pathway can be easily visualised resulting in the ability to interrogate a pathway more comprehensively, which could potentially explain the downstream or upstream results you may observe at a lower level of resolution. This is an especially interesting framework for analysis comparing healthy cells to aged cells, or healthy cells to diseased cells. Exploring data with frameworks such as this one opens the door for building computational models for specific signalling

pathways as it details how whole pathways are changed (or not changed) in different cellular states.

This framework can be further adapted to investigate temporal changes. For example, if data was available which had multiple timepoints (such as that found in SenOmic), this framework could be run for the different timepoints and the results directly compared. This would provide a high-level overview of how different pathways change temporally and evolve in different conditions. This KEGG-based analysis framework can be applied to any pathway in the KEGG repertoire.

Chapter 7: Conclusions and future perspectives.

Cellular senescence is an antagonistic hallmark of ageing typically characterised by stable cell cycle arrest, DNA damage, and an inflammatory secretome referred to as the SASP. Senescent cells are usually transient in the body and involved in processes including wound healing and embryonic development (Demaria et al., 2014; Muñoz-Espín et al., 2013). However, with age, the abundance of senescent cells typically increases leading to chronic low-grade inflammation and increased burdens of age-related diseases (He & Sharpless, 2017; Muñoz-Espín & Serrano, 2014). There is no gold standard and unique marker of senescence, with most studies taking multi-marker approaches. However, even when taking a multi-marker approach, not all markers translate from *in vitro* to *in vivo* (for example, flattened cell morphology) or are unique to senescence (for example, p53 is a key maker of senescence but is active in other cells including normal cells and cancerous cells). If a unique marker was identified, this would result in more robust and reproducible experiments which would lead to a deeper understanding of the basics of cellular senescence and therefore senotherapies.

This work aimed to create and explore impactful resources for investigating cellular senescence through the identification of transcriptomic and protein level temporal phenotypes of senescence and the curation of a future analysis framework for whole-pathway analysis and visualisation.

This thesis presents two resources – the SenOmic database and the Cellular Senescence Model – which utilise a systems biology approach to advance the basic understanding of senescence. SenOmic is a publicly accessible database which provides downloadable processed RNAseq data from 119 studies, offering the researcher the flexibility to analyse a variety of variables based on different study designs and aims. In parallel, the Cellular Senescence Model enables qualitative temporal simulation of interconnected and interacting protein networks, serving as a useful tool to investigate senescence dynamics and the effects of perturbations on the senescence network.

Using SenOmic, this thesis identified a Core Geneset of 28 significantly expressed genes when comparing senescent cells (BYS, DDIS, OIS, and REP) to proliferating control cells (**Figure 3.5**). Notably only one of these 28 genes (*CCNB2)* was present in the human cellular senescence KEGG pathway, while the remaining 27 genes are absent from this pathway and are not considered canonical senescence markers. Ultimately, this finding underscores the heterogeneity of senescence and the difficulty in determining a unique marker of senescence. Comparison of this Core Geneset with three further studies which non-systematically attempted to identify a core gene signature revealed minimal overlap (Casella et al., 2019; Hernandez-Segura et al., 2017; Saul et al., 2022). However, the smaller gene set identified in this thesis (compared to 68, 55, and 125 genes in prior studies, respectively) may have a greater potential for translation as a robust gene signature of senescence. Future work should focus on validating these 28 genes *in vitro* and *in vivo*, as well as comparing their expression across quiescent, diseased, or aged-but-not-senescent control cells to further refine their specificity to senescence.

Another key finding of this thesis was the identification of distinct clustering of senescence types (**Figure 3.4**), with BYS cells forming the most distinct cluster yet remaining comparable to OIS, the primary senescence type to induce BYS in these studies. This raises the intriguing possibility that the transcriptome of BYS cells closely resembles that of the primary senescent cells which initiate their state. Furthermore, upregulation of *NSD2* in BYS but its downregulation in DDIS, OIS and REP (**Figure 3.5B**) suggest that epigenetic modifications may play a critical role in induction of secondary senescence as these cells have not been subject to the DNA damage inducing stimulus as primary senescent cells have been. Given that NSD2 has histone methyltransferase activity and can alter the epigenome of cells (R. Chen et al., 2020; Weirich et al., 2024), investigating epigenomic differences between primary and secondary senescence could provide further insights into the mechanisms governing senescence induction. Ultimately, multi-omic integration – incorporating transcriptomic, epigenomic, and proteomic data – would enable a comprehensive analysis of senescence at multiple regulatory levels, offering deeper insights into both primary and secondary senescence dynamics.

One of the most significant contributions of SenOmic is its ability to capture the temporal evolution of senescence. This thesis demonstrated that senescent cells cluster by time_group (**Figure 4.1**), highlighting that senescent cells continue to evolve even at late timepoints. However, there are limited studies assessing late timepoints of senescence, and additional datasets would be beneficial for understanding whether senescent cells enter a stable transcriptional state over time or follow a cyclic pattern of gene expression fluctuations.

Temporal analysis of senescence in this thesis further identified a number of interesting observations including ORA identifying unique temporal features such as genes involved in protein secretion only being enriched for activation in time_group 5–7 days post-senescence induction and in no other time_groups (**Figure 4.3B**), consistent with the understood temporal delay in SASP expression (Coppé et al., 2008). Also, p53 transcript expression remained stable temporally relative to proliferating control cells (**Figure 4.8E**), while p53 signalling was significantly stronger in DDIS compared to OIS at both the transcriptomic and protein level (**Figures 4.8D-H** and **5.4A-C**). In contrast, p16 and p38 expression was significantly stronger in OIS compared to DDIS at the transcriptomic and protein level (**Figures 4.8H, 4.10A**, and **5.4D-F**), highlighting distinct molecular phenotypes in senescence. Together, these temporal findings emphasise the importance of considering which stage of senescence a cell may be at, as well as identifying phenotypes both common and unique to multiple senescence types and across multiple timepoints, which may provide targets for senotherapeutic interventions.

Alongside this transcriptomic approach, a protein level computational model was developed to simulate temporal changes in senescence (DDIS and OIS) and to assess the impact of p53 and RelA KDs on the whole network. This integrated approach highlights the necessity of investigating processes across multiple cellular levels as genes are not always translated after transcription, and the consequences of PTMs cannot always be observed at the transcript level. For example, p38 transcript expression remained similar to control cells between days 0–14 in DDIS and OIS (**Figure 4.10A**); however, when simulating the protein level, phosphorylation (and therefore activity) of p38 was clearly observed (**Figures 5.4E-F**), a phenotype also observed in the literature (Freund et al., 2011).

Additionally, this thesis identified novel senescence phenotypes which have not been studied in the literature, such as stronger p53 signalling in DDIS compared to OIS (**Figures 4.8D-G** and **5.4A-C**) and the KD of RelA leading to decreased p53 signalling (**Figures 3.15A-C** and **5.4A-C**). Identification of these phenotypes is not necessarily due to them not being recapitulated in experimental or biological settings, but rather that there is a lack of studies specifically investigating these aspects of senescence. Further research into these identified phenotypes could provide valuable insights into senescence progression and regulation, potentially aiding in senotherapy design.

Furthermore, this thesis establishes a framework for future analysis of SenOmic and senescence research, with the qualitative protein level computational model having the ability for future network adaptation, and the KEGG-based analysis framework having the capacity to incorporate any RNAseq dataset and KEGG pathway of interest. Notably, KEGG pathways are not limited to only human networks as KEGG offers the opportunity to explore the networks as understood in different organisms, including mice.

Overall, these resources, analyses, and outlined framework contribute and offer further opportunities to broadening the basic and temporal understanding of senescence. In understanding senescence, an integral hallmark of ageing, there is the possibility of reducing age-related disease burden and improving both healthspan and lifespan in humans.

There are, however, limitations to analysing big data; limitations which were apparent at different stages throughout this thesis. These included limitations to the creation of SenOmic as not all studies had details available for all variables such as the oxygen content cells were grown at or the PDL of cells (evidenced in the database itself, but not specifically presented in this work). In fact, even a critical database variable in timepoint of analysis was missing for some samples (however, as mentioned in **Chapter 2**, the timepoint of analysis was always enquired about if contact or study details were associated with the dataset). Furthermore, samples had different numbers of biological replicates between studies. Some studies argue a minimum of

3 replicates are recommended (Conesa et al., 2016), however it is becoming increasingly accepted that 6–10 biological replicates are required for accuracy and reproducibility (Schurch et al., 2016). In SenOmic, while all had two or more as this was set criteria in the systematic review, most samples had three biological replicates and less than ten samples had six biological replicates or more.

Another limitation lies in the choice of control type. In SenOmic there were multiple options for control type including quiescent. Few studies, however, included quiescent cells in their experiments and therefore the data is limited. There was much more data for proliferating control cells, and therefore proliferating cells were chosen as the control type in most of this thesis. Comparing senescent cells to quiescent cells would be of interest in future work as quiescence is likely closer biologically to senescence than proliferating cells due to both states involving cell cycle arrest. Therefore, if both control type avenues were explored, a gene signature unique to only senescence and no other biological states could be devised.

SenOmic also contains limited samples from primary cell lines, samples which were removed from this analysis during the filtering process described in **Chapter 2**. While they were not included in this analysis, additional lab work conducted in primary cells would benefit this database as such analyses could reveal key differences and similarities between *in vitro* grown primary cell lines and established cell lines. Recognising these patterns would help bridge findings across cell culture systems, animal models, and human clinical trials.

There are many avenues of analysis which can be explored using SenOmic as a data source due to the vastness of the data contained within. In addition to the suggestions discussed above, other areas include more deeply exploring the location of origin of established cell lines – for example with skin fibroblasts, do the cells have nasal or foreskin origins? It is possible that cells exposed to more external factors such as UV may respond differently to cells that are not? To perform this analysis a further variable would need adding to SenOmic detailing the specific location the cell originated from. While it would be interesting to see how cells from the same organ but different locations respond to the same inducer, some skin fibroblasts do not define their origin. Furthermore, whole-pathway visualisation using KEGG-based

analysis as proposed in **Chapter 6** would be an interesting avenue to explore as cellular senescence is a specific KEGG pathway and therefore can be visualised at different time points and in different experimental conditions, providing an easy visual for pathway wide changes in different experimental contexts.

SenOmic currently only contains transcriptomic data. In the future, expansion of SenOmic to other omics (such as epigenomics and proteomics) would improve this resource. Taking an integrated omic analysis would be the next stage of this project, seeing how and if the transcriptomic and proteomic levels compare. This project did explore the protein level, albeit not at an omic level, and the findings exemplify how phenotypes are not always observed across both macromolecule types. For example, p38 phosphorylation is increased and total p38 protein remains steady (**Figure 5.4 E-F**), however there was no observation of increased p38 transcript expression (**Figure 4.10A**). Another example lies with p53 expression; at the transcript level p53 expression remains similar to proliferating control cells (**Figure 4.8E**) despite it being well established that p53 signalling is active in senescence (Beauséjour et al., 2003; Freund et al., 2011; Rufini et al., 2013). In the computational model of cellular senescence, total p53 and phosphorylated p53 were increased upon senescence induction and persisted into late senescence (**Figure 5.4 A-B**). In the isolation of only transcript level investigation, both p53 and p38 do not appear active in senescence, highlighting the importance of an integrated approach. Therefore, improving SenOmic to include other omics will advance the basic understanding of senescence which will ultimately aid in the development of senotherapeutics and the reduction of senescence-related disease burdens.

References.

(ONS), O. f. N. S. (2024). *National life tables - life expectancy in England and Wales*. Retrieved from **https://www.ons.gov.uk/peoplepopulationandcommunity/birthsdeathsandmarriages/lifeexpectancies/bulletins/nationallifetablesunitedkingdom/2021to2023**

Aarts, M., Georgilis, A., Beniazza, M., Beolchi, P., Banito, A., Carroll, T.,…Gil, J. (2017). Coupling shRNA screens with single-cell RNA-seq identifies a dual role for mTOR in reprogramming-induced senescence. *Genes Dev*, *31*(20), 2085-2098. **https://doi.org/10.1101/gad.297796.117**

Abbas, T., & Dutta, A. (2009). p21 in cancer: intricate networks and multiple activities. *Nat Rev Cancer*, *9*(6), 400-414. **https://doi.org/10.1038/nrc2657**

Abe, T., & Barber, G. N. (2014). Cytosolic-DNA-mediated, STING-dependent proinflammatory gene induction necessitates canonical NF-κB activation through TBK1. *J Virol*, *88*(10), 5328-5341. **https://doi.org/10.1128/JVI.00037-14**

Ablasser, A., Schmid-Burgk, J. L., Hemmerling, I., Horvath, G. L., Schmidt, T., Latz, E., & Hornung, V. (2013). Cell intrinsic immunity spreads to bystander cells via the intercellular transfer of cGAMP. *Nature*, *503*(7477), 530-534. **https://doi.org/10.1038/nature12640**

Acosta, J. C., Banito, A., Wuestefeld, T., Georgilis, A., Janich, P., Morton, J. P.,…Gil, J. (2013). A complex secretory program orchestrated by the inflammasome controls paracrine senescence. *Nat Cell Biol*, *15*(8), 978-990. **https://doi.org/10.1038/ncb2784**

Acosta, J. C., O'Loghlen, A., Banito, A., Guijarro, M. V., Augert, A., Raguz, S.,…Gil, J. (2008). Chemokine signaling via the CXCR2 receptor reinforces senescence. *Cell*, *133*(6), 1006-1018. **https://doi.org/10.1016/j.cell.2008.03.038**

Admasu, T. D., Rae, M., & Stolzing, A. (2021). Dissecting primary and secondary senescence to enable new senotherapeutic strategies. *Ageing Res Rev*, *70*, 101412. **https://doi.org/10.1016/j.arr.2021.101412**

Akbari, M., Shanley, D. P., Bohr, V. A., & Rasmussen, L. J. (2021). Cytosolic Self-DNA-A Potential Source of Chronic Inflammation in Aging. *Cells*, *10*(12). **https://doi.org/10.3390/cells10123544**

Aksoy, O., Chicas, A., Zeng, T., Zhao, Z., McCurrach, M., Wang, X., & Lowe, S. W. (2012). The atypical E2F family member E2F7 couples the p53 and RB pathways during cellular senescence. *Genes Dev*, *26*(14), 1546-1557. **https://doi.org/10.1101/gad.196238.112**

Alcorta, D. A., Xiong, Y., Phelps, D., Hannon, G., Beach, D., & Barrett, J. C. (1996). Involvement of the cyclin-dependent kinase inhibitor p16 (INK4a) in replicative senescence of normal human fibroblasts. *Proc Natl Acad Sci U S A*, *93*(24), 13742-13747. **https://doi.org/10.1073/pnas.93.24.13742**

Alspach, E., Flanagan, K. C., Luo, X., Ruhland, M. K., Huang, H., Pazolli, E.,…Stewart, S. A. (2014). p38MAPK plays a crucial role in stromal-mediated tumorigenesis. *Cancer Discov*, *4*(6), 716-729. **https://doi.org/10.1158/2159-8290.CD-13-0743**

An, Y., Zhu, J., Wang, X., Sun, X., Luo, C., Zhang, Y.,…Xie, Z. (2022). Oridonin Delays Aging Through the AKT Signaling Pathway. *Front Pharmacol*, *13*, 888247. **https://doi.org/10.3389/fphar.2022.888247**

Anastassiou, D. (2007). Computational analysis of the synergy among multiple interacting genes. *Mol Syst Biol*, *3*, 83. **https://doi.org/10.1038/msb4100124**

Anerillas, C., Herman, A. B., Munk, R., Garrido, A., Lam, K. G., Payea, M. J.,…Gorospe, M. (2022). A BDNF-TrkB autocrine loop enhances senescent cell viability. *Nat Commun*, *13*(1), 6228. **https://doi.org/10.1038/s41467-022-33709-8**

Anerillas, C., Herman, A. B., Rossi, M., Munk, R., Lehrmann, E., Martindale, J. L.,…Gorospe, M. (2022). Early SRC activation skews cell fate from apoptosis to senescence. *Sci Adv*, *8*(14), eabm0756. **https://doi.org/10.1126/sciadv.abm0756**

Anerillas, C., Mazan-Mamczarz, K., Herman, A. B., Munk, R., Lam, K. G., Calvo-Rubio, M.,…Gorospe, M. (2023). The YAP-TEAD complex promotes senescent cell survival by lowering endoplasmic reticulum stress. *Nat Aging*, *3*(10), 1237-1250. **https://doi.org/10.1038/s43587-023-00480-4**

Ashcroft, M., Kubbutat, M. H., & Vousden, K. H. (1999). Regulation of p53 function and stability by phosphorylation. *Mol Cell Biol*, *19*(3), 1751-1758. **https://doi.org/10.1128/MCB.19.3.1751**

Baar, M. P., Brandt, R. M. C., Putavet, D. A., Klein, J. D. D., Derks, K. W. J., Bourgeois, B. R. M.,…de Keizer, P. L. J. (2017). Targeted Apoptosis of Senescent Cells Restores Tissue Homeostasis in Response to Chemotoxicity and Aging. *Cell*, *169*(1), 132-147.e116. **https://doi.org/10.1016/j.cell.2017.02.031**

Baker, D. J., Childs, B. G., Durik, M., Wijers, M. E., Sieben, C. J., Zhong, J.,…van Deursen, J. M. (2016). Naturally occurring p16(Ink4a)-positive cells shorten healthy lifespan. *Nature*, *530*(7589), 184-189. **https://doi.org/10.1038/nature16932**

Baker, D. J., & Petersen, R. C. (2018). Cellular senescence in brain aging and neurodegenerative diseases: evidence and perspectives. *J Clin Invest*, *128*(4), 1208-1216. **https://doi.org/10.1172/JCI95145**

Baker, D. J., Wijshake, T., Tchkonia, T., LeBrasseur, N. K., Childs, B. G., van de Sluis, B.,…van Deursen, J. M. (2011). Clearance of p16Ink4a-positive senescent cells delays ageing-associated disorders. *Nature*, *479*(7372), 232-236. **https://doi.org/10.1038/nature10600**

Baker, M., Denman-Johnson, S., Brook, B. S., Gaywood, I., & Owen, M. R. (2013). Mathematical modelling of cytokine-mediated inflammation in rheumatoid arthritis. *Math Med Biol*, *30*(4), 311-337. **https://doi.org/10.1093/imammb/dqs026**

Balistreri, C. R., Madonna, R., Melino, G., & Caruso, C. (2016). The emerging role of Notch pathway in ageing: Focus on the related mechanisms in age-related diseases. *Ageing Res Rev*, *29*, 50-65. **https://doi.org/10.1016/j.arr.2016.06.004**

Barnes, R. P., de Rosa, M., Thosar, S. A., Detwiler, A. C., Roginskaya, V., Van Houten, B.,…Opresko, P. L. (2022). Telomeric 8-oxo-guanine drives rapid premature senescence in the absence of telomere shortening. *Nat Struct Mol Biol*, *29*(7), 639-652. **https://doi.org/10.1038/s41594-022-00790-y**

Barnett, K., Mercer, S. W., Norbury, M., Watt, G., Wyke, S., & Guthrie, B. (2012). Epidemiology of multimorbidity and implications for health care, research, and medical education: a cross-sectional study. *Lancet*, *380*(9836), 37-43. **https://doi.org/10.1016/S0140-6736(12)60240-2**

Bartek, J., & Lukas, J. (2007). DNA damage checkpoints: from initiation to recovery or adaptation. *Curr Opin Cell Biol*, *19*(2), 238-245. **https://doi.org/10.1016/j.ceb.2007.02.009**

Barzilai, N., Crandall, J. P., Kritchevsky, S. B., & Espeland, M. A. (2016). Metformin as a Tool to Target Aging. *Cell Metab*, *23*(6), 1060-1065. **https://doi.org/10.1016/j.cmet.2016.05.011**

Basisty, N., Kale, A., Jeon, O. H., Kuehnemann, C., Payne, T., Rao, C.,…Schilling, B. (2020). A proteomic atlas of senescence-associated secretomes for aging biomarker development. *PLoS Biol*, *18*(1), e3000599. **https://doi.org/10.1371/journal.pbio.3000599**

Bauer, D. (1972). Constructing Confidence Sets Using Rank Statistics. *Journal of the American Statistical Association*, *67*(339), 687-690. **https://doi.org/10.1080/01621459.1972.10481279**

Beauséjour, C. M., Krtolica, A., Galimi, F., Narita, M., Lowe, S. W., Yaswen, P., & Campisi, J. (2003). Reversal of human cellular senescence: roles of the p53 and p16 pathways. *EMBO J*, *22*(16), 4212-4222. **https://doi.org/10.1093/emboj/cdg417**

Benhamed, M., Herbig, U., Ye, T., Dejean, A., & Bischof, O. (2012). Senescence is an endogenous trigger for microRNA-directed transcriptional gene silencing in human cells. *Nat Cell Biol*, *14*(3), 266-275. **https://doi.org/10.1038/ncb2443**

Bhat, R., Crowe, E. P., Bitto, A., Moh, M., Katsetos, C. D., Garcia, F. U.,…Torres, C. (2012). Astrocyte senescence as a component of Alzheimer's disease. *PLoS One*, *7*(9), e45069. **https://doi.org/10.1371/journal.pone.0045069**

Biernacka, A., Dobaczewski, M., & Frangogiannis, N. G. (2011). TGF-β signaling in fibrosis. *Growth Factors*, *29*(5), 196-202. **https://doi.org/10.3109/08977194.2011.595714**

Bodnar, A. G., Ouellette, M., Frolkis, M., Holt, S. E., Chiu, C. P., Morin, G. B.,…Wright, W. E. (1998). Extension of life-span by introduction of telomerase into normal human cells. *Science*, *279*(5349), 349-352. **https://doi.org/10.1126/science.279.5349.349**

Bond, M., Chase, A. J., Baker, A. H., & Newby, A. C. (2001). Inhibition of transcription factor NF-kappaB reduces matrix metalloproteinase-1, -3 and -9 production by vascular smooth muscle cells. *Cardiovasc Res*, *50*(3), 556-565. **https://doi.org/10.1016/s0008-6363(01)00220-6**

Borggrefe, T., & Oswald, F. (2009). The Notch signaling pathway: transcriptional regulation at Notch target genes. *Cell Mol Life Sci*, *66*(10), 1631-1646. **https://doi.org/10.1007/s00018-009-8668-7**

Borghesan, M., Fafián-Labora, J., Eleftheriadou, O., Carpintero-Fernández, P., Paez-Ribes, M., Vizcay-Barrena, G.,…O'Loghlen, A. (2019). Small Extracellular Vesicles Are Key Regulators of Non-cell Autonomous Intercellular Communication in Senescence via the Interferon Protein IFITM3. *Cell Rep*, *27*(13), 3956-3971.e3956. **https://doi.org/10.1016/j.celrep.2019.05.095**

Bracken, A. P., Ciro, M., Cocito, A., & Helin, K. (2004). E2F target genes: unraveling the biology. *Trends Biochem Sci*, *29*(8), 409-417. **https://doi.org/10.1016/j.tibs.2004.06.006**

Bray, S. J. (2006). Notch signalling: a simple pathway becomes complex. *Nat Rev Mol Cell Biol*, *7*(9), 678-689. **https://doi.org/10.1038/nrm2009**

Brown, J. P., Wei, W., & Sedivy, J. M. (1997). Bypass of senescence after disruption of p21CIP1/WAF1 gene in normal diploid human fibroblasts. *Science*, *277*(5327), 831-834. **https://doi.org/10.1126/science.277.5327.831**

Brugarolas, J., Chandrasekaran, C., Gordon, J. I., Beach, D., Jacks, T., & Hannon, G. J. (1995). Radiation-induced cell cycle arrest compromised by p21 deficiency. *Nature*, *377*(6549), 552-557. **https://doi.org/10.1038/377552a0**

Buj, R., Chen, C. W., Dahl, E. S., Leon, K. E., Kuskovsky, R., Maglakelidze, N.,…Aird, K. M. (2019). Suppression of p16 Induces mTORC1-Mediated Nucleotide Metabolic Reprogramming. *Cell Rep*, *28*(8), 1971-1980.e1978. **https://doi.org/10.1016/j.celrep.2019.07.084**

Bussian, T. J., Aziz, A., Meyer, C. F., Swenson, B. L., van Deursen, J. M., & Baker, D. J. (2018). Clearance of senescent glial cells prevents tau-dependent pathology and cognitive decline. *Nature*, *562*(7728), 578-582. **https://doi.org/10.1038/s41586-018-0543-y**

Campisi, J. (2001). Cellular senescence as a tumor-suppressor mechanism. *Trends Cell Biol*, *11*(11), S27-31. **https://doi.org/10.1016/s0962-8924(01)02151-1**

Carbo, A., Hontecillas, R., Kronsteiner, B., Viladomiu, M., Pedragosa, M., Lu, P.,…Bassaganya-Riera, J. (2013). Systems modeling of molecular mechanisms controlling cytokine-driven CD4+ T cell differentiation and phenotype plasticity. *PLoS Comput Biol*, *9*(4), e1003027. **https://doi.org/10.1371/journal.pcbi.1003027**

Carvalho, C., L'Hôte, V., Courbeyrette, R., Kratassiouk, G., Pinna, G., Cintrat, J. C.,…Thuret, J. Y. (2019). Glucocorticoids delay RAF-induced senescence promoted by EGR1. *J Cell Sci*, *132*(16). **https://doi.org/10.1242/jcs.230748**

Casella, G., Munk, R., Kim, K. M., Piao, Y., De, S., Abdelmohsen, K., & Gorospe, M. (2019). Transcriptome signature of cellular senescence. *Nucleic Acids Res*, *47*(21), 11476. **https://doi.org/10.1093/nar/gkz879**

Cellosaurus. (n.d.-a). *Cellosaurus HCA2 [Human foreskin fibroblast] (CVCL_E2UW)*. Swiss Institute of Bioinformatics. **https://www.cellosaurus.org/CVCL_E2UW**

Cellosaurus. (n.d.-b). *Cellosaurus HFL1 (CVCL_0298)*. Swiss Institute of Bioinformatics. **https://www.cellosaurus.org/CVCL_0298**

Cellosaurus. (n.d.-c). *Cellosaurus LF1 [Human fetal lung] (CVCL_C120)*. Swiss Institute of Bioinformatics. **https://www.culturecollections.org.uk/nop/product/hca-2**

Chalhoub, N., & Baker, S. J. (2009). PTEN and the PI3-kinase pathway in cancer. *Annu Rev Pathol*, *4*, 127-150. **https://doi.org/10.1146/annurev.pathol.4.110807.092311**

Chan, K. T., Blake, S., Zhu, H., Kang, J., Trigos, A. S., Madhamshettiwar, P. B.,…Pearson, R. B. (2020). A functional genetic screen defines the AKT-induced senescence signaling network. *Cell Death Differ*, *27*(2), 725-741. **https://doi.org/10.1038/s41418-019-0384-8**

Chan, M., Yuan, H., Soifer, I., Maile, T. M., Wang, R. Y., Ireland, A.,…Hendrickson, D. G. (2022). Novel insights from a multiomics dissection of the Hayflick limit. *Elife*, *11*. **https://doi.org/10.7554/eLife.70283**

Chan, T. S., Hsu, C. C., Pai, V. C., Liao, W. Y., Huang, S. S., Tan, K. T.,…Tsai, K. K. (2016). Metronomic chemotherapy prevents therapy-induced stromal activation and induction of tumor-initiating cells. *J Exp Med*, *213*(13), 2967-2988. **https://doi.org/10.1084/jem.20151665**

Chandrasegaran, S. (2023). Computational systems biology approaches to research cell senescence. In. Newcastle Upon Tyne: Newcastle University.

Chandrasegaran, S., Scanlan, R. L., Clark, P., Pease, L., Wordsworth, J., & Shanley, D. P. (2023). Systems Biology of Ageing. In J. R. Harris, Korolchuk, V.I. (Ed.), *Biochemistry and Cell Biology of Ageing: Part III Biomedical Science.* (Vol.

102, pp. 415-424). Springer, Cham.
https://doi.org/https://doi.org/10.1007/978-3-031-21410-3_16

Chandrasegaran, S., Sluka, J. P., & Shanley, D. (2024). Modelling the spatiotemporal dynamics of senescent cells in wound healing, chronic wounds, and fibrosis. *bioRxiv*. **https://doi.org/https://doi.org/10.1101/2024.07.04.602041**

Chase, A. J., Bond, M., Crook, M. F., & Newby, A. C. (2002). Role of nuclear factor-kappa B activation in metalloproteinase-1, -3, and -9 secretion by human macrophages in vitro and rabbit foam cells produced in vivo. *Arterioscler Thromb Vasc Biol*, *22*(5), 765-771.
https://doi.org/10.1161/01.atv.0000015078.09208.92

Chehab, N. H., Malikzay, A., Appel, M., & Halazonetis, T. D. (2000). Chk2/hCds1 functions as a DNA damage checkpoint in G(1) by stabilizing p53. *Genes Dev*, *14*(3), 278-288.

Chen, C., Liu, Y., & Zheng, P. (2009). mTOR regulation and therapeutic rejuvenation of aging hematopoietic stem cells. *Sci Signal*, *2*(98), ra75.
https://doi.org/10.1126/scisignal.2000559

Chen, C. Y., Chen, J., He, L., & Stiles, B. L. (2018). PTEN: Tumor Suppressor and Metabolic Regulator. *Front Endocrinol (Lausanne)*, *9*, 338.
https://doi.org/10.3389/fendo.2018.00338

Chen, G., Hitomi, M., Han, J., & Stacey, D. W. (2000). The p38 pathway provides negative feedback for Ras proliferative signaling. *J Biol Chem*, *275*(50), 38973-38980. **https://doi.org/10.1074/jbc.M002856200**

Chen, H., & Boutros, P. C. (2011). VennDiagram: a package for the generation of highly-customizable Venn and Euler diagrams in R. *BMC Bioinformatics*, *12*, 35. **https://doi.org/10.1186/1471-2105-12-35**

Chen, L., Liu, S., & Tao, Y. (2020). Regulating tumor suppressor genes: post-translational modifications. *Signal Transduct Target Ther*, *5*(1), 90.
https://doi.org/10.1038/s41392-020-0196-9

Chen, R., Chen, Y., Zhao, W., Fang, C., Zhou, W., Yang, X., & Ji, M. (2020). The Role of Methyltransferase NSD2 as a Potential Oncogene in Human Solid Tumors. *Onco Targets Ther*, *13*, 6837-6846.
https://doi.org/10.2147/OTT.S259873

Chen, S. J., Yuan, W., Mori, Y., Levenson, A., Trojanowska, M., & Varga, J. (1999). Stimulation of type I collagen transcription in human skin fibroblasts by TGF-beta: involvement of Smad 3. *J Invest Dermatol*, *112*(1), 49-57.
https://doi.org/10.1046/j.1523-1747.1999.00477.x

Chen, Z., Trotman, L. C., Shaffer, D., Lin, H. K., Dotan, Z. A., Niki, M.,…Pandolfi, P. P. (2005). Crucial role of p53-dependent cellular senescence in suppression of Pten-deficient tumorigenesis. *Nature*, *436*(7051), 725-730.
https://doi.org/10.1038/nature03918

Chicas, A., Wang, X., Zhang, C., McCurrach, M., Zhao, Z., Mert, O.,…Lowe, S. W. (2010). Dissecting the unique role of the retinoblastoma tumor suppressor during cellular senescence. *Cancer Cell*, *17*(4), 376-387.
https://doi.org/10.1016/j.ccr.2010.01.023

Chien, Y., Scuoppo, C., Wang, X., Fang, X., Balgley, B., Bolden, J. E.,…Lowe, S. W. (2011). Control of the senescence-associated secretory phenotype by NF-κB promotes senescence and enhances chemosensitivity. *Genes Dev*, *25*(20), 2125-2136. **https://doi.org/10.1101/gad.17276711**

Childs, B. G., Durik, M., Baker, D. J., & van Deursen, J. M. (2015). Cellular senescence in aging and age-related disease: from mechanisms to therapy. *Nat Med*, *21*(12), 1424-1435. **https://doi.org/10.1038/nm.4000**

Cho, H. J., Hwang, J. A., Yang, E. J., Kim, E. C., Kim, J. R., Kim, S. Y.,…Lee, Y. S. (2022). Nintedanib induces senolytic effect via STAT3 inhibition. *Cell Death Dis*, *13*(9), 760. **https://doi.org/10.1038/s41419-022-05207-8**

Choi, K., Medley, J. K., König, M., Stocking, K., Smith, L., Gu, S., & Sauro, H. M. (2018). Tellurium: An extensible python-based modeling environment for systems and synthetic biology. *Biosystems*, *171*, 74-79. **https://doi.org/10.1016/j.biosystems.2018.07.006**

Ciccone, L., Piragine, E., Brogi, S., Camodeca, C., Fucci, R., Calderone, V.,…Orlandini, E. (2022). Resveratrol-like Compounds as SIRT1 Activators. *Int J Mol Sci*, *23*(23). **https://doi.org/10.3390/ijms232315105**

Cimprich, K. A., & Cortez, D. (2008). ATR: an essential regulator of genome integrity. *Nat Rev Mol Cell Biol*, *9*(8), 616-627. **https://doi.org/10.1038/nrm2450**

Collado, M., Gil, J., Efeyan, A., Guerra, C., Schuhmacher, A. J., Barradas, M.,…Serrano, M. (2005). Tumour biology: senescence in premalignant tumours. *Nature*, *436*(7051), 642. **https://doi.org/10.1038/436642a**

Collins, K., & Mitchell, J. R. (2002). Telomerase in the human organism. *Oncogene*, *21*(4), 564-579. **https://doi.org/10.1038/sj.onc.1205083**

Colquitt, R., Colquhoun, D., & Thiele, R. (2011). *In silico* modelling of physiologic systems. *Best Practice and Research Clinical Anaesthesiology*, *25*(4), 499-510. **https://doi.org/https://doi.org/10.1016/j.bpa.2011.08.006**

Conesa, A., Madrigal, P., Tarazona, S., Gomez-Cabrero, D., Cervera, A., McPherson, A.,…Mortazavi, A. (2016). A survey of best practices for RNA-seq data analysis. *Genome Biol*, *17*, 13. **https://doi.org/10.1186/s13059-016-0881-8**

Contrepois, K., Coudereau, C., Benayoun, B. A., Schuler, N., Roux, P. F., Bischof, O.,…Mann, C. (2017). Histone variant H2A.J accumulates in senescent cells and promotes inflammatory gene expression. *Nat Commun*, *8*, 14995. **https://doi.org/10.1038/ncomms14995**

Contributors, S. P. (2024). *Spyder (Version 4.2.3)*. In Spyder Project. **https://www.spyder-ide.org**

Coppé, J. P., Desprez, P. Y., Krtolica, A., & Campisi, J. (2010). The senescence-associated secretory phenotype: the dark side of tumor suppression. *Annu Rev Pathol*, *5*, 99-118. **https://doi.org/10.1146/annurev-pathol-121808-102144**

Coppé, J. P., Patil, C. K., Rodier, F., Sun, Y., Muñoz, D. P., Goldstein, J.,…Campisi, J. (2008). Senescence-associated secretory phenotypes reveal cell-nonautonomous functions of oncogenic RAS and the p53 tumor suppressor. *PLoS Biol*, *6*(12), 2853-2868. **https://doi.org/10.1371/journal.pbio.0060301**

Correia-Melo, C., Marques, F. D., Anderson, R., Hewitt, G., Hewitt, R., Cole, J.,…Passos, J. F. (2016). Mitochondria are required for pro-ageing features of the senescent phenotype. *EMBO J*, *35*(7), 724-742. **https://doi.org/10.15252/embj.201592862**

Criscione, S. W., De Cecco, M., Siranosian, B., Zhang, Y., Kreiling, J. A., Sedivy, J. M., & Neretti, N. (2016). Reorganization of chromosome architecture in replicative cellular senescence. *Sci Adv*, *2*(2), e1500882. **https://doi.org/10.1126/sciadv.1500882**

d'Adda di Fagagna, F., Reaper, P. M., Clay-Farrace, L., Fiegler, H., Carr, P., Von Zglinicki, T.,…Jackson, S. P. (2003). A DNA damage checkpoint response in telomere-initiated senescence. *Nature*, *426*(6963), 194-198. **https://doi.org/10.1038/nature02118**

da Silva, P. F. L., Ogrodnik, M., Kucheryavenko, O., Glibert, J., Miwa, S., Cameron, K.,…von Zglinicki, T. (2019). The bystander effect contributes to the accumulation of senescent cells in vivo. *Aging Cell*, *18*(1), e12848. **https://doi.org/10.1111/acel.12848**

Dalle Pezze, P., Nelson, G., Otten, E. G., Korolchuk, V. I., Kirkwood, T. B., von Zglinicki, T., & Shanley, D. P. (2014). Dynamic modelling of pathways to cellular senescence reveals strategies for targeted interventions. *PLoS Comput Biol*, *10*(8), e1003728. **https://doi.org/10.1371/journal.pcbi.1003728**

Das, R. K., & Dusetzina, S. B. (2023). Gender-Affirming Hormone Therapy Spending and Use in the USA, 2013-2019. *J Gen Intern Med*, *38*(1), 260-262. **https://doi.org/10.1007/s11606-022-07693-0**

Davalli, P., Mitic, T., Caporali, A., Lauriola, A., & D'Arca, D. (2016). ROS, Cell Senescence, and Novel Molecular Mechanisms in Aging and Age-Related Diseases. *Oxid Med Cell Longev*, *2016*, 3565127. **https://doi.org/10.1155/2016/3565127**

Davis, S., & Meltzer, P. S. (2007). GEOquery: a bridge between the Gene Expression Omnibus (GEO) and BioConductor. *Bioinformatics*, *23*(14), 1846-1847. **https://doi.org/10.1093/bioinformatics/btm254**

De Cecco, M., Ito, T., Petrashen, A. P., Elias, A. E., Skvir, N. J., Criscione, S. W.,…Sedivy, J. M. (2019). L1 drives IFN in senescent cells and promotes age-associated inflammation. *Nature*, *566*(7742), 73-78. **https://doi.org/10.1038/s41586-018-0784-9**

de Sena Brandine, G., & Smith, A. D. (2019). Falco: high-speed FastQC emulation for quality control of sequencing data. *F1000Res*, *8*, 1874. **https://doi.org/10.12688/f1000research.21142.2**

Debès, C., Papadakis, A., Grönke, S., Karalay, Ö., Tain, L. S., Mizi, A.,…Beyer, A. (2023). Ageing-associated changes in transcriptional elongation influence longevity. *Nature*, *616*(7958), 814-821. **https://doi.org/10.1038/s41586-023-05922-y**

Decout, A., Katz, J. D., Venkatraman, S., & Ablasser, A. (2021). The cGAS-STING pathway as a therapeutic target in inflammatory diseases. *Nat Rev Immunol*, *21*(9), 548-569. **https://doi.org/10.1038/s41577-021-00524-z**

Demaria, M., Ohtani, N., Youssef, S. A., Rodier, F., Toussaint, W., Mitchell, J. R.,…Campisi, J. (2014). An essential role for senescent cells in optimal wound healing through secretion of PDGF-AA. *Dev Cell*, *31*(6), 722-733. **https://doi.org/10.1016/j.devcel.2014.11.012**

Demidenko, Z. N., & Blagosklonny, M. V. (2008). Growth stimulation leads to cellular senescence when the cell cycle is blocked. *Cell Cycle*, *7*(21), 3355-3361. **https://doi.org/10.4161/cc.7.21.6919**

Di Micco, R., Fumagalli, M., Cicalese, A., Piccinin, S., Gasparini, P., Luise, C.,…d'Adda di Fagagna, F. (2006). Oncogene-induced senescence is a DNA damage response triggered by DNA hyper-replication. *Nature*, *444*(7119), 638-642. **https://doi.org/10.1038/nature05327**

Dias, S. P., Brouwer, M. C., & van de Beek, D. (2022). Sex and Gender Differences in Bacterial Infections. *Infect Immun*, *90*(10), e0028322. **https://doi.org/10.1128/iai.00283-22**

Dikovskaya, D., Cole, J. J., Mason, S. M., Nixon, C., Karim, S. A., McGarry, L.,…Adams, P. D. (2015). Mitotic Stress Is an Integral Part of the Oncogene-Induced Senescence Program that Promotes Multinucleation and Cell Cycle Arrest. *Cell Rep*, *12*(9), 1483-1496. **https://doi.org/10.1016/j.celrep.2015.07.055**

Dimri, G. P., Lee, X., Basile, G., Acosta, M., Scott, G., Roskelley, C.,…Pereira-Smith, O. (1995). A biomarker that identifies senescent human cells in culture and in aging skin in vivo. *Proc Natl Acad Sci U S A*, *92*(20), 9363-9367. **https://doi.org/10.1073/pnas.92.20.9363**

Dou, Z., Ghosh, K., Vizioli, M. G., Zhu, J., Sen, P., Wangensteen, K. J.,…Berger, S. L. (2017). Cytoplasmic chromatin triggers inflammation in senescence and cancer. *Nature*, *550*(7676), 402-406. **https://doi.org/10.1038/nature24050**

Drosten, M., Dhawahir, A., Sum, E. Y., Urosevic, J., Lechuga, C. G., Esteban, L. M.,…Barbacid, M. (2010). Genetic analysis of Ras signalling pathways in cell proliferation, migration and survival. *EMBO J*, *29*(6), 1091-1104. **https://doi.org/10.1038/emboj.2010.7**

Edgar, R., Domrachev, M., & Lash, A. E. (2002). Gene Expression Omnibus: NCBI gene expression and hybridization array data repository. *Nucleic Acids Res*, *30*(1), 207-210. **https://doi.org/10.1093/nar/30.1.207**

Ei, Z. Z., Srithawirat, T., Chunhacha, P., Chaotham, C., Arunmanee, W., Phookphan, P., & Chanvorachote, P. (2024). Resveratrol Shows Potent Senescence Reversal in Experimental Cellular Models of Particular Matter 2.5-induced Cellular Senescence in Human Dermal Papilla Cells. *In Vivo*, *38*(2), 665-673. **https://doi.org/10.21873/invivo.13487**

el-Deiry, W. S., Tokino, T., Velculescu, V. E., Levy, D. B., Parsons, R., Trent, J. M.,…Vogelstein, B. (1993). WAF1, a potential mediator of p53 tumor suppression. *Cell*, *75*(4), 817-825. **https://doi.org/10.1016/0092-8674(93)90500-p**

Ergün, A., Lawrence, C. A., Kohanski, M. A., Brennan, T. A., & Collins, J. J. (2007). A network biology approach to prostate cancer. *Mol Syst Biol*, *3*, 82. **https://doi.org/10.1038/msb4100125**

Eritja, N., Felip, I., Dosil, M. A., Vigezzi, L., Mirantes, C., Yeramian, A.,…Dolcet, X. (2017). A Smad3-PTEN regulatory loop controls proliferation and apoptotic responses to TGF-β in mouse endometrium. *Cell Death Differ*, *24*(8), 1443-1458. **https://doi.org/10.1038/cdd.2017.73**

Estévez-Souto, V., Da Silva-Álvarez, S., & Collado, M. (2023). The role of extracellular vesicles in cellular senescence. *FEBS J*, *290*(5), 1203-1211. **https://doi.org/10.1111/febs.16585**

Ewels, P., Magnusson, M., Lundin, S., & Käller, M. (2016). MultiQC: summarize analysis results for multiple tools and samples in a single report. *Bioinformatics*, *32*(19), 3047-3048. **https://doi.org/10.1093/bioinformatics/btw354**

Fakatava, N., Mitarai, H., Yuda, A., Haraguchi, A., Wada, H., Hasegawa, D.,…Wada, N. (2023). Actin alpha 2, smooth muscle, a transforming growth factor-β1-induced factor, regulates collagen production in human periodontal ligament cells via Smad2/3 pathway. *J Dent Sci*, *18*(2), 567-576. **https://doi.org/10.1016/j.jds.2022.08.030**

Farage, M. A., Miller, K. W., Elsner, P., & Maibach, H. I. (2008). Intrinsic and extrinsic factors in skin ageing: a review. *Int J Cosmet Sci*, *30*(2), 87-95. **https://doi.org/10.1111/j.1468-2494.2007.00415.x**

Feng, X. H., Lin, X., & Derynck, R. (2000). Smad2, Smad3 and Smad4 cooperate with Sp1 to induce p15(Ink4B) transcription in response to TGF-beta. *EMBO J*, *19*(19), 5178-5193. **https://doi.org/10.1093/emboj/19.19.5178**

Fielder, E., von Zglinicki, T., & Jurk, D. (2017). The DNA Damage Response in Neurons: Die by Apoptosis or Survive in a Senescence-Like State? *J Alzheimers Dis*, *60*(s1), S107-S131. **https://doi.org/10.3233/JAD-161221**

Foundation, P. S. (2016). *Python (Version 3.6)*. In Python Software Foundation. **https://www.python.org**

Freund, A., Laberge, R. M., Demaria, M., & Campisi, J. (2012). Lamin B1 loss is a senescence-associated biomarker. *Mol Biol Cell*, *23*(11), 2066-2075. **https://doi.org/10.1091/mbc.E11-10-0884**

Freund, A., Patil, C. K., & Campisi, J. (2011). p38MAPK is a novel DNA damage response-independent regulator of the senescence-associated secretory phenotype. *EMBO J*, *30*(8), 1536-1548. **https://doi.org/10.1038/emboj.2011.69**

Friedman, H. M., & Koropchak, C. (1978). Comparison of WI-38, MRC-5, and IMR-90 cell strains for isolation of viruses from clinical specimens. *J Clin Microbiol*, *7*(4), 368-371. **https://doi.org/10.1128/jcm.7.4.368-371.1978**

Fritz García, J. H. G., Keller Valsecchi, C. I., & Basilicata, M. F. (2024). Sex as a biological variable in ageing: insights and perspectives on the molecular and cellular hallmarks. *Open Biol*, *14*(10), 240177. **https://doi.org/10.1098/rsob.240177**

Fujii, S., Maeda, H., Tomokiyo, A., Monnouchi, S., Hori, K., Wada, N., & Akamine, A. (2010). Effects of TGF-β1 on the proliferation and differentiation of human periodontal ligament cells and a human periodontal ligament stem/progenitor cell line. *Cell Tissue Res*, *342*(2), 233-242. **https://doi.org/10.1007/s00441-010-1037-x**

Fumagalli, M., Rossiello, F., Clerici, M., Barozzi, S., Cittaro, D., Kaplunov, J. M.,…d'Adda di Fagagna, F. (2012). Telomeric DNA damage is irreparable and causes persistent DNA-damage-response activation. *Nat Cell Biol*, *14*(4), 355-365. **https://doi.org/10.1038/ncb2466**

Funahashi, A., Matsuoka, Y., Jouraku, A., Morohashi, M., Kikuchi, N., Kitano, H. (2008). CellDesigner 3.5: A Versatile Modeling Tool for Biochemical Networks. *Proceedings of the IEEE*, *96*(8), 1254-1265. **https://doi.org/https://doi.org/10.1109/JPROC.2008.925458**

Furuse, M., Fujita, K., Hiiragi, T., Fujimoto, K., & Tsukita, S. (1998). Claudin-1 and -2: novel integral membrane proteins localizing at tight junctions with no sequence similarity to occludin. *J Cell Biol*, *141*(7), 1539-1550. **https://doi.org/10.1083/jcb.141.7.1539**

Gardner, M., Bann, D., Wiley, L., Cooper, R., Hardy, R., Nitsch, D.,…team, H. s. (2014). Gender and telomere length: systematic review and meta-analysis. *Exp Gerontol*, *51*, 15-27. **https://doi.org/10.1016/j.exger.2013.12.004**

Gautier, L., Cope, L., Bolstad, B. M., & Irizarry, R. A. (2004). affy--analysis of Affymetrix GeneChip data at the probe level. *Bioinformatics*, *20*(3), 307-315. **https://doi.org/10.1093/bioinformatics/btg405**

Geißler, C., Tahtali, A., Diensthuber, M., Gassner, D., Stöver, T., & Wagenblast, J. (2013). The role of p16 expression as a predictive marker in HPV-positive oral SCCHN--a retrospective single-center study. *Anticancer Res*, *33*(3), 913-916.

Georgilis, A., Klotz, S., Hanley, C. J., Herranz, N., Weirich, B., Morancho, B.,…Gil, J. (2018). PTBP1-Mediated Alternative Splicing Regulates the Inflammatory Secretome and the Pro-tumorigenic Effects of Senescent Cells. *Cancer Cell*, *34*(1), 85-102.e109. **https://doi.org/10.1016/j.ccell.2018.06.007**

Giacinti, C., & Giordano, A. (2006). RB and cell cycle progression. *Oncogene*, *25*(38), 5220-5227. **https://doi.org/10.1038/sj.onc.1209615**

Gladyshev, V. N., Kritchevsky, S. B., Clarke, S. G., Cuervo, A. M., Fiehn, O., de Magalhães, J. P.,…Cummings, S. R. (2021). Molecular Damage in Aging. *Nat Aging*, *1*(12), 1096-1106. **https://doi.org/10.1038/s43587-021-00150-3**

Glück, S., Guey, B., Gulen, M. F., Wolter, K., Kang, T. W., Schmacke, N. A.,…Ablasser, A. (2017). Innate immune sensing of cytosolic chromatin fragments through cGAS promotes senescence. *Nat Cell Biol*, *19*(9), 1061-1070. **https://doi.org/10.1038/ncb3586**

Going, J. J., Stuart, R. C., Downie, M., Fletcher-Monaghan, A. J., & Keith, W. N. (2002). 'Senescence-associated' beta-galactosidase activity in the upper gastrointestinal tract. *J Pathol*, *196*(4), 394-400. **https://doi.org/10.1002/path.1059**

Gong, D., & Ferrell, J. E. (2010). The roles of cyclin A2, B1, and B2 in early and late mitotic events. *Mol Biol Cell*, *21*(18), 3149-3161. **https://doi.org/10.1091/mbc.E10-05-0393**

González-Gualda, E., Baker, A. G., Fruk, L., & Muñoz-Espín, D. (2021). A guide to assessing cellular senescence in vitro and in vivo. *FEBS J*, *288*(1), 56-80. **https://doi.org/10.1111/febs.15570**

Gonçalves, S., Yin, K., Ito, Y., Chan, A., Olan, I., Gough, S.,…Hoare, M. (2021). COX2 regulates senescence secretome composition and senescence surveillance through PGE. *Cell Rep*, *34*(11), 108860. **https://doi.org/10.1016/j.celrep.2021.108860**

Govindaraju, D., Atzmon, G., & Barzilai, N. (2015). Genetics, lifestyle and longevity: Lessons from centenarians. *Appl Transl Genom*, *4*, 23-32. **https://doi.org/10.1016/j.atg.2015.01.001**

Greenberg, E. F., Voorbach, M. J., Smith, A., Reuter, D. R., Zhuang, Y., Wang, J. Q.,…Florian, H. (2024). Navitoclax safety, tolerability, and effect on biomarkers of senescence and neurodegeneration in aged nonhuman primates. *Heliyon*, *10*(16), e36483. **https://doi.org/10.1016/j.heliyon.2024.e36483**

Gregg, R. W., Sarkar, S. N., & Shoemaker, J. E. (2019). Mathematical modeling of the cGAS pathway reveals robustness of DNA sensing to TREX1 feedback. *J Theor Biol*, *462*, 148-157. **https://doi.org/10.1016/j.jtbi.2018.11.001**

Guan, L., Crasta, K. C., & Maier, A. B. (2022). Assessment of cell cycle regulators in human peripheral blood cells as markers of cellular senescence. *Ageing Res Rev*, *78*, 101634. **https://doi.org/10.1016/j.arr.2022.101634**

Guerrero, A., Herranz, N., Sun, B., Wagner, V., Gallage, S., Guiho, R.,…Gil, J. (2019). Cardiac glycosides are broad-spectrum senolytics. *Nat Metab*, *1*(11), 1074-1088. **https://doi.org/10.1038/s42255-019-0122-z**

Guerrero, A., Innes, A. J., Roux, P. F., Buisman, S. C., Jung, J., Ortet, L.,…Gil, J. (2022). 3-deazaadenosine (3DA) alleviates senescence to promote cellular fitness and cell therapy efficiency in mice. *Nat Aging*, *2*, 851-866. **https://doi.org/10.1038/s43587-022-00279-9**

Gulati, N., Laudet, B., Zohrabian, V. M., Murali, R., & Jhanwar-Uniyal, M. (2006). The antiproliferative effect of Quercetin in cancer cells is mediated via inhibition of the PI3K-Akt/PKB pathway. *Anticancer Res*, *26*(2A), 1177-1181.

Gulej, R., Nyúl-Tóth, Á., Ahire, C., DelFavero, J., Balasubramanian, P., Kiss, T.,…Ungvari, Z. (2023). Elimination of senescent cells by treatment with Navitoclax/ABT263 reverses whole brain irradiation-induced blood-brain barrier disruption in the mouse brain. *Geroscience*, *45*(5), 2983-3002. **https://doi.org/10.1007/s11357-023-00870-x**

Gulen, M. F., Koch, U., Haag, S. M., Schuler, F., Apetoh, L., Villunger, A.,…Ablasser, A. (2017). Signalling strength determines proapoptotic functions of STING. *Nat Commun*, *8*(1), 427. **https://doi.org/10.1038/s41467-017-00573-w**

Gulen, M. F., Samson, N., Keller, A., Schwabenland, M., Liu, C., Glück, S.,…Ablasser, A. (2023). cGAS-STING drives ageing-related inflammation and neurodegeneration. *Nature*, *620*(7973), 374-380. **https://doi.org/10.1038/s41586-023-06373-1**

Haga, M., & Okada, M. (2022). Systems approaches to investigate the role of NF-κB signaling in aging. *Biochem J*, *479*(2), 161-183. **https://doi.org/10.1042/BCJ20210547**

Hambright, W. S., Duke, V. R., Goff, A. D., Goff, A. W., Minas, L. T., Kloser, H.,…Huard, J. (2024). Clinical validation of C12FDG as a marker associated with senescence and osteoarthritic phenotypes. *Aging Cell*, *23*(5), e14113. **https://doi.org/10.1111/acel.14113**

Hanahan, D., & Weinberg, R. A. (2011). Hallmarks of cancer: the next generation. *Cell*, *144*(5), 646-674. **https://doi.org/10.1016/j.cell.2011.02.013**

Hancioglu, B., Swigon, D., & Clermont, G. (2007). A dynamical model of human immune response to influenza A virus infection. *J Theor Biol*, *246*(1), 70-86. **https://doi.org/10.1016/j.jtbi.2006.12.015**

Hannon, G. J., & Beach, D. (1994). p15INK4B is a potential effector of TGF-beta-induced cell cycle arrest. *Nature*, *371*(6494), 257-261. **https://doi.org/10.1038/371257a0**

Hari, P., Millar, F. R., Tarrats, N., Birch, J., Quintanilla, A., Rink, C. J.,…Acosta, J. C. (2019). The innate immune sensor Toll-like receptor 2 controls the senescence-associated secretory phenotype. *Sci Adv*, *5*(6), eaaw0254. **https://doi.org/10.1126/sciadv.aaw0254**

Harrison, D. E., Strong, R., Sharp, Z. D., Nelson, J. F., Astle, C. M., Flurkey, K.,…Miller, R. A. (2009). Rapamycin fed late in life extends lifespan in genetically heterogeneous mice. *Nature*, *460*(7253), 392-395. **https://doi.org/10.1038/nature08221**

Hasegawa, T., Oka, T., Son, H. G., Oliver-García, V. S., Azin, M., Eisenhaure, T. M.,…Demehri, S. (2023). Cytotoxic CD4+ T cells eliminate senescent cells by targeting cytomegalovirus antigen. *Cell*, *186*(7), 1417-1431.e1420. **https://doi.org/10.1016/j.cell.2023.02.033**

Hayflick, L., & Moorhead, P. S. (1961). The serial cultivation of human diploid cell strains. *Exp Cell Res*, *25*, 585-621. **https://doi.org/10.1016/0014-4827(61)90192-6**

He, S., & Sharpless, N. E. (2017). Senescence in Health and Disease. *Cell*, *169*(6), 1000-1011. **https://doi.org/10.1016/j.cell.2017.05.015**

Herbig, U., Jobling, W. A., Chen, B. P., Chen, D. J., & Sedivy, J. M. (2004). Telomere shortening triggers senescence of human cells through a pathway involving ATM, p53, and p21(CIP1), but not p16(INK4a). *Mol Cell*, *14*(4), 501-513. **https://doi.org/10.1016/s1097-2765(04)00256-4**

Hernandez-Segura, A., de Jong, T. V., Melov, S., Guryev, V., Campisi, J., & Demaria, M. (2017). Unmasking Transcriptional Heterogeneity in Senescent Cells. *Curr Biol*, *27*(17), 2652-2660.e2654. **https://doi.org/10.1016/j.cub.2017.07.033**

Herranz, N., Gallage, S., Mellone, M., Wuestefeld, T., Klotz, S., Hanley, C. J.,…Gil, J. (2015). mTOR regulates MAPKAPK2 translation to control the senescence-associated secretory phenotype. *Nat Cell Biol*, *17*(9), 1205-1217. **https://doi.org/10.1038/ncb3225**

Hewitt, G., Jurk, D., Marques, F. D., Correia-Melo, C., Hardy, T., Gackowska, A.,…Passos, J. F. (2012). Telomeres are favoured targets of a persistent DNA

damage response in ageing and stress-induced senescence. *Nat Commun*, *3*, 708. **https://doi.org/10.1038/ncomms1708**

Hickson, L. J., Langhi Prata, L. G. P., Bobart, S. A., Evans, T. K., Giorgadze, N., Hashmi, S. K.,…Kirkland, J. L. (2019). Senolytics decrease senescent cells in humans: Preliminary report from a clinical trial of Dasatinib plus Quercetin in individuals with diabetic kidney disease. *EBioMedicine*, *47*, 446-456. **https://doi.org/10.1016/j.ebiom.2019.08.069**

Hoare, M., Ito, Y., Kang, T. W., Weekes, M. P., Matheson, N. J., Patten, D. A.,…Narita, M. (2016). NOTCH1 mediates a switch between two distinct secretomes during senescence. *Nat Cell Biol*, *18*(9), 979-992. **https://doi.org/10.1038/ncb3397**

Hoare, M., & Narita, M. (2018). Notch and Senescence. *Adv Exp Med Biol*, *1066*, 299-318. **https://doi.org/10.1007/978-3-319-89512-3_15**

Hoffmann, A., & Baltimore, D. (2006). Circuitry of nuclear factor kappaB signaling. *Immunol Rev*, *210*, 171-186. **https://doi.org/10.1111/j.0105-2896.2006.00375.x**

Hopfner, K. P., & Hornung, V. (2020). Molecular mechanisms and cellular functions of cGAS-STING signalling. *Nat Rev Mol Cell Biol*, *21*(9), 501-521. **https://doi.org/10.1038/s41580-020-0244-x**

Hou, Y., Liang, H., Rao, E., Zheng, W., Huang, X., Deng, L.,…Fu, Y. X. (2018). Non-canonical NF-κB Antagonizes STING Sensor-Mediated DNA Sensing in Radiotherapy. *Immunity*, *49*(3), 490-503.e494. **https://doi.org/10.1016/j.immuni.2018.07.008**

Huan, T., Zhang, B., Wang, Z., Joehanes, R., Zhu, J., Johnson, A. D.,…Coronary ARteryDIsease Genome wide Replication and Meta-analysis (CARDIoGRAM) Consortium, I. t. C. f. B. P. G. I. (2013). A systems biology framework identifies molecular underpinnings of coronary heart disease. *Arterioscler Thromb Vasc Biol*, *33*(6), 1427-1434. **https://doi.org/10.1161/ATVBAHA.112.300112**

Huang, L. S., Hong, Z., Wu, W., Xiong, S., Zhong, M., Gao, X.,…Malik, A. B. (2020). mtDNA Activates cGAS Signaling and Suppresses the YAP-Mediated Endothelial Cell Proliferation Program to Promote Inflammatory Injury. *Immunity*, *52*(3), 475-486.e475. **https://doi.org/10.1016/j.immuni.2020.02.002**

Huang, W., Hickson, L. J., Eirin, A., Kirkland, J. L., & Lerman, L. O. (2022). Cellular senescence: the good, the bad and the unknown. *Nat Rev Nephrol*, *18*(10), 611-627. **https://doi.org/10.1038/s41581-022-00601-z**

Hubackova, S., Krejcikova, K., Bartek, J., & Hodny, Z. (2012). IL1- and TGFβ-Nox4 signaling, oxidative stress and DNA damage response are shared features of replicative, oncogene-induced, and drug-induced paracrine 'bystander senescence'. *Aging (Albany NY)*, *4*(12), 932-951. **https://doi.org/10.18632/aging.100520**

Hui, W., Young, D. A., Rowan, A. D., Xu, X., Cawston, T. E., & Proctor, C. J. (2016). Oxidative changes and signalling pathways are pivotal in initiating age-related changes in articular cartilage. *Ann Rheum Dis*, *75*(2), 449-458. **https://doi.org/10.1136/annrheumdis-2014-206295**

Hunziker, A., Jensen, M. H., & Krishna, S. (2010). Stress-specific response of the p53-Mdm2 feedback loop. *BMC Syst Biol*, *4*, 94. **https://doi.org/10.1186/1752-0509-4-94**

Idda, M. L., McClusky, W. G., Lodde, V., Munk, R., Abdelmohsen, K., Rossi, M., & Gorospe, M. (2020). Survey of senescent cell markers with age in human

tissues. *Aging (Albany NY)*, *12*(5), 4052-4066. **https://doi.org/10.18632/aging.102903**

Innes, A. J., Sun, B., Wagner, V., Brookes, S., McHugh, D., Pombo, J.,…Gil, J. (2021). XPO7 is a tumor suppressor regulating p21. *Genes Dev*, *35*(5-6), 379-391. **https://doi.org/10.1101/gad.343269.120**

Islam, M. T., Tuday, E., Allen, S., Kim, J., Trott, D. W., Holland, W. L.,…Lesniewski, L. A. (2023). Senolytic drugs, dasatinib and quercetin, attenuate adipose tissue inflammation, and ameliorate metabolic function in old age. *Aging Cell*, *22*(2), e13767. **https://doi.org/10.1111/acel.13767**

Ito, Y., Hoare, M., & Narita, M. (2017). Spatial and Temporal Control of Senescence. *Trends Cell Biol*, *27*(11), 820-832. **https://doi.org/10.1016/j.tcb.2017.07.004**

Jacobs, J. P., Jones, C. M., & Baille, J. P. (1970). Characteristics of a human diploid cell designated MRC-5. *Nature*, *227*(5254), 168-170. **https://doi.org/10.1038/227168a0**

Jacobsen, A., Wen, J., Marks, D. S., & Krogh, A. (2010). Signatures of RNA binding proteins globally coupled to effective microRNA target sites. *Genome Res*, *20*(8), 1010-1019. **https://doi.org/10.1101/gr.103259.109**

Jazayeri, A., Falck, J., Lukas, C., Bartek, J., Smith, G. C., Lukas, J., & Jackson, S. P. (2006). ATM- and cell cycle-dependent regulation of ATR in response to DNA double-strand breaks. *Nat Cell Biol*, *8*(1), 37-45. **https://doi.org/10.1038/ncb1337**

Jenkins, T. G., James, E. R., Alonso, D. F., Hoidal, J. R., Murphy, P. J., Hotaling, J. M.,…Aston, K. I. (2017). Cigarette smoking significantly alters sperm DNA methylation patterns. *Andrology*, *5*(6), 1089-1099. **https://doi.org/10.1111/andr.12416**

Johmura, Y., Shimada, M., Misaki, T., Naiki-Ito, A., Miyoshi, H., Motoyama, N.,…Nakanishi, M. (2014). Necessary and sufficient role for a mitosis skip in senescence induction. *Mol Cell*, *55*(1), 73-84. **https://doi.org/10.1016/j.molcel.2014.05.003**

Jun, J. I., & Lau, L. F. (2010). The matricellular protein CCN1 induces fibroblast senescence and restricts fibrosis in cutaneous wound healing. *Nat Cell Biol*, *12*(7), 676-685. **https://doi.org/10.1038/ncb2070**

Jung, S. H., Hwang, H. J., Kang, D., Park, H. A., Lee, H. C., Jeong, D.,…Lee, J. S. (2019). mTOR kinase leads to PTEN-loss-induced cellular senescence by phosphorylating p53. *Oncogene*, *38*(10), 1639-1650. **https://doi.org/10.1038/s41388-018-0521-8**

Jurk, D., Wang, C., Miwa, S., Maddick, M., Korolchuk, V., Tsolou, A.,…von Zglinicki, T. (2012). Postmitotic neurons develop a p21-dependent senescence-like phenotype driven by a DNA damage response. *Aging Cell*, *11*(6), 996-1004. **https://doi.org/10.1111/j.1474-9726.2012.00870.x**

Jurk, D., Wilson, C., Passos, J. F., Oakley, F., Correia-Melo, C., Greaves, L.,…von Zglinicki, T. (2014). Chronic inflammation induces telomere dysfunction and accelerates ageing in mice. *Nat Commun*, *2*, 4172. **https://doi.org/10.1038/ncomms5172**

Justice, J. N., Ferrucci, L., Newman, A. B., Aroda, V. R., Bahnson, J. L., Divers, J.,…Kuchel, G. A. (2018). A framework for selection of blood-based biomarkers for geroscience-guided clinical trials: report from the TAME Biomarkers Workgroup. *Geroscience*, *40*(5-6), 419-436. **https://doi.org/10.1007/s11357-018-0042-y**

Justice, J. N., Nambiar, A. M., Tchkonia, T., LeBrasseur, N. K., Pascual, R., Hashmi, S. K.,…Kirkland, J. L. (2019). Senolytics in idiopathic pulmonary fibrosis:

Results from a first-in-human, open-label, pilot study. *EBioMedicine*, *40*, 554-563. **https://doi.org/10.1016/j.ebiom.2018.12.052**
Kadler, K. E., Baldock, C., Bella, J., & Boot-Handford, R. P. (2007). Collagens at a glance. *J Cell Sci*, *120*(Pt 12), 1955-1958. **https://doi.org/10.1242/jcs.03453**
Kanehisa, M., Furumichi, M., Sato, Y., Matsuura, Y., & Ishiguro-Watanabe, M. (2025). KEGG: biological systems database as a model of the real world. *Nucleic Acids Res*, *53*(D1), D672-D677. **https://doi.org/10.1093/nar/gkae909**
Kaplon, J., Zheng, L., Meissl, K., Chaneton, B., Selivanov, V. A., Mackay, G.,…Peeper, D. S. (2013). A key role for mitochondrial gatekeeper pyruvate dehydrogenase in oncogene-induced senescence. *Nature*, *498*(7452), 109-112. **https://doi.org/10.1038/nature12154**
Kastan, M. B., Zhan, Q., el-Deiry, W. S., Carrier, F., Jacks, T., Walsh, W. V.,…Fornace, A. J. (1992). A mammalian cell cycle checkpoint pathway utilizing p53 and GADD45 is defective in ataxia-telangiectasia. *Cell*, *71*(4), 587-597. **https://doi.org/10.1016/0092-8674(92)90593-2**
Keeling, M. J. (2005). Models of foot-and-mouth disease. *Proc Biol Sci*, *272*(1569), 1195-1202. **https://doi.org/10.1098/rspb.2004.3046**
Kennedy, A. L., Morton, J. P., Manoharan, I., Nelson, D. M., Jamieson, N. B., Pawlikowski, J. S.,…Adams, P. D. (2011). Activation of the PIK3CA/AKT pathway suppresses senescence induced by an activated RAS oncogene to promote tumorigenesis. *Mol Cell*, *42*(1), 36-49. **https://doi.org/10.1016/j.molcel.2011.02.020**
Kennedy, B. K., Berger, S. L., Brunet, A., Campisi, J., Cuervo, A. M., Epel, E. S.,…Sierra, F. (2014). Geroscience: linking aging to chronic disease. *Cell*, *159*(4), 709-713. **https://doi.org/10.1016/j.cell.2014.10.039**
Kim, J. J., Lee, S. B., Yi, S. Y., Han, S. A., Kim, S. H., Lee, J. M.,…Lou, Z. (2017). WSB1 overcomes oncogene-induced senescence by targeting ATM for degradation. *Cell Res*, *27*(2), 274-293. **https://doi.org/10.1038/cr.2016.148**
Kirkland, J. L., & Tchkonia, T. (2020). Senolytic drugs: from discovery to translation. *J Intern Med*, *288*(5), 518-536. **https://doi.org/10.1111/joim.13141**
Kirkwood, T. B. (2005). Understanding the odd science of aging. *Cell*, *120*(4), 437-447. **https://doi.org/10.1016/j.cell.2005.01.027**
Kirschner, K., Samarajiwa, S. A., Cairns, J. M., Menon, S., Pérez-Mancera, P. A., Tomimatsu, K.,…Tavaré, S. (2015). Phenotype specific analyses reveal distinct regulatory mechanism for chronically activated p53. *PLoS Genet*, *11*(3), e1005053. **https://doi.org/10.1371/journal.pgen.1005053**
Kitano, H. (2002). Computational systems biology. *Nature*, *420*(6912), 206-210. **https://doi.org/10.1038/nature01254**
Klein, S. L., & Flanagan, K. L. (2016). Sex differences in immune responses. *Nat Rev Immunol*, *16*(10), 626-638. **https://doi.org/10.1038/nri.2016.90**
Kopan, R., & Ilagan, M. X. (2009). The canonical Notch signaling pathway: unfolding the activation mechanism. *Cell*, *137*(2), 216-233. **https://doi.org/10.1016/j.cell.2009.03.045**
Korolchuk, V. I., Miwa, S., Carroll, B., & von Zglinicki, T. (2017). Mitochondria in Cell Senescence: Is Mitophagy the Weakest Link? *EBioMedicine*, *21*, 7-13. **https://doi.org/10.1016/j.ebiom.2017.03.020**
Krizhanovsky, V., Xue, W., Zender, L., Yon, M., Hernando, E., & Lowe, S. W. (2008). Implications of cellular senescence in tissue damage response, tumor suppression, and stem cell biology. *Cold Spring Harb Symp Quant Biol*, *73*, 513-522. **https://doi.org/10.1101/sqb.2008.73.048**

Kuang, P. P., Zhang, X. H., Rich, C. B., Foster, J. A., Subramanian, M., & Goldstein, R. H. (2007). Activation of elastin transcription by transforming growth factor-beta in human lung fibroblasts. *Am J Physiol Lung Cell Mol Physiol*, *292*(4), L944-952. **https://doi.org/10.1152/ajplung.00184.2006**

Kuilman, T., Michaloglou, C., Vredeveld, L. C., Douma, S., van Doorn, R., Desmet, C. J.,…Peeper, D. S. (2008). Oncogene-induced senescence relayed by an interleukin-dependent inflammatory network. *Cell*, *133*(6), 1019-1031. **https://doi.org/10.1016/j.cell.2008.03.039**

Kuilman, T., & Peeper, D. S. (2009). Senescence-messaging secretome: SMS-ing cellular stress. *Nat Rev Cancer*, *9*(2), 81-94. **https://doi.org/10.1038/nrc2560**

Kumari, R., Hummerich, H., Shen, X., Fischer, M., Litovchick, L., Mittnacht, S.,…Jat, P. S. (2021). Simultaneous expression of MMB-FOXM1 complex components enables efficient bypass of senescence. *Sci Rep*, *11*(1), 21506. **https://doi.org/10.1038/s41598-021-01012-z**

Kumari, R., & Jat, P. (2021). Mechanisms of Cellular Senescence: Cell Cycle Arrest and Senescence Associated Secretory Phenotype. *Front Cell Dev Biol*, *9*, 645593. **https://doi.org/10.3389/fcell.2021.645593**

Kwong, J., Hong, L., Liao, R., Deng, Q., Han, J., & Sun, P. (2009). p38alpha and p38gamma mediate oncogenic ras-induced senescence through differential mechanisms. *J Biol Chem*, *284*(17), 11237-11246. **https://doi.org/10.1074/jbc.M808327200**

Laberge, R. M., Sun, Y., Orjalo, A. V., Patil, C. K., Freund, A., Zhou, L.,…Campisi, J. (2015). MTOR regulates the pro-tumorigenic senescence-associated secretory phenotype by promoting IL1A translation. *Nat Cell Biol*, *17*(8), 1049-1061. **https://doi.org/10.1038/ncb3195**

Lackner, D. H., Hayashi, M. T., Cesare, A. J., & Karlseder, J. (2014). A genomics approach identifies senescence-specific gene expression regulation. *Aging Cell*, *13*(5), 946-950. **https://doi.org/10.1111/acel.12234**

Lago, J. C., & Puzzi, M. B. (2019). The effect of aging in primary human dermal fibroblasts. *PLoS One*, *14*(7), e0219165. **https://doi.org/10.1371/journal.pone.0219165**

Lai, A., Marcellus, R. C., Corbeil, H. B., & Branton, P. E. (1999). RBP1 induces growth arrest by repression of E2F-dependent transcription. *Oncogene*, *18*(12), 2091-2100. **https://doi.org/10.1038/sj.onc.1202520**

Lan, Y. Y., Heather, J. M., Eisenhaure, T., Garris, C. S., Lieb, D., Raychowdhury, R., & Hacohen, N. (2019). Extranuclear DNA accumulates in aged cells and contributes to senescence and inflammation. *Aging Cell*, *18*(2), e12901. **https://doi.org/10.1111/acel.12901**

Lau, L., Porciuncula, A., Yu, A., Iwakura, Y., & David, G. (2019). Uncoupling the Senescence-Associated Secretory Phenotype from Cell Cycle Exit via Interleukin-1 Inactivation Unveils Its Protumorigenic Role. *Mol Cell Biol*, *39*(12). **https://doi.org/10.1128/MCB.00586-18**

Le Novère, N., Hucka, M., Mi, H., Moodie, S., Schreiber, F., Sorokin, A.,…Kitano, H. (2009). The Systems Biology Graphical Notation. *Nat Biotechnol*, *27*(8), 735-741. **https://doi.org/10.1038/nbt.1558**

Lee, J., Basak, J. M., Demehri, S., & Kopan, R. (2007). Bi-compartmental communication contributes to the opposite proliferative behavior of Notch1-deficient hair follicle and epidermal keratinocytes. *Development*, *134*(15), 2795-2806. **https://doi.org/10.1242/dev.02868**

Lee, K. W., & Pausova, Z. (2013). Cigarette smoking and DNA methylation. *Front Genet*, *4*, 132. **https://doi.org/10.3389/fgene.2013.00132**

Lee, Y., Kim, J., Kim, M. S., Kwon, Y., Shin, S., Yi, H.,…Kang, C. (2021). Coordinate regulation of the senescent state by selective autophagy. *Dev Cell*, *56*(10), 1512-1525.e1517. **https://doi.org/10.1016/j.devcel.2021.04.008**

Lenain, C., de Graaf, C. A., Pagie, L., Visser, N. L., de Haas, M., de Vries, S. S.,…Peeper, D. S. (2017). Massive reshaping of genome-nuclear lamina interactions during oncogene-induced senescence. *Genome Res*, *27*(10), 1634-1644. **https://doi.org/10.1101/gr.225763.117**

Leon, K. E., Buj, R., Lesko, E., Dahl, E. S., Chen, C. W., Tangudu, N. K.,…Aird, K. M. (2021). DOT1L modulates the senescence-associated secretory phenotype through epigenetic regulation of IL1A. *J Cell Biol*, *220*(8). **https://doi.org/10.1083/jcb.202008101**

Li, F., Huangyang, P., Burrows, M., Guo, K., Riscal, R., Godfrey, J.,…Simon, M. C. (2020). FBP1 loss disrupts liver metabolism and promotes tumorigenesis through a hepatic stellate cell senescence secretome. *Nat Cell Biol*, *22*(6), 728-739. **https://doi.org/10.1038/s41556-020-0511-2**

Li, X., Li, C., Zhang, W., Wang, Y., Qian, P., & Huang, H. (2023). Inflammation and aging: signaling pathways and intervention therapies. *Signal Transduct Target Ther*, *8*(1), 239. **https://doi.org/10.1038/s41392-023-01502-8**

Liu, P., Li, F., Lin, J., Fukumoto, T., Nacarelli, T., Hao, X.,…Zhang, R. (2021). m6A-independent genome-wide METTL3 and METTL14 redistribution drives the senescence-associated secretory phenotype. *Nature Cell Biology 23*(4), 355-365. **https://doi.org/10.1038/s41556-021-00656-3**

Liu, T., Zhang, L., Joo, D., & Sun, S. C. (2017). NF-κB signaling in inflammation. *Signal Transduct Target Ther*, *2*. **https://doi.org/10.1038/sigtrans.2017.23**

Liu, X. L., Ding, J., & Meng, L. H. (2018). Oncogene-induced senescence: a double edged sword in cancer. *Acta Pharmacol Sin*, *39*(10), 1553-1558. **https://doi.org/10.1038/aps.2017.198**

Liu, Y., & Pu, F. (2023). Updated roles of cGAS-STING signaling in autoimmune diseases. *Front Immunol*, *14*, 1254915. **https://doi.org/10.3389/fimmu.2023.1254915**

Liu, Y., Tan, Y., Zhang, Z., Yi, M., Zhu, L., & Peng, W. (2024). The interaction between ageing and Alzheimer's disease: insights from the hallmarks of ageing. *Transl Neurodegener*, *13*(1), 7. **https://doi.org/10.1186/s40035-024-00397-x**

Lizardo, D. Y., Lin, Y. L., Gokcumen, O., & Atilla-Gokcumen, G. E. (2017). Regulation of lipids is central to replicative senescence. *Mol Biosyst*, *13*(3), 498-509. **https://doi.org/10.1039/c6mb00842a**

Loayza-Puch, F., Drost, J., Rooijers, K., Lopes, R., Elkon, R., & Agami, R. (2013). p53 induces transcriptional and translational programs to suppress cell proliferation and growth. *Genome Biol*, *14*(4), R32. **https://doi.org/10.1186/gb-2013-14-4-r32**

Loo, T. M., Miyata, K., Tanaka, Y., & Takahashi, A. (2020). Cellular senescence and senescence-associated secretory phenotype via the cGAS-STING signaling pathway in cancer. *Cancer Sci*, *111*(2), 304-311. **https://doi.org/10.1111/cas.14266**

Lopes-Paciencia, S., Saint-Germain, E., Rowell, M. C., Ruiz, A. F., Kalegari, P., & Ferbeyre, G. (2019). The senescence-associated secretory phenotype and its regulation. *Cytokine*, *117*, 15-22. **https://doi.org/10.1016/j.cyto.2019.01.013**

Love, M. I., Huber, W., & Anders, S. (2014). Moderated estimation of fold change and dispersion for RNA-seq data with DESeq2. *Genome Biol*, *15*(12), 550. **https://doi.org/10.1186/s13059-014-0550-8**

Lujambio, A. (2016). To clear, or not to clear (senescent cells)? That is the question. *Bioessays*, *38 Suppl 1*, S56-64. **https://doi.org/10.1002/bies.201670910**

Luo, W., & Brouwer, C. (2013). Pathview: an R/Bioconductor package for pathway-based data integration and visualization. *Bioinformatics*, *29*(14), 1830-1831. **https://doi.org/10.1093/bioinformatics/btt285**

Lämmermann, I., Terlecki-Zaniewicz, L., Weinmüllner, R., Schosserer, M., Dellago, H., de Matos Branco, A. D.,…Grillari, J. (2018). Blocking negative effects of senescence in human skin fibroblasts with a plant extract. *NPJ Aging Mech Dis*, *4*, 4. **https://doi.org/10.1038/s41514-018-0023-5**

López-Antona, I., Contreras-Jurado, C., Luque-Martín, L., Carpintero-Leyva, A., González-Méndez, P., & Palmero, I. (2022). Dynamic regulation of myofibroblast phenotype in cellular senescence. *Aging Cell*, *21*(4), e13580. **https://doi.org/10.1111/acel.13580**

López-Otín, C., Blasco, M. A., Partridge, L., Serrano, M., & Kroemer, G. (2013). The hallmarks of aging. *Cell*, *153*(6), 1194-1217. **https://doi.org/10.1016/j.cell.2013.05.039**

López-Otín, C., Blasco, M. A., Partridge, L., Serrano, M., & Kroemer, G. (2023). Hallmarks of aging: An expanding universe. *Cell*, *186*(2), 243-278. **https://doi.org/10.1016/j.cell.2022.11.001**

Maclaine, N. J., & Hupp, T. R. (2009). The regulation of p53 by phosphorylation: a model for how distinct signals integrate into the p53 pathway. *Aging (Albany NY)*, *1*(5), 490-502. **https://doi.org/10.18632/aging.100047**

Madsen, H. B., Pease, L. I., Scanlan, R. L., Akbari, M., Rasmussen, L. J., Shanley, D. P., & Bohr, V. A. (2023). The DNA repair enzyme, aprataxin, plays a role in innate immune signaling. *Front Aging Neurosci*, *15*, 1290681. **https://doi.org/10.3389/fnagi.2023.1290681**

Mah, L. J., El-Osta, A., & Karagiannis, T. C. (2010). gammaH2AX: a sensitive molecular marker of DNA damage and repair. *Leukemia*, *24*(4), 679-686. **https://doi.org/10.1038/leu.2010.6**

Malkin, D. (1993). p53 and the Li-Fraumeni syndrome. *Cancer Genet Cytogenet*, *66*(2), 83-92. **https://doi.org/10.1016/0165-4608(93)90233-c**

Manchanda, H., Seidel, N., Krumbholz, A., Sauerbrei, A., Schmidtke, M., & Guthke, R. (2014). Within-host influenza dynamics: a small-scale mathematical modeling approach. *Biosystems*, *118*, 51-59. **https://doi.org/10.1016/j.biosystems.2014.02.004**

Mangelinck, A., Coudereau, C., Courbeyrette, R., Ourarhni, K., Hamiche, A., Redon, C.,…Mann, C. (2020). The H2A.J histone variant contributes to Interferon-Stimulated Gene expression in senescence by its weak interaction with H1 and the derepression of repeated DNA sequences. *bioRxiv*. **https://doi.org/https://doi.org/10.1101/2020.10.29.361204**

Marengoni, A., Angleman, S., Melis, R., Mangialasche, F., Karp, A., Garmen, A.,…Fratiglioni, L. (2011). Aging with multimorbidity: a systematic review of the literature. *Ageing Res Rev*, *10*(4), 430-439. **https://doi.org/10.1016/j.arr.2011.03.003**

Marin, I., Boix, O., Garcia-Garijo, A., Sirois, I., Caballe, A., Zarzuela, E.,…Serrano, M. (2023). Cellular Senescence Is Immunogenic and Promotes Antitumor Immunity. *Cancer Discov*, *13*(2), 410-431. **https://doi.org/10.1158/2159-8290.CD-22-0523**

Marthandan, S., Baumgart, M., Priebe, S., Groth, M., Schaer, J., Kaether, C.,…Hemmerich, P. (2016). Conserved Senescence Associated Genes and

Pathways in Primary Human Fibroblasts Detected by RNA-Seq. *PLoS One*, *11*(5), e0154531. **https://doi.org/10.1371/journal.pone.0154531**

Marthandan, S., Menzel, U., Priebe, S., Groth, M., Guthke, R., Platzer, M.,…Diekmann, S. (2016). Conserved genes and pathways in primary human fibroblast strains undergoing replicative and radiation induced senescence. *Biol Res*, *49*(1), 34. **https://doi.org/10.1186/s40659-016-0095-2**

Marthandan, S., Priebe, S., Groth, M., Guthke, R., Platzer, M., Hemmerich, P., & Diekmann, S. (2015). Hormetic effect of rotenone in primary human fibroblasts. *Immun Ageing*, *12*, 11. **https://doi.org/10.1186/s12979-015-0038-8**

Marthandan, S., Priebe, S., Hemmerich, P., Klement, K., & Diekmann, S. (2014). Long-term quiescent fibroblast cells transit into senescence. *PLoS One*, *9*(12), e115597. **https://doi.org/10.1371/journal.pone.0115597**

Martin, M. (2011). Cutadapt removes adapter sequences from high-throughput sequencing reads. *EMBnet.journal*, *17*(1).

Martinez-Zubiaurre, I., Fenton, C. G., Taman, H., Pettersen, I., Hellevik, T., & Paulssen, R. H. (2013). Tumorigenic Responses of Cancer-Associated Stromal Fibroblasts after Ablative Radiotherapy: A Transcriptome-Profiling Study. *Journal of Cancer Therapy*, *4*(1). **https://doi.org/10.4236/jct.2013.41031**

Martín-Escolano, R., Vidal-Alcántara, E. J., Crespo, J., Ryan, P., Real, L. M., Lazo-Álvarez, J. I.,…Fernández-Rodríguez, A. (2023). Immunological and senescence biomarker profiles in patients after spontaneous clearance of hepatitis C virus: gender implications for long-term health risk. *Immun Ageing*, *20*(1), 62. **https://doi.org/10.1186/s12979-023-00387-z**

Martínez-Zamudio, R. I., Roux, P. F., de Freitas, J. A. N. L., Robinson, L., Doré, G., Sun, B.,…Bischof, O. (2020). AP-1 imprints a reversible transcriptional programme of senescent cells. *Nat Cell Biol*, *22*(7), 842-855. **https://doi.org/10.1038/s41556-020-0529-5**

Maréchal, A., & Zou, L. (2013). DNA damage sensing by the ATM and ATR kinases. *Cold Spring Harb Perspect Biol*, *5*(9). **https://doi.org/10.1101/cshperspect.a012716**

Matjusaitis, M., Chin, G., Sarnoski, E. A., & Stolzing, A. (2016). Biomarkers to identify and isolate senescent cells. *Ageing Res Rev*, *29*, 1-12. **https://doi.org/10.1016/j.arr.2016.05.003**

Mc Auley, M. T., Wilkinson, D. J., Jones, J. J., & Kirkwood, T. B. (2012). A whole-body mathematical model of cholesterol metabolism and its age-associated dysregulation. *BMC Syst Biol*, *6*, 130. **https://doi.org/10.1186/1752-0509-6-130**

McHugh, D., Sun, B., Gutierrez-Muñoz, C., Hernández-González, F., Mellone, M., Guiho, R.,…Gil, J. (2023). COPI vesicle formation and N-myristoylation are targetable vulnerabilities of senescent cells. *Nat Cell Biol*, *25*(12), 1804-1820. **https://doi.org/10.1038/s41556-023-01287-6**

Mellone, M., Hanley, C. J., Thirdborough, S., Mellows, T., Garcia, E., Woo, J.,…Thomas, G. J. (2016). Induction of fibroblast senescence generates a non-fibrogenic myofibroblast phenotype that differentially impacts on cancer prognosis. *Aging (Albany NY)*, *9*(1), 114-132. **https://doi.org/10.18632/aging.101127**

Michael, D., & Oren, M. (2003). The p53-Mdm2 module and the ubiquitin system. *Semin Cancer Biol*, *13*(1), 49-58. **https://doi.org/10.1016/s1044-579x(02)00099-8**

Mijit, M., Caracciolo, V., Melillo, A., Amicarelli, F., & Giordano, A. (2020). Role of p53 in the Regulation of Cellular Senescence. *Biomolecules*, *10*(3). **https://doi.org/10.3390/biom10030420**

Miller, R. A., Harrison, D. E., Astle, C. M., Baur, J. A., Boyd, A. R., de Cabo, R.,…Strong, R. (2011). Rapamycin, but not resveratrol or simvastatin, extends life span of genetically heterogeneous mice. *J Gerontol A Biol Sci Med Sci*, *66*(2), 191-201. **https://doi.org/10.1093/gerona/glq178**

Mitra, M., Johnson, E. L., Swamy, V. S., Nersesian, L. E., Corney, D. C., Robinson, D. G.,…Coller, H. A. (2018). Alternative polyadenylation factors link cell cycle to migration. *Genome Biol*, *19*(1), 176. **https://doi.org/10.1186/s13059-018-1551-9**

Miwa, S., Kashyap, S., Chini, E., & von Zglinicki, T. (2022). Mitochondrial dysfunction in cell senescence and aging. *J Clin Invest*, *132*(13). **https://doi.org/10.1172/JCI158447**

Mo, J. S., Yoon, J. H., Ann, E. J., Ahn, J. S., Baek, H. J., Lee, H. J.,…Park, H. S. (2013). Notch1 modulates oxidative stress induced cell death through suppression of apoptosis signal-regulating kinase 1. *Proc Natl Acad Sci U S A*, *110*(17), 6865-6870. **https://doi.org/10.1073/pnas.1209078110**

Moiseeva, O., Deschênes-Simard, X., St-Germain, E., Igelmann, S., Huot, G., Cadar, A. E.,…Ferbeyre, G. (2013). Metformin inhibits the senescence-associated secretory phenotype by interfering with IKK/NF-κB activation. *Aging Cell*, *12*(3), 489-498. **https://doi.org/10.1111/acel.12075**

Montecino-Rodriguez, E., Berent-Maoz, B., & Dorshkind, K. (2013). Causes, consequences, and reversal of immune system aging. *J Clin Invest*, *123*(3), 958-965. **https://doi.org/10.1172/JCI64096**

Montes, M., Lubas, M., Arendrup, F. S., Mentz, B., Rohatgi, N., Tumas, S.,…Lund, A. H. (2021). The long non-coding RNA MIR31HG regulates the senescence associated secretory phenotype. *Nat Commun*, *12*(1), 2459. **https://doi.org/10.1038/s41467-021-22746-4**

Mufudza, C., Sorofa, W., & Chiyaka, E. T. (2012). Assessing the effects of estrogen on the dynamics of breast cancer. *Comput Math Methods Med*, *2012*, 473572. **https://doi.org/10.1155/2012/473572**

Muniz, L., Deb, M. K., Aguirrebengoa, M., Lazorthes, S., Trouche, D., & Nicolas, E. (2017). Control of Gene Expression in Senescence through Transcriptional Read-Through of Convergent Protein-Coding Genes. *Cell Rep*, *21*(9), 2433-2446. **https://doi.org/10.1016/j.celrep.2017.11.006**

Musi, N., Valentine, J. M., Sickora, K. R., Baeuerle, E., Thompson, C. S., Shen, Q., & Orr, M. E. (2018). Tau protein aggregation is associated with cellular senescence in the brain. *Aging Cell*, *17*(6), e12840. **https://doi.org/10.1111/acel.12840**

Muto, J., Fukuda, S., Watanabe, K., Dai, X., Tsuda, T., Kiyoi, T.,…Sayama, K. (2023). Highly concentrated trehalose induces prohealing senescence-like state in fibroblasts via CDKN1A/p21. *Commun Biol*, *6*(1), 13. **https://doi.org/10.1038/s42003-022-04408-3**

Muñoz-Espín, D., Cañamero, M., Maraver, A., Gómez-López, G., Contreras, J., Murillo-Cuesta, S.,…Serrano, M. (2013). Programmed cell senescence during mammalian embryonic development. *Cell*, *155*(5), 1104-1118. **https://doi.org/10.1016/j.cell.2013.10.019**

Muñoz-Espín, D., & Serrano, M. (2014). Cellular senescence: from physiology to pathology. *Nat Rev Mol Cell Biol*, *15*(7), 482-496. **https://doi.org/10.1038/nrm3823**

Mylonas, A., & O'Loghlen, A. (2022). Cellular Senescence and Ageing: Mechanisms and Interventions. *Front Aging*, *3*, 866718. **https://doi.org/10.3389/fragi.2022.866718**

Nagarajan, R. P., Zhang, J., Li, W., & Chen, Y. (1999). Regulation of Smad7 promoter by direct association with Smad3 and Smad4. *J Biol Chem*, *274*(47), 33412-33418. **https://doi.org/10.1074/jbc.274.47.33412**

Nakao, A., Afrakhte, M., Morén, A., Nakayama, T., Christian, J. L., Heuchel, R.,…ten Dijke, P. (1997). Identification of Smad7, a TGFbeta-inducible antagonist of TGF-beta signalling. *Nature*, *389*(6651), 631-635. **https://doi.org/10.1038/39369**

Nakao, A., Imamura, T., Souchelnytskyi, S., Kawabata, M., Ishisaki, A., Oeda, E.,…ten Dijke, P. (1997). TGF-beta receptor-mediated signalling through Smad2, Smad3 and Smad4. *EMBO J*, *16*(17), 5353-5362. **https://doi.org/10.1093/emboj/16.17.5353**

Nambiar, A., Kellogg, D., Justice, J., Goros, M., Gelfond, J., Pascual, R.,…Kirkland, J. (2023). Senolytics dasatinib and quercetin in idiopathic pulmonary fibrosis: results of a phase I, single-blind, single-center, randomized, placebo-controlled pilot trial on feasibility and tolerability. *EBioMedicine*, *90*, 104481. **https://doi.org/10.1016/j.ebiom.2023.104481**

Narita, M., Young, A. R., Arakawa, S., Samarajiwa, S. A., Nakashima, T., Yoshida, S.,…Shimizu, S. (2011). Spatial coupling of mTOR and autophagy augments secretory phenotypes. *Science*, *332*(6032), 966-970. **https://doi.org/10.1126/science.1205407**

Nelson, D. M., Jaber-Hijazi, F., Cole, J. J., Robertson, N. A., Pawlikowski, J. S., Norris, K. T.,…Adams, P. D. (2016). Mapping H4K20me3 onto the chromatin landscape of senescent cells indicates a function in control of cell senescence and tumor suppression through preservation of genetic and epigenetic stability. *Genome Biol*, *17*(1), 158. **https://doi.org/10.1186/s13059-016-1017-x**

Nelson, D. M., McBryan, T., Jeyapalan, J. C., Sedivy, J. M., & Adams, P. D. (2014). A comparison of oncogene-induced senescence and replicative senescence: implications for tumor suppression and aging. *Age (Dordr)*, *36*(3), 9637. **https://doi.org/10.1007/s11357-014-9637-0**

Nelson, G., Kucheryavenko, O., Wordsworth, J., & von Zglinicki, T. (2018). The senescent bystander effect is caused by ROS-activated NF-κB signalling. *Mech Ageing Dev*, *170*, 30-36. **https://doi.org/10.1016/j.mad.2017.08.005**

Nelson, G., Wordsworth, J., Wang, C., Jurk, D., Lawless, C., Martin-Ruiz, C., & von Zglinicki, T. (2012). A senescent cell bystander effect: senescence-induced senescence. *Aging Cell*, *11*(2), 345-349. **https://doi.org/10.1111/j.1474-9726.2012.00795.x**

Neyret-Kahn, H., Benhamed, M., Ye, T., Le Gras, S., Cossec, J. C., Lapaquette, P.,…Dejean, A. (2013). Sumoylation at chromatin governs coordinated repression of a transcriptional program essential for cell growth and proliferation. *Genome Res*, *23*(10), 1563-1579. **https://doi.org/10.1101/gr.154872.113**

Niccoli, T., & Partridge, L. (2012). Ageing as a risk factor for disease. *Curr Biol*, *22*(17), R741-752. **https://doi.org/10.1016/j.cub.2012.07.024**

Nichols, W. W., Murphy, D. G., Cristofalo, V. J., Toji, L. H., Greene, A. E., & Dwight, S. A. (1977). Characterization of a new human diploid cell strain, IMR-90. *Science*, *196*(4285), 60-63. **https://doi.org/10.1126/science.841339**

Novais, E. J., Tran, V. A., Johnston, S. N., Darris, K. R., Roupas, A. J., Sessions, G. A.,…Risbud, M. V. (2021). Long-term treatment with senolytic drugs Dasatinib and Quercetin ameliorates age-dependent intervertebral disc degeneration in mice. *Nat Commun*, *12*(1), 5213. **https://doi.org/10.1038/s41467-021-25453-2**

Oeckinghaus, A., & Ghosh, S. (2009). The NF-kappaB family of transcription factors and its regulation. *Cold Spring Harb Perspect Biol*, *1*(4), a000034. **https://doi.org/10.1101/cshperspect.a000034**

Ogrodnik, M., Carlos Acosta, J., Adams, P. D., d'Adda di Fagagna, F., Baker, D. J., Bishop, C. L.,…Demaria, M. (2024). Guidelines for minimal information on cellular senescence experimentation in vivo. *Cell*, *187*(16), 4150-4175. **https://doi.org/10.1016/j.cell.2024.05.059**

Omer, A., Barrera, M. C., Moran, J. L., Lian, X. J., Di Marco, S., Beausejour, C., & Gallouzi, I. E. (2020). G3BP1 controls the senescence-associated secretome and its impact on cancer progression. *Nat Commun*, *11*(1), 4979. **https://doi.org/10.1038/s41467-020-18734-9**

Orjalo, A. V., Bhaumik, D., Gengler, B. K., Scott, G. K., & Campisi, J. (2009). Cell surface-bound IL-1alpha is an upstream regulator of the senescence-associated IL-6/IL-8 cytokine network. *Proc Natl Acad Sci U S A*, *106*(40), 17031-17036. **https://doi.org/10.1073/pnas.0905299106**

Ouvrier, B., Ismael, S., & Bix, G. J. (2024). Senescence and SASP Are Potential Therapeutic Targets for Ischemic Stroke. *Pharmaceuticals (Basel)*, *17*(3). **https://doi.org/10.3390/ph17030312**

Pagano, M., Pepperkok, R., Verde, F., Ansorge, W., & Draetta, G. (1992). Cyclin A is required at two points in the human cell cycle. *EMBO J*, *11*(3), 961-971. **https://doi.org/10.1002/j.1460-2075.1992.tb05135.x**

Page-McCaw, A., Ewald, A. J., & Werb, Z. (2007). Matrix metalloproteinases and the regulation of tissue remodelling. *Nat Rev Mol Cell Biol*, *8*(3), 221-233. **https://doi.org/10.1038/nrm2125**

Palmer, A. K., Xu, M., Zhu, Y., Pirtskhalava, T., Weivoda, M. M., Hachfeld, C. M.,…Kirkland, J. L. (2019). Targeting senescent cells alleviates obesity-induced metabolic dysfunction. *Aging Cell*, *18*(3), e12950. **https://doi.org/10.1111/acel.12950**

Paluvai, H., Di Giorgio, E., Brancolini, C., & . (2018). Unscheduled HDAC4 repressive activity in human fibroblasts triggers TP53-dependent senescence and favors cell transformation. *Mol Oncol*, *12*(12), 2165-2181. **https://doi.org/10.1002/1878-0261.12392**

Pantazi, A., Quintanilla, A., Hari, P., Tarrats, N., Parasyraki, E., Dix, F. L.,…Finch, A. J. (2019). Inhibition of the 60S ribosome biogenesis GTPase LSG1 causes endoplasmic reticular disruption and cellular senescence. *Aging Cell*, *18*(4), e12981. **https://doi.org/10.1111/acel.12981**

Papaspyropoulos, A., Hazapis, O., Altulea, A., Polyzou, A., Verginis, P., Evangelou, K.,…Gorgoulis, V. (2023). Decoding of translation-regulating entities reveals heterogeneous translation deficiency patterns in cellular senescence. *Aging Cell*, *22*(9), e13893. **https://doi.org/10.1111/acel.13893**

Park, J. H., Ryu, S. J., Kim, B. J., Cho, H. J., Park, C. H., Choi, H. J. C.,…Park, S. C. (2021). Disruption of nucleocytoplasmic trafficking as a cellular senescence driver. *Exp Mol Med*, *53*(6), 1092-1108. **https://doi.org/10.1038/s12276-021-00643-6**

Parkinson, H., Kapushesky, M., Shojatalab, M., Abeygunawardena, N., Coulson, R., Farne, A.,…Brazma, A. (2007). ArrayExpress--a public database of microarray

experiments and gene expression profiles. *Nucleic Acids Res*, *35*(Database issue), D747-750. **https://doi.org/10.1093/nar/gkl995**

Parry, A. J., Hoare, M., Bihary, D., Hänsel-Hertsch, R., Smith, S., Tomimatsu, K.,…Narita, M. (2018). NOTCH-mediated non-cell autonomous regulation of chromatin structure during senescence. *Nat Commun*, *9*(1), 1840. **https://doi.org/10.1038/s41467-018-04283-9**

Passos, J. F., Nelson, G., Wang, C., Richter, T., Simillion, C., Proctor, C. J.,…von Zglinicki, T. (2010). Feedback between p21 and reactive oxygen production is necessary for cell senescence. *Mol Syst Biol*, *6*, 347. **https://doi.org/10.1038/msb.2010.5**

Passos, J. F., Saretzki, G., Ahmed, S., Nelson, G., Richter, T., Peters, H.,…von Zglinicki, T. (2007). Mitochondrial dysfunction accounts for the stochastic heterogeneity in telomere-dependent senescence. *PLoS Biol*, *5*(5), e110. **https://doi.org/10.1371/journal.pbio.0050110**

Patro, R., Duggal, G., Love, M. I., Irizarry, R. A., & Kingsford, C. (2017). Salmon provides fast and bias-aware quantification of transcript expression. *Nat Methods*, *14*(4), 417-419. **https://doi.org/10.1038/nmeth.4197**

Paul, B. D., Snyder, S. H., & Bohr, V. A. (2021). Signaling by cGAS-STING in Neurodegeneration, Neuroinflammation, and Aging. *Trends Neurosci*, *44*(2), 83-96. **https://doi.org/10.1016/j.tins.2020.10.008**

Pazolli, E., Luo, X., Brehm, S., Carbery, K., Chung, J. J., Prior, J. L.,…Stewart, S. A. (2009). Senescent stromal-derived osteopontin promotes preneoplastic cell growth. *Cancer Res*, *69*(3), 1230-1239. **https://doi.org/10.1158/0008-5472.CAN-08-2970**

Petrie, J. R., Chaturvedi, N., Ford, I., Brouwers, M. C. G. J., Greenlaw, N., Tillin, T.,…Group, R. S. (2017). Cardiovascular and metabolic effects of metformin in patients with type 1 diabetes (REMOVAL): a double-blind, randomised, placebo-controlled trial. *Lancet Diabetes Endocrinol*, *5*(8), 597-609. **https://doi.org/10.1016/S2213-8587(17)30194-8**

Pittayapruek, P., Meephansan, J., Prapapan, O., Komine, M., & Ohtsuki, M. (2016). Role of Matrix Metalloproteinases in Photoaging and Photocarcinogenesis. *Int J Mol Sci*, *17*(6). **https://doi.org/10.3390/ijms17060868**

Pratsinis, H., Armatas, A., Dimozi, A., Lefaki, M., Vassiliu, P., & Kletsas, D. (2013). Paracrine anti-fibrotic effects of neonatal cells and living cell constructs on young and senescent human dermal fibroblasts. *Wound Repair Regen*, *21*(6), 842-851. **https://doi.org/10.1111/wrr.12110**

Proctor, C. J., & Lorimer, I. A. (2011). Modelling the role of the Hsp70/Hsp90 system in the maintenance of protein homeostasis. *PLoS One*, *6*(7), e22038. **https://doi.org/10.1371/journal.pone.0022038**

Proctor, C. J., Pienaar, I. S., Elson, J. L., & Kirkwood, T. B. (2012). Aggregation, impaired degradation and immunization targeting of amyloid-beta dimers in Alzheimer's disease: a stochastic modelling approach. *Mol Neurodegener*, *7*, 32. **https://doi.org/10.1186/1750-1326-7-32**

Proctor, C. J., Soti, C., Boys, R. J., Gillespie, C. S., Shanley, D. P., Wilkinson, D. J., & Kirkwood, T. B. (2005). Modelling the actions of chaperones and their role in ageing. *Mech Ageing Dev*, *126*(1), 119-131. **https://doi.org/10.1016/j.mad.2004.09.031**

Purcell, M., Kruger, A., Tainsky, M. A., & . (2014). Gene expression profiling of replicative and induced senescence. *Cell Cycle*, *13*(24), 3927-3937. **https://doi.org/10.4161/15384101.2014.973327**

R core team. (2023). *R: A language and environment for statistical computing*. In R Foundation for Statistical Computing. **http://www.R-project.org/**

Rai, T. S., Cole, J. J., Nelson, D. M., Dikovskaya, D., Faller, W. J., Vizioli, M. G.,…Adams, P. D. (2014). HIRA orchestrates a dynamic chromatin landscape in senescence and is required for suppression of neoplasia. *Genes Dev*, *28*(24), 2712-2725. **https://doi.org/10.1101/gad.247528.114**

Rangarajan, A., Talora, C., Okuyama, R., Nicolas, M., Mammucari, C., Oh, H.,…Dotto, G. P. (2001). Notch signaling is a direct determinant of keratinocyte growth arrest and entry into differentiation. *EMBO J*, *20*(13), 3427-3436. **https://doi.org/10.1093/emboj/20.13.3427**

Rao, S. G., & Jackson, J. G. (2016). SASP: Tumor Suppressor or Promoter? Yes! *Trends Cancer*, *2*(11), 676-687. **https://doi.org/10.1016/j.trecan.2016.10.001**

Rayess, H., Wang, M. B., & Srivatsan, E. S. (2012). Cellular senescence and tumor suppressor gene p16. *Int J Cancer*, *130*(8), 1715-1725. **https://doi.org/10.1002/ijc.27316**

Reilly, D., & Lozano, J. (2021). Skin collagen through the lifestages: importance for skin health and beauty. *Plast Aesthet Res*, *8*(2). **https://doi.org/http://dx.doi.org/10.20517/2347-9264.2020.153**

Reinhardt, H. C., & Schumacher, B. (2012). The p53 network: cellular and systemic DNA damage responses in aging and cancer. *Trends Genet*, *28*(3), 128-136. **https://doi.org/10.1016/j.tig.2011.12.002**

Rena, G., Hardie, D. G., & Pearson, E. R. (2017). The mechanisms of action of metformin. *Diabetologia*, *60*(9), 1577-1585. **https://doi.org/10.1007/s00125-017-4342-z**

Rennie, K. J., Witham, M., Bradley, P., Clegg, A., Connolly, S., Hancock, H. C.,…Sayer, A. A. P. (2022). MET-PREVENT: metformin to improve physical performance in older people with sarcopenia and physical prefrailty/frailty - protocol for a double-blind, randomised controlled proof-of-concept trial. *BMJ Open*, *12*(7), e061823. **https://doi.org/10.1136/bmjopen-2022-061823**

Rey-Millet, M., Pousse, M., Soithong, C., Ye, J., Mendez-Bermudez, A., & Gilson, E. (2023). Senescence-associated transcriptional derepression in subtelomeres is determined in a chromosome-end-specific manner. *Aging Cell*, *22*(5), e13804. **https://doi.org/10.1111/acel.13804**

Ricard-Blum, S. (2011). The collagen family. *Cold Spring Harb Perspect Biol*, *3*(1), a004978. **https://doi.org/10.1101/cshperspect.a004978**

Rich, J. N., Zhang, M., Datto, M. B., Bigner, D. D., & Wang, X. F. (1999). Transforming growth factor-beta-mediated p15(INK4B) induction and growth inhibition in astrocytes is SMAD3-dependent and a pathway prominently altered in human glioma cell lines. *J Biol Chem*, *274*(49), 35053-35058. **https://doi.org/10.1074/jbc.274.49.35053**

Ritchie, M. E., Phipson, B., Wu, D., Hu, Y., Law, C. W., Shi, W., & Smyth, G. K. (2015). limma powers differential expression analyses for RNA-sequencing and microarray studies. *Nucleic Acids Res*, *43*(7), e47. **https://doi.org/10.1093/nar/gkv007**

Robles, S. J., & Adami, G. R. (1998). Agents that cause DNA double strand breaks lead to p16INK4a enrichment and the premature senescence of normal fibroblasts. *Oncogene*, *16*(9), 1113-1123. **https://doi.org/10.1038/sj.onc.1201862**

Rossi, M., Anerillas, C., Idda, M. L., Munk, R., Shin, C. H., Donega, S.,…Gorospe, M. (2023). Pleiotropic effects of BAFF on the senescence-associated secretome and growth arrest. *Elife*, *12*. **https://doi.org/10.7554/eLife.84238**

Rossiello, F., Jurk, D., Passos, J. F., & d'Adda di Fagagna, F. (2022). Telomere dysfunction in ageing and age-related diseases. *Nat Cell Biol*, *24*(2), 135-147. **https://doi.org/10.1038/s41556-022-00842-x**

Rovillain, E., Mansfield, L., Caetano, C., Alvarez-Fernandez, M., Caballero, O. L., Medema, R. H.,…Jat, P. S. (2011). Activation of nuclear factor-kappa B signalling promotes cellular senescence. *Oncogene*, *30*(20), 2356-2366. **https://doi.org/10.1038/onc.2010.611**

Rufini, A., Tucci, P., Celardo, I., & Melino, G. (2013). Senescence and aging: the critical roles of p53. *Oncogene*, *32*(43), 5129-5143. **https://doi.org/10.1038/onc.2012.640**

Sabath, N., Levy-Adam, F., Younis, A., Rozales, K., Meller, A., Hadar, S.,…Shalgi, R. (2020). Cellular proteostasis decline in human senescence. *Proc Natl Acad Sci U S A*, *117*(50), 31902-31913. **https://doi.org/10.1073/pnas.2018138117**

Saez-Atienzar, S., & Masliah, E. (2020). Cellular senescence and Alzheimer disease: the egg and the chicken scenario. *Nat Rev Neurosci*, *21*(8), 433-444. **https://doi.org/10.1038/s41583-020-0325-z**

Saint-Germain, E., Mignacca, L., Vernier, M., Bobbala, D., Ilangumaran, S., & Ferbeyre, G. (2017). SOCS1 regulates senescence and ferroptosis by modulating the expression of p53 target genes. *Aging (Albany NY)*, *9*(10), 2137-2162. **https://doi.org/10.18632/aging.101306**

Salminen, A., Kauppinen, A., & Kaarniranta, K. (2012). Emerging role of NF-κB signaling in the induction of senescence-associated secretory phenotype (SASP). *Cell Signal*, *24*(4), 835-845. **https://doi.org/10.1016/j.cellsig.2011.12.006**

Santoro, A., Bientinesi, E., & Monti, D. (2021). Immunosenescence and inflammaging in the aging process: age-related diseases or longevity? *Ageing Res Rev*, *71*, 101422. **https://doi.org/10.1016/j.arr.2021.101422**

Saul, D., Kosinsky, R. L., Atkinson, E. J., Doolittle, M. L., Zhang, X., LeBrasseur, N. K.,…Khosla, S. (2022). A new gene set identifies senescent cells and predicts senescence-associated pathways across tissues. *Nat Commun*, *13*(1), 4827. **https://doi.org/10.1038/s41467-022-32552-1**

Schade, A. E., Fischer, M., DeCaprio, J. A., & . (2019). RB, p130 and p107 differentially repress G1/S and G2/M genes after p53 activation. *Nucleic Acids Res*, *47*(21), 11197-11208. **https://doi.org/10.1093/nar/gkz961**

Schade, A. E., Schieven, G. L., Townsend, R., Jankowska, A. M., Susulic, V., Zhang, R.,…Maciejewski, J. P. (2008). Dasatinib, a small-molecule protein tyrosine kinase inhibitor, inhibits T-cell activation and proliferation. *Blood*, *111*(3), 1366-1377. **https://doi.org/10.1182/blood-2007-04-084814**

Schmitt, C. A., Wang, B., & Demaria, M. (2022). Senescence and cancer - role and therapeutic opportunities. *Nat Rev Clin Oncol*, *19*(10), 619-636. **https://doi.org/10.1038/s41571-022-00668-4**

Schmitz, C. R. R., Maurmann, R. M., Guma, F. T. C. R., Bauer, M. E., & Barbé-Tuana, F. M. (2023). cGAS-STING pathway as a potential trigger of immunosenescence and inflammaging. *Front Immunol*, *14*, 1132653. **https://doi.org/10.3389/fimmu.2023.1132653**

Schurch, N. J., Schofield, P., Gierliński, M., Cole, C., Sherstnev, A., Singh, V.,…Barton, G. J. (2016). How many biological replicates are needed in an RNA-seq experiment and which differential expression tool should you use? *RNA*, *22*(6), 839-851. **https://doi.org/10.1261/rna.053959.115**

Sebastiani, P., & Perls, T. T. (2012). The genetics of extreme longevity: lessons from the new England centenarian study. *Front Genet*, *3*, 277. **https://doi.org/10.3389/fgene.2012.00277**

Secomandi, L., Borghesan, M., Velarde, M., & Demaria, M. (2022). The role of cellular senescence in female reproductive aging and the potential for senotherapeutic interventions. *Hum Reprod Update*, *28*(2), 172-189. **https://doi.org/10.1093/humupd/dmab038**

Sedelnikova, O. A., Horikawa, I., Zimonjic, D. B., Popescu, N. C., Bonner, W. M., & Barrett, J. C. (2004). Senescing human cells and ageing mice accumulate DNA lesions with unrepairable double-strand breaks. *Nat Cell Biol*, *6*(2), 168-170. **https://doi.org/10.1038/ncb1095**

Sen, P., Lan, Y., Li, C. Y., Sidoli, S., Donahue, G., Dou, Z.,…Berger, S. L. (2019). Histone Acetyltransferase p300 Induces De Novo Super-Enhancers to Drive Cellular Senescence. *Mol Cell*, *73*(4), 684-698.e688. **https://doi.org/10.1016/j.molcel.2019.01.021**

Seoane, M., Costoya, J. A., & Arce, V. M. (2017). Uncoupling Oncogene-Induced Senescence (OIS) and DNA Damage Response (DDR) triggered by DNA hyper-replication: lessons from primary mouse embryo astrocytes (MEA). *Sci Rep*, *7*(1), 12991. **https://doi.org/10.1038/s41598-017-13408-x**

Serrano, M., Lin, A. W., McCurrach, M. E., Beach, D., & Lowe, S. W. (1997). Oncogenic ras provokes premature cell senescence associated with accumulation of p53 and p16INK4a. *Cell*, *88*(5), 593-602. **https://doi.org/10.1016/s0092-8674(00)81902-9**

Shah, P. P., Donahue, G., Otte, G. L., Capell, B. C., Nelson, D. M., Cao, K.,…Berger, S. L. (2013). Lamin B1 depletion in senescent cells triggers large-scale changes in gene expression and the chromatin landscape. *Genes Dev*, *27*(16), 1787-1799. **https://doi.org/10.1101/gad.223834.113**

Shamma, A., Takegami, Y., Miki, T., Kitajima, S., Noda, M., Obara, T.,…Takahashi, C. (2009). Rb Regulates DNA damage response and cellular senescence through E2F-dependent suppression of N-ras isoprenylation. *Cancer Cell*, *15*(4), 255-269. **https://doi.org/10.1016/j.ccr.2009.03.001**

Sharma, A. K., Roberts, R. L., Benson, R. D., Pierce, J. L., Yu, K., Hamrick, M. W., & McGee-Lawrence, M. E. (2020). The Senolytic Drug Navitoclax (ABT-263) Causes Trabecular Bone Loss and Impaired Osteoprogenitor Function in Aged Mice. *Front Cell Dev Biol*, *8*, 354. **https://doi.org/10.3389/fcell.2020.00354**

Shaw, R. J., & Cantley, L. C. (2006). Ras, PI(3)K and mTOR signalling controls tumour cell growth. *Nature*, *441*(7092), 424-430. **https://doi.org/10.1038/nature04869**

Shiloh, Y. (2003). ATM and related protein kinases: safeguarding genome integrity. *Nat Rev Cancer*, *3*(3), 155-168. **https://doi.org/10.1038/nrc1011**

Shiloh, Y., & Ziv, Y. (2013). The ATM protein kinase: regulating the cellular response to genotoxic stress, and more. *Nat Rev Mol Cell Biol*, *14*(4), 197-210.

Sierra-Ramirez, A., López-Aceituno, J. L., Costa-Machado, L. F., Plaza, A., Barradas, M., & Fernandez-Marcos, P. J. (2020). Transient metabolic improvement in obese mice treated with navitoclax or dasatinib/quercetin. *Aging (Albany NY)*, *12*(12), 11337-11348. **https://doi.org/10.18632/aging.103607**

Skea, D., Fotis, C., Tsolakos, N., Pliaka, V., Verrou, K.-M., & Alexopoulos, L. (2023). Conserved transcriptomic signatures and protein markers in cellular

senescence models. *Research Square*. **https://doi.org/https://doi.org/10.21203/rs.3.rs-3110821/v1**

Slater, L. (2014). PubMed PubReMiner. *Journal of the Canadian Health Libraries Association / Journal de l'Association des bibliothèques de la santé du Canada*, *33*(2), 106-107.

Smith, G. R., & Shanley, D. P. (2010). Modelling the response of FOXO transcription factors to multiple post-translational modifications made by ageing-related signalling pathways. *PLoS One*, *5*(6), e11092. **https://doi.org/10.1371/journal.pone.0011092**

Song, M. S., Salmena, L., & Pandolfi, P. P. (2012). The functions and regulation of the PTEN tumour suppressor. *Nat Rev Mol Cell Biol*, *13*(5), 283-296. **https://doi.org/10.1038/nrm3330**

Sozou, P. D., & Kirkwood, T. B. (2001). A stochastic model of cell replicative senescence based on telomere shortening, oxidative stress, and somatic mutations in nuclear and mitochondrial DNA. *J Theor Biol*, *213*(4), 573-586. **https://doi.org/10.1006/jtbi.2001.2432**

Stacklies, W., Redestig, H., Scholz, M., Walther, D., & Selbig, J. (2007). pcaMethods--a bioconductor package providing PCA methods for incomplete data. *Bioinformatics*, *23*(9), 1164-1167. **https://doi.org/10.1093/bioinformatics/btm069**

Stein, G. H., Drullinger, L. F., Soulard, A., & Dulić, V. (1999). Differential roles for cyclin-dependent kinase inhibitors p21 and p16 in the mechanisms of senescence and differentiation in human fibroblasts. *Mol Cell Biol*, *19*(3), 2109-2117. **https://doi.org/10.1128/MCB.19.3.2109**

Sternlicht, M. D., & Werb, Z. (2001). How matrix metalloproteinases regulate cell behavior. *Annu Rev Cell Dev Biol*, *17*, 463-516. **https://doi.org/10.1146/annurev.cellbio.17.1.463**

Storer, M., Mas, A., Robert-Moreno, A., Pecoraro, M., Ortells, M. C., Di Giacomo, V.,…Keyes, W. M. (2013). Senescence is a developmental mechanism that contributes to embryonic growth and patterning. *Cell*, *155*(5), 1119-1130. **https://doi.org/10.1016/j.cell.2013.10.041**

Stracker, T. H., Usui, T., & Petrini, J. H. (2009). Taking the time to make important decisions: the checkpoint effector kinases Chk1 and Chk2 and the DNA damage response. *DNA Repair (Amst)*, *8*(9), 1047-1054. **https://doi.org/10.1016/j.dnarep.2009.04.012**

Su, W., Hu, Y., Fan, X., & Xie, J. (2023). Clearance of senescent cells by navitoclax (ABT263) rejuvenates UHMWPE-induced osteolysis. *Int Immunopharmacol*, *115*, 109694. **https://doi.org/10.1016/j.intimp.2023.109694**

Suda, M., Tchkonia, T., Kirkland, J. L., & Minamino, T. (2025). Targeting senescent cells for the treatment of age-associated diseases. *J Biochem*, *177*(3), 177-187. **https://doi.org/10.1093/jb/mvae091**

Sun, C., Shi, H., Zhao, X., Chang, Y. L., Wang, X., Zhu, S., & Sun, S. (2023). The Activation of cGAS-STING in Acute Kidney Injury. *J Inflamm Res*, *16*, 4461-4470. **https://doi.org/10.2147/JIR.S423232**

Sun, P., Yoshizuka, N., New, L., Moser, B. A., Li, Y., Liao, R.,…Han, J. (2007). PRAK is essential for ras-induced senescence and tumor suppression. *Cell*, *128*(2), 295-308. **https://doi.org/10.1016/j.cell.2006.11.050**

Sun, T., Yang, W., Liu, J., & Shen, P. (2011). Modeling the basal dynamics of p53 system. *PLoS One*, *6*(11), e27882. **https://doi.org/10.1371/journal.pone.0027882**

Takaya, K., & Kishi, K. (2024). Combined dasatinib and quercetin treatment contributes to skin rejuvenation through selective elimination of senescent cells in vitro and in vivo. *Biogerontology*, *25*(4), 691-704. **https://doi.org/10.1007/s10522-024-10103-z**

Takebayashi, S., Tanaka, H., Hino, S., Nakatsu, Y., Igata, T., Sakamoto, A.,…Nakao, M. (2015). Retinoblastoma protein promotes oxidative phosphorylation through upregulation of glycolytic genes in oncogene-induced senescent cells. *Aging Cell*, *14*(4), 689-697. **https://doi.org/10.1111/acel.12351**

Tan, J. Z., Yan, Y., Wang, X. X., Jiang, Y., & Xu, H. E. (2014). EZH2: biology, disease, and structure-based drug discovery. *Acta Pharmacol Sin*, *35*(2), 161-174. **https://doi.org/10.1038/aps.2013.161**

Tanaka, T., Biancotto, A., Moaddel, R., Moore, A. Z., Gonzalez-Freire, M., Aon, M. A.,…consortium, C. (2018). Plasma proteomic signature of age in healthy humans. *Aging Cell*, *17*(5), e12799. **https://doi.org/10.1111/acel.12799**

Tasdemir, N., Banito, A., Roe, J. S., Alonso-Curbelo, D., Camiolo, M., Tschaharganeh, D. F.,…Lowe, S. W. (2016). BRD4 Connects Enhancer Remodeling to Senescence Immune Surveillance. *Cancer Discov*, *6*(6), 612-629. **https://doi.org/10.1158/2159-8290.CD-16-0217**

Tavenier, J., Nehlin, J. O., Houlind, M. B., Rasmussen, L. J., Tchkonia, T., Kirkland, J. L.,…Rasmussen, L. J. H. (2024). Fisetin as a senotherapeutic agent: Evidence and perspectives for age-related diseases. *Mech Ageing Dev*, *222*, 111995. **https://doi.org/10.1016/j.mad.2024.111995**

Tenenbaum, D., & Maintainer, B. (2024). *KEGGREST: Client-side REST access to the Kyoto Encyclopedia of Genes and Genomes (KEGG).* In.

Teo, Y. V., Rattanavirotkul, N., Olova, N., Salzano, A., Quintanilla, A., Tarrats, N.,…Chandra, T. (2019). Notch Signaling Mediates Secondary Senescence. *Cell Rep*, *27*(4), 997-1007.e1005. **https://doi.org/10.1016/j.celrep.2019.03.104**

Tominaga, K., & Suzuki, H. I. (2019). TGF-β Signaling in Cellular Senescence and Aging-Related Pathology. *Int J Mol Sci*, *20*(20). **https://doi.org/10.3390/ijms20205002**

Tordella, L., Khan, S., Hohmeyer, A., Banito, A., Klotz, S., Raguz, S.,…Gil, J. (2016). SWI/SNF regulates a transcriptional program that induces senescence to prevent liver cancer. *Genes Dev*, *30*(19), 2187-2198. **https://doi.org/10.1101/gad.286112.116**

Turinetto, V., & Giachino, C. (2015). Multiple facets of histone variant H2AX: a DNA double-strand-break marker with several biological functions. *Nucleic Acids Res*, *43*(5), 2489-2498. **https://doi.org/10.1093/nar/gkv061**

van Deursen, J. M. (2014). The role of senescent cells in ageing. *Nature*, *509*(7501), 439-446. **https://doi.org/10.1038/nature13193**

van Jaarsveld, M. T. M., Deng, D., Ordoñez-Rueda, D., Paulsen, M., Wiemer, E. A. C., & Zi, Z. (2020). Cell-type-specific role of CHK2 in mediating DNA damage-induced G2 cell cycle arrest. *Oncogenesis*, *9*(3), 35. **https://doi.org/10.1038/s41389-020-0219-y**

Varani, J., Dame, M. K., Rittie, L., Fligiel, S. E., Kang, S., Fisher, G. J., & Voorhees, J. J. (2006). Decreased collagen production in chronologically aged skin: roles of age-dependent alteration in fibroblast function and defective mechanical stimulation. *Am J Pathol*, *168*(6), 1861-1868. **https://doi.org/10.2353/ajpath.2006.051302**

Vassilieva, I., Kosheverova, V., Vitte, M., Kamentseva, R., Shatrova, A., Tsupkina, N.,…Burova, E. (2020). Paracrine senescence of human endometrial

mesenchymal stem cells: a role for the insulin-like growth factor binding protein 3. *Aging (Albany NY)*, *12*(2), 1987-2004. **https://doi.org/10.18632/aging.102737**

Velarde, M. C., & Menon, R. (2016). Positive and negative effects of cellular senescence during female reproductive aging and pregnancy. *J Endocrinol*, *230*(2), R59-76. **https://doi.org/10.1530/JOE-16-0018**

Venkatesh, D., Fredette, N., Rostama, B., Tang, Y., Vary, C. P., Liaw, L., & Urs, S. (2011). RhoA-mediated signaling in Notch-induced senescence-like growth arrest and endothelial barrier dysfunction. *Arterioscler Thromb Vasc Biol*, *31*(4), 876-882. **https://doi.org/10.1161/ATVBAHA.110.221945**

Victorelli, S., Lagnado, A., Halim, J., Moore, W., Talbot, D., Barrett, K.,…Passos, J. F. (2019). Senescent human melanocytes drive skin ageing via paracrine telomere dysfunction. *EMBO J*, *38*(23), e101982. **https://doi.org/10.15252/embj.2019101982**

Victorelli, S., Salmonowicz, H., Chapman, J., Martini, H., Vizioli, M. G., Riley, J. S.,…Passos, J. F. (2023). Apoptotic stress causes mtDNA release during senescence and drives the SASP. *Nature*, *622*(7983), 627-636. **https://doi.org/10.1038/s41586-023-06621-4**

Vincenti, M. P., Coon, C. I., & Brinckerhoff, C. E. (1998). Nuclear factor kappaB/p50 activates an element in the distal matrix metalloproteinase 1 promoter in interleukin-1beta-stimulated synovial fibroblasts. *Arthritis Rheum*, *41*(11), 1987-1994. **https://doi.org/10.1002/1529-0131(199811)41:11**<1987::AID-ART14>3.0.CO;2-8

Vizioli, M. G., Liu, T., Miller, K. N., Robertson, N. A., Gilroy, K., Lagnado, A. B.,…Adams, P. D. (2020). Mitochondria-to-nucleus retrograde signaling drives formation of cytoplasmic chromatin and inflammation in senescence. *Genes Dev*, *34*(5-6), 428-445. **https://doi.org/10.1101/gad.331272.119**

Volksdorf, T., Heilmann, J., Eming, S. A., Schawjinski, K., Zorn-Kruppa, M., Ueck, C.,…Brandner, J. M. (2017). Tight Junction Proteins Claudin-1 and Occludin Are Important for Cutaneous Wound Healing. *Am J Pathol*, *187*(6), 1301-1312. **https://doi.org/10.1016/j.ajpath.2017.02.006**

Waga, S., Hannon, G. J., Beach, D., & Stillman, B. (1994). The p21 inhibitor of cyclin-dependent kinases controls DNA replication by interaction with PCNA. *Nature*, *369*(6481), 574-578. **https://doi.org/10.1038/369574a0**

Wakita, M., Takahashi, A., Sano, O., Loo, T. M., Imai, Y., Narukawa, M.,…Hara, E. (2020). A BET family protein degrader provokes senolysis by targeting NHEJ and autophagy in senescent cells. *Nat Commun*, *11*(1), 1935. **https://doi.org/10.1038/s41467-020-15719-6**

Walker, A. E., Morgan, R. G., Ives, S. J., Cawthon, R. M., Andtbacka, R. H., Noyes, D.,…Donato, A. J. (2016). Age-related arterial telomere uncapping and senescence is greater in women compared with men. *Exp Gerontol*, *73*, 65-71. **https://doi.org/10.1016/j.exger.2015.11.009**

Wang, H., Guo, M., Wei, H., & Chen, Y. (2023). Targeting p53 pathways: mechanisms, structures, and advances in therapy. *Signal Transduct Target Ther*, *8*(1), 92. **https://doi.org/10.1038/s41392-023-01347-1**

Wang, T., Notta, F., Navab, R., Joseph, J., Ibrahimov, E., Xu, J.,…Tsao, M. S. (2017). Senescent Carcinoma-Associated Fibroblasts Upregulate IL8 to Enhance Prometastatic Phenotypes. *Mol Cancer Res*, *15*(1), 3-14. **https://doi.org/10.1158/1541-7786.MCR-16-0192**

Wang, T. W., Johmura, Y., Suzuki, N., Omori, S., Migita, T., Yamaguchi, K.,…Nakanishi, M. (2022). Blocking PD-L1-PD-1 improves senescence

surveillance and ageing phenotypes. *Nature*, *611*(7935), 358-364. **https://doi.org/10.1038/s41586-022-05388-4**

Wang, Y., Eapen, V., Kournoutis, A., Onorati, A., Li, X., Zhou, X.,…Dou, Z. (2022). Nuclear autophagy interactome unveils WSTF as a constitutive nuclear inhibitor of inflammation. *bioRxiv*. **https://doi.org/doi**: **https://doi.org/10.1101/2022.10.04.510822**

Warnes, G. R., Bolker, B., Bonebakker, L., Gentleman, R., Huber, W., Liaw, A.,…Venables, B. (2022). gplots: Various R Programming Tools for Plotting Data. In (R package version 3.1.3 ed.).

Watson, J. D. (1972). Origin of concatemeric T7 DNA. *Nat New Biol*, *239*(94), 197-201. **https://doi.org/10.1038/newbio239197a0**

Wechter, N., Rossi, M., Anerillas, C., Tsitsipatis, D., Piao, Y., Fan, J.,…Gorospe, M. (2023). Single-cell transcriptomic analysis uncovers diverse and dynamic senescent cell populations. *Aging (Albany NY)*, *15*(8), 2824-2851. **https://doi.org/10.18632/aging.204666**

Wei, Z., Chen, X. C., Song, Y., Pan, X. D., Dai, X. M., Zhang, J.,…Zhu, Y. G. (2016). Amyloid β Protein Aggravates Neuronal Senescence and Cognitive Deficits in 5XFAD Mouse Model of Alzheimer's Disease. *Chin Med J (Engl)*, *129*(15), 1835-1844. **https://doi.org/10.4103/0366-6999.186646**

Weichhart, T. (2018). mTOR as Regulator of Lifespan, Aging, and Cellular Senescence: A Mini-Review. *Gerontology*, *64*(2), 127-134. **https://doi.org/10.1159/000484629**

Weirich, S., Kusevic, D., Schnee, P., Reiter, J., Pleiss, J., & Jeltsch, A. (2024). Discovery of NSD2 non-histone substrates and design of a super-substrate. *Commun Biol*, *7*(1), 707. **https://doi.org/10.1038/s42003-024-06395-z**

Wickham, H. (2016). ggplot2: Elegant Graphics for Data Analysis. In.

Wickham, H., François, R., Henry, L., & Müller, K. (2023). dplyr: a Grammar of Data Manipulation.

Wiley, C. D., Velarde, M. C., Lecot, P., Liu, S., Sarnoski, E. A., Freund, A.,…Campisi, J. (2016). Mitochondrial Dysfunction Induces Senescence with a Distinct Secretory Phenotype. *Cell Metab*, *23*(2), 303-314. **https://doi.org/10.1016/j.cmet.2015.11.011**

Witkiewicz, A. K., Knudsen, K. E., Dicker, A. P., & Knudsen, E. S. (2011). The meaning of p16(ink4a) expression in tumors: functional significance, clinical associations and future developments. *Cell Cycle*, *10*(15), 2497-2503. **https://doi.org/10.4161/cc.10.15.16776**

Wong, E. S., Le Guezennec, X., Demidov, O. N., Marshall, N. T., Wang, S. T., Krishnamurthy, J.,…Bulavin, D. V. (2009). p38MAPK controls expression of multiple cell cycle inhibitors and islet proliferation with advancing age. *Dev Cell*, *17*(1), 142-149. **https://doi.org/10.1016/j.devcel.2009.05.009**

Wu, T., Hu, E., Xu, S., Chen, M., Guo, P., Dai, Z.,…Yu, G. (2021). clusterProfiler 4.0: A universal enrichment tool for interpreting omics data. *Innovation (Camb)*, *2*(3), 100141. **https://doi.org/10.1016/j.xinn.2021.100141**

Wyld, L., Bellantuono, I., Tchkonia, T., Morgan, J., Turner, O., Foss, F.,…Kirkland, J. L. (2020). Senescence and Cancer: A Review of Clinical Implications of Senescence and Senotherapies. *Cancers (Basel)*, *12*(8). **https://doi.org/10.3390/cancers12082134**

Xiao, Y., Hsiao, T. H., Suresh, U., Chen, H. I., Wu, X., Wolf, S. E., & Chen, Y. (2014). A novel significance score for gene selection and ranking. *Bioinformatics*, *30*(6), 801-807. **https://doi.org/10.1093/bioinformatics/btr671**

Xiong, Y., Hannon, G. J., Zhang, H., Casso, D., Kobayashi, R., & Beach, D. (1993). p21 is a universal inhibitor of cyclin kinases. *Nature*, *366*(6456), 701-704. **https://doi.org/10.1038/366701a0**

Xu, M., Pirtskhalava, T., Farr, J. N., Weigand, B. M., Palmer, A. K., Weivoda, M. M.,…Kirkland, J. L. (2018). Senolytics improve physical function and increase lifespan in old age. *Nat Med*, *24*(8), 1246-1256. **https://doi.org/10.1038/s41591-018-0092-9**

Xu, S., Cai, Y., & Wei, Y. (2014). mTOR Signaling from Cellular Senescence to Organismal Aging. *Aging Dis*, *5*(4), 263-273. **https://doi.org/10.14336/AD.2014.0500263**

Yang, E. J., Park, J. H., Cho, H. J., Hwang, J. A., Woo, S. H., Park, C. H.,…Lee, Y. S. (2022). Co-inhibition of ATM and ROCK synergistically improves cell proliferation in replicative senescence by activating FOXM1 and E2F1. *Commun Biol*, *5*(1), 702. **https://doi.org/10.1038/s42003-022-03658-5**

Yang, H., Wang, H., Ren, J., Chen, Q., & Chen, Z. J. (2017). cGAS is essential for cellular senescence. *Proc Natl Acad Sci U S A*, *114*(23), E4612-E4620. **https://doi.org/10.1073/pnas.1705499114**

Yang, J., Wang, J., Liang, X., Zhao, H., Lu, J., Ma, Q.,…Tian, F. (2019). IL-1β increases the expression of inflammatory factors in synovial fluid-derived fibroblast-like synoviocytes via activation of the NF-κB-mediated ERK-STAT1 signaling pathway. *Mol Med Rep*, *20*(6), 4993-5001. **https://doi.org/10.3892/mmr.2019.10759**

Yosef, R., Pilpel, N., Papismadov, N., Gal, H., Ovadya, Y., Vadai, E.,…Krizhanovsky, V. (2017). p21 maintains senescent cell viability under persistent DNA damage response by restraining JNK and caspase signaling. *EMBO J*, *36*(15), 2280-2295. **https://doi.org/10.15252/embj.201695553**

Yoshida, Y., Hayashi, Y., Suda, M., Tateno, K., Okada, S., Moriya, J.,…Minamino, T. (2014). Notch signaling regulates the lifespan of vascular endothelial cells via a p16-dependent pathway. *PLoS One*, *9*(6), e100359. **https://doi.org/10.1371/journal.pone.0100359**

Yoshimoto, S., Loo, T. M., Atarashi, K., Kanda, H., Sato, S., Oyadomari, S.,…Ohtani, N. (2013). Obesity-induced gut microbial metabolite promotes liver cancer through senescence secretome. *Nature*, *499*(7456), 97-101. **https://doi.org/10.1038/nature12347**

Young, A. R., Narita, M., Ferreira, M., Kirschner, K., Sadaie, M., Darot, J. F.,…Watt, F. M. (2009). Autophagy mediates the mitotic senescence transition. *Genes Dev*, *23*(7), 798-803. **https://doi.org/10.1101/gad.519709**

Yousefzadeh, M. J., Zhu, Y., McGowan, S. J., Angelini, L., Fuhrmann-Stroissnigg, H., Xu, M.,…Niedernhofer, L. J. (2018). Fisetin is a senotherapeutic that extends health and lifespan. *EBioMedicine*, *36*, 18-28. **https://doi.org/10.1016/j.ebiom.2018.09.015**

Yue, H., Brown, M., Knowles, J., Wang, H., Broomhead, D. S., & Kell, D. B. (2006). Insights into the behaviour of systems biology models from dynamic sensitivity and identifiability analysis: a case study of an NF-kappaB signalling pathway. *Mol Biosyst*, *2*(12), 640-649. **https://doi.org/10.1039/b609442b**

Yugawa, T., Handa, K., Narisawa-Saito, M., Ohno, S., Fujita, M., & Kiyono, T. (2007). Regulation of Notch1 gene expression by p53 in epithelial cells. *Mol Cell Biol*, *27*(10), 3732-3742. **https://doi.org/10.1128/MCB.02119-06**

Yun, J. M., Chien, A., Jialal, I., & Devaraj, S. (2012). Resveratrol up-regulates SIRT1 and inhibits cellular oxidative stress in the diabetic milieu: mechanistic

insights. *J Nutr Biochem*, *23*(7), 699-705. **https://doi.org/10.1016/j.jnutbio.2011.03.012**

Zenonos, K., & Kyprianou, K. (2013). RAS signaling pathways, mutations and their role in colorectal cancer. *World J Gastrointest Oncol*, *5*(5), 97-101. **https://doi.org/10.4251/wjgo.v5.i5.97**

Zhang, L., Pitcher, L. E., Prahalad, V., Niedernhofer, L. J., & Robbins, P. D. (2023). Targeting cellular senescence with senotherapeutics: senolytics and senomorphics. *FEBS J*, *290*(5), 1362-1383. **https://doi.org/10.1111/febs.16350**

Zhang, L. X., Li, C. X., Kakar, M. U., Khan, M. S., Wu, P. F., Amir, R. M.,…Li, J. H. (2021). Resveratrol (RV): A pharmacological review and call for further research. *Biomed Pharmacother*, *143*, 112164. **https://doi.org/10.1016/j.biopha.2021.112164**

Zhang, P., Kishimoto, Y., Grammatikakis, I., Gottimukkala, K., Cutler, R. G., Zhang, S.,…Mattson, M. P. (2019). Senolytic therapy alleviates Aβ-associated oligodendrocyte progenitor cell senescence and cognitive deficits in an Alzheimer's disease model. *Nat Neurosci*, *22*(5), 719-728. **https://doi.org/10.1038/s41593-019-0372-9**

Zhang, W., Ge, Y., Cheng, Q., Zhang, Q., Fang, L., & Zheng, J. (2018). Decorin is a pivotal effector in the extracellular matrix and tumour microenvironment. *Oncotarget*, *9*(4), 5480-5491. **https://doi.org/10.18632/oncotarget.23869**

Zhang, X., Liu, X., Du, Z., Wei, L., Fang, H., Dong, Q.,…Wang, X. (2021). The loss of heterochromatin is associated with multiscale three-dimensional genome reorganization and aberrant transcription during cellular senescence. *Genome Res*, *31*(7), 1121-1135. **https://doi.org/10.1101/gr.275235.121**

Zhao, J., Zheng, L., Dai, G., Sun, Y., He, R., Liu, Z.,…Duan, C. (2025). Senolytics cocktail dasatinib and quercetin alleviate chondrocyte senescence and facet joint osteoarthritis in mice. *Spine J*, *25*(1), 184-198. **https://doi.org/10.1016/j.spinee.2024.09.017**

Zhou, B., Yang, Y., Pang, X., Shi, J., Jiang, T., & Zheng, X. (2023). Quercetin inhibits DNA damage responses to induce apoptosis via SIRT5/PI3K/AKT pathway in non-small cell lung cancer. *Biomed Pharmacother*, *165*, 115071. **https://doi.org/10.1016/j.biopha.2023.115071**

Zhu, H., Chan, K. T., Huang, X., Cerra, C., Blake, S., Trigos, A. S.,…Kang, J. (2022). Cystathionine-β-synthase is essential for AKT-induced senescence and suppresses the development of gastric cancers with PI3K/AKT activation. *Elife*, *11*. **https://doi.org/10.7554/eLife.71929**

Zhu, Y., Doornebal, E. J., Pirtskhalava, T., Giorgadze, N., Wentworth, M., Fuhrmann-Stroissnigg, H.,…Kirkland, J. L. (2017). New agents that target senescent cells: the flavone, fisetin, and the BCL-X. *Aging (Albany NY)*, *9*(3), 955-963. **https://doi.org/10.18632/aging.101202**

Zhu, Y., Tchkonia, T., Fuhrmann-Stroissnigg, H., Dai, H. M., Ling, Y. Y., Stout, M. B.,…Kirkland, J. L. (2016). Identification of a novel senolytic agent, navitoclax, targeting the Bcl-2 family of anti-apoptotic factors. *Aging Cell*, *15*(3), 428-435. **https://doi.org/10.1111/acel.12445**

Zhu, Y., Tchkonia, T., Pirtskhalava, T., Gower, A. C., Ding, H., Giorgadze, N.,…Kirkland, J. L. (2015). The Achilles' heel of senescent cells: from transcriptome to senolytic drugs. *Aging Cell*, *14*(4), 644-658. **https://doi.org/10.1111/acel.12344**

Zirkel, A., Nikolic, M., Sofiadis, K., Mallm, J. P., Brackley, C. A., Gothe, H.,…Papantonis, A. (2018). HMGB2 Loss upon Senescence Entry Disrupts

Genomic Organization and Induces CTCF Clustering across Cell Types. *Mol Cell*, *70*(4), 730-744.e736. **https://doi.org/10.1016/j.molcel.2018.03.030**

Appendix.

Appendix Table A2.1 – Number of studies including:

Category	No. of studies	Category	No. of studies	Category	No. of studies
Senescence type					
OIS	54	DDIS	45	REP	24
BYS	3	OSKM	2	CR	2
RiboMature	1	NIS	1	RNIS	1
dNTP	1	MitoSkip	1	PIIPS	1
NBIS	1	Trehalose	1		
Control Condition					
Prolif	111	Quiesce	13	Apoptosis	1
Immortal	4				
Timepoint group					
0-4 days*	27	5-7 days*	40	8-11 days*	25
12-14 days*	8	15+ days*	6	0-40 days**	3
41+ days**	2				
Genes up					
None	118	ZFP36L1	1	DOT1L	1
GR	1	E1A	2	WSTF	1
SmallT	1	Unknown	1	E7	1
E6_E7	1	SV40smallT	1	TRF2	1
SmallT_E6_E7	1	TGFβ	1	Parkin_mtDNA	1
Parkin	3				
Genes down					
None	115	p21	3	IONpump	1
mTOR	2	pRb	4	miR34a	1
E2F7	1	pRb_E2F7	1	IL1R	1
p38	1	ETS1	1	laminA	1
JUN	1	RELA	4	HMGA1	1
p16	2	p107	1	p300	1
p130	2	H2AJ	3	BRD4	2
mitochondrial	2	cGAS	1	p53_pRb	1
G3BP1	1	CEBPb	1	HDAC	1
ABCD4	1	AKR1C1	1	DOT1L	1
ALOX5	1	ASB15	1	YBX1	1
BPIL1	1	BRD8	1	CBS	1
C20	1	CCL23	1	COX2	1
CTDSPL	1	DCAMKL3	1	BDNF	1
DUSP11	1	EMR4	1	ABCA1	1
ERCC3	1	GPRC5D	1	BAK_BAX	1
HSPC182	1	IFNA17	1	BAFF	1

IL15	1	IL17RE	1	DINO	1
ITCH	1	KCNA5	1	unknown	1
KCNQ4	1	LOC399818	1	Complex I	1
LOC51136	1	MAP3K6	1	E2F	1
MCFP	1	NRG1	1	p130_pRb	1
PEO1	1	PLCB1	1	CBP	1
PPP1CB	1	PROK2	1	p16_p21	1
PTBP1	3	PTPN14	1	ARID1B	1
RNF6	1	SHFM3	1	XPO7	1
SKP1A	1	TMEM219	1	MIR31HG	1
UBE2V21	1	p53	7	METTL14	1
EXOC7	1	LTR2	1	NF1	1
LTR10	1	caspase	1	NTRK2	1
COPB2	1				
Cell line					
IMR	59	WI38	19	CAF	3
BJ	16	MRC	8	HDF	5
LF1	1	HCA2	3	HFL1	2
FL2	1	Tig3	3	LFS_MDAH041	1
10-5_12-1	1	HDF161	1	Primary_fibroblast	1
HFF	5	HMF3A	1		
Organ					
Skin	34	Lung	90		

**DDIS, OIS, and BYS. **REP only. OIS, oncogene-induced senescence; DDIS, DNA damage-induced senescence; REP, replicative senescence; OSKM, senescence induced as a by-product of pluripotency induction via transcription factors Oct4, Sox2, Klf4 and c-Myc; RiboMature, senescence induced through ribosomal disruption; BYS, bystander induced senescence; dNTP, depletion of deoxyribonucleotide triphosphates; CR, chromatin remodelling induced senescence; NBIS, nuclear breakdown induced senescence; NIS, Notch induced senescence; RNIS, Ras and Notch induced senescence; MitoSkip, senescence induced by skipping mitosis; PIIPS, proteasome inhibition-induced premature senescence; Trehalose, Trehalose induced senescence; Prolif, proliferating cell; Quiesce, quiescent cell; Immortal, immortalised cell; CAF, cancer associated fibroblasts.*

Appendix Table A2.2 – Data informing computational model network.

Protein or process (***GENE***)	Interaction data		Temporal data		
	Interacting proteins	Summary of studies supporting the interactions	Summary of temporal data of the protein in senescence	Senescence type	Fibroblast cell line
NF-κB (p50/p65) (***NFKB1/ RELA***)	NF-κB and IL1α	In senescence, reduced IL1α activity reduced NF-κB transcriptional activity (Laberge et al., 2015).	In DDIS, NF-κB binding to DNA rises 24 hours post-senescence induction and continues to rise until the final timepoint at day 10. In OIS, there was increased binding of NF-κB to DNA (higher than in DDIS) at an unknown timepoint (Freund et al., 2011). In OIS, RelA bound to chromatin is increased in comparison to non-senescent cells on day 6 (Hoare et al., 2016).	DDIS (10 Gy) and OIS (4OHT-inducible RAS) OIS (4OHT-inducible RAS)	HCA2 IMR90
	NF-κB and p38	In OIS and DDIS, p38 activity induces SASP factors. These SASP factors were regulated by NF-κB, leading to the conclusion that p38 activity increases NF-κB transcriptional activity in a mechanism independent of DDR (Freund et al., 2011).			
IL6 (***IL6***)	IL6 and NF-κB	NF-κB is a transcription factor for IL6 (Liu et al., 2017).	Upregulated IL6 in OIS at unknown timepoint (Kuilman et al., 2008). Day 7 post-senescence induction in DDIS, IL6 expression began to increase and increased further at day 10 (Coppé et al., 2008). In DDIS, IL6 expression is upregulated at day 4, and upregulated further at days 10 and 20 (Hernandez-Segura et al., 2017).	OIS (BRAF retrovirus) DDIS (10 Gy) DDIS (10 Gray)	Tig3 WI38 HCA2
IL1α (**IL1A**)	IL1α and C/EBPβ	C/EBPβ binding sites identified in the IL1A locus. In OIS, there was increased C/EBPβ binding to the IL1A promoter and enhancer regions (Hoare et al., 2016).	IL1α mRNA the same on day 3 post-senescence induction in DDIS, however these increased at day 5 and 7 (Orjalo et al., 2009). On day 6 after OIS induction, mRNA levels of IL1α are approximately 35 times higher than in the control cells which do not have RAS induction (Hoare et al., 2016). I L1α is upregulated in DDIS at all time points (day 4, 10 and 20) (Hernandez-Segura et al., 2017).	DDIS (50mg/ml bleomycin) OIS (4OHT-inducible RAS) DDIS (10 Gy)	HCA2 IMR90 HCA2

C/EBPβ (***CEBPB***)	C/EBPβ and Notch	In OIS it was shown there was C/EBPβ expression, however when ectopic NICD was introduced, C/EBPβ expression was diminished (Hoare et al., 2016).	C/EBPβ is expressed at day 6 of OIS (Hoare et al., 2016).	OIS (4OHT-inducible RAS)	IMR90
RAS (***RAS***)	N/A	N/A	There was no RAS present in cells pre-OIS induction. On day 1 following induction, RAS levels increased and remained high throughout the 8 days assessed. Upon further inspection, RAS levels began to rise within 8 hours of senescence induction (Young et al., 2009). On days 2, 6 and 12 post senescence induction, RAS was strongly expressed (Kim et al., 2017).	OIS (4OHT-inducible RAS) OIS (4OHT-inducible RAS)	IMR90 MEFs
NOTCH1 (***NOTCH1***)	Notch and p53	NOTCH1 is a novel gene target of p53 (Yugawa et al., 2007).	On day 7 of DDIS and OIS, there was higher NOTCH1 protein expression in comparison to control proliferating cells. At day 0 of OIS, NOTCH1 expression levels were relatively low, however NOTCH1 expression increased at day 1 and further at day 2 before dropping slightly at day 4 and increasing again at days 6 and 8. NICD expression was only increased at days 2 and 4 and was diminished after day 4. In DDIS, NICD was increased on days 2 and 4 following senescence induction – all other timepoints had no detectable NICD (Hoare et al., 2016).	OIS (4OHT-inducible RAS) and DDIS (100μm etoposide)	IMR90
p38 (***MAPK14***)	p38, RAS and Notch1	RAS activates p38, and there is a negative feedback loop between p38 and RAS (Chen et al., 2000). In MEFs, NICD from Notch1 negatively regulates p38 signalling (Mo et al., 2013). In human umbilical vein endothelial cells, Notch signalling was crucial for senescence. Expression of MKP1 (inhibitor of p38) was associated with	Total p38 was present before ionising radiation treatment and remained at a similar expression level over 10 days. Phosphorylated p38 (p-p38) increased slightly after irradiation at days 2 and 4, with a significant increase from days 6 to 10 (Freund et al., 2011).	DDIS (10 Gy)	HCA2

		active Notch signalling in senescence (Yoshida et al., 2014).			
DNA damage response (DDR)	DDR and RAS	Activation of HRas-V12 in BJ human fibroblasts and MEFs triggered OIS in a DDR-dependent manner (Di Micco et al., 2006). Elevated N-Ras expression led to the activation of the DDR and ultimately OIS (Shamma et al., 2009). Activation of oncogenes such as RAS resulted in DDR activation due to hyperproliferation and double strand DNA breaks. Activation of the DDR can lead to senescence (Seoane et al., 2017).	Before irradiation there was no phosphorylated ATM (p-ATM) or Chk2 (p-Chk2). 2 hours after irradiation both increased significantly. p-ATM remained high until 24 hours when it dropped to pre-senescent levels. p-Chk2 had a strong increase over hours 2-8. At 24-72 hours expression was lower, but still higher than in pre-senescent cells. Total ATM and Chk2 were present in pre-senescent cells, with expression increasing through the whole 72-hour time period after irradiation (Freund et al., 2011). Protein expression of ATM remained relatively similar on days 2, 6 and 12 post-senescence induction. However, p-ATM increased across the time period. On day 2 there was minimal p-ATM, while on day 6 p-ATM was increased, followed by a further increase on day 12 (Kim et al., 2017).	DDIS (10 Gy) OIS (4OHT-inducible RAS)	HCA2 MEFs
p21 (***CDKN1A***)	p21 and p53	p21 (WAF1) was identified as a gene target of p53 (el-Deiry et al., 1993). This review discusses the role of p53 in senescence, including how p53 increases p21 expression in senescence (Rufini et al., 2013)	There was increased p21 protein levels as early as 2 hours post x-irradiation. p21 levels increased further at 4 hours and remained the same until 24 hours when p21 begins to decrease to pre-senescent levels (Freund et al., 2011). On days 2, 6 and 12 post senescence induction, p21 expression did not change much. It increased slightly from day 2 to day 6 but remained the same at day 12. In comparison to non-senescent cells, p21 expression was strongly increased at all three timepoints (Kim et al., 2017).	DDIS (10 Gy) OIS (4OHT-inducible RAS)	HCA2 MEFs
	p21 and Notch1	Endogenous Notch1 *in vitro* induced p21 expression (Rangarajan et al., 2001). Overexpression of Notch induced senescence, and the overexpression and activation of Notch resulted in increased p21 transcript and protein levels (Venkatesh et al., 2011).			

p53 (***TP53***)	p53 and the DDR	This study demonstrated that after DNA damage, DDR proteins such as ATM can phosphorylate p53 at serine 15 (Ashcroft et al., 1999).	p53 was present at low levels in the pre-senescent cells. 2 hours after senescence induction, p53 increased significantly and remained high until 24 hours when it began to decrease to pre-senescent levels. In pre-senescent cells there was no phosphorylated p53 (p-p53), however after senescence induction there was an increase in p-p53, with it beginning to decrease at around 8 hours but remaining significantly above pre-senescent levels at 72 hours (Freund et al., 2011). At day 2 post-senescence induction, p53 protein expression is increased in OIS cells in comparison to non-senescent cells, and continued to increase at day 6 and further still at day 12 (Kim et al., 2017).	DDIS (10 Gy) OIS (4OHT-inducible RAS)	HCA2 MEFs
		This study illustrated that in response to ionising radiation ATM mediated p53 phosphorylation (Maclaine & Hupp, 2009).			
	p53 and RAS	This review collated a variety of DDR mechanisms which activate p53 in response to DNA damage (Reinhardt & Schumacher, 2012).			
		There was ATM-dependent stimulation and expression of p53 in response to DNA damage (Shiloh & Ziv, 2013).			
Rb (***RB1***)	Rb and p21	p21 inhibits CDKs which allow hyperphosphorylation of pRb to p-pRb. Rb being hypophosphorylated leads to cell cycle arrest and senescence in certain contexts (Campisi, 2001).	N/A – no temporal data identified.	N/A	N/A
	Rb and p16	p16 inhibits CDK4 and CDK6, preventing hyperphosphorylation of pRb to p-pRb. This happens in senescence (Campisi, 2001).			
		p16 inhibits hyperphosphorylation of pRb (Giacinti & Giordano, 2006).			
p16 (***CDKN2A)***	p16 and p38	p38 regulates p16 expression in OIS via PRAK (Sun et al., 2007).	In OIS, over the course of 8 days p16 protein expression steadily increased. There were no further time points analysed. While p16 expression in DDIS follows the same trend of continually increasing over the 8 days, it appears	OIS (4OHT-inducible RAS) and DDIS (100μm etoposide)	IMR90
		p38 regulates increased expression of p16 in OIS via p53-independent mechanisms (Kwong et al., 2009).			

		Phosphorylated p38 regulates p16 expression (Wong et al., 2009).	to be of a lower concentration in DDIS than OIS (Hoare et al., 2016).		
	p16 and the DDR	The DDR increases p16 expression/formation via epigenetic changes and transcription factors activity (Rayess et al., 2012).	Before RAS induction, there were low levels of p16 protein. Days 1 and 2 have slightly higher p16 expression in comparison to day 0, followed by a strong increase on days 3-5, and an even larger increase on days 5-8. At the transcript level, there was some increase in expression on days 1-2, followed by a stronger increase from days 3-8. (Young et al., 2009).	OIS (4OHT-inducible RAS)	IMR90
		p16 expression is increased when senescence is induced with BRAF(V600E) via the activation of the DDR (Kaplon et al., 2013).	There was low p16 expression on day 2, followed by an increase at day 6 and again at day 12. (Kim et al., 2017).	OIS (4OHT-inducible RAS)	MEFs

ATM, ataxia-telangiectasia mutated; C/EBPβ, CCAAT/enhancer binding protein beta; CDK, cyclin dependent kinase; CHK, checkpoint kinase; DDIS, DNA damage-induced senescence; DDR, DNA damage response; MEFs, mouse embryonic fibroblasts; MKP, MAPK (mitogen-activated protein kinase) phosphatases; mRNA, messenger RNA; NF-κB, nuclear factor kappa light chain enhancer of activated B cells; NICD, Notch intracellular domain; OIS, oncogene-induced senescence; PRAK, p38-regulated/activated protein kinase; Rb, Retinoblastoma.

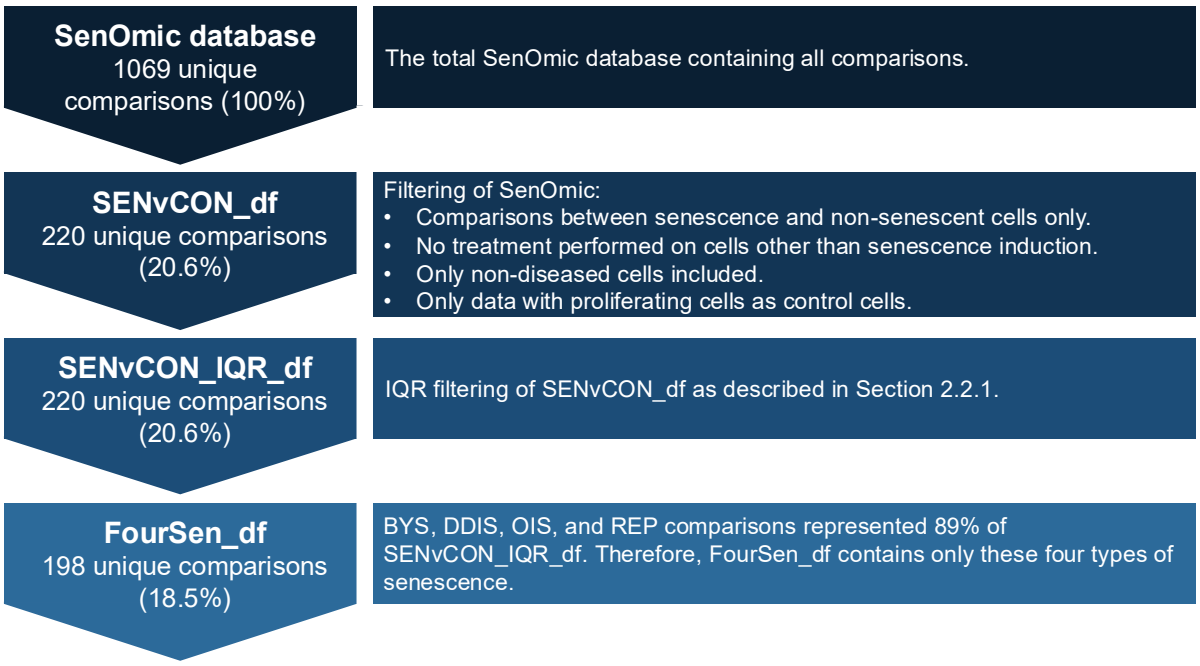

Appendix Figure A3.1 – Filtering of SenOmic to create FourSen_df.

BYS, bystander induced senescence; DDIS, DNA damage-induced senescence; IQR, interquartile range; OIS, oncogene-induced senescence; REP, replicative senescence.

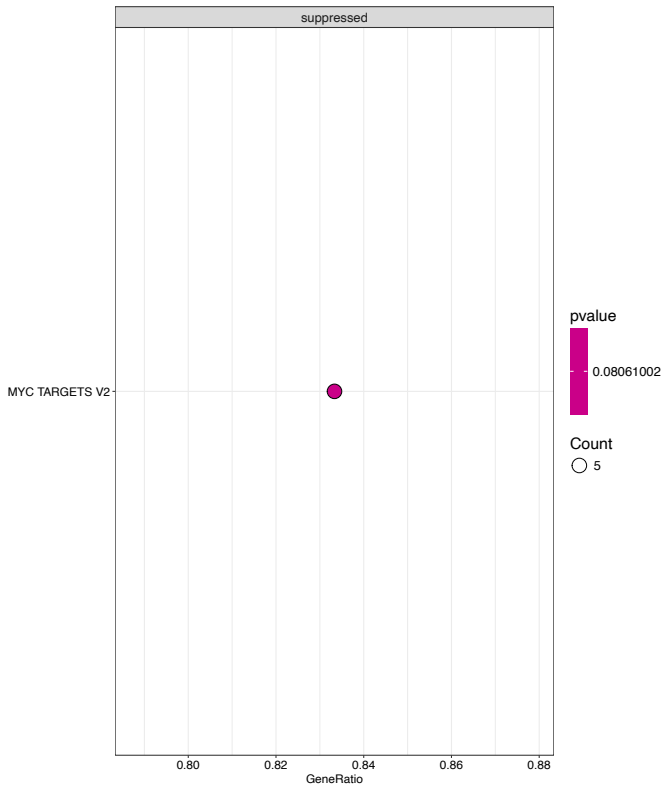

Appendix Figure A3.2 – ORA of the 3390 genes significantly expressed in lung fibroblasts with a p-value threshold of 0.1.

p-value refers to the significance of the overrepresentation of the pathway and count reflects the number of genes associated with the pathway.

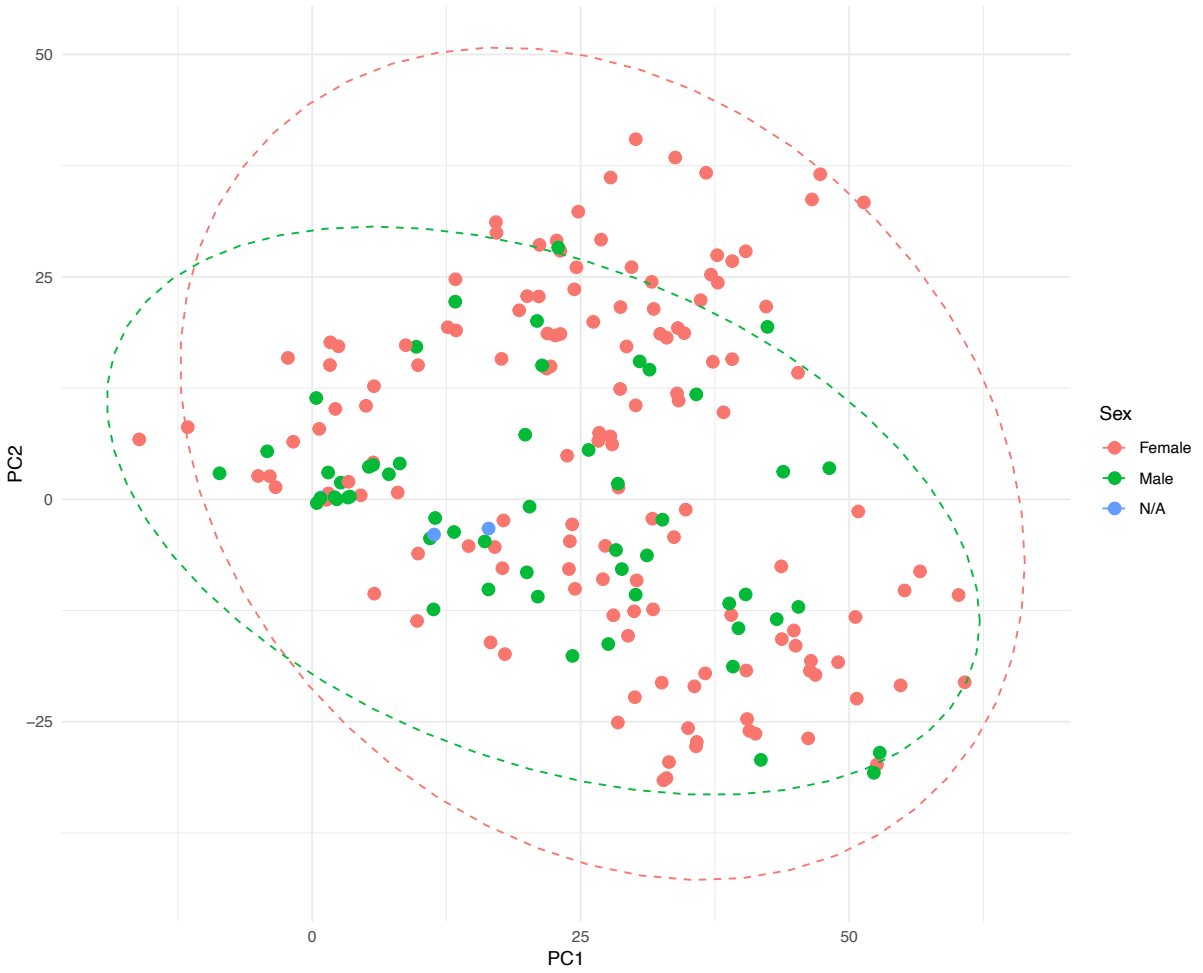

Appendix Figure A3.3 – PCA of FourSen_IQR labelled by variable Sex.

Using PCA Method 4, biplot with confidence ellipses labelled by Sex for the dataframe FourSen_IQR when datasets with the Sex variable == "NA" were included.

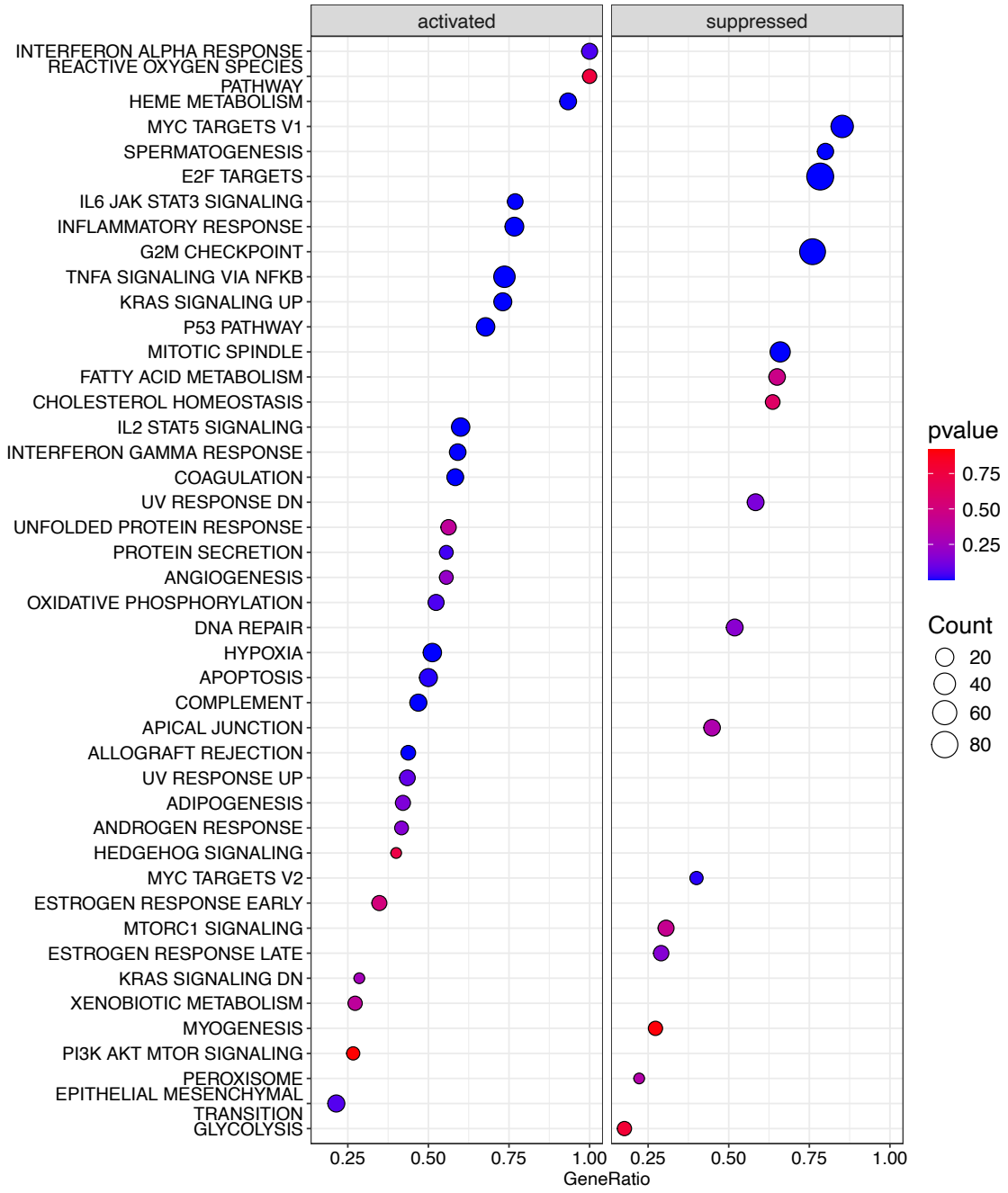

Appendix Figure A4.1 – Enriched pathways 5–7 days post-senescence induction.

Dot plot of pathways from ORA of activated and suppressed pathways identified in the 1461 genes common in DDIS and OIS 5–7 days post-senescence induction when there is no p-value threshold value. p-value refers to the significance of the overrepresentation of the pathway and count reflects the number of genes associated with the pathway. DDIS, DNA damage-induced senescence; OIS, oncogene-induced senescence; ORA, over-representation analysis.

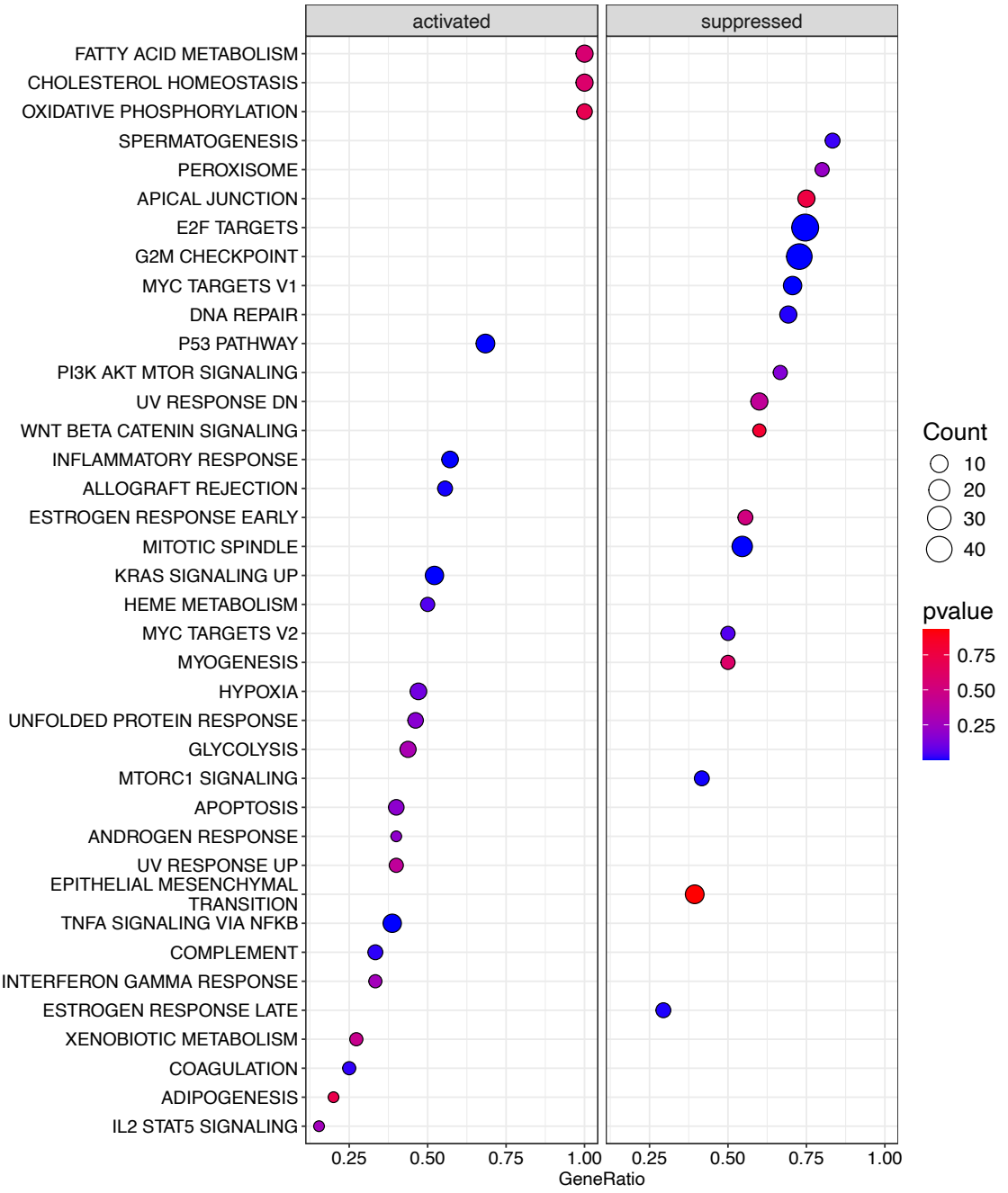

Appendix Figure A4.2 – Enriched pathways 0–4 days post-senescence induction.

Dot plot of pathways from ORA of activated and suppressed pathways identified in the 684 genes common in DDIS and OIS 0–4 days post-senescence induction when there is no p-value threshold value. p-value refers to the significance of the overrepresentation of the pathway and count reflects the number of genes associated with the pathway. DDIS, DNA damage-induced senescence; OIS, oncogene-induced senescence; ORA, over-representation analysis.

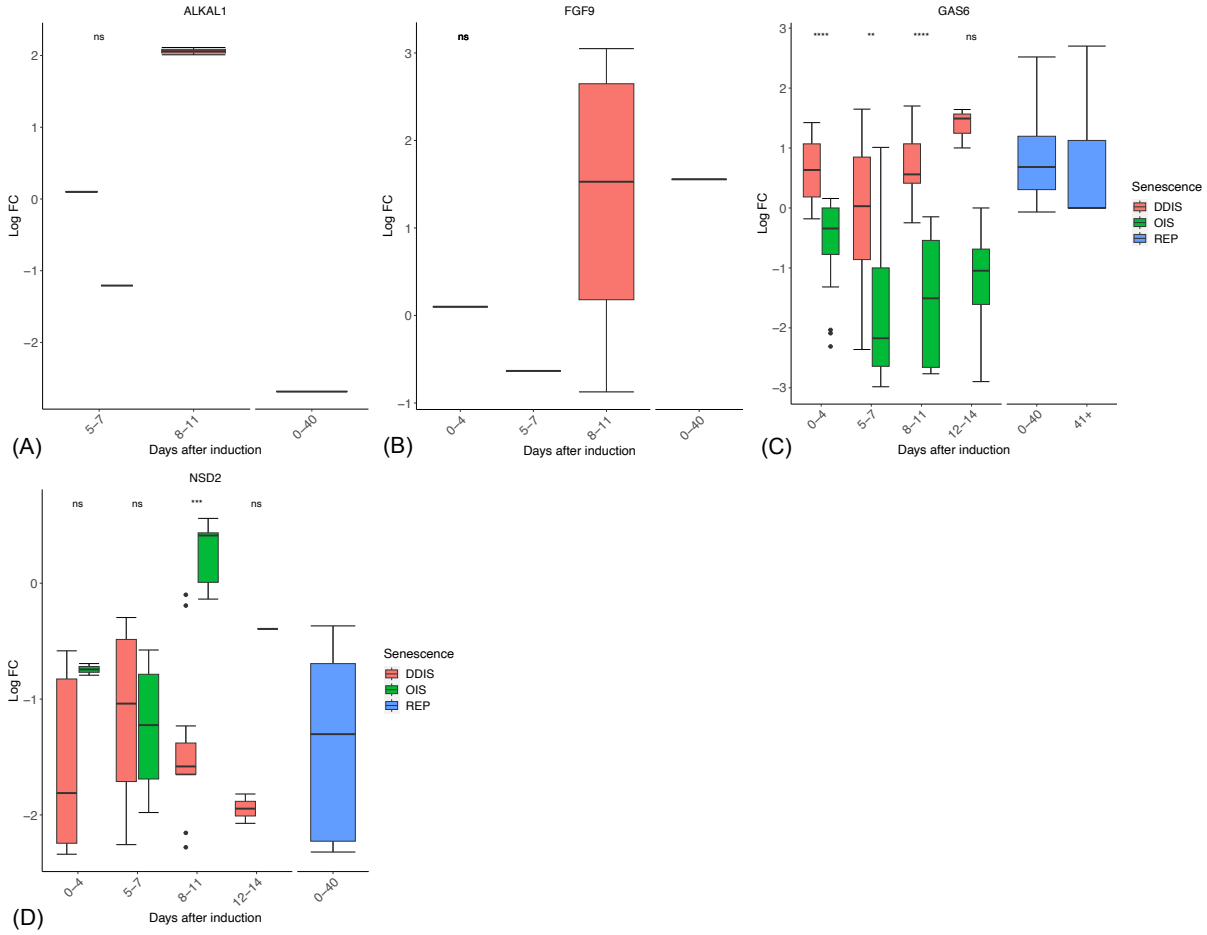

Appendix Figure A4.3 – Temporal expression of Core Geneset genes which had non-uniform expression.

*DDIS, DNA damage-induced senescence; OIS, oncogene-induced senescence; REP, replicative senescence; LogFC, log2 fold change; p-value refers to significance in expression between DDIS and OIS, *p-value <0.05; **p-value <0.01; ***p-value <0.001; ****p-value <0.0001. Figures produced using the methods and data from Scanlan et al. (2024).*

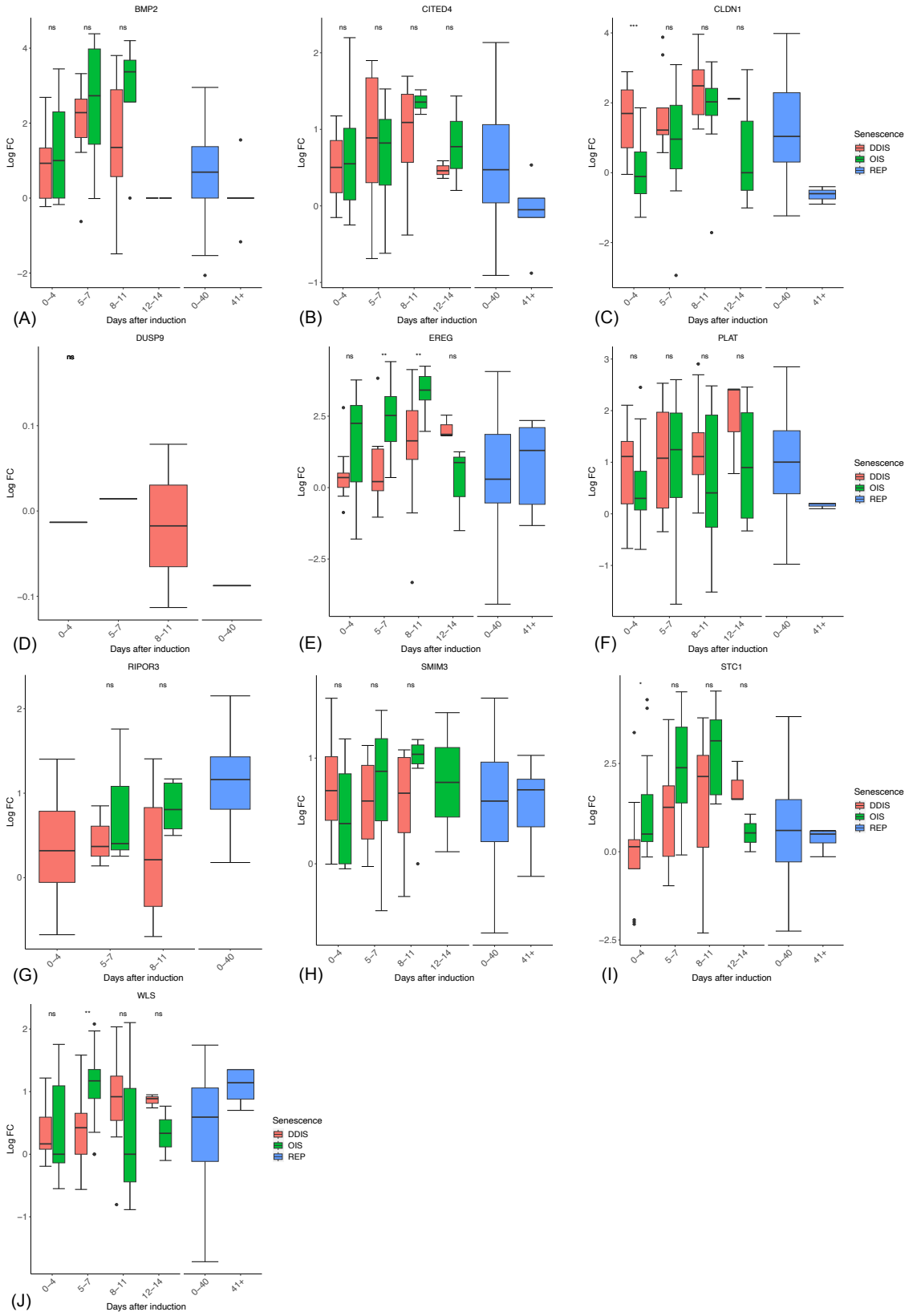

Appendix Figure A4.4 – Temporal expression of Core Geneset genes which were upregulated.

DDIS, DNA damage-induced senescence; OIS, oncogene-induced senescence; REP, replicative senescence; LogFC, log2 fold change; p-value refers to significance

*in expression between DDIS and OIS, *p-value <0.05; **p-value <0.01; ***p-value <0.001; ****p-value <0.0001. Figures produced using the methods and data from Scanlan et al. (2024).*

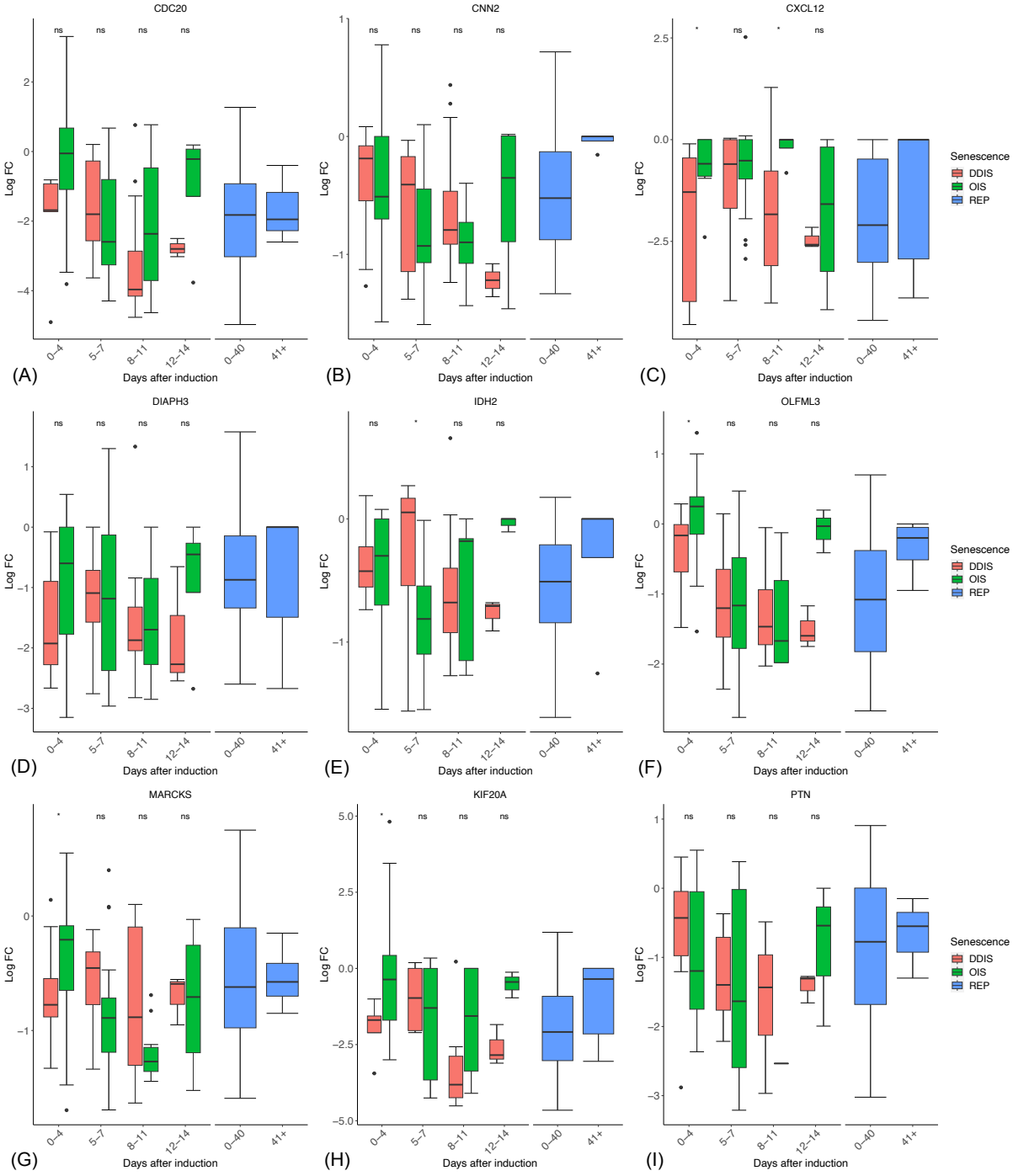

Appendix Figure A4.5 – Temporal expression of Core Geneset genes which were downregulated.

DDIS, DNA damage-induced senescence; OIS, oncogene-induced senescence; REP, replicative senescence; LogFC, log2 fold change; p-value refers to significance

*in expression between DDIS and OIS, *p-value <0.05; **p-value <0.01; ***p-value <0.001; ****p-value <0.0001. Figures produced using the methods and data from Scanlan et al. (2024).*

Appendix Table A5.1 – Data informing the model network of Model D.

Protein or process (***GENE***)	Interaction data		Temporal data		
	Interacting proteins	Summary of studies supporting the interactions	Summary of temporal data of the protein in senescence	Senescence type	Fibroblast cell line
PTEN (***PTEN***)	PTEN and p53	p53 can control transcriptional activation of PTEN (Chen et al., 2018)	N/A	N/A	N/A
	PTEN and SMAD3	A regulatory loop exists between PTEN and SMAD3, in which pSMAD3 binds the PTEN promoter, promoting PTEN transcription. SMAD3 KD and KO experiments reduce PTEN expression (Eritja et al., 2017).			
mTOR (***MTOR***)	mTOR and RAS	RAS activates the PI3K signalling pathway which activates mTOR (Shaw & Cantley, 2006).	N/A	N/A	N/A
	mTOR and PTEN	PTEN inhibits mTOR formation by preventing PI3K/Akt signalling (Chalhoub & Baker, 2009; Shaw & Cantley, 2006).			
p15 (***CDKN2B***)	p15 and SMAD3	Smad3 KO in mouse astrocytes resulted in a significant loss of p15 induction (Rich et al., 1999).	2 hours after induction there was an increase in p15 transcript expression, a trend which continued up until the end timepoint of day 8 (Young et al., 2009).	OIS (4OHT-inducible RAS)	IMR90
		Smad3 is directly involved in the induction of p15 gene transcription (Feng et al., 2000).			
Growth	Growth and RAS	RAS proteins are essential for cell proliferation in MEFs (Drosten et al., 2010).	Empty vector cells steadily increased in relative cell number across 6 days, while cells transfected with H-Ras-V12 entered a senescent state and relative cell number very slightly increased at day 2 but plateaued by the end of day 6 (Serrano et al., 1997).	OIS (4OHT-inducible RAS)	IMR90
		RAS promotes cell growth and survival (Zenonos & Kyprianou, 2013).			

	Growth and Rb	pRb is a key protein in the G1 checkpoint and inhibts growth by preventing transition into S phase of the cell cycle (Giacinti & Giordano, 2006). pRb binds and inhibits the transcription factor E2F to mediate growth arrest (Lai et al., 1999).	PD of cells was assessed for 8 days following senescence induction via ionising radiation. On day 1 there was no change compared to day 0 cells. At day 2 there was a steep drop in PD at day 2, followed by a slight increase up until day 5. On day 6, the population began to sharply decrease until day 7 when the PD as at 0%. There was no population doubling observed on day 8 (Passos et al., 2010).	DDIS (20Gy)	MRC5
	Growth and p21	This review details numerous studies in which p21 is described as inducing growth arrest and senescence (Kumari & Jat, 2021).	Cells which did not receive irradiation continued to increase their PD over a 10-day time period, whereas cells which experienced irradiation increased much slower and plateaued by day 10 (Freund et al., 2011).	DDIS (10Gy)	HCA2
	Growth and p15	Results from this study suggested that p15 may act to inhibit growth by inhibiting CDK4 and CDK6 (Hannon & Beach, 1994).	In this study cell number was assessed from day 2 to day 15 post senescence induction, comparing senescent cells and non-senescent cells. The senescent cells which have been induced via H-Ras-V12 initially peak at day 4 before decreasing at day 6 and 8. There was then a further decrease at day 10, followed by a slight increase on day 15 to levels similar to that on day 6/8. Meanwhile, the non-senescent cells had a continually increasing cell number (Kim et al., 2017).	OIS (4OHT-inducible RAS)	MEFs
TGFβ (***TGFB1***)	TGFβ and Notch	Notch signalling (mediated by NICD) regulates TGFβ expression. When Notch signalling was inhibited, TGFβ was significantly reduced (Hoare et al., 2016).	In OIS, TGFβ protein levels appeared low on day 0. This remained at day 1 and increased on day 2 and further again on day 4. TGFβ levels then dropped to below day 0 levels on days 6 and 8. In DDIS, there was slight presence of TGFβ indicated on day 0, followed by a moderate increase on days 1 and 2. TGFβ levels then began decreasing on day 4 before dropping below day 0 levels on day 6 and 8 (Hoare et al., 2016).	OIS (4OHT-inducible RAS) and DDIS (100μm etoposide)	IMR90
	TGFβ and decorin	Decorin diminished TGFβ activity by competing with TGFβ for binding to the TGF receptor (Zhang et al., 2018).			

Decorin (***DCN***)	N/A	N/A	On day 4 post-senescence induction, decorin levels were above control cell levels but still low. This was followed by a further drop in decorin levels at day 7, however it was still above control levels (Basisty et al., 2020).	OIS (4OHT-inducible RAS)	IMR90
SMAD3 (***SMAD3***)	SMAD3 and SMAD7	This study showed that SMAD7 inhibits TGFβ-mediated phosphorylation of SMAD3 (Nakao, Imamura, et al., 1997).	N/A	N/A	N/A
	SMAD3 and TGFβ	This study demonstrated that TGFβ signalling induces SMAD3 phosphorylation (Nakao, Afrakhte, et al., 1997).			
SMAD7 (***SMAD7***)	SMAD7 and SMAD3	This study showed that after TGFβ treatment, SMAD7 transcription increased through pSMAD3 stimulating the SMAD7 promoter (Nagarajan et al., 1999).	N/A	N/A	N/A
Elastin (***ELN***)	Elastin and SMAD3	In human embryonic lung fibroblasts, pSMAD3 activity stimulated elastin production (Kuang et al., 2007).	N/A	N/A	N/A
Collagen (***COL1A1***) (***COL1A2***) (***COL3A1***)	Collagens and SMAD3	In human skin fibroblasts, pSMAD3 stimulates collagen (specifically COL1A2) promoter activity. This can be achieved without TGFβ present but is enhanced by TGFβ presence (Chen et al., 1999).	Senescence was induced in two primary fibroblast cell lines (neonatal and adult). It was found in both the neonatal and adult senescent fibroblasts that COL1A1 was significantly downregulated at 24 hours (Pratsinis et al., 2013). 24 hours after receiving the final dose of UVB irradiation, mRNA was extracted and COL1A1, COL1A2 and COL3A1 levels were assessed and all three collagen genes were downregulated (Lago & Puzzi, 2019).	DDIS (8Gy/minute for 6 minutes) DDIS (UVB)	DSF22 & DSF76 primary skin fibroblasts Primary HDFs
	Collagens and MMP1	MMP proteins cleave collagen types I and III (Pittayapruek et al., 2016).			
		MMPs (such as MMP1) predominantly cleave and degrade collagen types I and III (Page-McCaw et al., 2007; Sternlicht & Werb, 2001).			

MMP1 (***MMP1***)	MMP1 and NF-κB	This study identified a NF-κB binding site on the MMP1 gene promoter (Vincenti et al., 1998).	In fibroblasts, it was found that on day 4 MMP1 transcript levels were lower than in control proliferating cells. By day 10, MMP1 levels had significantly increased to be much higher than in control cells, and this level of expression was maintained at day 20. (Hernandez-Segura et al., 2017).	DDIS (10Gy)	HCA2
		This study demonstrated that NF-κB plays an essential role in MMP1 upregulation (Bond et al., 2001).			
		In macrophages, NF-κB is key to MMP1 upregulation/secretion. When NF-κB was inhibited, MMP1 expression/secretion was drastically reduced (Chase et al., 2002).	In non-senescent cells, there was no MMP1 protein expression detected at any timepoint. On day 4 after Ras induction there was a strong increase in protein expression. On day 7 this expression was even stronger (Basisty et al., 2020).	OIS (4OHT-inducible RAS)	IMR90

DDIS, DNA damage induced senescence; OIS, oncogene induced senescence; PD, population doubling.